

Editor in Chief

P. J. Wyllie, Chicago, IL

Editors

A. El Goresy, Heidelberg

W. von Engelhardt, Tübingen · T. Hahn, Aachen

Jochen Hoefs

Stable Isotope Geochemistry

Third, Completely Revised and Enlarged Edition

With 62 Figures



Springer-Verlag
Berlin Heidelberg GmbH

Professor Dr. JOCHEN HOEFS
Geochemisches Institut der Universität
Goldschmidtstraße 1
D-3400 Göttingen, FRG

Volumes 1 to 9 in this series appeared under the title
Minerals, Rocks and Inorganic Materials

ISBN 978-3-662-10000-4 ISBN 978-3-662-09998-8 (eBook)
DOI 10.1007/978-3-662-09998-8

Library of Congress Cataloging-in-Publication Data. Hoefs, Jochen. Stable isotope geochemistry. (Minerals and rocks; 9). Bibliography: p. 1. Geochemistry. 2. Isotope geology. I. Title. II. Series. QE515.H54 1987 551.9 86-33876.

This work is subject to copyright. All rights are reserved, whether the whole or part of the material is concerned, specifically the rights of translation, reprinting, re-use of illustrations, recitation broadcasting, reproduction on microfilms or in other ways, and storage in data banks. Duplication of this publication or parts thereof is only permitted under the provisions of the German Copyright Law of September 9, 1965, in its version of June 24, 1985, and a copyright fee must always be paid. Violations fall under the prosecution act of the German Copyright Law.

© by Springer-Verlag Berlin Heidelberg 1973, 1980, and 1987.

Originally published by Springer-Verlag Berlin Heidelberg New York in 1987
Softcover reprint of the hardcover 3rd edition 1987

The use of registered names, trademarks, etc. in this publication does not imply, even in the absence of a specific statement, that such names are exempt from the relevant protective laws and regulations and therefore free for general use.

2132/3130-543210

Preface to the Third Edition

The first edition of this book was published in 1973, the second, totally rewritten, followed 7 years later in 1980. Because the field of stable isotopes is still growing and exerting an increasing influence on geosciences in general, it seems to be necessary, after a further 7 years, to revise the edition again accordingly.

Not only has the previous edition been updated, but two completely new chapters on the isotopic composition of mantle-derived material and on the isotopic composition of the ocean during the geologic past, have been added.

The references concentrate on recent literature. In some cases, older references have been omitted to save space. I do not intend to underrate the value of older publications, but only to keep the reference list – already very voluminous in relation to the total length – from becoming even larger.

An early draft has been reviewed by Russell Harmon and Alan Matthews. John Valley has sent me a preprint of an article on metamorphic rocks. To all three of them I owe my deepest thanks.

Göttingen, January 1987

Jochen Hoefs

Preface to the Second Edition

Since the first edition of this book appeared in 1973 knowledge in the field of isotope geochemistry has grown so fast that it appeared necessary to revise it accordingly. Although the main subdivisions have remained the same, the book has been totally revised and rewritten. Some reviewers of the first edition have criticized the subdivisions and proposed a more appropriate subdivision of the book along the line of different chemical elements. Since this book is mainly written for earth scientists and not for chemists, I believe the present subdivision to be more appropriate. I am fully aware that any subdivision is problematical and debatable (nature is indivisible), however, for practical purposes, geochemists have, for a long time, tried to subdivide the earth into certain "spheres". This book follows the classical scheme of subdivision with all its disadvantages, because I have no better one.

I am especially grateful to my colleagues who, during the various stages of the preparation of the manuscripts have read and criticized parts or whole drafts of the manuscript. I owe my deepest thanks to the following persons (in alphabetical order): W. Deuser (Woods Hole, Mass.), R. Harmon (East Kilbride, Scotland), T. Hoering (Washington, D.C.), H. Hubberten (Karlsruhe, FRG), Y. Kolodny (Jerusalem), J. O'Neil (Menlo Park, Calif.), B. Robinson (Wellington, N.Z.), W. Sackett (College Station, Texas), H. Sakai (Misasa, Japan), M. Schoell (Hannover, FRG), E. Usdowski (Göttingen, FRG).

However, I take, of course, full responsibility for any shortcomings.

Göttingen, January 1980

Jochen Hoefs

Contents

Chapter 1 Theoretical and Experimental Principles

1.1	General Characteristics of Isotopes	1
1.2	Isotope Effects	3
1.3	Isotope Fractionation Processes	6
1.3.1	Isotope Exchange	6
1.3.2	Kinetic Effects	11
1.3.3	Diffusion	13
1.3.4	Nonmass-Dependent Isotope Effects	15
1.3.5	Variation of Isotopic Composition with Chemical Composition and Crystal Structure	15
1.3.6	Isotope Geothermometers	16
1.4	Basic Principles of Mass Spectrometry . . .	19
1.5	Standards	22
1.6	General Remarks on Sample Handling . . .	25

Chapter 2 Isotopic Properties of Selected Elements

2.1	Hydrogen	26
2.1.1	Preparation Techniques and Mass Spectrometric Measurement	27
2.1.2	Standard	28
2.1.3	Fractionation Mechanisms	28
2.2	Carbon	31
2.2.1	Preparation Techniques	32
2.2.2	Standards	32
2.2.3	Fractionation Mechanisms of Carbon Isotopes	33
2.2.4	Interactions Between the Carbonate-Carbon Reservoir and Organic Carbon Reservoir .	36

2.3	Oxygen	37
2.3.1	Preparation Techniques	38
2.3.2	Standards	40
2.3.3	Fractionation Mechanisms	41
2.3.4	Water-Rock Interaction	47
2.4	Sulfur	49
2.4.1	Preparation Techniques	50
2.4.2	Standard	50
2.4.3	Fractionation Mechanisms	51
2.4.4	Experimental Determination of Sulfide Systems	56
2.5	Selenium	57
2.6	Nitrogen	57
2.7	Silicon	61
2.8	Boron	63
2.9	Chlorine	64
2.10	Calcium	64

Chapter 3 Variations of Stable Isotope Ratios in Nature

3.1	Extraterrestrial Materials	66
3.1.1	Meteorites	66
3.1.2	Tektites	72
3.1.3	The Moon	72
3.1.4	Mars	74
3.1.5	Venus	75
3.1.6	Interplanetary Dust	76
3.1.7	The Galaxy	76
3.2	The Isotopic Composition of Mantle Material	76
3.2.1	Oxygen	78
3.2.2	Hydrogen	80
3.2.3	Carbon	82
3.2.4	Sulfur	83
3.2.5	Nitrogen	85
3.3	Igneous Rocks	85

3.3.1	Differences Between Volcanic and Plutonic Igneous Rocks	86
3.3.2	Fractional Crystallization	86
3.3.3	Assimilation of Crustal Rocks	87
3.3.4	Secondary Alteration Processes	88
3.3.5	Basaltic Rocks	91
3.3.6	Granitic Rocks	93
3.3.7	Granitic Pegmatites	94
3.3.8	Hydrogen in Igneous Rocks	94
3.3.9	Carbon and Sulfur in Igneous Rocks	96
3.4	Volcanic Gases and Hot Springs	97
3.4.1	Volcanic Gases	97
3.4.2	Fluid Inclusions	99
3.4.3	Hot Springs	100
3.4.4	Origin of Carbon and Sulfur in Geothermal Fluids	101
3.4.5	Thermometers in Geothermal Systems	102
3.5	Ore Deposits	105
3.5.1	Origin of Ore Fluids	105
3.5.2	Wall Rock Alteration	108
3.5.3	Sulfur Isotope Composition of Hydro- thermal Ore Deposits	110
3.5.4	Hydrothermal Carbonates	116
3.6	Hydrosphere	117
3.6.1	Meteoric Water	118
3.6.2	Groundwater	124
3.6.3	Ocean Water	124
3.6.4	Pore Water	128
3.6.5	Formation Waters and Oil Field Brines	129
3.6.6	Water in Hydrated Salt Minerals	130
3.7	The Isotopic Composition of Dissolved and Suspended Compounds in Ocean and Fresh Waters	131
3.7.1	Nitrogen	131
3.7.2	Oxygen	132
3.7.3	Carbon Species in Water	133
3.7.4	Sulfate in Ocean and Fresh Water	135

3.8	Changes in the Isotopic Composition of the Ocean During Geologic History	138
3.8.1	Sulfur	138
3.8.2	Carbon	141
3.8.3	Oxygen	142
3.9	Atmosphere	143
3.9.1	Nitrogen	144
3.9.2	Oxygen	145
3.9.3	Carbon	147
3.9.4	Hydrogen	149
3.9.5	Sulfur	149
3.10	Biosphere	150
3.10.1	Living Organic Matter	151
3.10.2	Tree Rings	156
3.10.3	Organic Matter in Sediments	157
3.10.4	Oil	159
3.10.5	Coal	163
3.10.6	Natural Gas	164
3.11	Sedimentary Rocks	167
3.11.1	Clay Minerals	167
3.11.2	Cherts	169
3.11.3	Carbonates	170
3.11.4	Diagenesis of Limestones	178
3.11.5	Diagenesis of Clastic Rocks	180
3.11.6	Phosphates	181
3.11.7	Sedimentary Sulfides	182
3.12	Metamorphic Rocks	184
3.12.1	Metamorphic Fluids: Their Flow, Sources, and Water/Rock Ratios	184
3.12.2	Temperature Determination in Metamorphic Rocks	188
3.12.3	Contact Metamorphism	191
3.12.4	Regional Metamorphism	195
3.12.5	Granulite Facies Metamorphism	196
	References	198
	Subject Index	237

Chapter 1 Theoretical and Experimental Principles

1.1 General Characteristics of Isotopes

Isotopes are defined as atoms whose nuclei contain the same number of protons but a different number of neutrons. The term “isotopes” is derived from Greek (meaning equal places) and indicates that isotopes occupy the same position in the Periodic Table.

It is convenient to denote isotopes in the form ${}^m_n\text{E}$, where the superscript m represents the mass number and the subscript n represents the atomic number of an element E . For example, ${}^{12}_6\text{C}$ is the isotope of carbon which has six protons and six neutrons in its nucleus. This isotope has been assigned an atomic weight of exactly 12. All atomic weights are referred to this standard carbon isotope. The atomic weights of naturally occurring elements are averages of the weights contributed by the various kinds of isotopic nuclei.

Isotopes can be divided into stable and unstable (radioactive) species. The number of stable isotopes is about 300; whilst over 1200 unstable ones have been discovered so far. The term “stable” is relative, depending on the detection limits of radioactive decay times. In the range of atomic numbers from 1 (H) to 83 (Bi), stable nuclides of all masses except 5 and 8 are known. Only 21 elements are pure elements, in the sense that they have only one stable isotope. All other elements are mixtures of at least two isotopes. In some elements, the different isotope may be present in substantial proportions. In copper, for example, ${}^{63}_{29}\text{Cu}$ accounts for 69% and ${}^{65}_{29}\text{Cu}$ accounts for 31%. In most cases one isotope is predominant, the others being present only in trace amounts.

The stability of nuclides is characterized by several important rules, two of which are briefly discussed here. The first is the so-called symmetry rule, which states that in a stable nuclide with low atomic number, the number of protons is approximately equal to the number of neutrons, or the neutron-to-proton ratio, N/Z , is approximately equal to unity. In stable nuclei with more than 20 protons or neutrons, the N/Z ratio is always greater than unity, with a maximum value of about

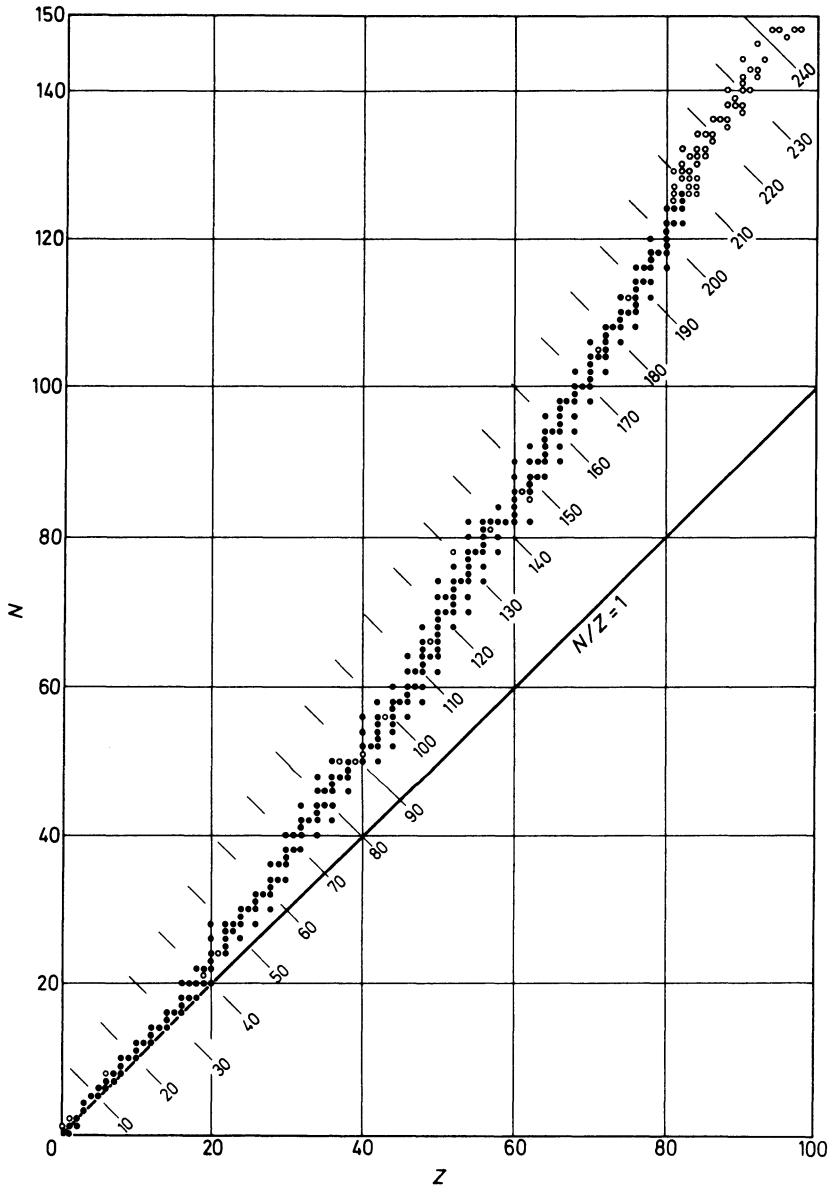


Fig. 1. Plot of number of protons (Z) and number of neutrons (N) in stable (●) and unstable (○) nuclides

Table 1. Types of atomic nuclei and their frequency of occurrence

Z-N combination	Number of stable nuclides
Even-even	160
Even-odd	56
Odd-even	50
Odd-odd	5

1.5 for the heaviest stable nuclei. The electrostatic Coulomb repulsion of the positively charged protons grows rapidly with increasing Z . To maintain the stability in the nuclei, electrically more neutral neutrons than protons are incorporated into the nucleus (see Fig. 1).

The second rule is the so-called Oddo-Harkins rule, which states that nuclides of even atomic numbers are more abundant than those with odd numbers. As shown in Table 1, the most common of the four possible combinations is even-even, the least common odd-odd.

The same relationship is demonstrated in Fig. 2, which shows that there are more stable isotopes with even than with odd proton numbers.

Radioactive isotopes can be classified into artificial and natural. Only the latter are of interest in geology, because they are the basis for radiometric age-dating methods. Radioactive decay processes are spontaneous nuclear reactions, characterized by the radiation emitted. This may be classified into α - β - γ -radiation and electron capture.

Radioactive decay is one process that produces isotope abundance variations. The second process is that of isotopic fractionation caused by small chemical and physical differences between the isotopes of an element. It is exclusively this process that we are discussing in the chapters which follow.

1.2 Isotope Effects

Differences in chemical and physical properties arising from differences in atomic mass of an element are called isotope effects. It is well known that the extranuclear structure of an element essentially determines its chemical behavior, whereas the nucleus is more or less responsible for its physical properties. Because all isotopes of a given element contain the same number and arrangement of electrons, a far-reaching similarity in chemical behavior is the logical consequence. But this similarity is

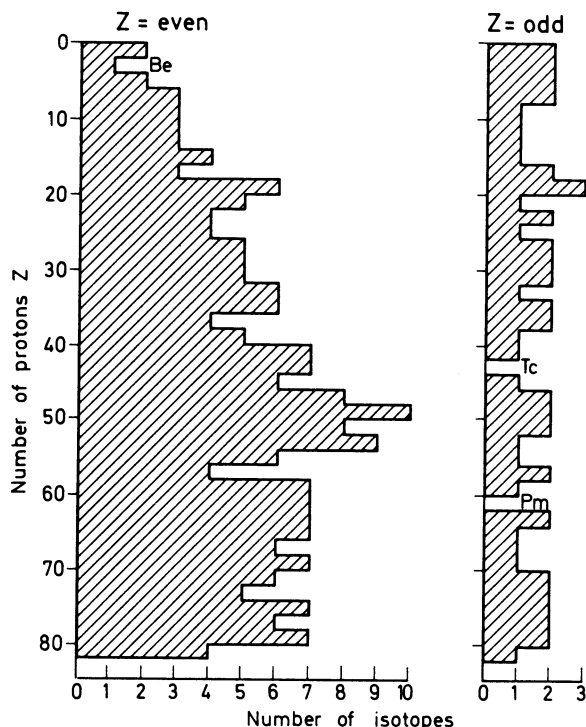


Fig. 2. Number of stable isotopes of elements with even and odd numbers of protons (radioactive isotopes with half-lives greater than 10^9 years are included)

not unlimited; certain differences exist in physicochemical properties due to the mass differences of different isotopes. The replacement of any atom in a molecule by one of its isotopes is one of the smallest of all the perturbations in chemical behavior. However, the addition of one neutron can, for instance, depress the rate of chemical reaction considerably. Furthermore, it leads, for example, to a shift of the lines in the Raman and IR spectra. These mass differences are most pronounced among the lightest elements. For example, in Table 2, some

Table 2. Characteristic constants of H_2O , D_2O , and H_2^{18}O

Constants	H_2^{16}O	D_2^{16}O	H_2^{18}O
Density (20 °C, in g cm^{-3})	0.9979	1.1051	1.1106
Temperature of greatest density (°C)	3.98	11.24	4.30
Melting point (760 Torr, in °C)	0.00	3.81	0.28
Boiling point (760 Torr, in °C)	100.00	101.42	100.14
Vapor pressure (at 100 °C, in Torr)	760.00	721.60	
Viscosity (at 20 °C, in centipoise)	1.002	1.247	1.056

differences in physicochemical properties of H_2^{16}O , H_2^{18}O , and D_2^{16}O are listed. To summarize, the properties of molecules differing only in isotopic substitution are qualitatively the same, but quantitatively different.

Since the discovery of the isotopes of hydrogen by Urey et al. (1932a,b), differences in the chemical properties of the isotopes of the elements H, C, N, O, S, and other elements have been calculated by the methods of statistical mechanics and also determined experimentally. These differences in the chemical properties can lead to considerable isotope effects in chemical reactions.

The theory of isotope effects and a related isotope fractionation mechanism will be discussed very briefly. For a more detailed introduction to the theoretical background see Bigeleisen and Mayer (1947), Urey (1947), Melander (1960), Roginsky (1962), Bigeleisen (1965), Bottinga and Javoy (1973), Javoy (1977), Richet et al. (1977), Hulston (1978), and others.

Differences in the physicochemical properties of isotopes arise as a result of quantum mechanical effects. Figure 3 shows schematically the energy of a diatomic molecule as a function of the distance between the two atoms. According to the quantum theory, the molecule cannot retain any energy on the continuous curve shown in Fig. 3, but is restricted to certain discrete energy levels. The lowest level is not at the minimum of the energy curve, but above it by an amount of $1/2 h\nu$, where h is Planck's constant and ν is the frequency with which the atoms in the molecule vibrate with respect to one another. Thus, even in the ground state at absolute zero temperature the vibrating molecule possesses a certain energy above the minimum of the potential energy curve of the molecule. It vibrates with its fundamental frequency which

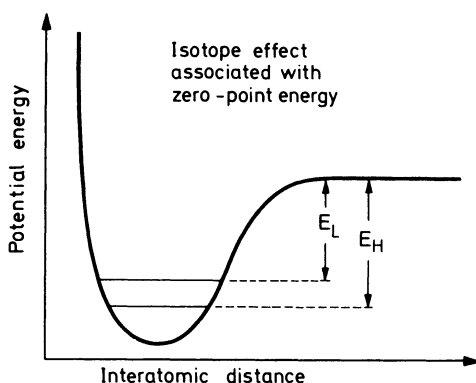


Fig. 3. Schematic potential-energy curve for the interaction of two atoms in a stable molecule or between two molecules in a liquid or solid. (After Bigeleisen 1965)

depends on the mass of the isotopes. Furthermore, it is worth mentioning that only vibrational motions cause isotope effects, rotational and translational motions have no effect on isotope separations. Therefore, different isotopic species will have different zero-point energies in molecules with the same chemical formula: the molecule of the heavy isotope will have a lower zero-point energy than the molecule of the light isotope. This is shown schematically in Fig. 3, where the upper horizontal line (E_L) represents the dissociation energy of the light molecule and the lower line (E_H), that of the heavy one. E_L is actually not a line, but an energy interval between the zero-point energy level and the “continuous” level. This means that the bonds formed by the light isotope are weaker than bonds involving the heavy isotope. Thus, during a chemical reaction, molecules bearing the light isotope will, in general, react slightly more readily than those with the heavy isotope.

1.3 Isotope Fractionation Processes

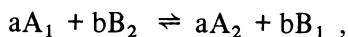
The largest isotope effect will not cause any fractionation if the reaction with which it is associated occurs quantitatively. Thus, an isotope fractionation will be observed when a reaction has an isotope effect and the formation of product is not quantitative. The partitioning of isotopes between two substances with different isotope ratios is called isotope fractionation. The main phenomena producing isotope fractionations are:

1. isotope exchange reactions,
2. kinetic processes, mainly depending on differences in reaction rates of isotopic molecules.

1.3.1 Isotope Exchange

This includes processes with very different mechanisms. In the following, the term “isotope exchange” is used for all processes in which ordinary changes in the chemical system do not occur, but in which the isotope distribution changes between different chemical substances, between different phases, or between individual molecules.

Isotope exchange reactions are a special case of general chemical equilibrium and can be written



where the subscripts indicate that species A and B contain either the light or heavy molecule 1 or 2. For this reaction the equilibrium constant will be equal to

$$K = \frac{\left(\frac{A_2}{A_1}\right)^a}{\left(\frac{B_2}{B_1}\right)^b}, \quad (1)$$

where the terms in parentheses may be, for example, the molar ratios of any species. Using the methods of statistical mechanics, the isotopic equilibrium constant may be expressed in terms of the partition functions Q of the various species

$$K = \frac{Q_{A_2}}{Q_{A_1}} / \frac{Q_{B_2}}{Q_{B_1}}. \quad (2)$$

The equilibrium constant then is simply the product or quotient of two partition function ratios, one for the two isotopic species of A, the other for B.

The partition function Q is defined by

$$Q = \sum_i (g_i \exp(-E_i/kT)), \quad (3)$$

where the summation is over all the allowed energy levels E_i of the molecules and g_i is the degeneracy or statistical weight of the i^{th} level [of E_i] and T is the temperature. Urey (1947) has shown that for the purpose of calculating partition function ratios of isotopic molecules, it is very convenient to introduce, for any chemical species, the ratio of its partition function to that of the corresponding isolated atom, which is called the reduced partition function. This reduced partition function ratio can be used in exactly the same way as the normal partition function ratio. The partition function of a molecule can be separated into factors corresponding to each type of energy: translation, rotation, and vibration

$$Q_2/Q_1 = (Q_2/Q_1)_{\text{trans}} \times (Q_2/Q_1)_{\text{rot}} \times (Q_2/Q_1)_{\text{vib}}. \quad (4)$$

The difference of the translation and rotation is more or less the same among the compounds appearing at the left- and right-hand side of the exchange reaction equation, except for hydrogen, where rotation must be taken into account. This leaves differences in vibrational energy as the source of "isotope effects". The vibrational energy term can be separated into two factors, the first is related to the zero-point energy

difference and accounts for most of the variation with temperature. The second term represents the contributions of all the other bound states and is not very different from unity. The complications which may occur relative to this simple model are mainly that the oscillator is not perfectly harmonic, so an “anharmonic” correction has to be added.

For geologic purposes the dependence of the equilibrium constant K on temperature is the most important property [Eq. (3)]. In principle, isotope fractionation factors for isotope exchange reactions are also slightly pressure-dependent. Experimental studies up to 20 kbar by Clayton et al. (1975) have shown that the pressure dependence is, however, less than the limit of detection. Thus, the pressure dependence seems to be of no importance for crustal and upper mantle environments. Isotope fractionations are equal to 1 at very high temperatures. However, the per mil fractionations do not decrease to zero monotonically with increasing temperatures. At higher temperatures, the fractionations may change sign and may increase in magnitude, but they must return a priori to zero at very high temperatures. Such crossover phenomena are due to the complex manner by which thermal excitation of the vibration of atoms contributes to an isotope effect (Stern et al. 1968). Some consequences of the crossover phenomenon for geologic material have been discussed by Muehlenbachs and Kushiro (1974).

Approaching 0° Kelvin, the equilibrium constant K tends towards zero, corresponding to complete isotope separation. Isotope fractionation, in general, disappears at high temperatures where the energy of an oscillator is given by the product kT , regardless of the mass of the vibrating atom or of the strength of the bond it forms with neighboring atoms.

For ideal gas reactions, there are two temperature regions where the behavior of the equilibrium constant K is simple: at low temperatures (generally much below room temperature) K follows in $K \sim 1/T$ where T is the absolute temperature. At high temperatures the approximation becomes $\ln K \sim 1/T^2$.

The definition of high and low temperature depends on the vibrational frequencies of the molecules involved in the reaction. We have seen that for the calculation of a partition function ratio for a pair of isotopic molecules, we have to know the vibrational frequencies of each. When solid materials are considered, the evaluation of partition function ratios becomes even more complicated, because it is necessary not

only to take into account the independent internal vibrations of each molecule, but also to consider the lattice vibrations.

1.3.1.1 Fractionation Factor (α)

Usually, we are interested in the fractionation factor, rather than in the equilibrium constant. The *fractionation factor* α is defined as the ratio of the numbers of any two isotopes in one chemical compound A divided by the corresponding ratio for another chemical compound B:

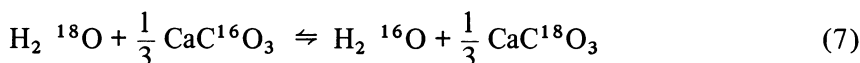
$$\alpha_{A-B} = \frac{R_A}{R_B} . \quad (5)$$

If the isotopes are randomly distributed over all possible positions in the compounds A and B, α is related to the equilibrium constant K by

$$\alpha = K^{1/n} , \quad (6)$$

where n is the number of atoms exchanged. For simplicity, isotope exchange reactions are written such that only one atom is exchanged [Eq. (7)]. In these cases, the equilibrium constant is identical with the fractionation factor, $K = \alpha$.

For example, the fractionation factor for the exchange of ^{18}O and ^{16}O between water and CaCO_3 according to



is given by

$$\alpha_{\text{CaCO}_3-\text{H}_2\text{O}} = \frac{(^{18}\text{O}/^{16}\text{O})_{\text{CaCO}_3}}{(^{18}\text{O}/^{16}\text{O})_{\text{H}_2\text{O}}} = 1.031 \text{ at } 25 \text{ } ^\circ\text{C} . \quad (8)$$

1.3.1.2 The Delta Value (δ)

The isotopic composition of two compounds A and B actually measured in the laboratory are expressed by δ -values:

$$\delta_A = \left(\frac{R_A}{R_{St}} - 1 \right) \cdot 10^3 \text{ (}\text{‰}\text{)} \quad (9)$$

and

$$\delta_B = \left(\frac{R_B}{R_{St}} - 1 \right) \cdot 10^3 \text{ (}\text{‰}\text{)} , \quad (10)$$

where R_{St} is the defined isotope ratio of a standard sample.

Table 3. Comparison between Δ , α , and $10^3 \ln \alpha$

δ_A	δ_B	Δ_{A-B}	α_{A-B}	$10^3 \ln \alpha_{A-B}$
1.00	0	1	1.001	0.9995
10.00	0	10	1.01	9.95
20.00	0	20	1.02	19.80
10.00	5.00	4.98	1.00498	4.96
20.00	15.00	4.93	1.00493	4.91
30.00	20.00	9.80	1.00980	9.76
30.00	10.00	19.80	1.01980	19.61

The δ -values and fractionation factor α are related by

$$\delta_A - \delta_B \cong \Delta_{A-B} \cong 10^3 \ln \alpha_{A-B} . \quad (11)$$

Table 3 illustrates the closeness of the approximation. Considering experimental errors, approximations are excellent for differences in δ -values of less than about 10.

1.3.1.3 Evaporation-Condensation Processes

Of special interest in stable isotope geochemistry are evaporation-condensation processes, because differences in the vapor pressures of isotopic compounds lead to fractionations. For example, from the vapor pressure data for water it is evident that the lighter molecular species are preferentially enriched in the vapor phase, the extent depending upon the temperature. Such an isotopic separation process can be treated theoretically in terms of fractional distillation or condensation under equilibrium conditions and is expressed by a Rayleigh (1896) equation. For a condensation process this equation is

$$\frac{R_v}{R_{v_0}} = f^{(\alpha-1)} , \quad (12)$$

where R_{v_0} is the isotope ratio of the initial bulk composition and R_v is the instantaneous ratio of the remaining vapor (v); f is the fraction of the residual vapor, and the fractionation factor is $\alpha = R_l/R_v$ ($l = \text{liquid}$). The instantaneous isotope ratio of the condensate leaving the vapor (R_l) is given by

$$\frac{R_l}{R_{v_0}} = \alpha f^{(\alpha-1)} \quad (13)$$

and the average isotope ratio of the separated and accumulated condensate (\bar{R}_l) at any time of condensation is expressed by

$$\frac{\bar{R}_l}{R_{v_0}} = \frac{1 - f^\alpha}{1 - f} \quad (14)$$

For a distillation process the instantaneous isotope ratios of the remaining liquid and the vapor leaving the liquid are given by

$$\frac{R_l}{R_{l_0}} = f \left(\frac{1}{\alpha} - 1 \right) \quad (15)$$

and

$$\frac{R_v}{R_{l_0}} = \frac{1}{\alpha} f \left(\frac{1}{\alpha} - 1 \right) \quad (16)$$

The average isotope ratio of the separated and accumulated vapor is expressed by

$$\frac{\bar{R}_v}{R_{l_0}} = \frac{1 - f^{\frac{1}{\alpha}}}{1 - f} \quad (f = \text{fraction of residual liquid}) \quad (17)$$

Any isotope fractionation carried out in such a way that the products are isolated from the reactants immediately after formation will show a characteristic trend in isotopic composition. As condensation or distillation proceed the residual vapor or liquid become progressively depleted or enriched with respect to the heavy isotope. A natural example is the fractionation between oxygen isotopes in the water vapor of a cloud and the raindrops released from that cloud. The resulting depletion of the $^{18}\text{O}/^{16}\text{O}$ ratio in the residual vapor and the instantaneous isotopic composition of the raindrops released from that cloud are given as a function of the fraction of vapor remaining in the cloud (Fig. 4).

1.3.2 Kinetic Effects

These are the second main phenomena producing fractionations. The theory of kinetic isotope effects has been reviewed by Bigeleisen and Wolfsberg (1958), Melander (1960), and Melander and Saunders (1980). Knowledge of kinetic isotope effects is very important, because it can provide information about details of reaction pathways. A kinetic isotope effect occurs when the rate of a chemical reaction is sensitive to atomic mass at a particular position in one of the reacting species.

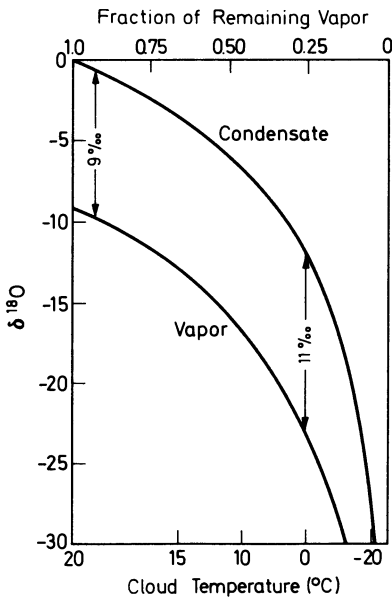


Fig. 4. $\delta^{18}\text{O}$ in a cloud vapor and condensate plotted as a function of the fraction of remaining vapor in the cloud for a Rayleigh process. The temperature of the cloud is shown on the lower axis. The increase in fractionation with decreasing temperature is taken into account. (After Dansgaard 1964)

Quantitatively, many observed deviations from the simple equilibrium processes can be interpreted as consequences of the various isotopic components having different rates of reaction.

Isotope fractionation measurements taken during unidirectional chemical reactions always show a preferential enrichment of the lighter isotope in the reaction products. The isotope fractionation introduced in the course of a unidirectional reaction may be considered in terms of the ratio of rate constants for the isotopic substances.

Thus, for two competing isotopic reactions



the ratio of rate constants for the reaction of light and heavy isotope species k_1/k_2 as in the case of equilibrium constants, is expressed in terms of two partition function ratios, one for the two isotopic reactant species, and one for the two isotopic species of the activated complex or transition state A^* :

$$\frac{k_1}{k_2} = \left[\frac{Q^*(A_2)}{Q^*(A_1)} \right] \frac{v_1}{v_2} \quad (19)$$

The factor v_1/v_2 in the expression is a mass term ratio for the two isotopic species. The determination of the ratio of rate constants is, there-

fore, principally the same as the determination of an equilibrium constant, although the calculations are not so precise because of the need for detailed knowledge of the transition state. By “transition state” is meant that molecular configuration which is most difficult to attain along the path between the reactants and the products. This theory is based on the idea that a chemical reaction proceeds from some initial state to a final configuration by a continuous change, and that there is some critical intermediate configuration called the activated species or transition state. There are a small number of activated molecules in equilibrium with the reacting species and the rate of reaction is controlled by the rate of decomposition of these activated species.

1.3.3 Diffusion

The process of diffusion can cause significant isotope fractionations. As is well known, gaseous diffusion is used in the nuclear industry to separate ^{235}U from ^{238}U . Generally light isotopes are more mobile than heavy isotopes. The ratio of the diffusion coefficients expresses the isotopic enrichment factors. For gases the ratio is equivalent to the square root of their masses.

In solutions and solids the relationships are much more complicated. The term “solid state diffusion” generally includes volume diffusion and diffusion mechanisms where the atoms move along paths of easy diffusion such as grain boundaries and surfaces. The diffusion coefficient D is usually represented as depending exponentially on an activation energy E and the absolute temperature T according to

$$D = D_0^{(-E/RT)},$$

where R is the universal gas constant and D_0 is a term which is temperature-independent. Attempts to determine diffusion coefficients have been carried out by Yund and Anderson (1974), Giletti and Anderson (1975), Giletti et al. (1978), Graham (1981), Freer and Dennis (1982), and Elphick et al. (1986). Perhaps the most promising method is the use of the Secondary Ion Mass Spectrometer (SIMS).

With the acquisition of kinetic data for oxygen diffusion in various minerals the effect of diffusion during cooling can be evaluated. Figure 5 shows an Arrhenius plot of diffusion coefficients versus reciprocal temperature for several minerals. At 600 °C, for example, feldspar, quartz, and hornblende have diffusion coefficients that differ by three orders

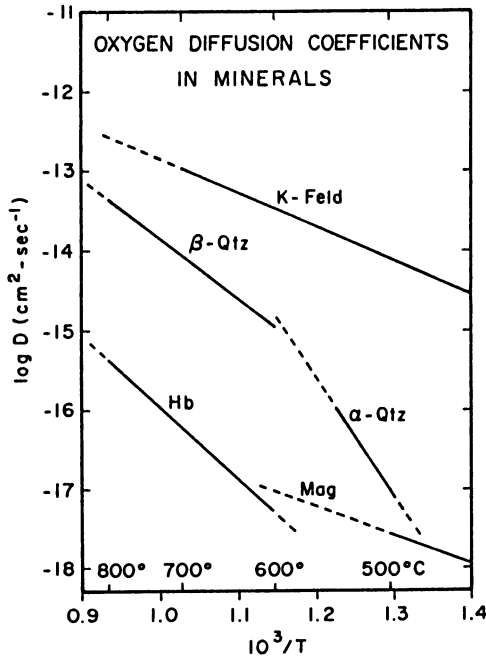


Fig. 5. Arrhenius plots of oxygen self-diffusion coefficients for K-feldspar, quartz, hornblende, and magnetite. Silicate data are for $p_{\text{H}_2\text{O}} = 1$ kbar, magnetite data are for approximately 1 bar and $(p_{\text{H}_2}/p_{\text{H}_2\text{O}}) = 1.0$. Solid lines show range of observed data (Giletti 1986)

of magnitude. That means in a given rock these minerals exchange oxygen at different rates and become closed systems at different temperatures.

Oxygen diffusion in silicate minerals under hydrothermal conditions is characterized by low activation energies (typically 30 kcal mol^{-1}) and comparatively high diffusion rates, whereas under essentially dry conditions several orders of magnitude higher activation energies and lower diffusion rates are observed. The differences are believed to arise from variations in the oxygen exchange and transport mechanisms. The study of Matthews et al. (1983c) on oxygen isotope exchange between quartz or feldspar and water has shown that exchange mechanisms are a complex function of $p_{\text{(H}_2\text{O)}}$, T , extent of exchange, grain size and morphology, and other variables and that, particularly for quartz, it may be unsafe to generalize on the mechanisms of oxygen exchange from diffusion data. Nevertheless, the determination of diffusion coefficients is of considerable importance in interpreting oxygen isotope temperatures (Giletti 1986), in studying hydrothermal water-rock interactions, and in estimating the rates of diffusion-controlled ductile deformation processes in minerals (Giletti and Yund 1984).

1.3.4 Nonmass-Dependent Isotope Effects

It has been a common belief that chemically produced isotope effects arise solely because of differences in isotopic mass. This means that for an element with more than two isotopes such as oxygen the enrichment of ^{18}O relative to ^{16}O is expected to be approximately twice as large as the enrichment of ^{17}O relative to ^{16}O . This yields a slope of 0.52 (Matsuhisa et al. 1979) on a three-isotope correlation diagram of $\delta^{17}\text{O}$ versus $\delta^{18}\text{O}$. On this basis, nonmass-dependent isotope fractionations have been ascribed solely to nuclear processes. However, Heidenreich and Thiemens (1983, 1985) have shown experimentally that during the formation of ozone from molecular oxygen and during the dissociation of carbon dioxide in a high frequency discharge, nonmass-dependent isotope fractionations do occur. To explain those unexpected isotope effects Heidenreich and Thiemens (1983) first assumed an isotopic self-shielding process which leads to the preferential dissociation of ^{18}O -containing molecules, but later (1985) demonstrated that during the dissociation of CO_2 the reaction product (O_2) is also depleted in ^{17}O and ^{18}O which would not be the case in a self-shielding process. From a kinetic standpoint it appears that both the ozone formation and the CO_2 dissociation represent the same phenomena. According to Heidenreich and Thiemens (1985), the most likely process in producing this effect is either the formation or relaxation of ozone in an excited electronic state. More experiments are needed to estimate the frequency and the importance of such nonmass-dependent isotope effects. The effects described may be of relevance to cosmochemical studies, whereas it is very likely that terrestrial processes are accompanied by mass-dependent fractionations.

1.3.5 Variation of Isotopic Composition with Chemical Composition and Crystal Structure

This aspect has been reviewed by O'Neil (1977).

Chemical Composition. Qualitatively, the isotopic composition of a mineral depends to a very high degree upon the nature of the chemical bonds within the mineral and to a smaller degree upon the atomic mass. In general, bonds to ions with a high ionic potential and low atomic mass are associated with high vibrational frequencies and have a ten-

dency to incorporate preferentially the heavy isotope. This relationship can be easily demonstrated considering the bonding of oxygen to the small, highly charged Si^{4+} ion compared to the relatively large Fe^{2+} ion: In natural mineral assemblages quartz is always the most ^{18}O -rich mineral and magnetite is always the most ^{18}O -deficient mineral. Furthermore, carbonates are always enriched in ^{18}O relative to most other mineral groups because oxygen is bonded to the small, highly charged C^{4+} ion. The nature of the divalent cation is only of secondary importance to the C-O bonding. However, the mass effect is apparent in ^{34}S distributions among sulfides where, for example, ZnS always concentrates ^{34}S relative to coexisting PbS.

Crystal Structure. Structural effects are secondary in importance to those arising from the primary chemical bonding: the heavy isotope being concentrated in the more closely packed or well-ordered structures. Such effects can be large, for example, between graphite and diamond. The calculated diamond-graphite fractionation ranges from 11.5 ‰ at 0 °C to 0.4 ‰ at 1000 °C (Bottinga 1969b), conversely, the ^{18}O and ^{13}C fractionations between aragonite and calcite at 25 °C are relatively small at 0.6 ‰ and 1.8 ‰, respectively (Rubinson and Clayton 1969; Tarutani et al. 1969).

Stable isotope studies can also provide information on details of crystal structure. For instance, Heinzinger (1969) identified two kinds of water released from $\text{CuSO}_4 \times 5 \text{H}_2\text{O}$ below and above 50 °C, differing in their bonding characteristic in the crystal. The oxygens of four water molecules are bonded to the copper ion, that of the fifth molecule is hydrogen-bonded. Heinzinger (1969) demonstrated that this fifth hydrogen-bonded molecule is enriched in deuterium by 57‰ relative to the water coordinated by the copper ion.

1.3.6 Isotope Geothermometers

Isotopic thermometry has become well established since the classic paper of Urey (1947) on the thermodynamic properties of isotopic substances. The partitioning of two stable isotopes of an element between two mineral phases can be viewed as a special case of element partitioning between two minerals. There are, however, quantitative differences between these two exchange reactions, the most important being that isotope partitioning is more or less pressure independent,

which represents the greatest advantage relative to the numerous other geothermometers.

Recently, Rumble (1982), however, argued that changing pressure has a significant influence on isotope fractionations in rocks. The pressure effect arises because changing pressure causes changes in the proportions of volatile species in fluids, which in turn leads to changes in fractionation between bulk fluid and bulk rock.

The necessary condition to apply the different geothermometers is isotope equilibrium. Conclusions concerning the nature and extent of isotope equilibrium are influenced by the criteria used to test for attainment of equilibrium and the spatial scale over which measurements have been made.

In a mineral assemblage of n -phases we can obtain $n-1$ independent temperatures, one temperature for each mineral pair. If each mineral pair gives concordant temperatures, we can be nearly certain that isotope equilibrium was attained and that equilibrium was frozen in at the same temperature in every mineral. A necessary requirement of the concordant temperature approach is that temperature calibrations must be accurate, which, however, is far from being the case. Theoretical studies show that the fractionation factor α , for isotope exchange between minerals is a linear function of $1/T^2$, where T is in degrees Kelvin at crustal temperatures. Bottinga and Javoy (1973) were the first to show that isotope fractionations between anhydrous mineral pairs at $T > 500$ °C can be expressed in terms of the equation:

$$1000 \ln \alpha = A/T^2 ,$$

which means that for a temperature determination factor A has to be known. Fractionations between minerals and fluids at < 500 °C can, on the other hand, be expressed by the equation:

$$1000 \ln \alpha = A/T^2 + B .$$

Three different methods have been used to determine the equilibrium constants for isotope exchange reactions:

1. calculation from statistical mechanical theory, which is specially suitable for gas reactions,
2. experimental determination in the laboratory;
3. calibration on an empirical basis.

The latter method is based on the idea that the calculated “formation temperature” of a rock in which other minerals are also present serves as a calibration to the measured fractionations of other minerals,

providing that all minerals were at equilibrium. However, because there is evidence that totally equilibrated systems are not very common in nature, such empirical calibrations should be regarded with extreme caution.

The theoretical calculation of isotope fractionation factors for solids is exceedingly difficult, because all vibrational frequencies of the crystalline lattice must be taken into account. Calculation of equilibrium isotope fractionation factors have been particularly successful for gases (Richet et al. 1977) and various quartz-silicate systems (Kieffer 1982). Theoretical methods are likely to play an increasing role in improving the quality of the basis for extrapolating the experimental fractionation data outside of the practical laboratory temperature range.

In a number of cases two or more approaches have been applied. For example, for the system calcite-H₂O, theoretical, experimental, and empirical methods have given coherent results.

The most promising approach seems to be the experimental determination of isotope fractionation factors. In principle, the experimental determinations of isotope exchange equilibrium constants can be carried out by simply holding the phases at a fixed temperature. By a suitable choice of isotopic compositions of the starting materials, it is possible to approach equilibrium from opposite directions, thus satisfying the classical criterion for equilibrium. However, the driving forces for the exchange reactions are small and rates of exchange are often very low. In such cases a variety of techniques have been used to facilitate exchange, and have been summarized by Clayton (1981):

1. recrystallization of a very finely ground powder;
2. crystallization of a gel or glass;
3. crystallization as a result of polymorphic phase transition;
4. synthesis of a new phase by cation exchange;
5. complete mineral synthesis.

All of these techniques depart from an ideal exchange experiment in that there are driving forces for a reaction other than the differences in isotopic composition. These obvious limitations result in various calibration curves for which significant discrepancies exist.

Experimental calibrations of isotopic geothermometers have been typically performed between 250° and 800°C. The upper temperature limit is generally determined by the stability of the mineral or by limitations of the equipment. The lower temperature limit is determined by the decreasing rate of exchange. Various procedures have been used to

establish isotope equilibrium. For direct mineral-fluid exchange experiments isotope equilibrium can be approached from opposite directions. For mineral-fluid experiments where only an approach towards equilibrium is achieved an extrapolation technique is used (Northrop and Clayton 1966), which has been widely applied for the low temperature experiments. However, the predicted "equilibrium" fractionation is often larger than the actual equilibrium value. An important modification of the Northrop and Clayton method has been introduced by Matsuhisa et al. (1979) and Matthews et al. (1983a,b), by using a three-isotope exchange method, which is discussed in more detail in Sect. 2.3.

Many of the experiments designed to calibrate an isotope thermometer yield additional information concerning the kinetics and mechanisms involved in the isotope exchange reaction. Such information is important to understand fluid/rock interaction processes. In the simplest case of direct exchange experiments, where no material is created or destroyed during the exchange process, the grain size remains constant and the volume diffusion of the element is the mechanism for isotope exchange. In many of the other hydrothermal experiments the grain size was observed to change due to chemical breakdown (e.g., feldspars), recrystallization, and/or the solution-precipitation process. The rate of isotope exchange in such systems may vary with time and thus kinetic effects cannot be dismissed (Matthews et al. 1983a). For example, in feldspar-water isotope exchange, diffusion appears to be the dominant process rather than dissolution and redeposition (O'Neil and Taylor 1967). On the other hand, in other systems, such as quartz-water, both recrystallization and diffusional exchange mechanisms may be occurring (Matthews et al. 1983c).

1.4 Basic Principles of Mass Spectrometry

Mass spectrometric methods are by far the most effective means of measuring isotope abundances. A mass spectrometer separates charged atoms and molecules on the basis of their masses based on their motions in magnetic and/or electrical fields. The design and the applications of the many types of mass spectrometers are too broad to cover here. Only the principles of mass analysis will be briefly discussed.

In principle, a mass spectrometer may be divided into four different parts: (1) the inlet system, (2) the ion source, (3) the mass analyzer, and (4) the ion detector (see Fig. 6).

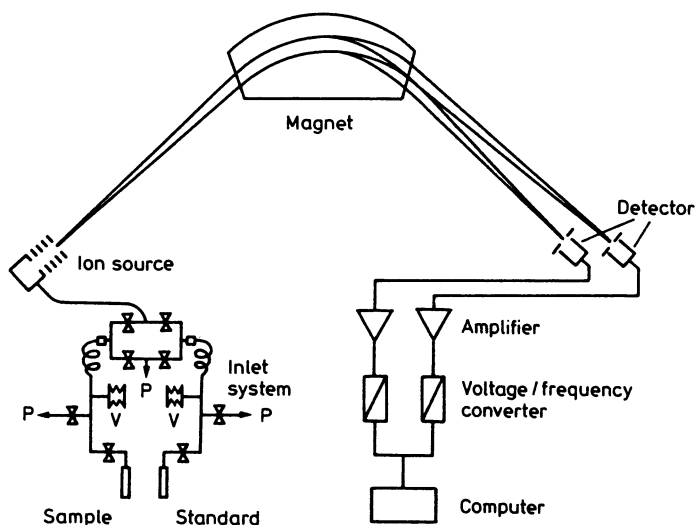


Fig. 6. Schematic drawing of a mass spectrometer for stable isotope measurements. *P* denotes pumping system, *V* denotes a variable volume

1. Special arrangements for the *inlet system* are necessary because the instability of the ions produced and the mass separation require a high vacuum. If the mean free path length (flight without collision with other molecules) of molecules is large compared with the dimensions of the tubing through which the gas is flowing, then we refer to this as molecular flow. During molecular flow the gas particles do not influence each other. Therefore, the gas flow velocity of the lighter component is greater than that of the heavier component, and this means that the heavier isotope becomes enriched in the reservoir from which the gas flows into the mass spectrometer. To avoid such a mass discrimination, normally the isotope abundance measurements of gaseous substances are carried out utilizing viscous gas flow. During the viscous gas flow the free path length of molecules is small and no mass separation takes place. The normal gas pressure is around 100 Torr. At the end of the inlet system through which we have viscous gas flow, there is a "leak", a constriction in the flow line.

2. The *ion source* is the part of the mass spectrometer where ions are formed, accelerated, and focused into a narrow beam. In the ion source, the gas flow is always molecular.

In general, ions are produced thermally or by electron impact. Ions of gaseous samples are provided most reliably by electron bombard-

ment. A beam of electrons is emitted by a heated filament, usually tungsten or rhenium, and is directed to pass between two parallel plates. The beam is collimated by means of a weak magnetic field. Positive ions are formed between the two parallel plates as a result of gas molecule-electron collisions. The ions are drawn out of the electron beam by the action of an electric field, and are further accelerated up to several kV. The positive ions entering the magnetic field are essentially monoenergetic, i.e., they will possess the same kinetic energy, according to the equation:

$$1/2 mv^2 = eV .$$

There is a minimum threshold energy below which ionization does not occur. The energy of electrons used for ionization generally is about 50 to 70 V, because this range of energy maximizes the efficiency of single ionization, but is too low to produce a significant number of multiply charged ions. The principal advantage of an electron-bombardment ion source is the stability of the resulting ion beam, the disadvantage is that the vacuum system must be extremely clean, because the electrons will ionize any gases present in the ionization chamber.

3. The *mass analyzer* separates the ion beams emerging from the ion source according to their M/e (mass/charge) ratios. From the many possible mass analyzer configurations only the first-order direction, focusing mass analyzer is used in stable isotope research. As the ion beam passes through the magnetic field, the ions are deflected into circular paths, the radii of which are proportional to the square root of M/e . Thus, the ions are separated into beams, each with a particular value of M/e .

In 1940 Nier introduced the sector magnetic analyzer. In this type of analyzer, deflection takes place in a wedge-shaped magnetic field. The ion beam enters and leaves the field at right angles to the boundary, so the deflection angle is equal to the wedge angle, for instance, 60° . The sector instrument has the advantage of its source and detector being comparatively free from the mass-discriminating influence of the analyzer field.

4. After passing through the magnetic field, the separated ions are collected in the *ion detector* and converted into an electrical impulse, which is then fed into an amplifier. For relatively large ion currents a simple metal cup (Faraday cage) is used. The cup is grounded through a high ohmic resistor. As the ion current passes to the ground, the potential drop in the resistor acts as a measure of the ion current.

By collecting two ions beams of the isotopes in question simultaneously, and by measuring the ratio of this ion current directly, a much higher precision can be obtained than from a single ion beam collection. With simultaneous collection, the isotope ratios of two samples can be compared quickly under nearly identical conditions. Nier et al. (1947) developed this technique for routine measurements and McKinney et al. (1950) improved this type of mass spectrometer, which became the standard type for isotope ratio analysis for many years. The double collecting mass spectrometer employed a precision voltage divider in a null circuit (Kelvin bridge type). With this technique the isotope ratios could be accurately measured using the chart recorder output of a vibrating reed electrometer.

During the 1960's and early 1970's, instrument makers automated their mass spectrometers, changing the measurement system from the null technique to one employing voltage-to-frequency converters and counters on each electrometer output. Today, the newest mass-spectrometer generation is fully automated and computerized, improving the reproducibility to values better than $\pm 0.02\%$.

The overall instrumental error of the mass-spectrometric measurement may be increased by nonlinearities within the individual measurement devices. The probable variation between different instruments may reach a level of 1% to 2% of the measured δ -values. This is not critical for small differences in isotopic composition. However, the uncertainty in comparing data from different laboratories increases when samples of very different isotopic compositions are compared. Blattner and Hulston (1978), by distributing a pair of calcite reference samples, showed that the individual differences between $\delta^{18}\text{O}$ determinations in more than 10 laboratories range from 23.0‰ to 23.6‰.

1.5 Standards

The accuracy with which *absolute* isotope abundances can be measured is substantially poorer than the precision with which *relative* differences in isotope abundances between two samples can be determined. Nevertheless, the determination of absolute isotope ratios is very important, because these numbers form the basis for the calculation of the relative differences, the δ -values. Table 4 summarizes absolute isotope ratios of primary standards.

Table 4. Absolute isotope ratios of international standards. (After Hayes 1983)

Standard	Ratio	Accepted value ($\times 10^6$) (with 95% confidence interval)	Source
SMOW	D/H	155.76 ± 0.10	Hagemann et al. (1970)
	$^{18}\text{O}/^{16}\text{O}$	$2,005.20 \pm 0.43$	Baertschi (1976)
	$^{17}\text{O}/^{16}\text{O}$	373 ± 15	Nier (1950), corrected by Hayes (1983)
PDB	$^{13}\text{C}/^{12}\text{C}$	$11,237.2 \pm 2.9$	Craig (1957)
	$^{18}\text{O}/^{16}\text{O}$	$2,067.1 \pm 2.1$	
	$^{17}\text{O}/^{16}\text{O}$	379 ± 15	
Air nitrogen	$^{15}\text{N}/^{14}\text{N}$	$3,676.5 \pm 8.1$	Junk and Svec (1958)
Canyon Diablo Troilite (CDT)	$^{34}\text{S}/^{32}\text{S}$	$45,004.5 \pm 9.3$	Jensen and Nakai (1962)

Irregularities and problems concerning standards have been evaluated by Friedman and O'Neil (1977), Gonfiantini (1978, 1984), and Coplen et al. (1983). The accepted unit of isotope ratio measurements is the delta value (δ), given in per mil (‰). The δ -value is defined as

$$\delta \text{ in } \text{‰} = \frac{R_{(\text{sample})} - R_{(\text{standard})}}{R_{(\text{standard})}} \times 1000 ,$$

where R represents the isotope ratio. If $\delta_A > \delta_B$, we speak of A being enriched in the rare isotope or "heavier" than B. Unfortunately, not all of the δ -values cited in the literature are given relative to a single universal standard, so that often several standards of one element are in use. To convert δ -values from one standard to another, the following equation may be used

$$\delta_{X-A} = \left[\left(\frac{\delta_{B-A}}{10^3} + 1 \right) \left(\frac{\delta_{X-B}}{10^3} + 1 \right) - 1 \right] 10^3 ,$$

where X represents the sample, A and B different standards.

For different elements a convenient "working standard" is used in each laboratory. However, all values measured relative to the "working standard" are reported in the literature relative to a universal standard. Unfortunately, there has sometimes been a lack of agreement among researchers in this field as to what standard should be designated as the universal standard. A standard should fulfill the following requirements:

1. be used worldwide as the zero point;
2. be homogeneous in composition;
3. be available in relatively large amounts;
4. be easy to handle for chemical preparation and isotopic measurement;
5. have an isotope ratio near the middle of the natural variation range.

Among the reference samples now used, relatively few meet all of these requirements. For example, the most widely used carbon isotope standard, PDB, a sample of a belemnite guard, is exhausted. The worldwide standards now in use are given in Table 5.

The problems related to standards have been discussed by an advisory group, who met in 1983 for the third time in Vienna. As a result of these meetings (Coplen et al. 1983; Confiantini 1984) several new standards can be cited.

A further advancement comes from interlaboratory comparison of two standards having different isotopic composition, which, for instance, has been carried out by Blattner and Hulston (1978) on two carbonates. Such an interlaboratory calibration can then be used for a normalization procedure, which corrects for all proportional errors due to the mass spectrometer and to the sample preparation. Ideally, the two standard samples should have isotope ratios as different as possible, but still within the range of natural variations. There are, however, some problems connected with the data normalization, which are still under debate. For example, the CO₂ equilibration of waters and the acid extraction of CO₂ from carbonates are indirect analytical procedures, involving temperature-dependent fractionation factors (whose values are not well defined) with respect to the original samples and which might be reevaluated on the normalized scale.

Table 5. Worldwide standards in use for the isotopic composition of hydrogen, carbon, oxygen, sulfur, and nitrogen

Element	Standard	Standard abbreviated
H	Standard Mean Ocean Water	SMOW
C	Belemnitella americana from the Cretaceous Peedde formation, South Carolina	PDB
O	Standard Mean Ocean Water	SMOW
S	Troilite (FeS) from the Canyon Diablo iron meteorite	CD
N	Air	N ₂ (atm.)

1.6 General Remarks on Sample Handling

Isotopic differences between samples to be measured are often extremely small. Therefore, great care has to be taken to avoid any isotope fractionation during chemical or physical treatment of the sample.

To convert geologic samples to a suitable form for analysis, many different preparation techniques must be used. They have, nevertheless, one general feature in common: any preparation procedure providing a yield of less than 100% may produce a reaction product that is isotopically different from the original specimen, because the different isotopic species have different reaction rates.

A quantitative yield of a pure gas is usually necessary for the mass spectrometric measurement in order to prevent not only isotope fractionation during sample preparation, but also interference in the mass spectrometer. Contamination with gases having the same molecular masses and having similar physical properties may be a serious problem. This is especially critical with CO_2 and N_2O , on the one hand (Craig and Keeling 1963), and N_2 and CO , on the other. When CO_2 is used, interference by hydrocarbons and a CS^+ ion may also be a problem.

Contamination may result from incomplete evacuation of the vacuum system and/or from degassing of the sample. How gases are transferred, distilled, or otherwise processed in vacuum lines is briefly discussed under the different elements. All errors due to chemical preparation limit the overall precision of an isotope ratio measurement to 0.1‰ to 0.2‰, while modern mass spectrometer instrumentation enables a precision better than 0.02‰ for light elements other than hydrogen. Still larger errors must be expected when elements of very low concentration are extracted by chemical methods (e.g., carbon and sulfur from igneous rocks). Table 6 summarizes which gases are used for mass-spectrometric analysis of the various elements.

Table 6. Gases most commonly used in isotope ratio in mass spectrometry

Element	Gas
H	H_2
C	CO_2
N	N_2
O	$\text{CO}_2, (\text{O}_2)$
S	SO_2, SF_6
Si	SiF_4

Chapter 2 Isotopic Properties of Selected Elements

The foundations of stable isotope geochemistry were laid in 1947 by Urey's paper on the thermodynamic properties of isotopic substances and by Nier's development of the ratio mass spectrometer. Before going into details of the naturally occurring variations of stable isotope ratios, it is useful to discuss some general trends pertinent to the whole field of isotope geochemistry.

1. Detectable isotope fractionation occurs only when the relative mass differences between the isotopes of a specific element are large, i.e., measurable isotope fractionations should be detectable only for the light elements (in general up to a mass number of about 40).
2. All those elements that form solid, liquid, and gaseous compounds which are stable over a wide temperature range, are likely to have variations of isotopic composition. Generally, the heavy isotope is concentrated in the solid phase in which it is more tightly bound. Heavier isotopes tend to concentrate in molecules in which they are present in the highest oxidation state.
3. Isotopic variations in most biological systems can be best explained by assuming kinetic effects. During biological reactions (e.g., during photosynthesis, bacterial reactions, and other microbiological processes) the lighter isotope is very often enriched in the reaction product relative to the starting substances.

2.1 Hydrogen

Until 1931 it was assumed that hydrogen consisted of only one isotope. Urey et al. (1932a,b) detected the presence of a second, heavy, stable isotope, which was called deuterium. Way et al. (1950) gave the following average abundances of the stable hydrogen isotopes:

^1H : 99.9844%

^2D : 0.0156% .

Hagemann et al. (1970) reported the absolute abundance of deuterium in the SMOW standard to be 155.8 ppm. In addition to these two stable isotopes there is a third naturally occurring but radioactive isotope, ^3H , tritium, with a half-life of approximately 12.5 years.

The isotope geochemistry of the stable hydrogen isotopes is one of the most interesting, for several reasons:

1. Hydrogen has by far the largest relative mass difference between its two stable isotopes. This results in hydrogen showing the largest variations in stable isotope ratios of all elements.
2. Hydrogen is nearly omnipresent in the forms of H_2O , OH^- , H_2 , and CH_4 , even at great depths in the earth's mantle. Therefore, it is conceivable that hydrogen plays a major role, directly or indirectly, in many naturally occurring geologic processes.

In Fig. 7 the ranges of hydrogen isotope composition of some geologically important reservoirs are given. The isotope geochemistry of hydrogen has been reviewed by Taylor (1974a) and Friedman and O'Neil (1978).

2.1.1 Preparation Techniques and Mass Spectrometric Measurement

The determination of the D/H ratios is usually performed on H_2 gas. Water is converted to hydrogen by passage over hot zinc or uranium at about 750°C , e.g., as described by Bigeleisen et al. (1952), Friedman

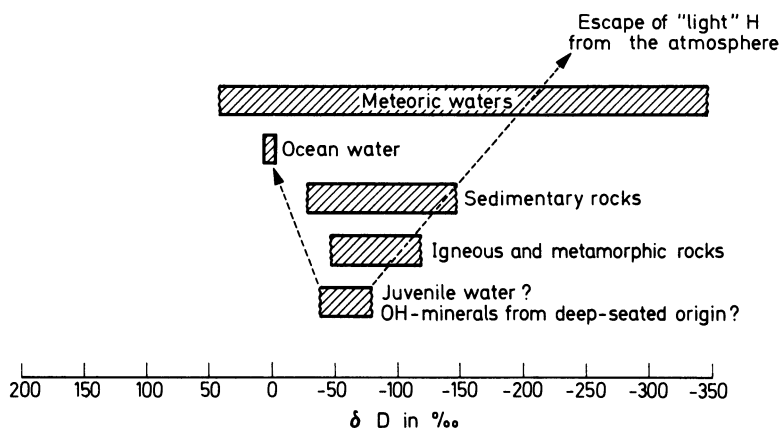


Fig. 7. D/H ratios of some geologically important materials (δD relative SMOW)

(1953), Craig (1961a), and Godfrey (1962). Most of the hydrogen generated from hydroxyl-bearing minerals is liberated in the form of water, but some is liberated as molecular hydrogen (Savin and Epstein 1970a). The resulting H_2 gas is converted in many laboratories to water by reaction with copper oxide. The water is then treated as described above.

A difficulty in measuring D/H isotope ratios is that along with the H_2^+ and HD^+ formation in the ion source, H_3^+ is produced as a by-product of ion-molecule collisions. Therefore, an H_3^+ correction has to be made. The relevant procedures have been evaluated by Schoeller et al. (1983), who also introduced a new alternative. The analytical error for hydrogen isotope data is usually given as $\pm 0.5\%$ to $\pm 2\%$ depending on different laboratories.

2.1.2 Standard

In the past there has been some confusion due to the fact that different laboratories have expressed their results in noncorresponding scales. To resolve this confusion, in 1976 a consultant meeting of the International Atomic Energy Agency in Vienna recommended that the zero point of the δD scale should be Vienna SMOW. The I.A.E.A. distributes a second water standard called SLAP (Standard Light Antarctic Precipitation) which has a δ -value of -428% .

2.1.3 Fractionation Mechanisms

2.1.3.1 Vapor Pressure and Freezing-Point Differences

The most effective processes that produce hydrogen isotope variations are those due to vapor pressure differences of water, and to a much smaller degree, those due to differences in freezing points. Because the vapor pressure of HDO is slightly lower than that of H_2O , the concentration of D is higher in the liquid than in the vapor phase.

The physical processes responsible for the fractionation of hydrogen isotopes in water and the distribution of the resulting fractionations in nature are the same as those applying to the fractionation of oxygen isotopes in water. Therefore, the fractionation of ^{18}O parallels that of D in most cases.

2.1.3.2 Equilibrium Exchange Reactions

Bottinga (1969a) and Richet et al. (1977) calculated the hydrogen isotope fractionations for gaseous hydrogen compounds. They demonstrated that very large fractionations on the order of several hundred per mil occur in the systems water vapor-methane, $\text{H}_2\text{O}-\text{H}_2$, and $\text{H}_2\text{O}-\text{H}_2\text{S}$. D/H fractionation factors between hydrous minerals and water have been determined experimentally by Suzuoki and Epstein (1976), Sakai and Tsutsumi (1978), Graham et al. (1980, 1984, 1986), Satake and Matsuo (1984), and Liu and Epstein (1984). The resulting fractionation curves (see Fig. 8) are much more complex than originally thought by Suzuoki and Epstein (1976). As Fig. 8 demonstrates the forms of the curves are extremely variable, even within one mineral group. Therefore, extrapolations to temperatures outside of the convenient experimental range are not justified. The linear relationship between $1/T^2$ and the mineral water fractionations proposed by Suzuoki and Epstein

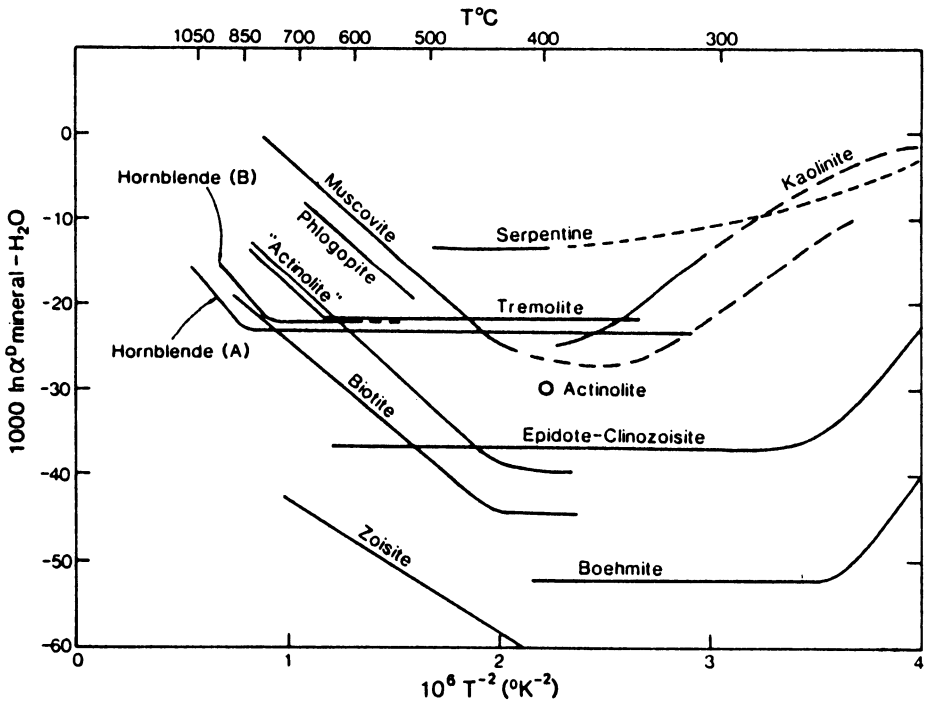


Fig. 8. Some experimentally determined mineral-water hydrogen isotope fractionation curves (Sheppard 1984)

(1976) for micas and amphiboles in the temperature range from 800° to 450 °C is not followed by epidotes (Graham et al. 1980), by tremolite (Graham et al. 1984), or by chlorite (Graham et al., in press). Furthermore, the near linear relationship between atomic mass/charge ratio of the octahedrally coordinated cation and the mineral-H₂O fractionation noted by Suzuoki and Epstein (1976) has not been verified for other minerals (Graham et al. 1980).

Hydrogen isotope fractionations in the temperature range below 400 °C are not well known, because the exchange rates between water and mineral are slow. O'Neil and Kharaka (1976) reported that $\approx 30\%$ of hydrogen isotope exchange between kaolinite and water was reached after 8 months of reaction at 200 °C. With a modified technique – relative to conventional techniques – Liu and Epstein (1984) determined the fractionation for kaolinite-water in the temperature range from 200° to 350 °C. The relationship found by them is opposite to that observed for temperatures above 400 °C. These data, combined with data on natural samples (Lambert and Epstein 1980; Marumo et al. 1980), suggest that there is a reversal in isotope fractionation at temperatures around 200 °C.

One reason for this complicated behavior of hydrogen isotope fractionation might be that hydrogen occurs in some minerals in more than one structural site (Graham et al., in press). In minerals where hydrogen bonding occurs there is a qualitative relationship between the length of the O–H–O bridge and the fractionation factor: the shorter the bond length in the mineral, the more strongly the mineral concentrates protium. Satake and Matsuo (1984) demonstrated that besides the hydrogen bond effect, structural effects such as distortion of the Mg-octahedron may also control the D/H fractionation.

When applying these experimental data to natural assemblages isotope equilibrium is a necessary prerequisite. However, in the case of hydrogen it is especially difficult to establish whether isotope equilibrium is commonly preserved in high-temperature environments, because the rate of hydrogen isotope exchange is – compared to oxygen – relatively rapid. Graham (1981) could demonstrate that for micas closure temperatures for hydrogen are about 200 °C lower than those for oxygen. Rapid hydrogen transport may proceed by hydrolysis of Si–O and Al–O bonds, thus supporting the idea that water appears to be essential for isotope exchange. Graham (1981) could further demonstrate that hydrogen isotope exchange between coexisting hydrous minerals proceeds by a quite different mechanism in the absence of hydrous

fluid than in its presence. The presence of water greatly facilitates diffusion rates by at least two orders of magnitude. The kinetics of the hydrogen exchange reaction may be quantified by the determination of activation energies for hydrogen diffusion in hydrous minerals (Graham 1981).

2.1.3.3 Other Fractionation Effects

It is well known that clays and shales may act as semipermeable membranes. This effect is also known as “ultrafiltration”. Coplen and Hanshaw (1973) demonstrated that both hydrogen and oxygen isotope fractionations may occur during ultrafiltration in such a way that the residual water is enriched in the heavier isotopes, which is due to the preferential adsorption of the heavier isotopes at the clay minerals. This phenomenon has important implications in explaining the isotopic compositions of formation waters.

In salt solutions, isotope fractionation can occur between the water in the “hydration sphere” and the free water (Truesdell 1974). The influence of hydration on the D/H activity ratio is discussed briefly in Sect. 2.3. Very interesting fractionation effects have been observed between crystal water and the mother fluid. Barrer and Denny (1964) and Matsuo et al. (1972) reported that D is depleted in hydrated salts and enriched in the aqueous solution with which salts were in equilibrium. In the gypsum-water system, Matsubaya and Sakai (1973) gave, for instance, a fractionation factor of 0.980 at 25 °C. There are a few examples, such as ice-water, where deuterium is enriched in the solid phase (O’Neil 1968).

Appreciable hydrogen isotope fractionations seem probable in biochemical processes, e.g., during bacterial production of molecular hydrogen and methane (Krichevsky et al. 1961). Cloud et al. (1958) observed that hydrogen gas given off by a bacterial culture was depleted in deuterium by a factor of 20, rather than 3.7 expected if the hydrogen gas had been in isotopic equilibrium with water.

2.2 Carbon

Carbon is one of the most abundant elements in the universe, but it occurs in the earth as a trace element. The average carbon content of

the crust and the mantle probably lies in the range of several hundred parts per million. Besides playing a key role in the biosphere, inorganic carbon also exists in a diversity of compounds with different oxidation states like in diamond and in carbon dioxide. This distribution of more oxidized carbon compounds of inorganic origin and of more reduced carbon in the biosphere is an ideal situation for naturally occurring isotope fractionations.

Carbon has two stable isotopes:

$^{12}\text{C} = 98.89\%$ (reference mass for atomic weight scale),

$^{13}\text{C} = 1.11\%$ (Nier 1950).

The naturally occurring variations of the carbon isotope composition is greater than 100‰. Heavy carbonates with a δ -value of more than +20 and light methane of around -90‰ have been reported in the literature (see also Fig. 11).

2.2.1 Preparation Techniques

The gas used in all $^{13}\text{C}/^{12}\text{C}$ measurements is CO_2 , for which the following preparation methods exist:

1. a) *Carbonates* are reacted with 100% phosphoric acid at temperatures between 25° and 75 °C (depending on the carbonate) to liberate CO_2 (see also Sect. 2.3).
b) Thermal decomposition.
2. *Organic compounds* are generally oxidized at ≈ 1000 °C in a stream of oxygen or by an oxidizing agent like CuO. Systems in use have been described, for instance, by Wedeking et al. (1983).

The determination of isotope abundances at specific positions within organic molecular structures can be of great interest. Special degradative techniques have been devised to produce CO_2 quantitatively from the positions of interest (DeNiro and Epstein 1977; Monson and Hayes 1982).

2.2.2 Standards

As the commonly used international reference standard PDB has been exhausted for several years there was a need for introducing new stan-

Table 7. $\delta^{13}\text{C}$ -values of NBS-reference samples relative to PDB. (After Coplen et al. 1983)

NBS-16	CO_2	-41.48
NBS-17	CO_2	- 4.41
NBS-18	Carbonatite	- 5.00
NBS-19	Marble	+ 1.92
NBS-20	Limestone (Solenhofen)	- 1.06
NBS-21	Graphite	-28.10
NBS-22	Oil	-29.63

dards. Coplen and Kendall (1982) prepared two new standards in the form of gaseous CO_2 , which is particularly useful, because it avoids any errors during chemical preparation procedures. Table 7 summarizes the $\delta^{13}\text{C}$ -values of the presently available NBS standards.

With respect to the oil standard, one may ask whether this material can be regarded as a suitable standard substance, because in a recent intercalibration study Schoell et al. (1983) concluded that -29.81 is the correct $\delta^{13}\text{C}$ -value.

2.2.3 Fractionation Mechanisms of Carbon Isotopes

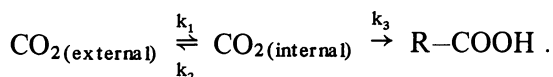
The two main carbon reservoirs, organic matter and sedimentary carbonates, are isotopically quite different from each other because of the operation of two different reaction mechanisms:

1. a kinetic effect during photosynthesis, leading to a depletion of ^{12}C in the remaining CO_2 , and concentrating the light ^{12}C in the synthesized organic material;
2. a chemical exchange effect in the system: atmospheric CO_2 -dissolved HCO_3^- , which leads to an enrichment of C^{13} in the bicarbonate.

1. Carbon isotope fractionations by organisms grown in the laboratory have been reported by Park and Epstein (1960), Abelson and Hoering (1961), Smith and Epstein (1971), Seckbach and Kaplan (1973), Pardue et al. (1976), Wong and Sackett (1978), Fuchs et al. (1979), and Wong et al. (1979). Recent reviews by Deines (1980b) and O'Leary (1981) have summarized the biochemical background of carbon isotope fractionation during CO_2 uptake.

The main isotope-discriminating steps during biological carbon fixation are (1) the uptake and intracellular diffusion of CO_2 and (2) the

first CO₂-fixing carboxylation reaction. Such a two-step model was first proposed by Park and Epstein (1960):



From this simplified scheme follows that the diffusional process is reversible, while the enzymatic carbon fixation is irreversible. However, in specific cases such as aquatic plants, natural conditions are probably further complicated by additional fractionations (i.e., hydration of CO₂). Furthermore, this model nicely explains why organic substances derived from atmospheric CO₂ or oceanic HCO₃⁻ differ in their ¹³C-content, namely that the isotopic composition depends upon the carbon source available.

The total isotope fractionation depends on which of the two steps becomes dominant or rate-controlling. Following O'Leary (1981) fractionations associated with *k*₁ and *k*₂ are roughly -4‰. The fractionation of the irreversible enzymatic carboxylation reaction (*k*₃) is considerably larger, but may vary from -17‰ to -40‰ or even lower. The initial chemical product formed during the carboxylation reaction in the majority of plant families is a three-carbon molecule, phosphoglyceric acid. These species are therefore called C₃ plants and this type of photosynthesis is called the "Calvin cycle".

In contrast, carboxylation by phosphoenolpyruvate carboxylase yields a C₄ dicarboxylic acid as the first product of carbon fixation. These C₄ plants discriminate by only -2 to -3‰ relative to bicarbonate which is the active species in this reaction (Reibach and Benedict 1977). This is one of the reasons for the small overall fractionation observed in the C₄ (or "Hatch-Slack") pathway.

Since the work of Park and Epstein (1960) and Abelson and Hoering (1961) it is well known that ¹³C is not uniformly distributed among the total organic matter, but varies between lipids, carbohydrates, and proteins. Although the causes of these δ¹³C-differences are not entirely clear, kinetic isotope effects seem to be more plausible (DeNiro and Epstein 1977, Monson and Hayes 1982) than thermodynamic equilibrium effects (Galimov 1973). The latter author postulated that ¹³C-concentrations at individual carbon positions within organic molecules are principally controlled by structural factors. Approximate calculations suggested that reduced C-H bonded positions are systematically depleted in ¹³C, while oxidized C-O bonded positions are enriched in ¹³C. Many of the observed relationships are qualitatively consistent

with that concept, however, it is difficult to identify any general mechanism by which thermodynamic factors should be able to control chemical equilibrium within a complex organic structure. Experimental evidence presented by Monson and Hayes (1982) suggests that kinetic effects will be dominant in most biological systems.

2. Isotopic equilibria in the system $\text{CaCO}_3 - \text{CO}_2 - \text{H}_2\text{O}$ have been summarized by Usdowski (1982). The overall reaction of carbonate precipitation, either abiotically or by biological consumption, is given by:



with the largest ^{13}C fractionation between CaCO_3 and CO_2 .

The temperature dependence for carbon solute species with respect to CaCO_3 is shown in Fig. 9. At low temperatures ($< 50^\circ\text{C}$) the largest fractionation step occurs between $\text{CO}_2(\text{gas})$ and HCO_3^- . Several experimental studies have attempted to determine this equilibrium fractionation factor and of these it is generally regarded that the values determined by Mook et al. (1974) are the most reliable. The isotope exchange takes place through the hydration-dehydration of CO_2 gas, which is a relatively slow process (Mills and Urey (1940)). Besides the overwhelming importance of equilibrium effects, kinetic effects are also observed in the carbonate- CO_2 - H_2O system (Usdowski et al. 1979; Turner 1982; Michaelis et al. 1985). In supersaturated solutions precipitation of calcite occurs without fractionation between solid and solution due to the fact that precipitation is faster than isotopic equilibration.

Other equilibrium fractionation reactions occur in the systems involving calcite, CO_2 , graphite, and CH_4 , which have been calculated

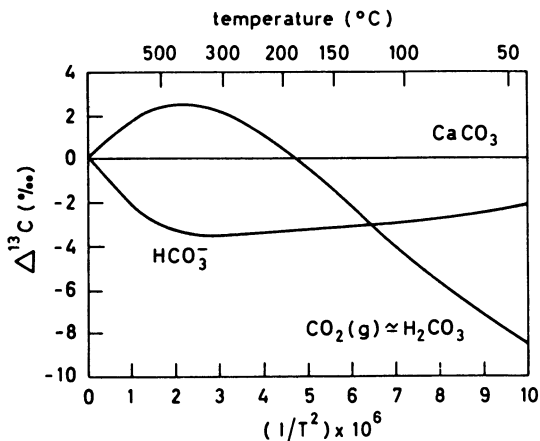


Fig. 9. Temperature dependence of carbon isotope fractionation for carbon solute species with respect to CaCO_3 . The $\Delta^{13}\text{C}$ -value is equal to the difference in $\delta^{13}\text{C}$ -values between the solute species and CaCO_3 (note the crossover point on the H_2CO_3 curve at about 190°C (Robinson 1975))

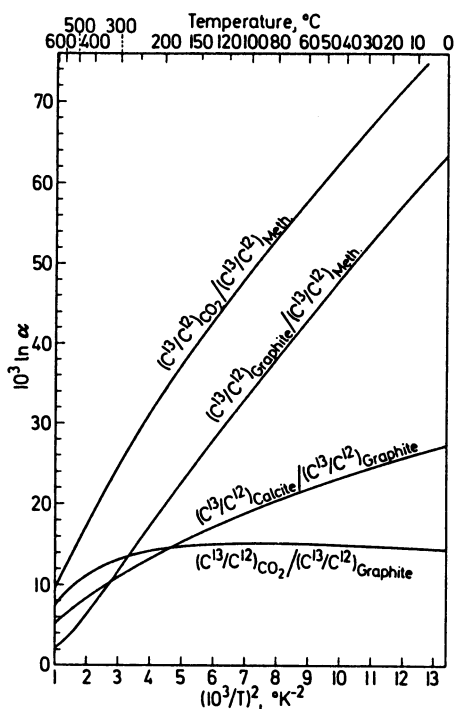


Fig. 10. Calculated carbon isotope fractionation factors for exchange among graphite, calcite, carbon dioxide, and methane. (After Bottinga 1969a)

by Bottinga (1969a) (see Fig. 10). Of these, the calcite-graphite fractionation has become a useful geothermometer, especially at high temperatures (i.e., Valley and O'Neil 1981), discussed in more detail on p. 190).

2.2.4 Interactions Between the Carbonate-Carbon Reservoir and Organic Carbon Reservoir

In Fig. 11, $\delta^{13}\text{C}$ -variations of some important carbon compounds are schematically demonstrated. As has already been mentioned, the two most important carbon reservoirs on earth, the carbonate and the reduced carbon of biological origin are characterized by very different isotopic compositions: the carbonates being isotopically heavy with a mean $\delta^{13}\text{C}$ -value around 0‰ and the biogenically reduced carbon compounds being isotopically light with a mean $\delta^{13}\text{C}$ -value around -25‰. Furthermore, large $^{13}\text{C}/^{12}\text{C}$ -fractionation can be found between the possible decay products of the carbonates – CO_2 formed during decar-

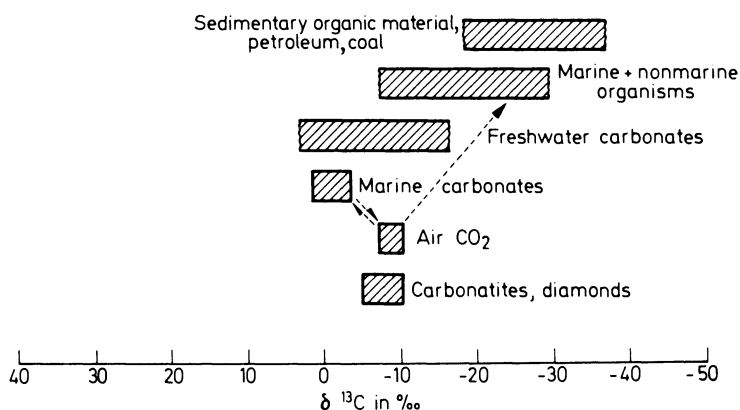


Fig. 11. $^{13}\text{C}/^{12}\text{C}$ ratios of some important carbon compounds ($\delta^{13}\text{C}$ relative PDB)

bonatization – and the decay products of the organic material, CH_4 and CO_2 . In a closed system containing these different carbon species, variations in $\delta^{13}\text{C}$ can occur as a result of oxidation-reduction reactions. Carbonates with strongly negative $\delta^{13}\text{C}$ -values are, therefore, usually interpreted as resulting from participation of organic matter carbon (see, for instance, Presley and Kaplan 1968; for interstitial waters, Hoefs 1970 and Sass and Kolodny 1972; for carbonate concretions, Kolodny and Gross 1974; for carbonates from the Mottled Zone, Israel, i.e., thermal metamorphism by combustion of organic matter). In all these cases the relative contribution of organic carbon has been estimated.

2.3 Oxygen

Oxygen is the most abundant element on earth. It occurs in gaseous, liquid, and solid compounds, most of which are thermally stable over large temperature ranges. These facts make oxygen one of the most interesting elements in isotope geochemistry. Oxygen has three stable isotopes with the following abundances (Garlick 1969):

$$^{16}\text{O} = 99.763\%$$

$$^{17}\text{O} = 0.0375\%$$

$$^{18}\text{O} = 0.1995\%$$

Because of the higher abundance and the greater mass difference, the $^{18}\text{O}/^{16}\text{O}$ ratio is normally determined. Baertschi (1976) determined

the absolute value for the $^{18}\text{O}/^{16}\text{O}$ ratio in Standard Mean Ocean Water (SMOW) as $(2005.20 \pm 0.45) \times 10^{-6}$. The $^{18}\text{O}/^{16}\text{O}$ ratio may vary by about 10% or in absolute numbers from about 1:475 to 1:525.

2.3.1 Preparation Techniques

In almost all cases CO_2 is the gas used in mass-spectrometric measurement. Different methods are used to liberate the oxygen from the various oxygen-containing compounds.

The oxygen in *silicates* and *oxides* is usually converted to CO_2 through fluorination with F_2 , BrF_5 , or ClF_3 in nickel tubes at 500° to 600°C . Decomposition by carbon reduction at 1000°C to 2000°C is suitable for quartz and iron oxides, but not for all silicates (Clayton and Epstein 1958). The liberation of oxygen by F_2 , BrF_5 , or ClF_3 has been described by Taylor and Epstein (1962), Clayton and Mayeda (1963), and Borthwick and Harmon (1982). Unwanted product gases are removed from the oxygen by cold traps, and excess F_2 is removed by reaction with KBr to form KF . The oxygen is converted to CO_2 over a heated graphite rod.

Care must be taken to ensure quantitative oxygen yields. Low yields caused by inadequate reaction temperatures or reaction times result in anomalous $^{18}\text{O}/^{16}\text{O}$ ratios, high yields are often due to excess moisture.

Stepwise fluorination techniques are useful in studying isotopic gradients in mineral grains, such as quartz and feldspar which have been hydrothermally altered. Haimson and Knauth (1983) applied a partial fluorination technique to several hydrous silica samples by reducing the amount of fluorine. With this technique they tried to react away various amounts of water, organic matter, and other impurities leaving the stronger silicon-oxygen bonds unreacted. Hamza and Epstein (1980) described a stepwise fluorination procedure to isotopically analyze the oxygen of hydroxyls in several silicate minerals. They suggested that the difference in $\delta^{18}\text{O}$ -values of the total mineral and the OH group can be used as a geothermometer.

Phosphates must be treated in a similar way first described by Tudge (1960), subsequently modified by Kolodny et al. (1983).

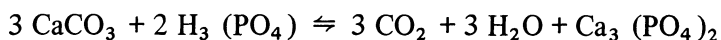
Sulfates are precipitated as BaSO_4 , and then reduced at 1000°C with carbon to CO_2 and CO . The CO is converted to CO_2 by sparking between platinum electrodes (Longinelli and Craig 1967). Care has to be taken that no memory effects occur (Sakai and Krouse 1971).

Table 8. Isotope fractionations for various carbonates occurring during CO₂ liberation with phosphoric acid at 25 °C (Rosenbaum and Sheppard 1986)

Carbonate	α	$10^3 \ln \alpha$
Calcite	1.01025	10.20
Aragonite	1.01034	10.29
Dolomite	1.01178	11.71
Siderite	1.01163	11.56

Carbonates are reacted with 100% phosphoric acid at various temperatures between 25° and 150 °C (McCrea 1950; Rosenbaum and Sheppard 1986).

The following reaction scheme:



shows that only two-thirds of the oxygen originally present in the carbonates is liberated. Since there are characteristic differences in the isotopic fractionation factors associated with the phosphoric acid liberation of CO₂ from various carbonates, this has to be considered when the isotopic composition of different carbonates is compared (see Table 8).

Wachter and Hayes (1985) demonstrated that careful attention must be given to the concentration of phosphoric acid. In their experiments best results were obtained by using 105% phosphoric acid and a reaction temperature of 75 °C. This high reaction temperature has the advantage of reducing the reaction time, but should not be applied when attempting to discriminate between mineralogically distinct carbonates by means of differential rates of phosphorolysis.

The ¹⁸O/¹⁶O ratio in *water* is usually determined by equilibration of a small amount of CO₂ with a surplus of water and analyzing the resulting CO₂. For this technique the exact value of the fractionation for the CO₂ ⇌ H₂O equilibrium at a given temperature is of crucial importance. In addition, this fractionation factor enters also all δ¹⁸O-values of waters analyzed with respect to carbonate standards and all δ¹⁸O-values of silicates. Therefore, it is logical that a number of authors have experimentally determined this fractionation factor ranging from 40.7‰ to 42.4‰ at 25 °C. The more recent determinations by O'Neil et al. (1975) and Brenninkmeijer et al. (1983) suggest that the best

value is

$$\alpha_{\text{H}_2\text{O}}^{18}(\text{CO}_2) = 1.04115 \pm 0.00005 .$$

It is also possible to quantitatively convert all water oxygen directly to CO_2 by reaction with guanidine hydrochloride. This technique was described by Dugan et al. (1985) and has the advantage that it is not necessary to assume a value for the $\text{H}_2\text{O}-\text{CO}_2$ isotope fractionation to arrive at a $\delta^{18}\text{O}$ -value.

2.3.2 Standards

Two different δ -scales are in use: $\delta^{18}\text{O}_{(\text{SMOW})}$ and $\delta^{18}\text{O}_{(\text{PDB})}$, because of two different categories of users. The SMOW standard was originally a hypothetical water sample defined by Craig (1961b). Today, the International Atomic Energy Agency (IAEA) distributes two different water standards: Vienna SMOW and SLAP (Standard Light Antarctic Precipitation), with a normalized $\delta^{18}\text{O}$ -value of -55.5‰ (Gonfiantini 1978, 1984). The original standard introduced for the paleotemperature determinations was the PDB standard, a Cretaceous belemnite from the Pee Dee formation, which has been long exhausted. The need of introducing additional stable isotope standards was recognized at an IAEA consultants' meeting in 1976. Table 9 gives the $\delta^{18}\text{O}$ -values of these new standards (Coplen et al. 1983).

Table 9. $\delta^{18}\text{O}$ -values of isotope standards relative to PDB now being distributed by the NBS. (After Coplen et al. 1983)

NBS 16	CO_2	-36.09
NBS 17	CO_2	-18.71
NBS 18	Carbonatite	-23.00
NBS 19	Marble	- 2.19
NBS 20	Limestone (Solenhofen)	- 4.14

It is relatively difficult to intercompare results between different kinds of samples, e.g., water and calcium carbonate. The conversion equation of $\delta^{18}\text{O}_{\text{PDB}}$ versus $\delta^{18}\text{O}_{\text{SMOW}}$ is

$$\delta_{\text{SMOW}} = 1.03086 \delta_{\text{PDB}} + 30.86\text{‰}$$

and for CO₂ samples

$$\delta_{\text{SMOW}} = 1.04143(\delta_{\text{PDB-CO}_2}) + 41.43\text{‰}$$

and

$$\delta_{\text{SMOW}} = 1.4115(\delta_{\text{SMOW-CO}_2}) + 41.15\text{‰} .$$

2.3.3 Fractionation Mechanisms

The ¹⁸O/¹⁶O-ratio varies in nature by about 100‰. These variations result from both equilibrium and kinetic fractionation effects. Figure 12 presents a schematic diagram of the naturally occurring variations of oxygen isotopes.

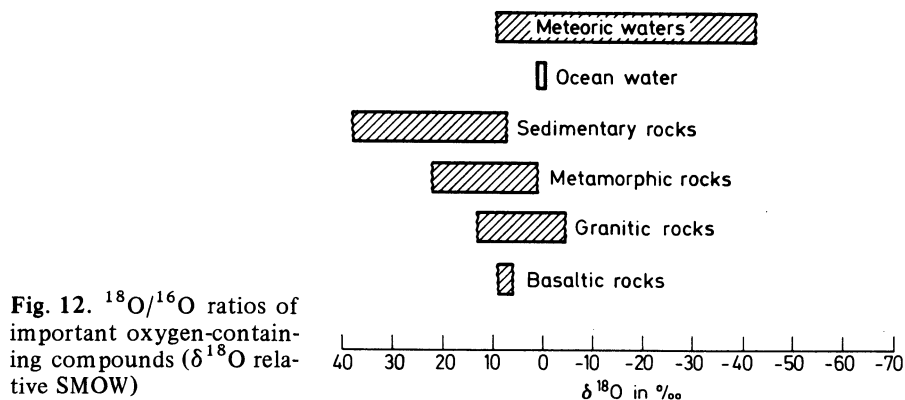


Fig. 12. ¹⁸O/¹⁶O ratios of important oxygen-containing compounds (δ¹⁸O relative SMOW)

2.3.3.1 Equilibrium Exchange Reactions

An excellent consistency in the relative ¹⁸O-contents of different minerals can be found in nature. Taylor (1967) made an attempt to arrange coexisting minerals according to their relative tendencies to concentrate ¹⁸O (Table 10). This order of decreasing ¹⁸O-content is due to a crystal-chemical relationship associated with the relative affinity for ¹⁸O. The more highly polymerized the silicate, the greater is the tendency to concentrate ¹⁸O, except for the OH group in silicates, which do not follow this relationship. Qualitatively the equilibrium isotope effect might be separated into a bond strength factor and a mass factor. The ¹⁸O-rich minerals have the most strongly bonded oxygen and/or the

Table 10. Sequence of minerals in the order (bottom to top) of their increasing tendency to concentrate O^{18} during equilibrium oxygen isotopic exchange

Minerals	δ Value ^a
1. Quartz (tridymite)	15.0
2. Dolomite	14.2
3. K-feldspar, albite	13.0
4. Calcite	12.8
5. Na-rich plagioclase	12.5
6. Ca-rich plagioclase	11.5
7. Muscovite, paragonite	11.3
8. Augite, orthopyroxene, diopside (kyanite, glaucophane)	10.5
9. Hornblende (sphene, lawsonite)	10.0
10. Olivine, garnet (zircon, apatite)	9.5
11. Biotite	8.5
12. Chlorite	8.0
13. Ilmenite	5.5
14. Magnetite, hematite	4.5

^a The δ -values given above are completely hypothetical, but they are reasonably typical of low- to middle-grade metamorphism of pelitic schists. The minerals in parentheses are less well placed in the sequence than are the major minerals.

oxygen is bonded to cations of the lowest atomic weight or highest ionic potential (charge to size ratio).

Each oxygen atom in quartz is very strongly bonded between 2 Si-atoms and Si-bonds are the strongest in the silicate structures. The Al–O bond is longer and, therefore, weaker than the Si–O bond and the atomic weight of Al is almost the same as that of Si. Therefore, all else being equal, feldspars have lower $^{18}O/^{16}O$ ratios than quartz and calcic plagioclases lower $^{18}O/^{16}O$ ratios than alkali feldspars.

The mass effect for carbonates with divalent cations is demonstrated in Table 11 (O'Neil et al. 1969). As seen in Table 11 the masses of the

Table 11. Oxygen isotope fractionation between various carbonates and water at 250 °C

Carbonate	1000 ln α	Atomic weight of cation
CaCO ₃	7.9	40.07
SrCO ₃	7.4	87.63
CdCO ₃	6.8	112.41
BaCO ₃	6.2	137.37
PbCO ₃	5.6	207.20

It should be mentioned, that the effects are much larger at lower temperatures than 250 °C.

divalent cations have a relatively small effect on the ^{18}O -content of carbonates. However, carbonates, all being relatively ^{18}O -rich, seem to be primarily influenced by the strongest bond in their structure, namely the bond between the oxygen and the small, highly charged C^{4+} ion. For silicates this seems to imply that the mass effect, i.e., the substitutions of octahedral cations in silicate structures, will generally influence the fractionation behavior slightly compared to the $\text{Al-Si-Fe}^{3+}\text{-O}$ substitutions.

Kieffer (1982) presented a theoretical model with which oxygen isotope fractionations can be predicted. Her model confirms, in general, the relative order of ^{18}O -enrichment and defines the region in which the fractionation factors do not follow a $1/T^2$ trend. Furthermore, Kieffer (1982) was able to show that crossovers in fractionation factors generally do not occur in silicate minerals of comparable composition. Thus, she found no indication for a crossover between olivine and pyroxene at $\sim 1200^\circ\text{C}$, as has been proposed by Kyser et al. (1981).

On the basis of these systematic trends in the $^{18}\text{O}/^{16}\text{O}$ -ratios of many minerals, it has become apparent that significant temperature information could be obtained up to temperatures of 1000°C and even higher in natural assemblages, if calibration curves could be worked out for the various mineral pairs.

Table 12 summarizes the principal experimental methods that have been applied to determine oxygen fractionation factors. Various criteria have been used to establish the attainment of isotopic equilibrium or the percentage of exchange. For direct mineral-fluid exchange experiments, isotopic equilibrium can be approached from opposite directions. For those experiments where equilibrium is only approached, not attained, an extrapolation technique is used (Northrop and Clayton 1966). This technique assumes that the measured amount of exchange is directly proportional to the distance the system is off from isotopic equilibrium. An important modification of the Northrop and Clayton (1966) technique has been introduced by Matsuhisa et al. (1979) and Matthews et al. (1983a, b) by using a three-isotope exchange method as illustrated in Fig. 13. The initial $^{18}\text{O}/^{16}\text{O}$ -fractionation for the mineral-water system is selected to be close to the assumed equilibrium. In contrast the initial $^{17}\text{O}/^{16}\text{O}$ -fractionation is chosen to be very different from the equilibrium value. In this way the change in the $^{17}\text{O}/^{16}\text{O}$ -fractionations monitor the extent of isotopic exchange, while $^{18}\text{O}/^{16}\text{O}$ -fractionations closely bracket the equilibrium value enabling accurate determination of its value. Using the three-isotope

Table 12. Experimental calibration methods for oxygen-containing mineral systems. (After Sheppard 1984)

Method	System	Remarks	Reference
1. Direct mineral-fluid exchange experiments	Calcite-H ₂ O Quartz-H ₂ O	Recrystallization evident	O'Neil et al. (1969) Clayton et al. (1972) Matsuhisa et al. (1979)
2. Direct mineral-mineral exchange	Quartz-K-feldspar Enstatite-basalt magma	Both minerals in common solution Exchange via O ₂ or CO ₂ 1250°–1500 °C	Blattner and Bird (1974) Muehlenbachs and Kushiro (1974)
3. Crystallization	Quartz-H ₂ O	Synthesis from silica gel restricted to very limited T-range	Clayton et al. (1972)
a) Gel	Muscovite-H ₂ O		O'Neil and Taylor (1969)
b) Glass	Jadeite-H ₂ O		Matthews et al. (1983a)
4. Polymorphic transformation	Calcite-H ₂ O Quartz-H ₂ O	Aragonite-calcite Cristobalite-quartz	Clayton (1959) Matsuhisa et al. (1979)
5. Synthesis			
a) Cation exchange	Albite-H ₂ O Muscovite-H ₂ O	K-feldspar + NaCl → Na Feldspar + KCl Paragonite + KCl → Muscovite + NaCl	O'Neil and Taylor (1967) O'Neil and Taylor (1969)
b) Complete	Muscovite-H ₂ O Magnetite-H ₂ O Magnetite-H ₂ O Quartz-H ₂ O	Kaolinite + KCl → Muscovite + HCl + H ₂ O FeCO ₃ + H ₂ O → Fe ₃ O ₄ + CO ₂ + H ₂ Fe ₂ O ₃ + H ₂ + (H ₂ O) → Fe ₃ O ₄ + H ₂ O Hydrothermal synthesis of silicic acid (265–465 °C) Fayalite + H ₂ O → Magnetite + quartz + H ₂ Calcite → high Mg-calcite → dolomite solution and reprecipitation	O'Neil and Taylor (1969) O'Neil and Taylor (1969) Bertenrath et al. (1973) Matthews and Beckinsale (1979) Downs et al. (1981) Matthews and Katz (1977)

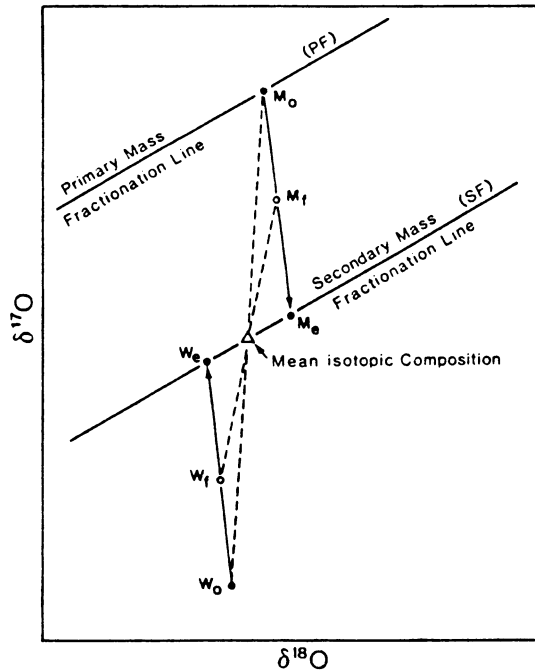


Fig. 13. Schematic diagram of the three-isotope exchange method. Natural samples plot on the primary mass fractionation line (*PF*). Initial isotopic compositions are mineral (M_0) and water (W_0) which is well removed from equilibrium with M_0 in $\delta^{17}\text{O}$, but very close to equilibrium with M_0 in $\delta^{18}\text{O}$. Complete isotopic equilibrium is defined by a secondary mass fractionation line (*SF*) parallel to *PF* and passing through the bulk isotopic composition of the mineral plus water system. Isotopic compositions of partially equilibrated samples are M_f and W_f and completely equilibrated samples are M_e and W_e . Values for M_e and W_e can be determined by extrapolation from the measured values of M_0 , M_f , W_0 , and W_f . (After Matthews et al. 1983a; Sheppard 1984)

technique Matthews et al. (1983a,b) provided a consistent set of temperature coefficients for silicate pairs (see Table 13).

For most minerals, the upper temperature limit of these experimental calibrations is around 700 °C. Mayeda et al. (1986) extended the experimental calibrations up to 1200 °C in dry systems, using calcite as the common exchange phase. Most of the experimentally determined equilibrium constants are in good agreement with the calculations of Kieffer (1982).

Isotope exchange reactions between minerals and fluids have been attributed to two major processes, diffusion and dissolution-precipitation. Available oxygen isotope data suggest that the exchange reactions

Table 13. Coefficient A for silicate-pair fractionations. (After Matthews et al. 1983a,b)

	Ab	Cc	Jd	Zo	An	Di	Wo	Mt
Qz	0.5	0.5	1.09	1.56	1.59	2.08	2.20	6.11
Ab	—	0.0	0.59	1.06	1.09	1.58	1.70	5.61
Cc	—	—	0.59	1.06	1.09	1.58	1.70	5.61
Jd	—	—	—	0.47	0.50	0.99	1.11	5.02
Zo	—	—	—	—	0.03	0.52	0.64	4.55
An	—	—	—	—	—	0.49	0.61	4.52
Di	—	—	—	—	—	—	0.12	4.03
Wo	—	—	—	—	—	—	—	3.91

$$(1000 \ln \alpha_{A-B} = \frac{A}{T^2} 10^6)$$

Abbreviations: Qz = quartz; Ab = albite; Cc = calcite; Jd = jadeite; Zo = zoisite; An = anorthite; Di = diopside; Wo = wollastonite; Mt = magnetite.

proceed in two steps, the first through surface controlled dissolution-precipitation reactions when the fluids and minerals are out of chemical equilibrium and when chemical equilibrium is attained through a diffusional mechanism (Matthews et al. 1983c; Cole et al. 1983). The most obvious general trend with respect to diffusion rates is the difference of several orders of magnitude between wet and dry conditions. Relatively high diffusion rates are observed in hydrothermal experiments probably due to lowering of the activation energies, whereas under dry conditions exchange rates are characterized by high activation energies and slow diffusion rates (Graham 1981; Freer and Dennis 1982, Dennis 1984; Giletti and Yund 1984).

2.3.3.2 Fractionations Due to Kinetic Processes

Oxygen isotope fractionations occurring during photosynthesis (Dole and Jenks 1944) and respiration (Lane and Dole 1956) are kinetic processes. This is discussed in more detail on p. 145.

2.3.3.3 Fractionations Due to Other Processes

Vapor Pressure Difference. Variations found in the isotopic composition of natural waters are due to vapor pressure differences. The light

isotopic component has a higher vapor pressure than the heavy one, as has already been discussed.

Hydration. Oxygen isotope fractionation occurs during the hydration of most ions. The distinction between the activity isotope ratio and the concentration isotope ratio of water is rarely made and is only of academic interest in dilute solutions, since the difference between these ratios is within the precision of the method. However, Feder and Taube (1952), Taube (1954), Sofer and Gat (1972), and Truesdell (1974) have reported significant deviations of the $^{18}\text{O}/^{16}\text{O}$ -activity ratio from the atom ratio of water in highly saline solutions. These effects have to be considered in the study of naturally occurring brines, such as oil field brines, hydrothermal solutions, and strongly evaporated water bodies, e.g., the Dead Sea.

2.3.4 Water-Rock Interaction

Oxygen isotope geochemistry is especially useful when applied to the study of water/rock interactions. The geochemical effect of such an interaction between water and rock or mineral is a shift of the oxygen isotope ratios of the rock and/or the water away from their initial values. Two end-member models can be considered:

1. Rock \gg water. In this case, the $\delta^{18}\text{O}$ -value of the rock remains unchanged and that of the fluid is modified. Examples are the positive $\delta^{18}\text{O}$ -shifts up to 15‰ observed in geothermal waters (for instance, Craig 1963).
2. Water \gg rock. The $\delta^{18}\text{O}$ -value of the rock is modified and that of the fluid remains constant. Examples are the effects observed in submarine weathered basalts which have interacted with an infinitely large reservoir of seawater.

Besides the water/rock ratio, the other factor which affects the oxygen isotope systematics is the temperature of alteration. These parameters can vary independently, and, therefore, it is difficult to assess the relative importance of these two variables. Water rock ratios have often been calculated from oxygen isotope analyses of whole rocks and fluid, using a simplified, closed-system, material balance calculation (Taylor 1974, 1977):

$$W/R = \frac{\delta_{\text{rock}f} - \delta_{\text{rock}i}}{\delta_{\text{H}_2\text{O}i} - (\delta_{\text{rock}f} - \Delta)}$$

where $\Delta = \delta_{\text{rock}f} - \delta_{\text{H}_2\text{O}f}$. This model requires adequate knowledge of both the initial (i) and final (f) isotopic states of the system.

The above model bases on closed-system conditions, which assume continuous recirculation and cyclic reequilibration of the water with the rock. However, some of the heated water will be lost from the system by escape to the surface. In the open system, in which each increment of water makes only a single pass through the rock, the water/rock is lower than under closed-system conditions (Taylor 1977, 1978).

The intergrated W/R ratio is given by the equation:

$$W/R = \log_e [W/R_{\text{closed system}} + 1] .$$

In Fig. 14 comparisons are made between the “closed” and “open” system for the two specific parameters 500° and 300 °C and a $\delta^{18}\text{O}_{\text{H}_2\text{O}}^i$ of -14‰.

In actual hydrothermal systems, the true 500 °C curve would lie between the two 500 °C curves plotted in Fig. 14, probably close to the right-hand curve, as the single-pass system is an unrealistic one. It should be noted that such models only give minimum values of W/R because appreciable water may move through fractures without exchanging (i.e., after the wall rocks next to the fractures have become already markedly depleted in ^{18}O).

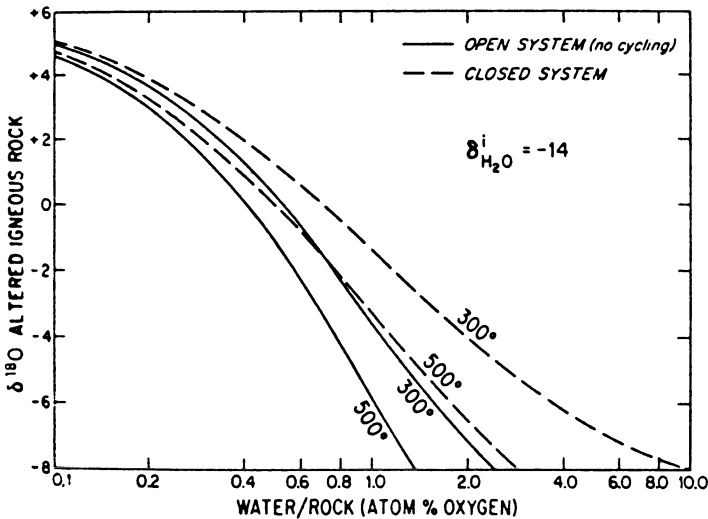


Fig. 14. $\delta^{18}\text{O}$ -values of altered igneous rocks the calculated water/rock ratios for open and closed system conditions, assuming initial values of $\delta_{\text{rock}}^i = +6.5$ and $\delta_{\text{H}_2\text{O}}^i = -14\text{‰}$ (Taylor 1978)

2.4 Sulfur

Sulfur has four stable isotopes with the following abundances (Mac-Namara and Thode 1950):

^{32}S : 95.02%

^{33}S : 0.75%

^{34}S : 4.21%

^{36}S : 0.02%

Sulfur is present in nearly all natural environments: as a minor component in igneous and metamorphic rocks, mostly as sulfides; in the biosphere and related organic substances, like crude oil and coal; in ocean water as sulfate and in marine sediments as both sulfide and sulfate. It may be a major component: in ore deposits, where it is the dominant nonmetal, and as sulfates in evaporites. These occurrences cover the whole temperature range of geologic interest. Sulfur is bound in various oxidation states, from sulfides to elemental sulfur, to sulfates. From these facts it is quite clear that sulfur is of special interest in stable isotope geochemistry.

Thode et al. (1949) and Trofimov (1949) were the first to observe wide variations in the abundances of sulfur isotopes. Today, variations on the order of 150‰ have been found, e.g., the “heaviest” sulfates have $\delta^{34}\text{S}$ -values greater than +90‰ and the “lightest” sulfides have δ -values of around -65‰. For a schematic diagram, see Fig. 15.

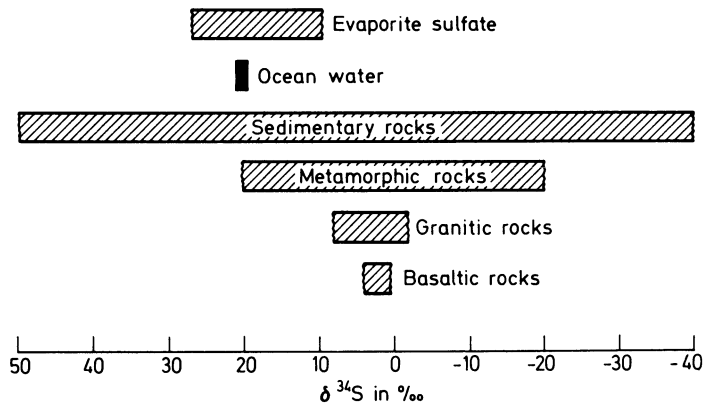


Fig. 15. $^{34}\text{S}/^{32}\text{S}$ ratios in some geologically important materials ($\delta^{34}\text{S}$ relative CD troilite)

The following papers have summarized the whole field or broader aspects of the naturally occurring variations: Thode (1970), Rye and Ohmoto (1974), Nielsen (1978, 1979), Ohmoto and Rye (1979).

2.4.1 Preparation Techniques

Some aspects concerning the chemical preparation of the various sulfur compounds have been discussed by Rafter (1957), Ricke (1964), and Robinson and Kusakabe (1975). The gas used in mass-spectrometric measurement is usually SO_2 . Puchelt et al. (1971) and Rees (1978) described a method using SF_6 which has some distinct advantages, because (1) it is without any memory effect and (2) fluorine is monoisotopic avoiding any correction of the raw data.

Pure sulfides are converted to SO_2 by reaction with an oxidizing agent, like CuO , Cu_2O , V_2O_5 , and O_2 . For any method used, it is particularly important to minimize the production of sulfur trioxide and sulfates. Combustions in vacuum with a solid oxidant minimize the presence of contaminant gases, particularly CO_2 , and purification of the SO_2 is often unnecessary.

For the extraction of sulfates and total sulfur a suitable solvent and reducing agent are needed. Thode et al. (1961) used a reducing agent which was a mixture of HCl , H_3PO_2 , and HJ . Tin(II)-phosphoric acid (Kiba solution) has been used by Sasaki et al. (1979). Sakai et al. (1978) and Ueda and Sakai (1983) described a method in which sulfate and sulfide disseminated in rocks are converted to SO_2 and H_2S , respectively. These authors showed that when sulfate and sulfide were attacked at 280°C under vacuum by dehydrated phosphoric acid containing stannous ions, both SO_2 and H_2S can be obtained separately, but simultaneously, from the same specimen.

2.4.2 Standard

The reference standard commonly used is sulfur from troilite of the Canon Diablo iron meteorite, while Russian investigators refer to troilite from the Sikhote Alin meteorite.

2.4.3 Fractionation Mechanisms

There are two types of reactions producing mainly the naturally occurring sulfur isotope variations:

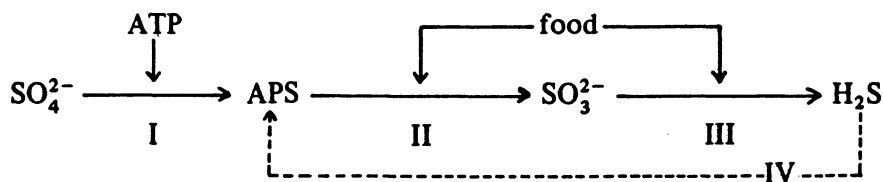
- a kinetic effect, during the bacterial reduction of sulfate to “light” H₂S, which gives by far the largest fractionations in the sulfur cycle;
- various chemical exchange reactions, e.g., between sulfate and sulfides, on the one hand, and between the sulfides themselves, on the other, where there is a definite order of concentrating ³⁴S.

1. The principal organisms which transform sulfate to H₂S are the sulfate-reducing bacteria belonging to the genera *Desulfovibrio* and *Desulfatovacuum*. These bacteria gain their energy for growth by coupling anaerobic oxidation of hydrogen and organic matter to the reduction of sulfate. Many of the environmental limitations on the sulfate-reducing bacteria were reviewed by ZoBell (1958) and are summarized in Table 14. A more recent review was given by Chambers and Trudinger (1979).

Table 14. Some environmental limits of sulfate-reducing bacteria (ZoBell 1958)

Factor	Limits
E _H	+350 to -500 mV
pH	4.2 to 10.4
Pressure	1 to 1000 atm
Temperature	0 to 100 °C
Salinity	< 1 to 30% NaCl

Harrison and Thode (1957a,b), Kaplan et al. (1960), Nakai and Jensen (1964), Kemp and Thode (1968), McCready et al. (1974), and McCready (1975) showed that fractionations of up to nearly 5% could be achieved in the laboratory under a variety of conditions. In the experiments cited above, such parameters as temperature, electron source, sulfate concentration, and bacterial population density are varied. The reaction chain during anaerobic sulfate reduction can be described schematically as follows:



ATP = Adenosine triphosphate, APS = Adenosine-5'-phosphosulfate. For more details, see Goldhaber and Kaplan (1974).

Under normal conditions the rate-controlling step is reaction II, that is the breaking of the first S—O bond. However, extremely low sulfate concentration or extraordinarily high food supply makes reaction I rate-controlling and brings the net fractionation to zero (Kemp and Thode 1968, McCready 1975).

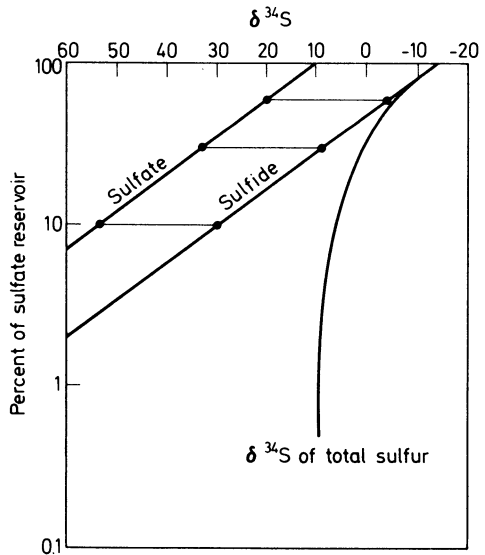
In contrast to the conditions in laboratory cultures, bacterial activity in natural environments is characterized by much slower growth rates and hence a much slower turnover of sulfur through the cells. Then reaction IV, the back reaction between the enzymatically bound sulfur species, may become important (Trudinger and Chambers 1973).

Two different model environments are representative for natural reduction of sulfate to sulfide:

a) The simplest model case is achieved in a body of stagnant water, which has become anoxic due to insufficient vertical mixing. Sulfate-reducing bacteria may grow rapidly under these conditions until the environment becomes poisoned due to H_2S production. Typical examples are the Black Sea and local oceanic deeps. In all these cases, the H_2S is extremely depleted in ^{34}S , while the sulfate consumption and change in $\delta^{34}\text{S}$ remain negligible (open-system environment, see also p. 182).

b) When H_2S is continually extracted from the system, for instance, by degassing or by precipitation of iron sulfide, the bacteria continue to reduce sulfate until no more food or sulfate is available. The extraction of the light sulfur isotope from the system changes the observed δ -patterns drastically following the Rayleigh equation, given on p. 10–11: the $\delta^{34}\text{S}$ of the residual sulfate increases with decreasing sulfate concentration and, consequently, the H_2S produced at a later stage also exhibits “heavier” $\delta^{34}\text{S}$ -values. The change in $\delta^{34}\text{S}$ of residual sulfate and of produced H_2S with decreasing sulfate concentration follows the relation shown in Fig. 16. The curves indicate that extremely heavy sulfate may be found in the final stage of bacterial activity in a “closed-system” environment.

Fig. 16. Variations of $\delta^{34}\text{S}$ -values of sulfide-produced and residual sulfate in a closed system (Rayleigh-type fractionation). Assumed fractionation factor: 1.025, assumed starting composition of sulfate +10‰



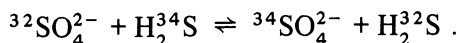
Besides the respiratory sulfate reduction other biological sulfur isotope fractionations occur in nature. Comparatively little is known on isotope effects associated with sulfur-oxidizing organisms. Fry et al. (1986) summarized the recent literature and demonstrated that isotope effects associated with bacterial oxidation of inorganic sulfur compounds are small.

During assimilation of sulfate by microorganisms, plant and animals sulfur isotope fractionation is in the range of -2 to -3‰ (Kaplan 1983). This is similar to the small effect measured during nitrogen fixation (Delwiche and Steyn 1970), but is in marked contrast to assimilated carbon, where a considerable ^{12}C -enrichment occurs. In the case of sulfur and nitrogen, fractionation only occurs in the initial activation step. Once sulfate or nitrogen has been transferred into the cell, it is completely reduced to the protein.

2. Under low temperature conditions ($T < 50\text{ }^\circ\text{C}$) bacterial activity seems to be the only mechanism for the reduction of sulfate. However, at appreciably higher temperatures ($> 250\text{ }^\circ\text{C}$) sulfate will be reduced to H_2S by reactions with Fe^{2+} components in rocks (Ohmoto and Rye 1979). Such a process is an important mechanism in environments where circulation of ocean water through hot volcanic rocks is established.

At these relatively high temperatures ($> 250\text{ }^\circ\text{C}$) probably isotopic equilibrium seems to be established between sulfate and hydrogen sul-

vide. The isotope exchange between sulfate and sulfide may be written:



The theoretical value for the exchange reaction is $\alpha \approx 1.075$ at 25 °C (Tudge and Thode 1950). Therefore, if this exchange takes place, although no mechanism is yet known, it should lead to sulfides being depleted in ^{34}S by up to 75‰ relative to sulfates. Sakai (1957) has extended this calculation up to temperatures of 1000 °C. Thode et al. (1971) have measured the equilibrium constant K between SO_2 and H_2S in the temperature range 500° to 1000 °C and compared the results with theoretical calculations. Robinson (1973) measured the fractionation between H_2S and HSO_4^- and found fractionation factors slightly lower than Sakai's theoretical values. Sakai (1957) first suggested that isotope fractionation between different metallic sulfides would bring about a slight variation in the isotope ratios during their deposition. Theoretical studies of fractionations between sulfides have been done by Sakai (1968) and Bachinski (1969), who reported the reduced partition function ratios and the bond strength of sulfide minerals and their relationship to isotope fractionation. Similar to oxygen in silicates, a relative order of ^{34}S -enrichment in coexisting sulfide minerals can be arranged (Bachinski 1969; Table 15).

Instead of directly comparing the equations for the fractionation factors suggested by various investigators, Ohmoto and Rye (1979) critically examined all the available experimental raw data in terms of (1) attainment of equilibrium, (2) uncertainties in the measurements, (3) minimum or maximum fractionation factors when equilibrium was not attained, and (4) compatibility with the fractionation factors

Table 15. Equilibrium isotope fractionation factors of important sulfides with respect to H_2S . The temperature dependence is given by the equation $10^3 \ln \alpha = A/T^2 + B$. (After Ohmoto and Rye 1979)

Mineral	Chemical composition	A
Molebdenite	MoS_2	0.45
Pyrite	FeS_2	0.40
Sphalerite	ZnS	0.10
Pyrrhotite	FeS	0.10
Chalcopyrite	CuFeS_2	-0.05
Covelline	CuS	-0.40
Galena	PbS	-0.63
Chalcosite	Cu_2S	-0.75
Argentite	Ag_2S	-0.80

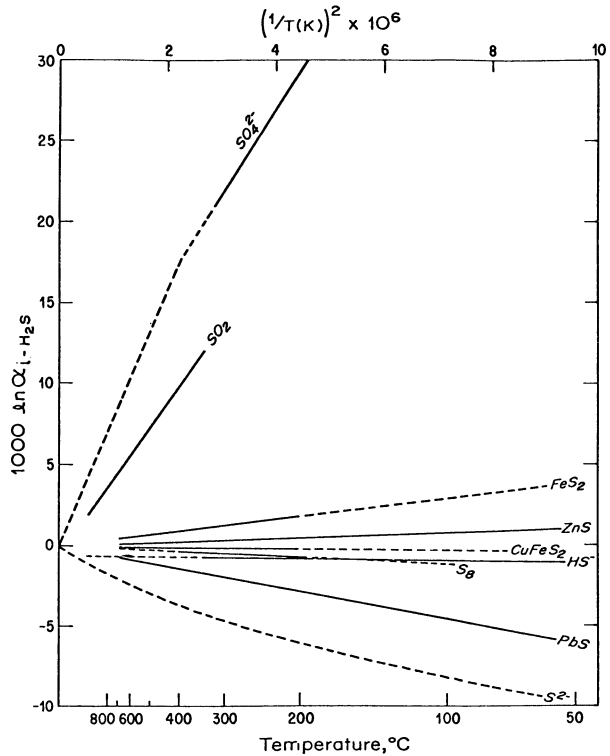


Fig. 17. Equilibrium fractionation factors among sulfur compounds relative H_2S (solid lines experimentally determined, dashed lines extrapolated or theoretically calculated) (Ohmoto and Rye 1979)

estimated from other sets of experiments. Figure 17 and Table 15 give a summary of what Ohmoto and Rye (1979) believe to be the best fractionation factors relative to H_2S .

3. As already mentioned in Sect. 2.1 both hydrogen and oxygen isotopic compositions of residual water may become heavier during the passage through clay-rich sediments (ultrafiltration). A similar phenomenon was observed by Nriagu (1974) on $\delta^{34}S$ -values of sulfate in solution. He demonstrated that ^{32}S was preferentially absorbed into sediments and the remaining sulfate was enriched in ^{34}S up to 6‰. The fractionation factor was dependent on the sulfate concentration in the solution and on the amount of sulfate absorbed in the sediment. This process could play an important role for the sulfur isotopic composition in formation and connate waters.

2.4.4 Experimental Determination of Sulfide Systems

In the last years more and more experimental determinations of the distribution of sulfur isotopes in sulfides under "hydrothermal" conditions have become available. Some of the more recent investigations are those by Kiyosu (1973), Czamanske and Rye (1974), and Hubberten (1980).

Two essentially similar approaches have been used. One approach is to have both sulfides present in the equilibrium vessel but to keep them physically separated and to effect isotope exchange between them via transport of sulfur vapor. The second approach uses hydrothermal solutions instead of a gas phase. The problem involved in this technique comes from the difficulties involved in the exchange reactions between a mineral pair.

The experimental determinations of equilibrium constants performed so far do not agree very well with each other. For example, sulfur fractionations in sphalerite-galena pairs can vary considerably depending on which experimental curve is used. For a fractionation of 2‰ the calculated temperatures from the three experimental curves are $319^{\circ} \pm 15^{\circ} \text{C}$ (Czamanske and Rye 1974), $286^{\circ} \pm 19^{\circ} \text{C}$ (Grootenboer and Schwarcz 1969), and $360^{\circ} \pm 30^{\circ} \text{C}$ (Kajiwara and Krouse 1971). Rye (1974) has argued that the Czamanske and Rye (1974) curve gives the best agreement with filling temperatures of fluid inclusions over the temperature range from 370° to 125°C . Mineral pairs may give geologically reasonable temperatures as long as the two minerals were formed in equilibrium with the ore-bearing solution which in turn was uniform in temperature and in physicochemical conditions such as f_{O_2} and p_{H} . Sphalerite-galena pairs in many deposits give reasonable temperatures even when these minerals are not contemporaneous, suggesting that during the deposition of sphalerite and galena the conditions have not changed very much. Examples for which galena-sphalerite pairs agree well with the filling temperatures of fluid inclusions have been reported from Providencia (Mexico), Casapalca (Peru), and Creede (Colorado, USA) by Rye (1974). With the sphalerite-galena pair temperatures can be determined to within $\pm 40^{\circ} \text{C}$, even taking into account the uncertainty in the calibration curves. This sulfur isotope geothermometer is especially useful on massive or metamorphosed ore deposits where other methods such as filling temperatures in fluid inclusions fail.

Pyrite-galena pairs, on the other hand, are not very suitable for a temperature determination, because pyrite often seems to precipitate over larger portions of ore deposition than galena and the chemistry of the solutions and the temperature might have changed considerably over this period.

2.5 Selenium

Because selenium is, to some extent, chemically similar to sulfur, one might expect to find some analogous fractionations of the selenium isotopes in nature.

Six stable selenium isotopes are known with the following abundances:

^{74}Se : 0.87% ^{78}Se : 23.52%

^{76}Se : 9.02% ^{80}Se : 49.82%

^{77}Se : 7.58% ^{82}Se : 9.19%

$^{82}\text{Se}/^{76}\text{Se}$ ratios have been determined by Krouse and Thode (1962), Rees and Thode (1966), and Rashid et al. (1978). Selenium is extracted in its elemental form from natural samples and then fluorinated to SeF_6 which is introduced into the mass spectrometer.

From theoretical calculations Krouse and Thode (1962) deduced that ^{76}Se and ^{82}Se differ in their chemical properties to the extent that isotope fractionations up to 60‰ are predicted for $^{76}\text{Se}/^{82}\text{Se}$ exchange processes, provided that mechanisms are available for such exchanges.

In this connection it is interesting to note that in addition to sulfate-reducing bacteria, other anaerobic bacteria are known to reduce selenates and selenites. Rashid et al. (1978) showed that numerous organisms fractionate selenium isotopes during SeO_3^{2-} reduction. For instance, six different *Salmonella* species were found to reduce $^{76}\text{SeO}_3^{2-}$ faster than $^{82}\text{SeO}_3^{2-}$ with $\delta^{82}\text{Se}$ values ranging from -5‰ to -40‰.

2.6 Nitrogen

More than 99% of the known nitrogen on or near the earth's surface is present as atmospheric N_2 or as dissolved N_2 in the ocean. Only a

minor amount is combined with other elements, mainly C, O, and H. Nevertheless, this small part plays a decisive role in the biological world. Since nitrogen occurs in various oxidation states and in gaseous, liquid, and solid forms, it is a highly suitable element for the search of natural variations in its isotopic composition.

Nitrogen consists of two stable isotopes, ^{14}N and ^{15}N . Atmospheric nitrogen, determined by Nier (1950), has the following composition:

^{14}N : 99.64%

^{15}N : 0.36%

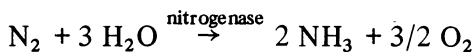
Much progress has been achieved during the last years concerning nitrogen isotope geochemistry (Sweeney et al. 1978; Letolle 1980; Kaplan 1983). One important application is the problem whether it is possible to distinguish fertilizer nitrogen from compounds of natural origin. Artificial fertilizers are systematically depleted in ^{15}N compared with soil organic matter due to their synthesis from air. Therefore, one might expect that $\delta^{15}\text{N}$ -values of cultivated soil organic matter may show a shift towards lighter values. So far, none of the detailed studies in progress have confirmed this shift (Letolle 1980).

Preparation procedures have been described by Bremner and Keeney (1966) and Ross and Martin (1970). The conversion of organic nitrogen is done by the Kjeldahl procedure. Nitrate is reduced to ammonium and then oxidized to N_2 by the use of lithium hypobromide. Overall analytical precision can be better than $\pm 0.2\text{‰}$.

As has been mentioned earlier, isotope ratios are measured in the form of N_2 . The standard gas used is atmospheric nitrogen (Mariotti 1983). It is imperative that N_2 be free of carbon monoxide, which gives an interfering peak in the mass spectrum.

Basic biochemical reactions of nitrogen are:

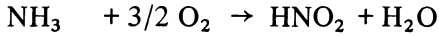
1. Nitrogen Fixation



In the nodules of the roots of plants many bacteria can convert molecular nitrogen into nitrogen compounds. However, the high energy needed to break molecular nitrogen makes natural nitrogen fixation a very inefficient process.

2. *Nitrification*. When organic matter decays in the soil, bacteria utilize the complex nitrogen-containing molecules to form ammonia, which is

oxidized by nitrifying bacteria first to NO_2^- and subsequently to NO_3^- . Conversion of ammonia into nitrate can thus be written as:



Bacteria such as *Nitrosomonas* can accomplish the first oxidation while *Nitrobacter* the second. Under normal aerobic conditions, nitrate is the most common form of combined nitrogen in the ocean. Nitrate can be utilized by vascular plants.

3. Denitrification. Denitrification by organisms such as *Pseudomonas denitrificans* or *Thiobacillus denitrificans* results in the conversion of nitrate to nitrogen gas and seems to be the only significant mechanism to convert combined nitrogen into N_2 . Denitrification takes place in poorly aerated soil and in stratified anaerobic water bodies. Denitrification supposedly balances the natural fixation of nitrogen. If it did not occur atmospheric nitrogen would be exhausted in less than 100 million years.

A model for denitrification may involve two consecutive steps:

- a) Uptake of substrate into the cell with little or no isotope fractionation.
- b) Reduction of the substrate with breaking of an N–O bond which produces a large isotope effect. It is generally agreed that biological denitrification occurs as the following reaction sequence $\text{NO}_3^- \rightarrow \text{NO}_2^- \rightarrow \text{NO} \rightarrow \text{N}_2\text{O} \rightarrow \text{N}_2$. The denitrification step $\text{NO}_2^- \rightarrow \text{N}_2\text{O}$ was investigated by Mariotti et al. (1982). The fractionation factor changed from 10 to 30‰, the largest values were obtained under lowest reduction rates. Generally, the same factors that influence isotope fractionations during bacterial sulfate reduction are also operative during bacterial denitrification.

The fractionation factors for the three main processes involved in biogenic utilization are summarized in Table 16. As Table 16 demonstrates, isotope fractionations during nitrogen fixation are small compared to bacterial nitrification and denitrification. Equilibrium processes are ammonia volatilization from ammonia ion and the solution of nitrogen gas. The first process only seems to have a significant isotope effect.

Since in igneous rocks the main source of nitrogen seems to be present as ammonium, temperature dependence of the $\text{NH}_4^+ - \text{NH}_3$ isotope exchange reaction is of great importance. Experimental data by

Table 16. Nitrogen isotope fractionation factors for the major biological processes occurring in nature [calculated fractionation factors among gaseous nitrogen compounds by Richet et al. (1977) are excluded]

<i>Kinetic Isotope Effects</i>				
Nitrogen fixation	Atm. $N_2 \rightarrow$ fixed nitrogen	$\alpha = 1.000$	Hoering and Ford (1960)	
		$\alpha = 1.004$	Delwiche and Steyn (1970)	
Nitrification	$NH_4^+ \rightarrow NO_2^-$	$\alpha = 1.02$	Miyake and Wada (1971)	
		$\alpha = 1.035$	Mariotti et al. (1981)	
Denitrification	$NO_3^- \rightarrow N_2$	$\alpha = 1.02$	Miyake and Wada (1971)	
			Wellmann et al. (1968)	
		$\alpha = 1.01-1.03$	Delwiche and Steyn (1970) Mariotti et al. (1982)	
<i>Equilibrium Isotope Effects</i>				
Ammonia volatilization	$NH_4^+(aq) \rightleftharpoons NH_3(g)$	$25^\circ C$	$\alpha = 1.034$	Kirschenbaum et al. (1947)
Solution of nitrogen gas	$N_2(soln.) \rightleftharpoons N_2(g)$	$0^\circ C$	$\alpha = 1.00085$	Klots and Benson (1963)

Nitzsche and Stiehl (1984) indicate fractionation factors of 1.0143 at 250° and of 1.0126 at $350^\circ C$.

Other fractionation effects affecting the ammonium ion may be ion exchange in soils. Delwiche and Steyn (1970) studied the fractionation between aqueous solution and kaolinite clays, however, a general conclusion on the efficiency of this process in natural systems cannot yet be made.

Still another process causing isotope fractionations might be diffusional migration of natural gas. Stahl et al. (1977) concluded that migration of nitrogen within porous rocks results in decreasing ^{15}N -contents with increasing migration distance. Into the same direction point the large differences found in mantle-derived rocks, which may be explained by differential degassing of mantle nitrogen. This point will be discussed later on p. 85.

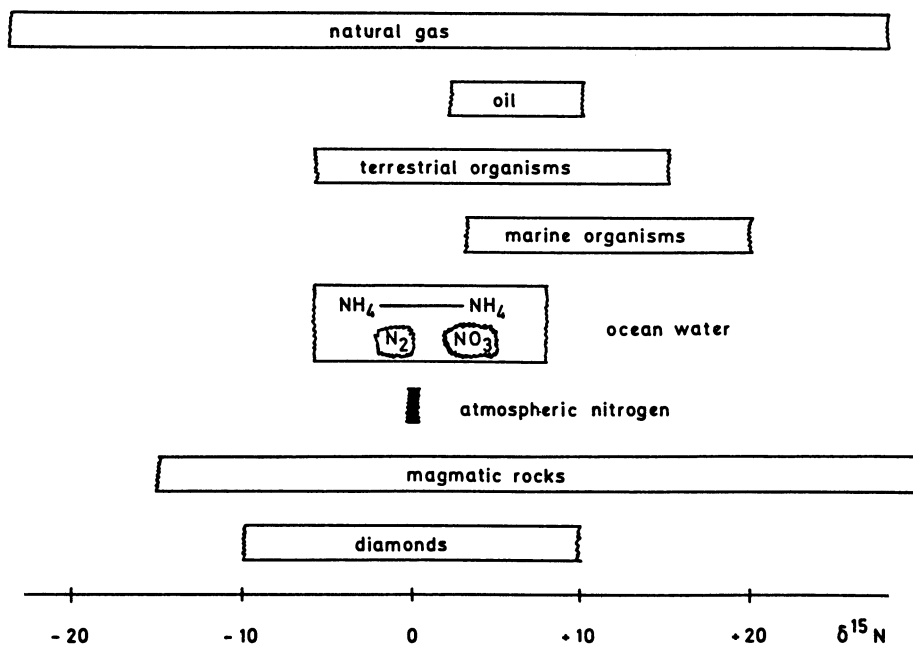


Fig. 18. $^{15}\text{N}/^{14}\text{N}$ ratios of some geologically important nitrogen compounds ($\delta^{15}\text{N}$ relative atmospheric nitrogen)

These various fractionation mechanisms lead to considerable differences in $^{15}\text{N}/^{14}\text{N}$ ratios of natural substances (see Fig. 18).

2.7 Silicon

Silicon has three stable isotopes with the following abundances (Bainbridge and Nier 1950):

^{28}Si : 92.27%

^{29}Si : 4.68%

^{30}Si : 3.05%

We might expect small fractionations, small, because there are no redox reactions: Si is always bound to oxygen. Furthermore, no geologically important gaseous silicon compound is known and the liquid components are of minor importance.

Douthitt (1982) has summarized the literature data and added 132 measurements on terrestrial materials. The total variation range is

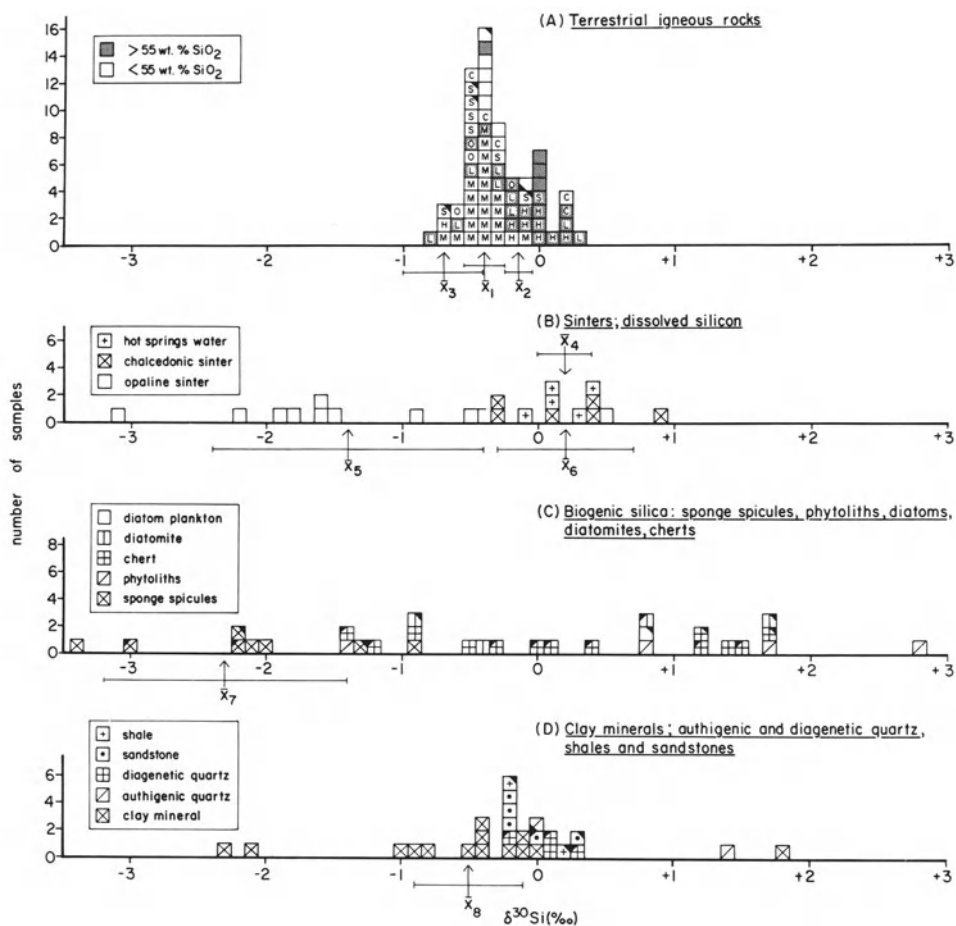


Fig. 19. Histogram of $\delta^{30}\text{Si}$ -values for various terrestrial samples ($\delta^{30}\text{Si}$ -values relative CalTech Rose Quartz Standard) (Douthitt 1982)

6.2‰ (see Fig. 19). However, $\delta^{30}\text{Si}$ -values show little variation (1.1‰) in igneous rocks and minerals. Coexisting minerals exhibit small, systematic, silicon isotope fractionations. In a general way $\delta^{30}\text{Si}$ increases with the silicon contents of igneous rocks and minerals. Relatively large fractionations occur in opaline sinters, biogenic opal, clay minerals, and authigenic quartz. A kinetic isotope fractionation of $\sim 3.5\%$ has been postulated by Douthitt (1982) to occur during the low precipitation of opal and possibly, poorly ordered phyllosilicates. This fractionation coupled with a Rayleigh precipitation model is capable of explaining most nonmagmatic $\delta^{30}\text{Si}$ -variations.

2.8 Boron

Boron has two stable isotopes (Bainbridge and Nier 1950):

^{10}B : 18.98%

^{11}B : 81.02%

Boron is well known to be a highly mobile element geochemically and, therefore, variations in its isotopic composition might be expected. The large relative mass difference between ^{10}B and ^{11}B (only hydrogen and oxygen have larger relative mass differences) and large chemical isotope effects (Bigeleisen 1965) make boron a very promising element to look for isotope variations. Because boron is difficult to handle in mass-spectrometric measurements, data on boron isotope variations, reported in the past, partly contradict each other. However, recent studies by Spivack and Edmond (1986) and Swihart et al. (1986) obviously have overcome these experimental difficulties, thus a renewed interest in boron isotope variations is expected for the very near future.

Since earlier studies by Schwarcz et al. (1969) it is well known that there is a tremendous kinetic isotope effect during the absorption of dissolved ^{10}B onto clay minerals. The magnitude of this isotope effect depends on the specific clay minerals, the solution temperature, and the boron concentration. This isotope effect is thought to be responsible for the observed ^{11}B -enrichment of ocean water by about 4% relative to crustal material. It is also reflected in marine and nonmarine evaporite borates (Swihart et al. 1986). Thus, it should be possible to use boron isotopic compositions as a tracer for boron of marine origin.

Spivack (1985) demonstrated that the mean $\delta^{11}\text{B}$ of unaltered mid-ocean ridge basalts is $-3.6 \pm 0.5\text{‰}$ relative to NBS 951 Boric Acid Standard. Altered basalts have $\delta^{11}\text{B}$ -values between 0 and 9‰. Hydrothermal solutions from midoceanic ridges fall on a mixing line between ocean water and fresh basalt (Spivack 1985).

As shown by Kanzaki et al. (1979) the boron isotopic composition of high-temperature fumarolic products should be closely related to that of the parent magma. Based on such fumarolic products, Nomura et al. (1982) proposed an average andesite value of about 6‰ for Japanese island arc rocks.

2.9 Chlorine

Chlorine has two stable isotopes with the following abundances (Boyd et al. 1955):

^{35}Cl : 75.53%

^{37}Cl : 24.47%

Older measurements by Hoering and Parker (1961) reported no detectable differences in the isotopic composition lying outside the analytical precision. By using methyl chloride as the gas being introduced into the mass spectrometer, Kaufmann et al. (1984) reported isotopic variations up to 1.3‰ in natural chlorides. Dissolved chloride in groundwaters shows both enrichment and depletion with respect to seawater chloride. Kaufmann et al. (1984) suggested that variations in the chlorine isotope ratio may be significant in diffusion-controlled systems. And, indeed, Desaulniers et al. (1986) observed a preferential upward diffusion of ^{35}Cl relative to ^{37}Cl in slow flowing groundwater systems.

In brines from deep aquifers Kaufmann et al. (1986) observed a positive correlation between $\delta^{37}\text{Cl}$ -values and chloride concentrations. They suggested that diffusion processes may be responsible for this apparent relationship.

2.10 Calcium

Isotopic variations of the alkali and alkaline earth elements have been reported in the literature, however, the results are often contradictory and will not be repeated here. We are still unable to give a well-defined picture of the possible naturally occurring differences. Calcium is the only element which has been recently analyzed with a sophisticated technique (Russel et al. 1978). Calcium has six stable isotopes in the mass range of 40 to 48 with the following abundances (Bainbridge and Nier 1950).

^{40}Ca : 96.97%

^{42}Ca : 0.64%

^{43}Ca : 0.145%

^{44}Ca : 2.06%

^{46}Ca : 0.0033%

^{48}Ca : 0.185%

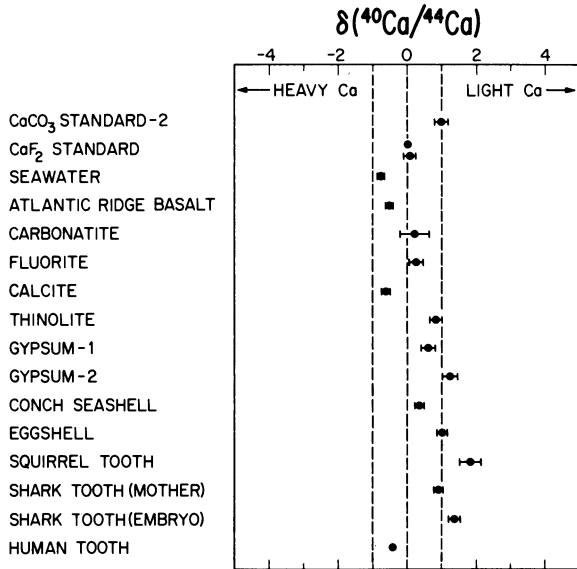


Fig. 20. ⁴⁰Ca/⁴⁴Ca ratios of some terrestrial samples [δ -values relative to a CaF₂ standard (Russell et al. 1978)]

Due to the large mass difference between ⁴⁰Ca and ⁴⁸Ca (the percent mass difference is the next highest after ²H and ¹H) and due to the low abundance of all Ca isotopes other than ⁴⁰Ca, Ca isotope abundance measurements are especially subjected to instrumental fractionation effects. By using a double-spike technique and by using a mass-dependent law for correction of instrumental mass fractionation Russell et al. (1978) were able to demonstrate that differences in the ⁴⁰Ca/⁴⁴Ca ratio are clearly resolvable to a level of 0.5‰. Russell et al. (1978) found (1) no samples which have Ca fractionated by more than 2.5‰, (2) meteorites, lunar, and terrestrial samples show the same small range of ⁴⁰Ca/⁴⁴Ca, and (3) small Ca isotope fractionations (~2.5‰) are definitely present in nature. Ca of biological origin does not show fractionation effects larger than observed for nonbiogenic samples. In Fig. 20 the variation range for the terrestrial samples analyzed by Russell et al. (1978) are given.

Chapter 3 Variations of Stable Isotope Ratios in Nature

3.1 Extraterrestrial Materials

3.1.1 Meteorites

Formerly, it was generally agreed that the initial material of the solar system was isotopically homogeneous, but in recent years it has become quite clear that this is not the case. Traces of presolar matter, which have survived in some primitive meteorites, can be recognized by their anomalous isotopic composition, which lies outside the range normally found on the earth and in the solar system. Shima (1986) has summarized the extremes of isotopic variations in extraterrestrial materials.

During the past few years tremendous progress has been achieved in this field. A recent summary of the vast amount of new data has been presented by Pillinger (1984). For carbon and nitrogen isotope studies this success is partly due to the introduction of a new mass-spectrometric measurement technique similar to that used for noble gas techniques, namely the static mass spectrometer. Details for the experimental procedure were published by Gardiner and Pillinger (1979). With this technique sensitivities at the nanogram and even the picogram level are possible with precisions of the order $\pm 1\%$ or even better (Wright et al. 1983). A limitation of the static method is that it is not immediately applicable to hydrogen, oxygen, and sulfur because of instrument background, sample degradation, or adsorption problems.

In meteorites and other extraterrestrial materials a totally new class of isotope effects has to be considered, namely isotope fractionation due to spallogenic effects. This includes all effects caused by the interaction of primary and secondary particles, for example, protons, neutrons, α -particles, and mesons from both galactic radiation and solar cosmic radiation. The reaction products of such elemental interactions with cosmic particles cover the total range in mass number up to, and even slightly above, those of the target elements themselves and they

are characterized by an approximately equal production rate for the different isotopes of a given element. Consequently, a spallogenic admixture manifests itself most pronouncedly in an enhanced abundance of the rare isotopes.

3.1.1.1 Oxygen

It was the work of Clayton et al. (1973a) on oxygen isotope variations in carbonaceous chondrites which caused a revision of theories regarding solar system formation. Once oxygen isotope anomalies had been discovered, attempts to characterize them and to establish the extent of their occurrence followed by the Chicago group. Excess ^{16}O occurs in all samples of carbonaceous chondrites (C2, C3, and C4) (Clayton et al. 1976, 1977, Clayton and Mayeda 1984; see Fig. 21). Almost 5% excess ^{16}O was found in spinel, pyroxene, and sometimes olivine, smaller amounts of about 1% in melilite, feldspars, and grossular. Clayton et al. (1977) proposed that the first material condensing from the solar nebula had an oxygen isotope composition of $\delta^{18}\text{O} - 40$ and $\delta^{17}\text{O} - 43\text{‰}$. The initial condensates later underwent a partial exchange close to the terrestrial fractionation.

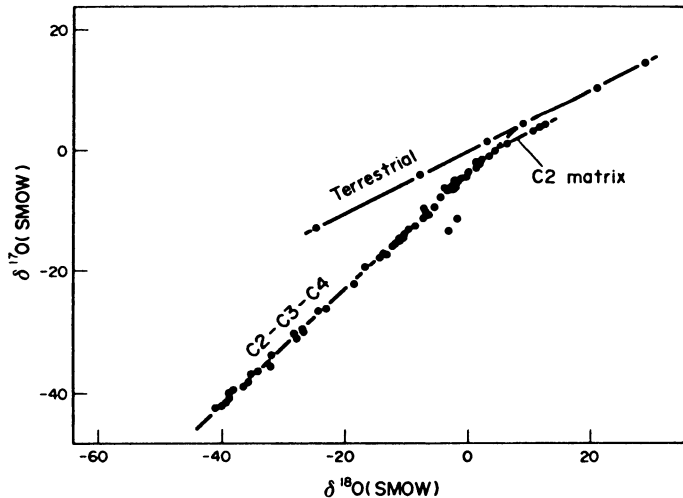


Fig. 21. Three isotope plots for terrestrial samples and some anhydrous phases in C2, C3, and C4 carbonaceous chondrites. The maximum observed ^{16}O excess is 5% (Clayton et al. 1977)

The supposition that measurement of three isotopes can distinguish between nuclear and chemical/physical fractionation effects was questioned by Thiemens and Heidenreich (1983), who found a mass-independent fractionation process during the photochemical dissociation of ozone. The mechanism postulated for the dissociation process also works with other gases such as CO_2 , however, it may, of course, be irrelevant with respect to understanding the internal isotopic systematics in meteorites.

Whatever the cause of ^{16}O -isotope variations in meteorites might be, their presence has permitted a classification into seven categories (Clayton and Mayeda 1978). In the order of increasing ^{16}O -contents, they are: (1) L and LL chondrites; (2) H chondrites, (3) E chondrites and aubrites; (4) eucrites, howardites, and diogenites; (5) ureilites; (6) C2 carbonaceous chondrites hydrous matrix; (7) C2, C3, and C4 carbonaceous chondrites anhydrous minerals.

These characteristic ^{18}O -contents are obviously due to the different oxygen isotope compositions of the parent bodies from which the different types of meteorites were derived. There is a peculiar group of achondrites, the so-called SNC meteorites, which are considered to have originated from a large planet, perhaps Mars. Clayton and Mayeda (1983) demonstrated that the SNC achondrites and eucrites each have characteristic oxygen isotope compositions being near the terrestrial isotope composition. The two groups could not have been derived from the same oxygen reservoir and thus probably had different parent bodies.

Clayton and Mayeda (1978) have tried further to relate the above groups to the various iron meteorite classes through the oxygen isotope analysis of minor oxygen-bearing phases in iron meteorites. The aim is to elucidate the genetic links between stones and irons which could have been originally part of the same planetary body.

3.1.1.2 The Volatiles Hydrogen, Carbon, Nitrogen

Before considering the wealth of information currently being obtained from the analysis of individual components, the bulk isotopic composition of carbonaceous chondrites is briefly discussed. Kerridge (1985) analyzed δD , $\delta^{13}\text{C}$, and $\delta^{15}\text{N}$ -values for 26 carbonaceous chondrites and mainly confirmed the ranges observed by earlier workers. In addition, Kerridge (1985) could demonstrate that several chondrites reveal

unusual compositions which are not only useful for classification of carbonaceous chondrites, but also strengthen the conclusion that some specimens such as Al Rais and Renazzo are clearly different from other carbonaceous chondrites.

One of the basic questions in the interpretation of meteoritic δD , $\delta^{13}C$, and $\delta^{15}N$ -values is the distinction of nuclear from mass-dependent processes. By using stepwise combustion techniques Kerridge (1983) observed systematic patterns of isotopic heterogeneity for H, C, and N in the insoluble organic fraction from the Orgueil and Murray carbonaceous chondrites. The insoluble organic matter contains a number of components with distinct origins, either nucleogenetic or chemical, or both, which were mixed together with little or no equilibration. Kerridge's data cannot be reconciled with a single mass fractionation process acting upon a single precursor composition.

Hydrogen. Considerable efforts have been undertaken in recent years to analyze D/H ratios in meteoritic materials (Robert et al. 1978, 1979a,b; Kolodny et al. 1980; McNaughton et al. 1981, 1982; Becker and Epstein 1982; Robert and Epstein 1982; Fallick et al. 1983; Kerridge 1983; Yang and Epstein 1983).

The D/H ratio of our solar system cannot be obtained directly from a study of the sun, because deuterium is most easily destroyed in thermonuclear reactions. Therefore, the analysis of meteorites is the next best choice, especially of primitive chondrites. In these meteorites hydrogen is bound in hydrated minerals and in organic matter. The most exciting result from these studies is that exceptional deuterium enrichments occur - up to a δD -value of 10000‰ (Yang and Epstein 1983) - in special deuterium-carrier phases associated with the organic matter. Pillinger (1984) suggested that ion-molecule reactions which seem to operate independently of temperature appear to be the only feasible fractionation mechanisms to be responsible for the extreme deuterium enrichments in the organic matter. The δD -values in the phyllosilicates of carbonaceous chondrites are relatively constant at about 110‰ (Yang and Epstein 1982).

Carbon. The $^{12}C/^{13}C$ -ratio varies greatly in stars from 4 to > 100 in late-type stars and even the mean interstellar ratio of 60 ± 8 or 67 ± 19 (Penzias 1980) differs appreciably from the terrestrial ratio of 89. Thus, exotic carbon in meteorites should be easily recognizable by its anomalous isotopic ratio. In a direct search for exotic carbon Swart et al.

(1983) measured several carbonaceous chondrites enriched in anomalous noble gases. The Murchison and Allende chondrites contain up to 5 ppm C that is enriched in ^{13}C by up to 1100‰. The $^{12}\text{C}/^{13}\text{C}$ -ratio is approximately 42 compared to 89 for terrestrial carbon.

Part of the carbon isotope variation of the total carbon in carbonaceous chondrites ($\delta^{13}\text{C}$ -values from -30 to +65‰) is related to the presence of ^{13}C -enriched carbonate. The ^{13}C -enrichment in the carbonate has been attributed to kinetic isotope effects in Fischer-Tropsch-type reactions in the formation of organic compounds in these meteorites (Lancet and Anders 1970). Yuen et al. (1984) have questioned the Fischer-Tropsch model on the ground that individual hydrocarbons (C_1 to C_5) of increasing molecular weight show decreasing ^{13}C -abundances as might be expected for a kinetically controlled process rather than thermochemical equilibrium. Higher molecular weight alkanes (greater than C_{17}) follow the opposite trend which implies that they were produced by cracking (Gilmour and Pillinger 1983).

Using stepped heating techniques to resolve contamination and to distinguish between different carbon phases, Carr et al. (1983), Grady et al. (1983), and Grady et al. (1985) demonstrated consistent carbon isotope patterns for ordinary chondrites, enstatite chondrites, and ureilite achondrites which have aided in establishing intergroup/class relationships.

Nitrogen. ^{14}N and ^{15}N are synthesized in two different astrophysical processes: ^{14}N during hydrostatic hydrogen burning and ^{15}N during explosive hydrogen and helium burning (Prombo and Clayton 1985). Thus, it can be expected that nitrogen should be isotopically heterogeneous in interstellar matter.

What was considered by Kaplan (1975) to be a wide range of ^{15}N -values in meteorites has continuously expanded (Kung and Clayton 1978; Robert and Epstein 1980, 1982; Grady et al. 1983; Lewis et al. 1983; Prombo and Clayton 1985). The lowest $\delta^{15}\text{N}$ -value directly measured so far, is -326‰ in a fraction of an Allende acid residue (Lewis et al. 1983), the highest $\delta^{15}\text{N}$ -value is 973‰ in a whole-rock sample of the stony-iron meteorite of Bencubbin (Prombo and Clayton 1985). Two possibilities exist to explain the ^{15}N -enrichments: either by extreme chemical or photochemical fractionation processes, which would require very low temperatures below 40 K in a presolar molecular cloud or by nucleosynthetic reactions, which would require failure of homogenization in nova explosions (Prombo and Clayton 1985).

There are three groups of rare achondrites, the so-called SNC meteorites, which differ from other achondrites. It has been suggested that these meteorites may have originated on Mars. This idea has been supported by Becker and Pepin (1984), who found a nitrogen component trapped in a glass inclusion, but not present in the surrounding basaltic matrix, with a $\delta^{15}\text{N}$ -value of at least as high as 190‰. Such a δ -value can be explained with dilution of a Martian atmospheric component ($\delta^{15}\text{N}$: 620 ± 160 ‰) by either terrestrial atmosphere absorbed on the samples or by indigenous nitrogen from the rock.

3.1.1.3 Sulfur

The most intense research on sulfur isotopes was in the 1960's (Thode et al. 1961; Jensen and Nakai 1962; Hulston and Thode 1965; Monster et al. 1965; Kaplan and Hulston 1966).

Troilite is the most abundant sulfur compound of iron meteorites and has $\delta^{34}\text{S}$ -values from 0‰ to 0.6‰ relative to Cañon Diablo troilite (Kaplan and Hulston 1966). Stony meteorites also contain a wide variety of sulfur compounds. Monster et al. (1965) and Kaplan and Hulston (1966) separated the various sulfur constituents. The results are summarized in Table 17.

In contrast to most terrestrial environments, sulfate in the Orgueil meteorite is isotopically the lightest sulfur compound. Monster et al. (1965) suggested that kinetic isotope effects in a sulfur-water reaction may be responsible for the genesis of sulfur compounds in meteorites. There is no evidence for biological activity having occurred in meteorites, because biogenic sulfate would be characterized by an enrichment in the heavy isotope. Measurements of more than two isotopes of sulfur might help in identifying genetic relationships between mete-

Table 17. Distribution and isotopic composition of sulfur in the Orgueil carbonaceous chondrite. (After Monster et al. 1965)

Form of sulfur	Sulfur (wt.%)	$\delta^{34}\text{S}$
$\text{MgSO}_4 \times 7 \text{H}_2\text{O}$	2.1	-1.3
Elemental sulfur	1.8	1.5
Troilite sulfur	0.8	2.6
Other forms of sulfur	0.3	-
Total sample	5.0	0.4

orites in a similar way to that already known from oxygen isotope studies. Hulston and Thode (1965) and Kaplan and Hulston (1966) have measured the $^{33}\text{S}/^{32}\text{S}$ and $^{36}\text{S}/^{32}\text{S}$ ratios in meteoritic material. Their data give strong evidence against variations due to inhomogeneities in the processes of nucleosynthesis and due to cosmic ray effects. The occurrence of an excess of ^{33}S and ^{36}S from spallation processes has been demonstrated by Hulston and Thode (1965) in the iron (non-troilite) phase. McEwing et al. (1983) found a slight ^{34}S excess in metal spheroids from the rim of the Canyon Diablo crater which they interpreted as an impact-induced fractionation effect.

3.1.2 Tektites

Tektites are derived from terrestrial rocks, which were hit by asteroids or comets (Bentor 1986). They consist of a silica-rich glass (average 75% SiO_2) resembling obsidian, yet distinct from obsidians in composition and texture.

Taylor and Epstein (1964, 1966a, 1969) have shown that the oxygen isotope composition of tektites usually ranges from 8.9‰ to 11.8‰. Various tektite groupings based on chemical composition and geographic occurrence all show a systematic increase in ^{18}O with decreasing SiO_2 content. These systematic correlations, as noted by Taylor and Epstein (1969), are caused probably by vapor fractionation of the tektite material during impact.

3.1.3 The Moon

Three different kinds of material are recognized on the lunar surface: (1) crystalline rocks of different composition, (2) brecciated rocks (rock fragment and fine-grained debris) from meteorite impact, and (3) fines or soils with grain sizes down to $< 1 \mu\text{m}$. The crystalline rocks represent deep-seated lunar materials which are generally very poor in volatiles, such as carbon and nitrogen, but rich in sulfur. The brecciated rocks represent an intermediate group, while the dust and fines are heavily influenced through the bombardment of the solar wind.

Starting with the oxygen isotope composition of the common rock-forming minerals in lunar igneous rocks, one can say that they vary little from one sampled locality to another (Epstein and Taylor 1970,

1971, 1972; Onuma et al. 1970a; Clayton et al. 1973b). The $\delta^{18}\text{O}$ of pyroxene is always between 5.3‰ and 5.8‰, olivines are between 4.9‰ and 5.1‰, and plagioclase between 5.6‰ and 6.4‰. The small range of variation implies that the source regions of the rocks are very similar in oxygen isotope composition. Assuming that the source regions are composed largely of a mixture of olivine, pyroxene, and plagioclase, the lunar interior should have a $\delta^{18}\text{O}$ -value of $5.5‰ \pm 0.2‰$. Lunar igneous rocks are, therefore, essentially identical to many mafic and ultramafic rocks on earth. The fractionations observed among co-existing minerals indicate temperatures of crystallization of $\approx 1000^\circ\text{C}$ or higher, similar to values observed in terrestrial basalts (Onuma et al. 1970a,b). Furthermore, it seems to imply that the water content of lunar basalts is negligible.

In comparison with other terrestrial rocks, the range of observed ^{18}O -values is narrow. For instance, the group of terrestrial plagioclase exhibits a variation which is at least ten times greater than that for all lunar rocks (Taylor 1968). This difference may be attributed to the much greater role of low-temperature processes in the evolution of the earth's crust and to the presence of water on the earth.

The question of the presence of water on the moon is very important in understanding the origin and conditions of its formation. Small amounts of water have been found in lunar soils (Epstein and Taylor 1970, 1971, 1972; Friedman et al. 1970, 1974). This water is typically present in concentrations between 120 and 360 ppm. Epstein and Taylor (1970, 1971) argued that the absolute concentration and the isotope data strongly suggest that terrestrial atmospheric water vapor is the dominant source of this "lunar water", meaning that the water is largely a result of terrestrial contamination.

3.1.3.1 Sulfur

The most notable feature of the sulfur isotope geochemistry of lunar rocks is their uniformity and proximity to the Canon Diablo meteorite standard. The range of published values is between $-2‰$ and $+2.5‰$, however, as noted by Des Marais (1983), the actual range is likely to be considerably narrower than $4.5‰$ due to systematic discrepancies either between laboratories or between analytical procedures. The average $\delta^{34}\text{S}$ -value of all measurements is $0.55‰$, but it is not yet clear whether this small ^{34}S enrichment relative to the Canon Diablo standard

reflects the real sulfur isotope composition of lunar rocks or whether it reflects an artifact. The very small range in $\delta^{34}\text{S}$ -values supports the idea that the very low oxygen fugacities on the moon prevent the formation of SO_2 or sulfate and thus eliminating exchange reactions between oxidized and reduced sulfur species.

3.1.3.2 Nitrogen and Carbon

As shown by Des Marais (1983) nitrogen and carbon abundances are extremely low in lunar rocks. Des Marais (1983) presented compelling evidence that all lunar rocks are contaminated by complex carbon compounds during sample handling. This carbon which is released at relatively low combustion temperatures, exhibits low $\delta^{13}\text{C}$ -values between -23‰ and -31‰ , whereas the carbon liberated at higher temperatures has higher $\delta^{13}\text{C}$ -values. However, we must ask if the extremely low C- and N-contents of lunar materials indicate that the moon is strongly depleted in these elements. Perhaps the losses of carbon and nitrogen in rocks which crystallized at depth were less extensive. Another complication for the determination of the indigenous isotope ratios of lunar carbon and nitrogen arises from spallation effects (which results from the interaction of primary and secondary particles of cosmic ray origin with the lunar surface). These spallation effects lead to an increase in the $\delta^{13}\text{C}$ - and $\delta^{15}\text{N}$ -values depending upon cosmic ray exposure ages of the rocks.

Summarizing, enrichments of the heavy isotopes on the surfaces of the lunar fines are found in ^{13}C , ^{15}N , ^{34}S , and ^{41}K (Barnes et al. 1973). This suggests that all enrichments are due to the same processes, most probably the influence of the solar wind. Detailed interpretation of their isotopic variations is difficult due to the lack of knowledge of the isotopic composition of the solar wind and due to uncertainties of the mechanisms for trapping. However, it seems obvious that the lighter isotopes have been preferentially lost from the moon because of kinetic effects involved in the vaporization-condensation processes.

3.1.4 Mars

Measurements from the Viking mission have shown that the Martian atmosphere consists mainly of CO_2 with traces of N_2 , Ar, O_2 , CO,

Table 18. Comparison of the isotope ratios in the Martian and terrestrial atmosphere. (After Owen et al. 1977)

Isotope ratio	Mars	Earth
$^{12}\text{C}/^{13}\text{C}$	90	89
$^{16}\text{O}/^{18}\text{O}$	500	499
$^{14}\text{N}/^{15}\text{N}$	165	277
$^{40}\text{Ar}/^{36}\text{Ar}$	3000	292

and O. The relative abundance of oxygen and carbon isotopes seems to be similar to values measured for the terrestrial atmosphere, however, a strong enrichment in ^{15}N by about 75% relative to the earth has been found (Biemann et al. 1976; Nier et al. 1976; Owen et al. 1977). This ^{15}N -enrichment is attributed to selective escape, implying a higher initial nitrogen abundance during the early stages of Martian history. In Table 18 a comparison of the isotope ratios in the Martian and terrestrial atmosphere is made (Owen et al. 1977).

3.1.5 Venus

The mass spectrometer on the Pioneer mission, which entered the Venus atmosphere on December 9, 1978 measured the atmospheric composition relative to CO_2 , the dominant constituent. The $^{13}\text{C}/^{12}\text{C}$ and $^{18}\text{O}/^{16}\text{O}$ ratios have been found to be close to the earth value, while the $^{15}\text{N}/^{14}\text{N}$ ratio is within 20% of that of the Earth (Hoffman et al. 1979).

One of the major problems related to the origin and evolution of Venus is that of its "missing water". There is no liquid water on the surface of Venus today and the water vapor content in the atmosphere is probably not more than 220 ppm (Hoffman et al. 1979). This means that either Venus was formed of material very poor in water or whatever water was originally present has disappeared, possibly by the escape of hydrogen into space. By measuring the D/H ratio Donahue et al. (1982) tested this idea. The D/H ratio they measured was $1.6 \pm 0.2 \times 10^{-2}$. The 100-fold enrichment of deuterium relative to the Earth is consistent with an outgassing process, however, the magnitude of this process is difficult to understand.

3.1.6 Interplanetary Dust

In the last few years a new type of extraterrestrial material has become available for isotope investigations: micrometeorites collected as stratospheric dust particles by aircraft at 20-km altitude. Ion microprobe measurements of D/H ratios by McKeegan et al. (1985) gave δD -values between -386 to $+2534\%$. The hydrogen isotope composition is heterogeneous on a scale of a few microns demonstrating that the dust is unequilibrated. Elemental and molecular ion signals in different dust fragments show that a carbonaceous phase, not water, is the carrier of the hydrogen. Carbon isotope ratios are similar to terrestrial values within the limits of analytical uncertainties.

3.1.7 The Galaxy

The galactic distributions of some stable isotope ratios have been derived from the study of interstellar molecules by means of their radio spectra (see Table 19, after Penzias 1980). Two observations are especially important: (1) the heavy isotopes are enriched substantially in the galaxy relative to the Earth and (2) there is a distinct difference in isotopic composition between the galactic center and the galactic plane.

Table 19. Estimated isotope abundances and corresponding $\approx 90\%$ confidence uncertainties in our interstellar/solar system. (After Penzias 1980)

	$^{13}\text{C}/^{12}\text{C}$	$^{18}\text{O}/^{16}\text{O}$	$^{17}\text{O}/^{16}\text{O}$	$^{14}\text{N}/^{15}\text{N}$
Galactic plane	1.3 ± 0.2	0.7 ± 0.3	1.2 ± 0.4	1.4 ± 0.2
Galactic center	3.9 ± 1.0	2.0 ± 0.6	3.2 ± 1.0	2.0 ± 0.6

3.2 The Isotopic Composition of Mantle Material

Considerable geochemical and isotopic evidence has accumulated supporting the concept that many parts of the mantle have experienced a complex history of partial melting, intrusion, crystallization, recrystallization, deformation, and alkali metasomatism. The result of this complex history is that the mantle is chemically and isotopically heterogeneous.

Heterogeneities in radiogenic isotopes are relatively easy to detect because the processes which produce basaltic melts and a refractory residue do not fractionate radiogenic isotopes and if they do, these effects are corrected for by measurement of the nonradiogenic isotopes. Heterogeneities in stable isotopes are more difficult to detect: stable isotope ratios are affected by the various partial melting-crystal fractionation processes because they are governed by the temperature-dependent fractionation factors between residual crystals and partial melt and between cumulate crystals and residual liquid.

Sources for information about the composition of the mantle are from the direct analysis of unaltered ultramafic xenoliths brought rapidly to the surface in explosive volcanic vents. Due to the rapid transport these peridotite nodules are in many cases chemically fresh and by most workers considered as the best sample available from the mantle. The other source of information about the mantle is from basalts, which represent partial melts from the mantle. The problem with basalts is that they do not necessarily represent the mantle composition if partial melting causes isotope fractionations relative to the precursor material. Partial melting of Ca-Al-containing peridotites would result in extraction of various basaltic magmas as the Ca-Al-rich minerals were dissolved, leaving behind refractory residues dominated by olivine and orthopyroxene which may differ in the isotopic composition from the original materials. With respect to the volatiles it has to be kept in mind that during partial melting the volatiles will be enriched in the melt and depleted in the parent material. At present, knowledge of isotope fractionations related to this process is more or less nonexistent, but probably this effect should be small at the very high temperatures present in the mantle.

Let us first consider which isotope fractionation processes might have modified the original mantle isotope composition in the samples analyzed. Both, extrapolation of experimental data and theory demand that isotope fractionation factors in the magmatic temperature range should be small ($\alpha \approx 1.000$), but relatively little is known about the exact isotope fractionation factors at very high temperatures ($> 1000^\circ\text{C}$). For gases, Stern et al. (1968) predicted isotopic reversals to occur, even more complex behavior is expected for liquids and solids.

With respect to volatiles a further complication has to be kept in mind. Assuming that the volatiles are stored in various accessory minerals present in the mantle, the volatiles will be preferentially depleted in the parent material during partial melting and enriched in the melt.

This process alone may cause isotope fractionation. During further ascent of the melts the volatiles are degassed preferentially, which in turn might be accompanied by isotope fractionation. Two different examples might exemplify the possible phenomena. Javoy et al. (1978) observed experimentally a difference of 4‰ between CO₂ and carbon dissolved in a basaltic melt at 1200 °C. The effect of degassing upon the sulfur isotope composition in basalts has been discussed by Sakai et al. (1982). Normally ³²S will be enriched in the melt due to the preferential degassing of SO₂ enriched in ³⁴S. At especially high oxygen fugacities loss of SO₂ will cause an enrichment of ³⁴S in the melt, because the sulfate/sulfide ratio is significantly increased.

In summary, the assumption that partial melting of peridotitic mantle material will not produce any measurable fractionations between the magma and the residual phases may be true only to a first approximation. In detail, the effects might be very complex and might cause some small but measurable shifts in the isotopic composition relative to the precursor material. With this in mind, we will now discuss the various evidences of oxygen, hydrogen, carbon, sulfur, and nitrogen isotope compositions of the mantle.

3.2.1 Oxygen

Basalts. There is general agreement that unaltered midocean ridge tholeiitic basalts and ocean island tholeiites have relatively constant $\delta^{18}\text{O}$ -values with an average value of $5.7 \pm 0.5\text{‰}$ (Muehlenbachs and Clayton 1972a; Pineau et al. 1976a; Kyser et al. 1982). Ocean island alkalic basalts are enriched in ¹⁸O by approximately 0.5‰ (Kyser et al. 1982; Harmon and Hoefs 1984; see Fig. 22). These differences in ¹⁸O-contents, although not well understood, may be interpreted as indicating a heterogeneous mantle source.

Many island-arc and continental basalts have ¹⁸O/¹⁶O ratios similar to those of their oceanic counterparts, but $\delta^{18}\text{O}$ -values in excess of 7‰ have been reported from a variety of localities, which will be discussed in more detail under “magmatic rocks”.

Spinel and Garnet Lherzolites. Figure 22 illustrates the range in $\delta^{18}\text{O}$ -values for spinel and garnet lherzolites which is between 5.0 and 7.0, the spinel lherzolites show a pronounced maximum around 5.7 (Javoy 1980; Kyser et al. 1981, 1982).

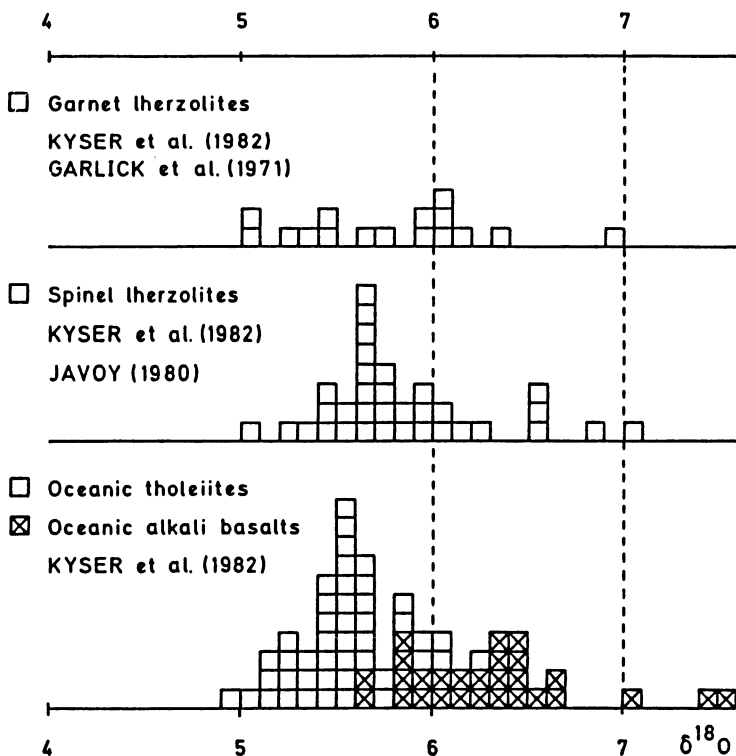


Fig. 22. Oxygen isotope variations in spinel and garnet lherzolites and in oceanic tholeiites and oceanic alkali basalts

When we look at separated minerals the ^{18}O -spread becomes even larger (Javoy 1980; Kyser et al. 1981, 1982). To explain this large spread Kyser et al. (1981) described a temperature-dependent fractionation between coexisting pyroxene and olivine. This interpretation was, however, questioned by Gregory and Taylor (1986), who noted that olivines had a much larger spread (4.4 to 7.5‰) than pyroxenes (5.6 to 6.5‰). They attributed this phenomenon to secondary mantle heterogeneities produced by nonequilibrium processes. This intermineral disequilibrium in the xenoliths does not necessarily demonstrate that the mantle in the basalt source regions will show similar disequilibrium, but is suggestive that this may indeed be the case.

Of special significance with respect to the oxygen isotope composition of mantle-derived rocks is the process of mantle metasomatism in which metasomatic fluids rich in Fe^{3+} , Ti, K, LREE, P, and other LIL

elements tend to react with peridotite mantle-forming micas, amphiboles, and other accessory minerals. The origin of metasomatic fluids is likely to be either (1) exsolved fluids from an ascending magma or (2) fluids or melts derived from subducted, hydrothermally altered oceanic crust.

Hydrothermally altered oceanic crust can show large $\delta^{18}\text{O}$ -variations from 2.0 to $\sim 20\text{‰}$ (Spooner et al. 1974; Magaritz and Taylor 1976; Gregory and Taylor 1981). During subduction, homogenization processes operate within the ocean crust, which reduce the overall oxygen isotope variation. If the typical scale of homogenization were a few tens of meters within the basalt-sediment section, $\delta^{18}\text{O}$ -values in melts produced from this volume should be around $+10\text{‰}$. Because such high $\delta^{18}\text{O}$ -values have not been observed in mantle-derived rocks, the homogenization process must be more effective and operate on a larger scale.

3.2.2 Hydrogen

The concept of juvenile water has a long tradition and has influenced thinking in various fields in igneous petrology and ore genesis. Juvenile water is defined as water that originates by degassing from the mantle and that has never been in contact with the Earth's surface. To analyze the isotopic composition of juvenile water two different approaches have been made: firstly, the direct analysis of water in and from mantle-derived materials, secondly the analysis of OH-bearing minerals such as micas and amphiboles of deep-seated origin (see Fig. 23).

Water. The difficulty in analyzing the water content of basaltic and other mantle-derived materials lies in the fact, that degassing, mixing, and contamination with other water sources may have modified the primary composition. In addition, the fine-grained and glassy matrix material of volcanic rocks is susceptible to low temperature hydrous alteration processes. Altogether this complicates the interpretation of δD -values in basaltic rocks (Kyser and O'Neil 1984). Therefore, it is desirable to analyze separated hydrous minerals rather than whole-rock samples.

OH-Bearing Minerals. Micas and amphiboles in rapidly quenched volcanic rocks will probably preserve their primary isotopic composition,

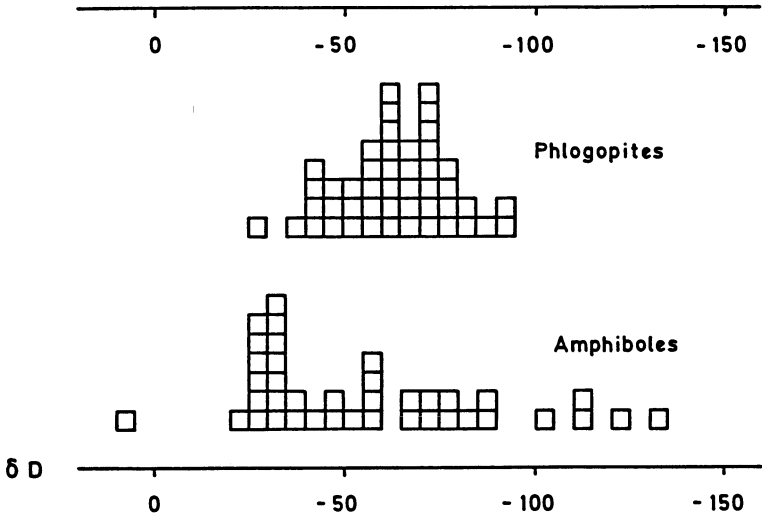


Fig. 23. Deuterium isotope variations in mantle-derived minerals. (Data source: Sheppard and Epstein 1970; Boettcher and O’Neil 1980; Kuroda et al. 1975; Javoy 1980; Graham et al. 1982)

however, because of the limited knowledge on fractionation factors and unknown temperatures of final isotope equilibration between the minerals and water, the calculation of the isotopic composition of water is rather crude and uncertain. Assuming that the temperature of isotopic equilibration lies in the range between 850° and 1000 °C, the fractionation factor between phlogopite and water is around 1.000 (Suzuoki and Epstein 1976), whereas in the case of amphiboles the fractionation factor is about 0.985 (Graham et al. 1984). From these estimates and the phlogopite data shown in Fig. 23, it is quite clear that the hydrogen isotope composition of mantle water should lie, in general, between - 50 and - 80, a range which was first proposed by Sheppard and Epstein (1970) and subsequently by several other authors. Furthermore, Fig. 23 demonstrates that the mantle is heterogeneous with respect to hydrogen isotopes.

The δD -range for amphiboles is much larger than that for phlogopites (Boettcher and O’Neil 1980); the reasons for this are not well understood. The lowest δD -values are from K-richterites, whereas paragasites are relatively D-rich by comparison. One interesting interpretation for the deuterium-enriched amphiboles has been offered by Graham et al. (1982), namely the derivation from seawater via subduction.

3.2.3 Carbon

The presence of CO_2 in the upper mantle has been well documented through the following observations:

1. CO_2 is a quantitatively significant constituent in volcanic gases associated with basaltic eruptions (see discussion in Sect. 3.4.1).
2. The eruption of carbonatite and kimberlite rocks testifies to the storage of CO_2 in the upper mantle. Experimental petrologists agree, for instance, that kimberlitic liquids can be produced by a small degree of partial melting of garnet lherzolite containing H_2O and CO_2 (Eggler and Wendtlandt 1979; Wyllie 1979).

Besides as CO_2 , mantle carbon may exist as methane, graphite, and diamond.

Figure 24 summarizes data from fluid-inclusion CO_2 , from ocean ridge basalts, from kimberlites and carbonatites, and from diamonds. Most $\delta^{13}\text{C}$ -values are between -8 and -3‰ . Although the mean isotopic composition of selected carbonatite complexes is indistinguishable from that of kimberlite pipes as well as that of most diamonds, at a single locality the $\delta^{13}\text{C}$ -values of carbonatites, kimberlites, and diamonds may vary in the per mil range for different complexes or pipes. Deines et al. (1984) have convincingly documented this heterogeneity

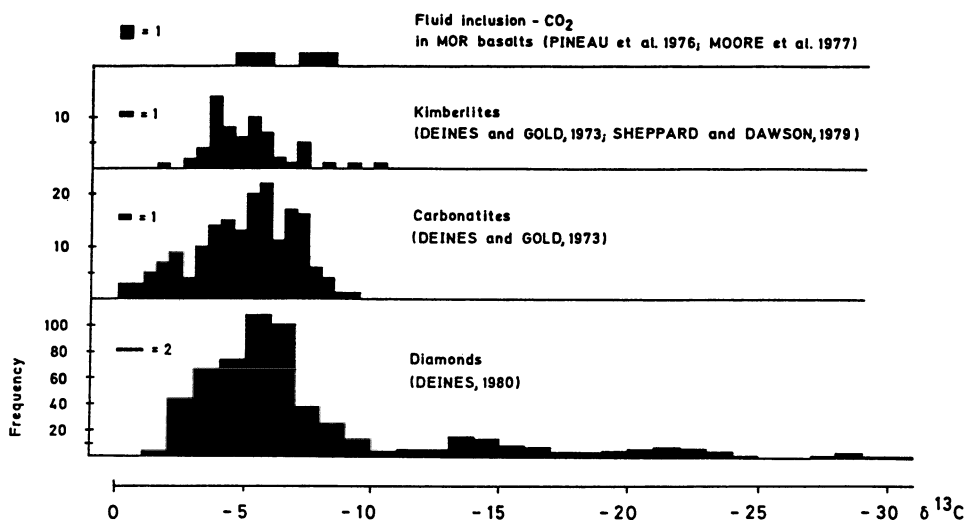


Fig. 24. Carbon isotope variations in fluid inclusion CO_2 from MORB, in kimberlites, carbonatites, and diamonds

by comparing diamonds from the Finsch and Premier kimberlite. Maybe the most puzzling fact is the large variation range observed in diamonds (see Fig. 24). While maybe more than 90% of all diamonds analyzed fall in the restricted $\delta^{13}\text{C}$ -range between -8 and -3‰ , some of them are extremely depleted in ^{13}C with δ -values lower than -30‰ (Galimov 1985). By discussing different models of diamond genesis Deines (1980a) demonstrated that carbon isotope fractionations during the formation of diamonds should be on the order of a few per mil. Therefore, the observed large range of $\delta^{13}\text{C}$ -values should reflect mainly carbon isotope variations in the mantle source.

3.2.4 Sulfur

Basalts. As previously mentioned degassing of SO_2 , which is the predominant sulfur species at basaltic temperatures, may cause some isotope fractionation in subaerial basalts. Therefore, we will concentrate on the sulfur isotope composition of submarine basalts; where fractionation effects due to degassing should be minimized. As shown in Fig. 25, deep-sea basalts from the Atlantic and Pacific Ocean (data from Kanehira et al. 1973; Grinenko et al. 1975; Hubberten and Puchelt 1980; Sakai et al. 1982; Hubberten 1984) reveal that

1. in general, the primary sulfide sulfur fraction has slightly negative $\delta^{34}\text{S}$ -values between -1.2 and 0‰ ;
2. the sulfate-sulfur fraction, which may amount up to 36%, varies between 2.3 and 5.5‰ (Sakai et al. 1982) and
3. the total sulfur exhibits values in the range between 0.4 to 1.2‰ , pointing to small, but nevertheless distinct, heterogeneities.

Sulfur from Peridotites and Mantle Xenoliths. Heilmann and Lensch (1977) analyzed sulfides and whole-rock sulfur from peridotites of the Ivrea Zone. The different bodies showed slightly different $\delta^{34}\text{S}$ -values with mean values of 0.5 , 0.8 , and 1.9‰ , respectively (see Fig. 25).

In xenoliths of upper mantle origin sulfides are relatively rare, but they occur in some ultramafic and eclogitic xenoliths from kimberlites. Bulk rock lherzolites and garnet pyroxenite xenoliths from the Obnazhennaya kimberlite give $\delta^{34}\text{S}$ -values from 0.5 to 2.1‰ (Grinenko and Ukhanov 1977), while eclogites from the Premier and Roberts Victor kimberlite yields values between 0.2 to 2.1‰ (Tsai et al. 1979).

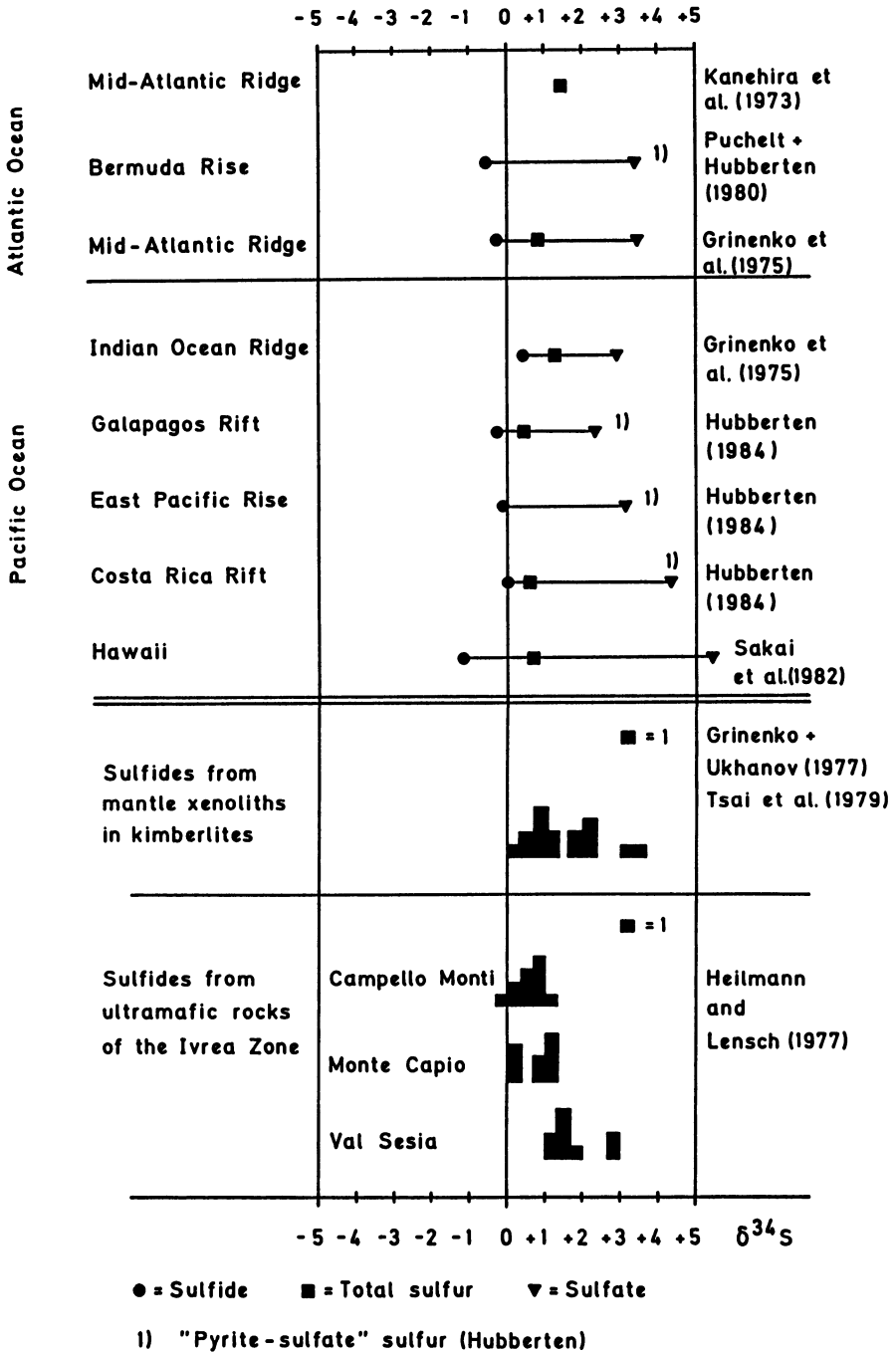


Fig. 25. Sulfur isotope variations in ridge basalts and in sulfides from kimberlites and peridotites

In conclusion, the observed spread of $\delta^{34}\text{S}$ mean values between 0.0 and +2‰ indicates mantle heterogeneities and favor a slight enrichment in ^{34}S relative to meteoritic sulfur. The reasons for this enrichment are not at all clear, but might be due to the loss of volatiles preferentially enriched in ^{32}S .

3.2.5 Nitrogen

The data base for evaluating the nitrogen isotope composition of the mantle, although increased in the past few years, is still rather limited. Becker and Clayton (1977) were the first to report a large range in $\delta^{15}\text{N}$ -values between 6 and 20‰ in mantle-derived rocks. In the meantime more $\delta^{15}\text{N}$ -values became available and the majority of them show distinct negative $\delta^{15}\text{N}$ -values (Javoy and Pineau 1986). In diamonds, for instance, which may contain 1.7 to 3.7 vol% N_2 (Melton and Giardini 1974) an inverse correlation between N concentrations and ^{15}N contents exists (Javoy et al. 1984): low ^{15}N contents are correlated with high N concentrations. In basaltic glasses Exley et al. (1986b) observed low N-contents between 0.2 and 2 ppm and $\delta^{15}\text{N}$ -values between -4 and 14‰ (average 7.5‰) with no correlation between both parameters. These findings suggest that the primary mantle is depleted in ^{15}N relative to the atmosphere and that the residual nitrogen in the mantle may be enriched in ^{15}N due to degassing processes.

3.3 Igneous Rocks

As was stated in the introductory section, igneous rocks show relatively small differences in isotopic composition because of their high temperature of formation. However, especially due to secondary alteration processes, the variation in isotopic composition is sometimes larger than expected from their temperature of formation. The importance of $^{18}\text{O}/^{16}\text{O}$ measurements to some of the classical problems of igneous petrology is well established (see, e.g. Taylor 1968).

Provided an igneous rock has not been affected by subsolidus isotope exchange or hydrothermal alteration, its oxygen isotope composition will be determined by:

1. the $^{18}\text{O}/^{16}\text{O}$ ratio of the source region in which the magma was generated;

2. the temperature of magma generation and crystallization;
3. the mineralogical composition;
4. the evolutionary history of a magma including such additional processes as isotope exchange, assimilation of country rocks, magma mixing, etc..

In the following sections some of these points are discussed in more detail.

3.3.1 Differences Between Volcanic and Plutonic Igneous Rocks

Relatively large differences in O-isotope composition are observed between fine-grained, rapidly quenched volcanic rocks and their coarse-grained plutonic equivalents (Taylor 1968; Anderson et al. 1971). Fractionations in mafic plutonic rocks are on the average about twice as great as for the corresponding fractionations in mafic extrusive rocks. This difference may result from the retrograde exchange or postcrystallization exchange reactions of the plutonic rocks with a fluid phase. This interpretation is supported by the fact that basaltic and gabbroic rocks from the lunar surface have the same “isotopic temperatures” corresponding to their initial crystallization. Due to the absence of water on the moon, no retrograde exchange took place.

3.3.2 Fractional Crystallization

Because fractionation factors between liquid and solid are small at the relatively high temperatures of magmatic melts, fractional crystallization seems to play only a minor role in influencing the oxygen isotopic composition of magmatic rocks. Matsuhisa (1979) reported that within a lava sequence from Japan $\delta^{18}\text{O}$ increased by approximately 1‰ from basalt to dacite. Muehlenbachs and Byerly (1982) analyzed an extremely differentiated suite of volcanic rocks at the Galapagos spreading center and showed that 90% fractionation only enriches the residual melt by about 1.2‰. On Ascension Island Sheppard and Harris (1985) observed a difference of nearly 1‰ in a volcanic suite ranging from alkali basalt to obsidian.

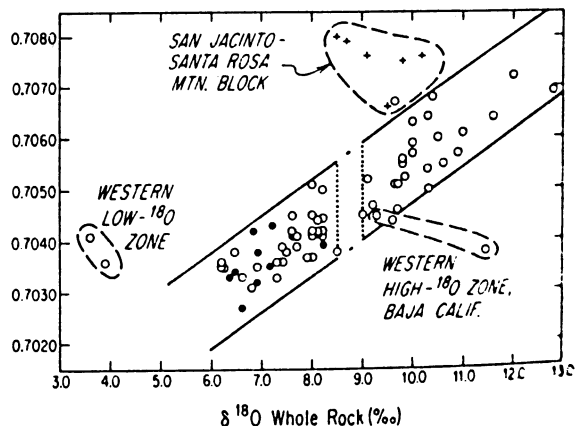
In summary, modelling for closed-system, crystal fractionation predicts an ^{18}O -enrichment of about 0.4‰ per 10 wt% increase in SiO_2 content (Sheppard and Harris 1985; Harmon and Hoefs, in press).

3.3.3 Assimilation of Crustal Rocks

Because the various surface and crustal environments are characterized by different and distinctive isotope compositions, stable isotopes provide a powerful tool of discriminating between the relative role of mantle and crust in magma genesis. This is especially true when stable isotopes are considered together with radiogenic isotopes, because variations within these independent isotopic systems arise from unrelated geologic processes. A mantle melt that has been affected by upper crustal contamination will exhibit increases in $^{18}\text{O}/^{16}\text{O}$ and $^{87}\text{Sr}/^{86}\text{Sr}$ ratios that correlate with increase in SiO_2 and decrease in Sr content. In contrast, a mantle melt which evolves only through differentiation unaccompanied by interaction with crustal material, will mainly reflect the isotopic compositions of the source region, independent of variations in chemical composition. In this latter case, correlated stable and radiogenic isotope variations would be an indication of variable crustal contamination of the source region, i.e. crustal material which has been recycled into the mantle via subduction. In many igneous provinces a positive correlation between O- and Sr-isotope compositions has been observed. One of the most striking examples is shown in Fig. 26.

The feature presented in Fig. 26 is generally interpreted to reflect a mixing between a mantle-derived melt with low $^{18}\text{O}/^{16}\text{O}$ and low $^{87}\text{Sr}/^{86}\text{Sr}$ ratios and a crustal component enriched in both ^{18}O and ^{87}Sr . This mixing is viewed as a combined fractional crystallization-assimilation process (AFC process, Taylor 1980) occurring at relatively shallow depths during magma residence in a magma chamber. Thus, a

Fig. 26. Whole-rock $\delta^{18}\text{O}$ -values versus initial $^{87}\text{Sr}/^{86}\text{Sr}$ ratios for plutonic igneous rocks, Peninsular Ranges batholith. *Solid circles* indicate gabbros. The $\delta^{18}\text{O}$ gap between 8.5 and 9.0‰ divides the western group of granodiorites and tonalites from the eastern group (Taylor and Silver 1978)



two-component mixing process is an oversimplification for crustal contamination and at least three end members have to be considered: the magma, the country rocks, and the cumulates.

Modelling by Taylor (1980) and James (1981) has demonstrated that it is possible to distinguish between the effects of source contamination as well as crustal contamination. Magma mixing and source contamination are two-component mixing processes which obey two-component hyperbolic mixing relations, while crustal contamination is a three-component mixing process, involving the magma, the crustal contaminant, and the cumulates.

3.3.4 Secondary Alteration Processes

It is now generally recognized that the emplacement of a hot magma into relatively permeable, water-saturated country rocks commonly initiates the development of a hydrothermal circulation system. As the magma cools and crystallizes, these hydrothermal systems alter the recently solidified igneous rocks. The amount of interaction between igneous rocks and the hydrothermal fluid depends upon the permeability of the affected rocks, the water/rock ratio of the system, and the chemical and isotopic differences between the rock and the fluid. In subaerial regions the circulating fluid is dominantly meteoric water, while in submarine environments the fluid is ocean water. Since both types of water are very different in isotopic composition the observed alteration effects are also different. Therefore, these two different environments are discussed separately.

3.3.4.1 *Ocean Water Interaction*

Evidence of altered oceanic crust comes from samples dredged from the seafloor, from DSPD drilling sites, and from the study of ophiolite complexes, which presumably represents pieces of old oceanic crust. Two types of alteration can be distinguished: low-temperature weathering may markedly enrich the groundmass of basalts, but does not affect the isotopic composition of phenocrysts. It is well known that volcanic glasses are readily altered to more stable phases, generally smectites or other clay minerals. This low-temperature alteration leads to an ^{18}O -enrichment by 1 to 3‰ of the whole rock, but may increase

to about 10‰ (Muehlenbachs and Clayton 1972a,b, 1976). The amount of ^{18}O -enrichment correlates with the H_2O content: the higher the water content, the higher the $\delta^{18}\text{O}$ -values.

At temperatures in excess of about 300 °C hydrothermal systems beneath the midocean ridges have depleted deeper parts of the oceanic crust by 1 to 2‰. Similar findings have been reported from ophiolite complexes, see, for instance, the oxygen isotope study of the Oman ophiolite by Gregory and Taylor (1981). At Oman maximum $\delta^{18}\text{O}$ -values occur in the uppermost part of the pillow lavas and decrease through the sheeted dike complex. Normal mantle values are observed at the base of the dike complex and below that depth down to the MOHO $\delta^{18}\text{O}$ -values are lower than mantle values by about 1 to 2‰. The oxygen isotopic composition of oceanic crust subducted into the mantle in the geologic past will depend upon the variation in the oxygen isotope composition of seawater during earth history. Muehlenbachs and Clayton (1976) have concluded that the ^{18}O -enrichment is balanced by the ^{18}O -depletion in the oceanic crust. Gregory and Taylor (1981) reached the same conclusion which implies that the $\delta^{18}\text{O}$ of the oceans has not changed much with time. This point will be also discussed again on p. 142.

3.3.4.2 Interactions Between Meteoric Groundwaters and Igneous Intrusions

Mainly through the work of H.P. Taylor and co-workers it has become well established that many epizonal igneous intrusions have interacted with meteoric groundwaters on a very large scale. The interaction and transport of large amounts of meteoric water through hot igneous rocks produces a depletion of ^{18}O in the igneous rocks by as much as 10 to 15‰ and a corresponding shift in the $\delta^{18}\text{O}$ -values of the water. Igneous complexes that are abnormally low in ^{18}O characteristically display the following geologic, petrologic, and isotopic features (after Taylor 1974b).

1. The intrusions are emplaced into highly jointed volcanic rocks that are permeable to groundwater movement.
2. The feldspars are commonly depleted in ^{18}O to a greater degree than the other coexisting minerals and the feldspars, particularly the alkali feldspars, commonly show a “clouding” or a turbidity.

3. The primary igneous pyroxenes and olivines are usually altered to amphibole, chlorite, Fe-Ti oxides, and/or epidote.
4. Intergrowths of turbid alkali feldspars and quartz are quite common.
5. Miarolitic cavities are locally present in the intrusives.
6. The OH-bearing minerals have abnormally low δD -values relative to "normal" igneous rocks.

Low ^{18}O -igneous rocks have now been observed in many localities, the best documented are in the Skaergaard intrusion in Greenland, in the Scottish Hebrides, and in portions of the Idaho batholith, the southern California batholith, and the Coast Range batholith, British Columbia (Taylor and Forester 1971, 1979; Magaritz and Taylor 1976, 1986; Criss and Taylor 1983, and others).

These types of hydrothermal systems seem to represent the "fossil" equivalents of the deep portions of modern geothermal systems such as occur at Wairakei, New Zealand, Steamboat Springs, Nevada, and Yellowstone Park, Wyoming. The enormous scale of interaction between meteoric groundwaters and epizonal igneous intrusions is best documented in the Challis Volcanic Field, Idaho, where thousands of square kilometers are involved (Criss et al. 1984). The amounts of meteoric water needed to produce these effects are large but not unreasonable, however, considering the tens of thousands of years during which such hydrothermal systems probably persist. Assuming normal amounts of rainfall, only about 5% of the annual precipitation has to be added to the geothermal system, to produce the observed O-isotope shifts.

Recently Ferry (1985a,b) has integrated the isotope data of Taylor and Forester (1971) and Forester and Taylor (1977) on Skye with chemical and mineralogical changes observed in the gabbros and granites. Both isotopic and petrologic data point to pervasive flow of fluid through gabbros at 500° to 1000 °C and through granites at 450° to 550 °C. The difference between the behavior of the granites and gabbro can be attributed to the difference between the solidus temperatures of the two rock types.

For the granitic rocks Ferry (1985b) postulated that during cooling an interconnected set of channelways along grain boundaries between quartz and feldspar developed due to the volume decrease of quartz during β - to α -transformation. These channelways would allow access to hydrothermal fluids that could then chemically and isotopically react with minerals preferentially at grain boundaries.

3.3.5 Basaltic Rocks

Before discussing the primary isotopic composition of volcanic rocks, secondary factors that can modify the primary composition are discussed briefly. Because of their glass content and very fine grain size volcanic rocks are very susceptible to low-temperature ^{18}O -enrichment processes such as hydrothermal alteration, hydration, and weathering. The whole-rock $\delta^{18}\text{O}$ -values of all whole-rock samples must be regarded with suspicion, unless the lavas were very recently erupted or unless the results have been checked by $\delta^{18}\text{O}$ -analysis of the phenocrysts, which, however, is often not possible. Although there is no way to exactly correct for this O-enrichment effect, a crude estimate can be made by determining the water (and carbon dioxide) content of the rocks to be analyzed (Taylor et al. 1984; Ferrara et al. 1985). Although it is difficult to estimate the primary water content of basaltic magmas, there is some general consensus that primary magmas should not have more than 0.5%, certainly not more than 0.9% as determined for some Hawaiian alkali basalts (Moore 1970). Thus, any water content $> 0.5\%$ or $> 0.9\%$ should be of secondary origin, and has to be corrected for when the primary $\delta^{18}\text{O}$ -value of the rock is evaluated. Such corrections are schematically demonstrated in Fig. 27.

Basaltic rocks from different tectonic settings exhibit characteristic differences in oxygen isotope composition. This was first suggested by Kyser et al. (1982) and subsequently verified in an extensive compilation by Harmon and Hoefs (1984) (see Table 20). MORB basalts have

Table 20. Comparison of O-isotope variations of basalts erupted in different tectonic settings. (Data from Harmon and Hoefs 1984)

Tectonic setting	Number of analyses	$\delta^{18}\text{O}$ range	$\bar{x} \delta^{18}\text{O} \pm 1 \sigma$
Midocean ridges	(67)		
Tholeiitic basalts		+5.4 to +6.6	+5.78 \pm 0.23
Oceanic islands	(110)		
Tholeiitic basalts		+5.0 to +5.8	+5.38 \pm 0.23
Alkali basalts		+5.5 to +8.2	+6.34 \pm 0.62
Continental intraplate settings	(92)		
Tholeiitic basalts		+6.4 to +9.0	+6.91 \pm 0.59
Alkali basalts		+5.9 to +8.2	+6.88 \pm 0.89
Oceanic island arcs	(165)	+5.0 to +9.7	+6.31 \pm 0.79
Continental margin arcs	(323)	+5.2 to +8.8	+6.71 \pm 1.08

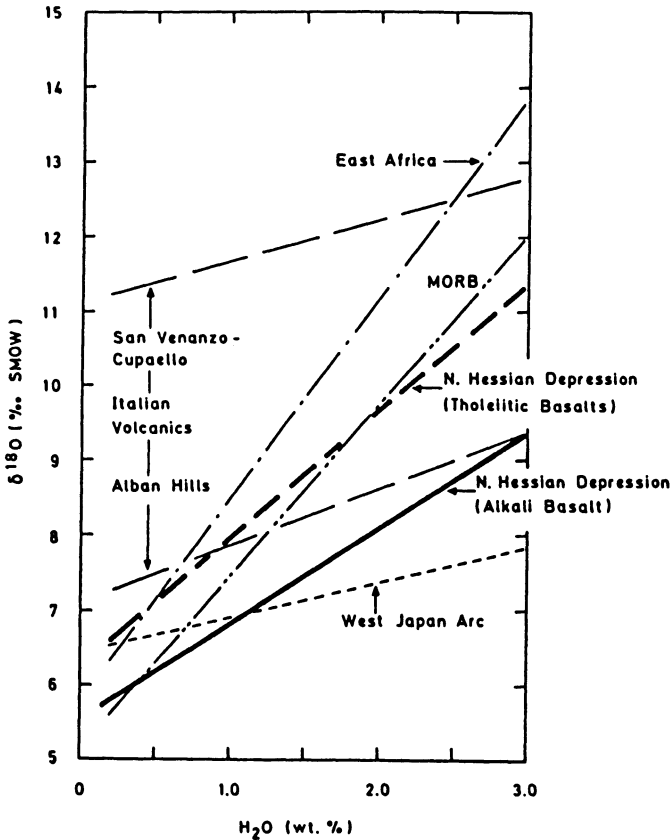


Fig. 27. Plot of $\delta^{18}\text{O}$ versus H_2O which compares the effect of secondary water uptake on the oxygen isotope composition of volcanic rocks and glasses of different chemical character (Harmon et al. 1987)

the lowest average $\delta^{18}\text{O}$ -values (5.82 ± 0.3) with the smallest overall O-isotope variation. The ^{18}O -enrichment observed for continental volcanic rocks compared to their oceanic counterparts of equivalent bulk composition either implies that the subcontinental upper mantle is enriched in ^{18}O due to mantle metasomatism (Holm and Munksgaard 1982) or that contamination by ^{18}O -rich continental crust is an important process in the magma genesis of continental magmas (e.g., Taylor et al. 1979). Although there is strong evidence that the subcontinental mantle shows some enrichment in radiogenic isotopes, evidence for an ^{18}O -enrichment due to metasomatic processes is much weaker. In many cases where ^{18}O -enriched volcanics have been ob-

served these can be best explained by assuming different mechanisms of crustal interaction in different tectonic settings. Examples of such crustal interaction – besides others – have been described from the Andes (Harmon et al. 1984), from the Lesser Antilles (Davidson 1985), and from Antarctica (Hoefs et al. 1980).

The highest ^{18}O -enrichments are found in K-rich leucite-bearing rocks. Taylor et al. (1984) argued that these extreme ^{18}O -enrichments are due to secondary subsolidus processes, because these K-rich volcanic rocks containing leucite are especially susceptible to hydration and other low-temperature alteration processes.

3.3.6 Granitic Rocks

On the basis of their $^{18}\text{O}/^{16}\text{O}$ ratios, Taylor (1977, 1978) subdivided granitic rocks into three groups: (1) “normal ^{18}O -granitic rocks” with $\delta^{18}\text{O}$ -values between 6 and 10‰, (2) high ^{18}O -granitic rocks with $\delta^{18}\text{O}$ -values $> 10\text{‰}$, and (3) low ^{18}O -granitic rocks with $\delta^{18}\text{O}$ -values $< 6\text{‰}$.

Although this is a somewhat arbitrary grouping it allows some generalizations.

Many plutonic granites throughout the world have relatively uniform $\delta^{18}\text{O}$ -values between 6 and 10‰. Granitoids at the low ^{18}O -end of the normal group have been described in island-arc areas where continental crust is absent, such as the Koloulo Igneous Complex of Guadalcanal (Chivas et al. 1982), which are considered to be entirely mantle-derived. Similar $\delta^{18}\text{O}$ -values have been measured in granites which could be derived by partial melting of lower crustal granulitic rocks. Granites at the high end of the normal granitic rock $\delta^{18}\text{O}$ -range may have formed by partial melting of crust that contained both a sedimentary and a volcanic fraction. Furthermore, it is interesting to note that many of the “normal” granites are of Precambrian age in which metasediments quite often have $\delta^{18}\text{O}$ -values below 10‰ (Longstaffe and Schwarcz 1977).

Granitic rocks with $\delta^{18}\text{O}$ -values higher than 10‰ require derivation from some type of ^{18}O -enriched sedimentary or metamorphic rock. For instance, such high ^{18}O -contents are observed in some Caledonian granitoids in Scotland (Halliday et al. 1980), in Hercynian granites of western Europe (Michard-Vitrac et al. 1980; Hoefs and Emmermann 1983), in Damaran granites, SW Africa (Haack et al. 1982), and in

granites from the Himalaya (Blattner et al. 1983). All these granites are easily attributed to anatexis within a heterogeneous crustal source, containing a large metasedimentary component.

Granitic rocks with $\delta^{18}\text{O}$ -values lower than 6‰ cannot be derived by any known differentiation process from “normal” basaltic magmas. Excluding those low ^{18}O -granites which have exchanged with ^{18}O -depleted meteoric-hydrothermal fluids under subsolidus conditions, a few primary low ^{18}O -granitoids have been observed. These granites obviously inherited ^{18}O depletions when still predominantly liquid, prior to their primary crystallization as low ^{18}O -magmas. Examples are described from Iceland (Hattori and Muehlenbachs 1982), from southern Nevada (Lipman and Friedman 1975), and from Yellowstone (Hildreth et al. 1984). In all cases, the ^{18}O -depletions can be attributed to the interactions of magmas with ^{18}O -depleted country rocks in high-level magma chambers.

3.3.7 Granitic Pegmatites

Stable isotope data on granitic pegmatites are mostly available from oxygen isotope studies (Taylor et al. 1979; Taylor and Friedrichsen 1983; Longstaffe 1982). The interpretation of these data is complex because of the small size of these bodies and their volatile, rich nature. Rather surprisingly, only a relatively small spread in $\delta^{18}\text{O}$ -values is observed, the $^{18}\text{O}/^{16}\text{O}$ of quartz, for example, varies from 8.6 to 11.8‰ (Taylor and Friedrichsen 1983). The whole-rock isotopic composition appears to reflect the composition of the melt. Isotope exchange with the wall rocks may occur, but the extent is difficult to assess, because the country rocks intruded by granitic pegmatites often have similar $\delta^{18}\text{O}$ -values (Longstaffe 1982). Oxygen isotope fractionations among pegmatitic minerals yield temperatures for crystallization between 540° and 750 °C. Hydrogen isotope data have shown that interaction with meteoric waters is atypical of pegmatite crystallization and emplacement (Taylor et al. 1979; Taylor and Friedrichsen 1983).

3.3.8 Hydrogen in Igneous Rocks

H-isotopes provide the primary guide to the source of the water present in a magma or in volcanic rocks. δD -values also indicate to what extent

vapor-phase exsolution or assimilation may have affected a magma prior to eruption and crystallization (Nabelek et al. 1983; Taylor et al. 1983).

It is well known that volcanic rocks are quite susceptible to post-eruptive, subsolidus alteration. Kyser and O'Neil (1984) demonstrated that D/H ratios and water contents in fresh submarine basalt glasses from midoceanic ridges can be altered by (1) outgassing, (2) addition of seawater at magmatic temperature, and (3) low-temperature hydration. Extrapolations to possible unaltered δD -values indicate the primary δD -value of most tholeiite and alkali basalts near $-80 \pm 5\%$.

The H-isotope composition of subaerial volcanic rocks can be modified by slow inward diffusion of meteoric water into interstitial glass and fine-grained groundmass at low temperature. Such an uptake should produce a decrease in δD -values concomitant with increasing H_2O content. Kyser and O'Neil (1984) observed that the outer rims of volcanic glasses can undergo low-temperature hydration by hydroxyl groups having δD -values of -100% .

In addition to low temperature hydration, exsolution of water from a magma can deplete the magma in deuterium (Nabelek et al. 1983; Taylor et al. 1983). In contrast, a D-enrichment would occur if H_2 or CH_4 is lost from the melt because these gases are strongly depleted in D relative to the melt at magmatic temperatures (Richet et al. 1977).

The hydrogen isotopic composition of biotite and hornblende from granitic rocks in most cases is within the range between -90% and -50% (Godfrey 1962; Sheppard and Epstein 1970; Kuroda et al. 1974; Taylor 1974b). However, quite a significant number of hornblendes and biotites, mostly from shallow intrusions, have lower and more variable δD -values (down to -180%). This variation seems to be a consequence of the interaction of meteoric groundwaters of different isotopic composition with magmas or hot igneous rocks. The D/H ratios of igneous rocks and minerals are much more sensitive to such processes than are the $^{18}O/^{16}O$ ratios because igneous rocks contain about 60 atom% oxygen and it thus requires exchange with a very large amount of H_2O to change their $^{18}O/^{16}O$ ratios appreciably. The water/rock ratios in these hydrothermal convective systems are typically so low that over wide areas the only evidence for meteoric water exchange is given by δD -values. Figure 28 illustrates the changes in $\delta D_{(biotite)}$ and $\delta^{18}O_{(feldspar)}$ due to isotope exchange between a granodiorite and high-latitude meteoric water as a function of the water/rock ratio. Such L-shaped patterns are characteristic of hydrothermal alteration (Taylor 1978).

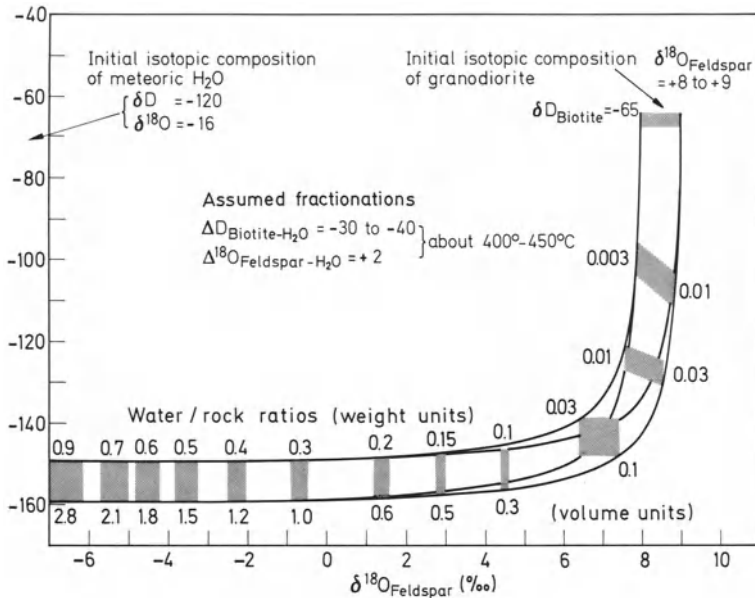


Fig. 28. Plot of calculated values of $\delta D(\text{biotite})$ and $\delta^{18}O(\text{feldspar})$ that would be obtained during hypothetical meteoric-hydrothermal alteration of a typical granodiorite at varying water/rock ratios, assuming the initial conditions shown in the diagram (Taylor 1978)

3.3.9 Carbon and Sulfur in Igneous Rocks

Earlier measurements by Hoefs (1973) and Fuex and Baker (1973) demonstrated that reduced carbon in igneous rocks was isotopically depleted relative to “mantle” $\delta^{13}\text{C}$ -values. Two models have been developed to explain this duality: Pineau and Javoy (1983) suggested that the isotopically light carbon is the residue after partial outgassing from the magma. By employing a stepwise combustion technique to extract carbon Des Marais and Moore (1984) and Matthey et al. (1984) considered the isotopically light carbon, which was released at low combustion temperatures, to be surficial organic contamination. At very high temperatures isotopically heavy carbon with typical mantle values was released from midocean ridge basalts and glasses. However, island-arc glasses yielded lower $\delta^{13}\text{C}$ -values which might be explained by mixing of two different carbon compounds in the source regions: a MORB-like carbon and an organic carbon component from subducted pelagic sediments. More measurements from other tectonic settings are needed to confirm this relationship.

Sulfur. Midocean ridge basalts and submarine Hawaiian basalts have a very narrow range in sulfur isotope composition around zero (Sakai et al. 1982, 1984). In subaerial volcanic rocks the variation in $\delta^{34}\text{S}$ -values is larger and generally shifted towards positive values. One of the reasons for this larger variation is certainly degassing of sulfur. The effects of this process on the sulfur isotope fractionation depends on the ratio of sulfate to sulfide in the magma which is directly proportional to the fugacity of oxygen (Sakai et al. 1982). Especially enriched in ^{34}S (up to $\delta^{34}\text{S}$ -values of +20‰) are arc-volcanic rocks (Ueda and Sakai 1984; Harmon and Hoefs 1986). This overall enrichment is considered to be mainly a product of mantle heterogeneities resulting from the recycling of marine sulfate during subduction.

3.4 Volcanic Gases and Hot Springs

In the fluid phase of magmatic melts, H_2O is the main constituent, followed by CO_2 and SO_2 . Most workers agree that typical concentrations in basaltic and andesitic magmas are in the ranges: H_2O from 35 to 90 mol%, CO_2 from 5 to 50 mol%, and SO_2 from 2 to 30 mol%. The ultimate origin of these volatiles – whether juvenile in the sense that they originate from primary mantle degassing or recycled during subduction processes – is an important question which might be solved by detailed isotope studies in suitable cases.

There are three sources of information on the isotopic composition of the fluid and gaseous phase related to magmatic processes: (1) volcanic gases, (2) fluid inclusions, and (3) hot springs.

3.4.1 Volcanic Gases

The chemical compositions of volcanic gases vary significantly with distance from volcanic vent, eruption history, temperature of collection, and sampling techniques. Volcanic gases are frequently subject to several sources of contamination. It is relatively simple to recognize and correct modifications from atmospheric contamination. More problematic are those which involve usual magmatic constituents such as meteoric water. The complexities involved have been discussed by Anderson (1975) among others.

Water. A long-standing problem is the source of the water vapor observed in many volcanic eruptions. How much is derived from the magma itself and how much is recycled meteoric water? Deuterium measurements can help to solve this problem. As will be discussed below, in most cases meteoric surface waters are the dominant source. However, in a few cases a magmatic water component is not excluded. Fumarolic water from Surtsey, Iceland gave a δD -value of -53‰ (Arnason and Sigurgeirsson 1968). Viglino et al. (1985) determined the isotopic composition of fumarole condensates from Augustine Volcano, an active stratovolcano in the Aleutian Arc. The isotopic data for the condensates form a linear δD - $\delta^{18}O$ array from low-temperature fluids ($< 100\text{ }^\circ\text{C}$), which are essentially local meteoric water ($\delta D \sim -150$, $\delta^{18}O \sim -19$), to high temperature ($> 450\text{ }^\circ\text{C}$) fluids collected at the volcano summit, which are enriched in both D and ^{18}O ($\delta D \sim -35$, $\delta^{18}O \sim -13.5$). These authors suggest that the isotopically enriched condensates are "magmatic" fluids released into the hydrothermal system during the 1976 eruption.

CO₂. CO₂ is the second most abundant magmatic gas species. Its importance for determining the composition of mafic magmas in the source region and for governing the vapor phase at elevated pressure became recognized recently. The volcano where gases have been collected and analyzed for the longest time (since 1912) is Kilauea in Hawaii. Gerlach and Thomas (1986) observed a constant $\delta^{13}C$ -value of -3.2‰ , which is heavier than common estimates for mantle carbon. These authors argued that the analyzed $\delta^{13}C$ -value of the CO₂ reflects the $\delta^{13}C$ -value of the parental magma. They attributed the observed ^{13}C -enrichment to be a typical feature of Hawaiian hot-spot volcanism. However, glasses from Loihi seamount – some 30 km south of Kilauea – contain indigenous carbon with typical mantle values between -5.8‰ and -7.1‰ (Exley et al. 1986a). $\delta^{13}C$ -values of CO₂ from many other volcanoes around the world have been also interpreted to represent "mantle carbon". Sometimes, a ^{13}C -enrichment may be due to local contamination from carbonate-rich sediments in the volcano's basement (Allard 1979).

Sulfur. Sulfur is a major component of magmatic volatiles. The equilibrium proportions of H₂S, S₂, SO₂, and SO₃ depend upon temperature, pressure, oxygen fugacity, and bulk composition (Anderson 1975). In high-temperature gases SO₂ is the dominant gas phase. $\delta^{34}S$ -

values of SO_2 collected from fumaroles between 1971 and 1979 at Kilauea have remained relatively constant at 0.9‰ (Sakai et al. 1982). However, elemental sulfur may show quite different and much more variable $\delta^{34}\text{S}$ -values. The origin of sulfur and the fractionation behavior of different sulfur components is discussed below.

3.4.2 Fluid Inclusions

There are two different methods whereby gases may be extracted from rocks: (1) decrepitation by heating in vacuum and (2) crushing and grinding in vacuum. Both techniques may cause serious analytical difficulties. The major disadvantage of the thermal decrepitation technique is that although the amount of gas liberated is higher than by crushing at elevated temperatures, the different compounds present may begin to exchange isotopically or even to react with each other. This is especially crucial for hydrogen and carbon isotope measurements, when water and methane or carbon dioxide and methane coexist with each other. Crushing in vacuum avoids isotope exchange processes, however, during crushing large new surfaces are created which easily absorb some of the liberated gases. These absorption processes may also cause some fractionation effects. Both techniques preclude separating the different generations of inclusions in a sample. Therefore, in general, the results obtained represent the average isotopic composition of all generations of inclusions.

H-isotope data are particularly important in defining the origin of inclusion fluids and in detecting the mixing of different fluids if two or more sources are involved. The $\delta^{18}\text{O}$ -value of inclusion waters in silicate is likely to have been modified through isotope exchange with the host mineral. Rye and O'Neil (1968) analyzed the ^{18}O -content of fluid inclusions in minerals from the Providencia ore deposit and found that the water present in oxygen-bearing minerals such as quartz and calcite indicated that the inclusions had exchanged ^{18}O with their host minerals. Only the $\delta^{18}\text{O}$ -values of water in sphalerites with a very narrow $\delta^{18}\text{O}$ -range between 5.8 and 6.2‰ were found to represent the primary isotopic composition.

Since the possibilities of isotope exchange are much more restricted for hydrogen than for oxygen, δD -values of magmatic waters should represent their primary isotopic composition.

3.4.3 Hot Springs

One of the principal conclusions drawn from stable isotope studies of fluids in geothermal systems is that most hot spring waters (perhaps 95% or more) are meteoric waters derived from local precipitation (Craig et al. 1956; Craig 1966; Clayton et al. 1968; Clayton and Steiner 1975; Truesdell and Hulston 1980). Most hot spring waters have deuterium contents similar to those of local precipitation, but are usually enriched in ^{18}O by isotope exchange with the country rock at elevated temperatures. This so-called oxygen-isotope shift is demonstrated in Fig. 29. However, in areas where the D/H ratios of the local meteoric waters are similar to "magmatic" water values, stable isotope techniques cannot distinguish conclusively between the meteoric-hydrothermal and the magmatic-hydrothermal solutions.

The magnitude of the oxygen isotope shift depends on the original $\delta^{18}\text{O}$ -value of both water and rock, the mineralogy of the rock, the temperature, the water/rock ratio, and the time of contact. Waters from systems containing carbonate rocks – having originally $\delta^{18}\text{O}$ be-

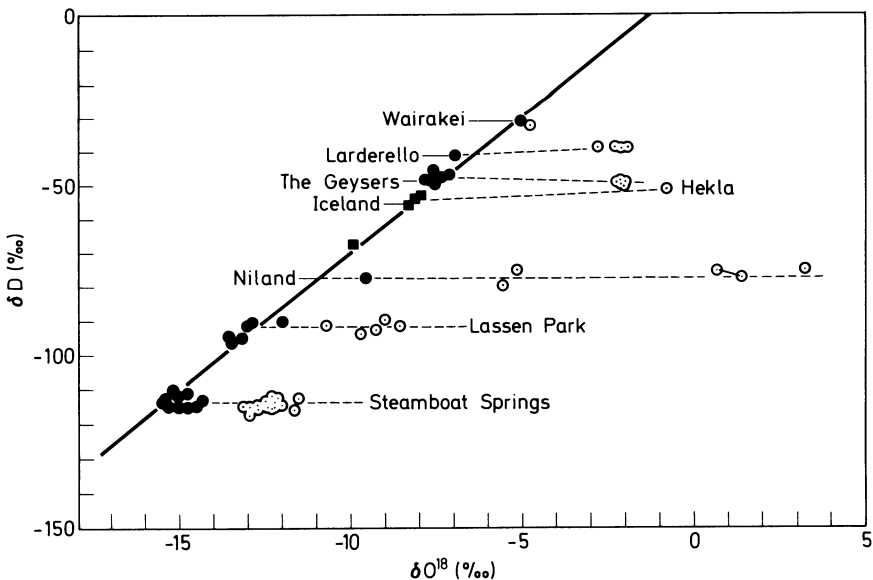


Fig. 29. Observed isotopic variations in near-neutral, chloride-type geothermal waters and in geothermal steam. ■ Local meteoric waters or slightly heated, near-surface groundwaters; ● hot spring geothermal water; ○ high temperature, high pressure, geothermal steam. Niland = Salton Sea Geothermal Area. (After Craig 1963)

tween 20 and 30‰ – high temperatures and low water/rock ratios exhibit large oxygen shifts. One such example is the Salton Sea, where large $\delta^{18}\text{O}$ -shifts in the fluid ($\approx +13\text{‰}$) have indicated approximately equal amounts of water and rock (by mass) (Clayton et al. 1968). In the Broadlands-Wairakei area, New Zealand, much smaller $\delta^{18}\text{O}$ -shifts accompany the hydrothermal alteration (Clayton and Steiner 1975), implying that the ratio of the mass of the water to the mass of the hydrothermally altered rock is large. In the Valles Caldera, New Mexico, Lambert and Epstein (1980) observed an even larger fluid/rock ratio than in the Wairakei geothermal system.

A second class of geothermal waters consists of seawater. Sakai and Matsubaya (1974) showed that such thermal water systems at ocean coasts are mixtures of heated oceanic and local meteoric waters. They are characterized by $\delta^{18}\text{O}$ - and δD -values intermediate between ocean and local meteoric waters. Similar conclusions may hold true for hot spring waters in Iceland.

What is sometimes neglected are the effects of boiling: loss of steam from a geothermal fluid can cause isotope fractionations. ^{16}O is concentrated in the vapor at all temperatures below the critical temperature, while hydrogen is increasingly concentrated in the vapor below 221 °C (Truesdell et al. 1977).

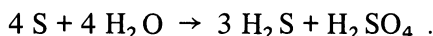
Quantitative estimates of the effects of boiling on the isotopic composition of water can be made using known temperature-dependent fractionation coefficients and assumptions as to the extent to which the generated steam remains in contact with liquid water during the boiling process (Truesdell and Hulston 1980). If steam stays with ascending water and separates when it reaches the surface, maximum isotope effects are found. If steam separation is continuously minimum isotope effects are observed.

3.4.4 Origin of Carbon and Sulfur in Geothermal Fluids

Most $\delta^{13}\text{C}$ -values of CO_2 from geothermal waters fall in the range between -5‰ and -1‰ (Craig 1953; Hulston and McCabe 1962; Lyon 1974a,b; Panichi et al. 1977). Because those $\delta^{13}\text{C}$ -values are close to the ratio for deep-seated carbon (see p. 82), these values might possibly indicate a magmatic origin. However, high temperature leaching of carbonate rocks, or mixing between decarbonation CO_2 and CO_2 derived from carbonaceous matter could also produce such $\delta^{13}\text{C}$ -values.

The CH₄ content in these fluids rarely exceeds 1% and thus is generally less than the CO₂ content. Therefore, the isotopic composition of methane is probably the result of high-temperature equilibration with CO₂ and thus not indicative of the source of the methane.

Elucidation of the origin of geothermal sulfur is complicated by the fact that besides H₂S, SO₂, and sulfate, elemental sulfur can form in appreciable amounts. A further complication arises from the fact that contamination may be very important. Sakai et al. (1980) demonstrated that seawater sulfate plays a decisive role in the Reykjanes geothermal systems of Iceland. The same is true for the solfataras of the Santorini volcano in Greece (Hubberten et al. 1975). For the active volcano White Island, New Zealand Giggenbach and Robinson (1976) found δ³⁴S-values between +1‰ and +9‰, the low values being observed during high-temperature periods. The high values measured for the low-temperature periods are considered to be due to the kinetically controlled precipitation of isotopically light elemental sulfur in the fumaroles. Native sulfur, which usually has higher δ³⁴S-values than 0‰, could fractionate into heavy sulfate and light H₂S through reactions such as



3.4.5 Thermometers in Geothermal Systems

Although there are many isotope exchange processes occurring within a geothermal fluid which have the potential to provide thermometric information, only a few have been generally applied, because of suitable exchange rates for achieving isotopic equilibrium (Hulston 1977; McKenzie and Truesdell 1977; Panichi et al. 1977; Sakai 1977; Panichi and Gonfiantini 1978; Truesdell and Hulston 1980; Giggenbach 1982).

In a single geothermal system several different reservoirs may exist which generally increase in temperature with depth. The presence of such reservoirs at different temperatures may be indicated by different isotope thermometers equilibrating at different rates. The reaction rates of these exchange reactions determine whether they will equilibrate in deep geothermal reservoirs or if they will reequilibrate in shallower reservoirs. Some isotopic reactions appear not to equilibrate at temperatures below 350 °C, whereas others equilibrate so rapidly that only the temperature of collection is indicated (see Table 21).

Figure 30 summarizes the calculated fractionation factors as a function of temperature for some gases of geologic interest (after Richet

Table 21. Isotope temperature and rates of exchange to establish equilibrium for the hydrothermal fluid at Wairakei, New Zealand (Hulston 1977)

Element	Species	Isotope temperature	Rates of exchange
C	$^{13}\text{CH}_4 - ^{12}\text{CO}_2$	350 °C	$10^2 - 10^5$ y
S	$\text{H}^{34}\text{SO}_4 - \text{H}_2^{32}\text{S}$	350 °C	10^3 y
O	$\text{S}^{16}\text{O}_4 - \text{H}_2^{18}\text{O}$	280 °C	1 y
H	$\text{H}_2 - \text{HDO}$	260 °C	1-2 weeks
	Drill hole temperature	260 °C	

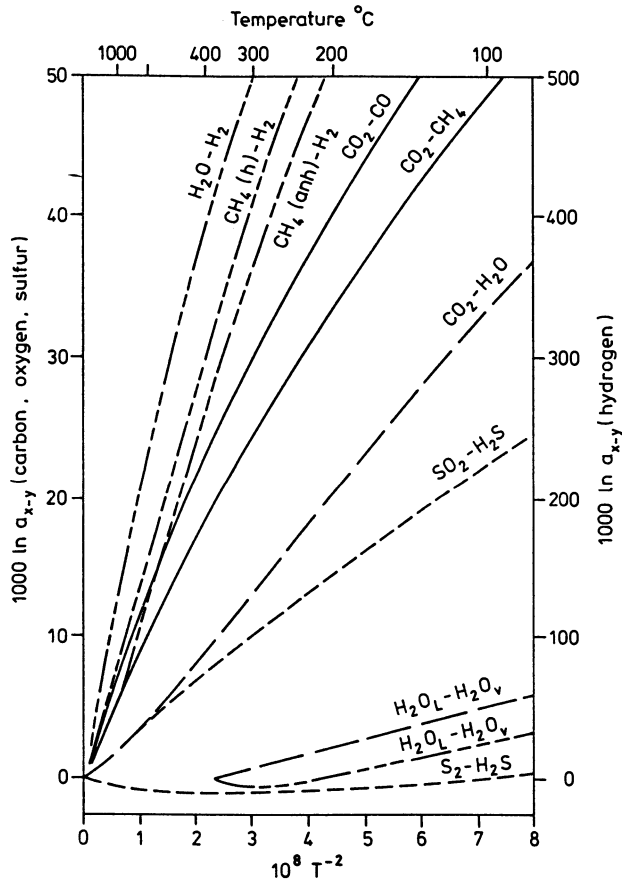
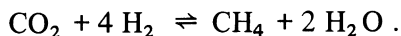


Fig. 30. Calculated equilibrium hydrogen, carbon, oxygen, and sulfur isotope fractionation factors as a function of temperature for some gases of geological interest. (After Richet et al. 1977, in Sheppard 1984)

et al. 1977, from Sheppard 1984) and the following paragraphs discuss the details of the more common geothermometers.

CO_2-CH_4 . This thermometer was the first to be applied (Craig 1953; Hulston and McCabe 1962) on the basis of the exchange reaction:



These early workers postulated close agreement between actually measured underground temperatures and isotope temperatures. However, more recently it became apparent that calculated temperatures are frequently much higher than those measured at the base of the geothermal wells (Ellis 1979; see also Table 21).

Giggenbach (1982) demonstrated that the observed $\Delta_{CO_2-CH_4}$ values are likely to represent frozen-in compositions attained after minimum residence times of 20 Ka at 400 °C or 10 Ma at 300 °C.

Hydrogen Isotope Geothermometers. At least five hydrogen-containing gases (H_2O , H_2S , H_2 , CH_4 , and NH_3) occur in major amounts in geothermal fluids. Of the various possible geothermometers only two have been widely used: (1) hydrogen-water and (2) hydrogen-methane. Arnason (1977) measured δD -values of hydrogen gas and water from drill holes and hot springs of Iceland. He found excellent agreement with measured downhole temperatures in most areas. In other regions variable degrees of reequilibration between the reservoir and the sampling point seem to occur (Lyon 1974a,b; Kiyosu 1983). Kiyosu (1983) observed that the hydrogen from low-temperature fumarolic gases (~ 100 °C) in northeastern Japan is lighter than from hot-water dominated geothermal gases from Iceland, which suggests that the hydrogen in low-temperature volcanic gases have equilibrated with water vapor at temperatures between 200°–400 °C.

The exchange for H_2-CH_4 is probably slower than that for H_2-H_2O . This has been found by a comparison of temperatures in Yellowstone Park and Broadlands, New Zealand samples (Lyon 1974b).

Oxygen Isotope Geothermometers. These geothermometers have the basic disadvantage that by far the largest oxygen reservoir is contained in the water itself and boiling during ascent produces isotope fractionation. Nevertheless, the most “well-behaved” geothermometer appears to be the sulfate-water system (McKenzie and Truesdell 1977; Sakai 1977; Truesdell and Hulston 1980). The exchange reaction is both suf-

ficiently rapid to attain equilibrium and sufficiently slow to retain the indication of temperatures above 300 °C. Another oxygen geothermometer is the CO₂–H₂O pair, which has been applied with apparent success at Lardarello, Italy (Panichi et al. 1977). In those uncommon systems where both steam and water can be sampled separately the water-steam geothermometer can be useful (Truesdell and Hulston 1980).

Sulfur Isotope Geothermometers. Large isotope fractionations occur between oxidized and reduced sulfur species, namely between H₂S and HS⁻ and between SO₂, SO₄²⁻, and HSO₄⁻. In laboratory studies the exchange between H₂S or HS⁻ and HSO₄⁻ and SO₄²⁻ has been found to be very fast under acid conditions and very slow under alkaline conditions (Thode et al. 1971; Robinson 1973, 1978). Thus, the application of sulfur isotope geothermometers requires an estimate of the pH of the fluid. Using the SO₄²⁻–H₂S fractionation factors of Robinson (1973), the temperature in the Wairakei geothermal system is about 350 °C (see Table 21).

3.5 Ore Deposits

Stable isotope analyses provide the best geochemical data available for discerning the origin of the ore fluid, the sulfur, and the carbon species involved in ore deposition.

Of particular importance has been the ability to identify sources of water in hydrothermal ore deposits by their hydrogen and oxygen isotope ratios. The major isotopic characteristic of hydrothermal fluids is that, at a given locality, there is commonly a wide range in δ¹⁸O, but a narrow range in δD-values. We, thus, find the relationship for hot springs, shown in Fig. 30, where waters have undergone an ¹⁸O-enrichment at more or less constant H-isotope compositions.

3.5.1 Origin of Ore Fluids

Ore fluids may be generated in a variety of ways. With respect to their isotopic composition five end-member components may be defined (see Fig. 31):

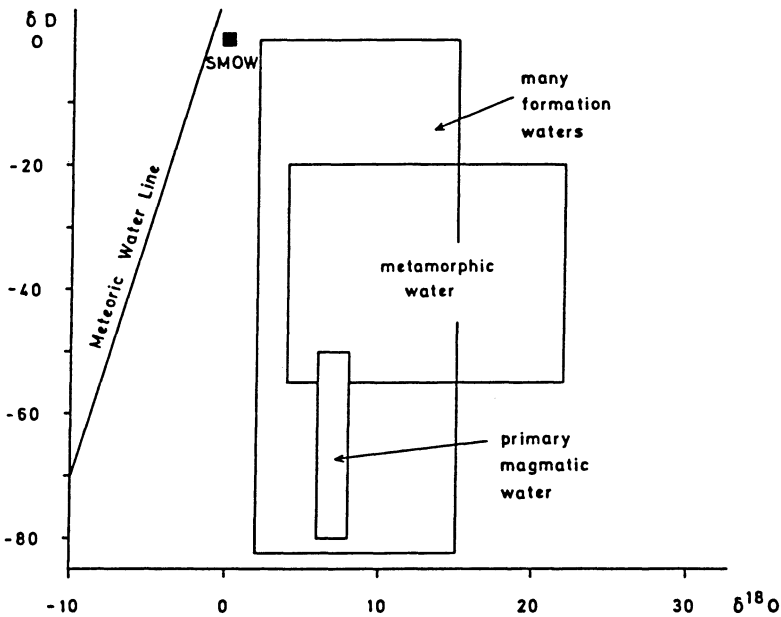


Fig. 31. Plot of δD versus $\delta^{18}O$ of waters of different origin

1. meteoric waters;
2. ocean water;
3. formation waters;
4. metamorphic waters;
5. magmatic waters.

Waters (1), (2), and (3) can be obtained as actual samples and measured isotopically. Waters (4) and (5) normally cannot be measured directly, except for fluid inclusions present in certain minerals such as quartz, but can be calculated from the analysis of hydroxyl minerals if the fractionation factors between the mineral and water and the temperature of formations are known.

1. Heated meteoric waters are a major constituent of the ore-forming fluids in many ore deposits and may become dominant in the latest stages of ore deposition. O'Neil and Silberman (1974), for instance, demonstrated that epidermal Au–Ag vein deposits of the Great Basin, Nevada are probably exclusively deposited from meteoric waters. The majority of vein minerals from these deposits have very low $\delta^{18}O$ -values, whereas the D-values of fluid inclusions are *uniformly* low with

a range from -90 to -140‰ identical to that of recent spring waters in the area.

2. Many volcanogenic massive sulfide deposits are formed in submarine environments from heated oceanic waters. This concept gains support from the recently observed hydrothermal systems at ocean ridges, where the actually measured fluids show a slightly modified isotopic composition relative to 0‰ . Bowers and Taylor (1985) have modelled the δD - and $\delta^{18}\text{O}$ -values of the evolving hydrothermal solution. At low temperatures the $\delta^{18}\text{O}$ of the fluid decreases relative to ocean water because the alteration products in the oceanic crust are ^{18}O -rich. At around $250\text{ }^{\circ}\text{C}$ the solution is back to its initial value of seawater. Further reaction with basalt at 350° increases the modified seawater to 2‰ . The δD of the solution increases at all temperatures because mineral-water fractionations are nearly all less than zero. At $350\text{ }^{\circ}\text{C}$ the δD -value of the solution is 2.5‰ . The best documented example for the role of ocean water during ore deposition is for the Kuroko-type deposits (see the extensive monograph by Ohmoto and Skinner 1983: *Econ. Geol. Monogr.* 5).

3. Connate and formation waters tend to increase in salinity as well as in temperature as they descend. During descent their ability to extract and transport metal increases as their chlorinity increases. One type of ore deposit which is associated with connate waters is the Mississippi-Valley-type ore deposit (Pinckney and Rye 1972; Heyl et al. 1974). More details about the isotopic composition of formation waters is discussed on p. 129.

A special type of water has been introduced by Charef and Sheppard (1986): "organic water" which is defined to be water whose deuterium content at least is derived from transformations of organic compounds during thermal maturation. Its D/H ratio is predicted to be very similar to that of the organic precursor material as fractionations during biodegradation and oxidation reactions are generally quite small. Charef and Sheppard (1986) postulated that organic water should have δD -values below -90‰ . Such organic waters may play an important role during the dewatering of sedimentary basins, transporting probably both metals and sulfur.

4. Metamorphic waters are generated by dehydration reactions. This process occurs not only in metamorphic rocks, but also in altered wall rocks accompanying many ore deposits. Typical ore deposits formed by the action of metamorphic fluids are skarn deposits. Combined petrologic and stable isotope studies by Taylor and O'Neil (1977),

Brown et al. (1985), and Bowman et al. (1985) have helped to resolve the complexities of formation. For instance, Bowman et al. (1985) concluded that meteoric water was unimportant during the main stage of skarn formation and that decarbonation of marble could supply the needed ^{18}O -rich fluid to mix with magmatic water. Into the category of metamorphic waters belong also the hydrothermal fluids that deposited gold-bearing quartz veins. These fluids are generally heavy, have $\delta^{18}\text{O}$ -values between 8 and 14 and δD -values between -10 and -50‰ (Kerrick 1980; Marshall and Taylor 1981; Böhlke and Kistler 1986), and appear to owe their characteristics to deep crustal sources.

5. The isotopic composition of magmatic water has already been discussed on p. 98f. The classical theory of a hydrothermal solution arising from a cooling magma remains a reasonable explanation for many ore deposits. Fluids associated with porphyry copper and molybdenum deposits show the clearest evidence for a dominant magmatic water compound (Sheppard et al. 1971; Rice et al. 1985). Some involvement of nonmagmatic waters is indicated during ore-emplacment stages and became dominant during postore stages. Isotopic evidence supports a genetic model in which a magmatic-hydrothermal system is surrounded by a cooler meteoric-hydrothermal system that collapses inward and downward as the magmatic-hydrothermal system cools.

3.5.2 Wall Rock Alteration

Information on the origin and genesis of ore deposits can also be obtained by analyzing the alteration products in wall rocks. Delineation of hypogene and supergene ore deposits is possible by stable isotope analysis of the ores and associated alteration products. Because temperatures and isotopic compositions of the hydrothermal fluids are variable, hydrothermal clays exhibit a large scatter of points on a plot of δD versus $\delta^{18}\text{O}$ (see Fig. 32). All supergene clays plot either on the "Kaolinite Line" or slightly to the left of it. This is explained by slightly higher temperatures of formation than those occurring during surface weathering. Note that not only do supergene clays correlate with the Meteoric Water Line, but hypogene clays also correlate. This indicates that meteoric water was also a dominant constituent in the hypogene-hydrothermal system.

Whole rock $\delta^{18}\text{O}$ -data in alteration halos can be used as an exploration guide for volcanogenic massive sulfide deposits (Green et al. 1983).

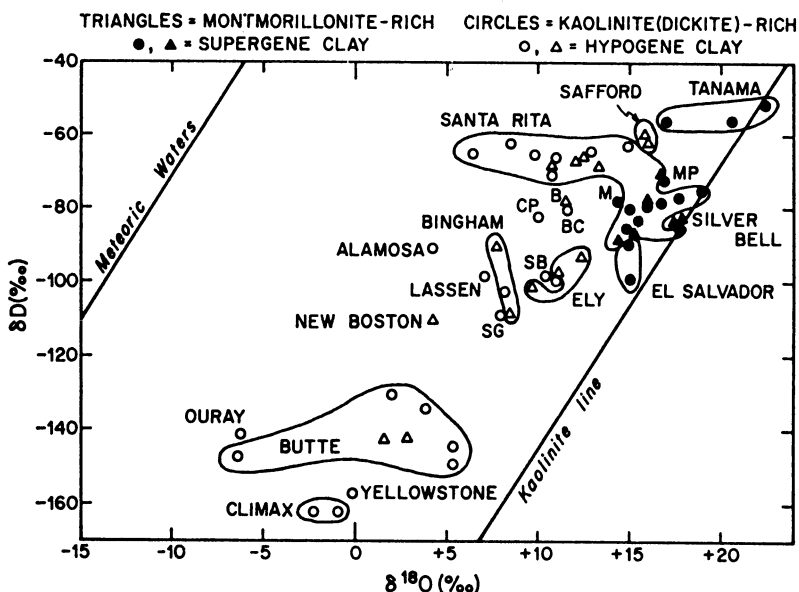


Fig. 32. δD versus $\delta^{18}O$ for hypogene and supergene clay minerals from various ore deposits (Taylor 1974a)

According to the generally accepted model for this type of deposit, the ore-forming fluid passes through the submarine sediment-volcanic section, emerges into the ocean, and precipitates the ore at or near the ocean floor. The conduit of altered rocks is thus subjected to large water fluxes, producing intense hydrothermal alteration and generally causing a depletion in $\delta^{18}O$ -values. Thus, fossil hydrothermal conduits can be outlined by following the zones of ^{18}O -depletion. If a set of alteration zones has been mapped from field and petrographic data, $\delta^{18}O$ -values might indicate zones of greatest water fluxes and of temperatures most appropriate for ore deposition. Oxygen isotope data are especially valuable in rock types which do not show diagnostic alteration mineral assemblages as well as those in which the assemblages have been obliterated by subsequent metamorphism (Beaty and Taylor 1982). In another example, Criss et al. (1985) found excellent spatial correlations between low $\delta^{18}O$ -values and economic mineralizations. Such empirical spatial associations of mineralization with zones having anomalous low $\delta^{18}O$ -values may be a useful guide for exploration of hydrothermal ore deposits.

3.5.3 Sulfur Isotope Composition of Hydrothermal Ore Deposits

A huge amount of literature exists on the sulfur isotope composition in hydrothermal ore deposits. Some of these data are discussed in the first and second editions of this book and, therefore, are not repeated here. Of the numerous papers on the subject the reader is referred to extensive reviews by Rye and Ohmoto (1974), Ohmoto and Rye (1979), and Nielsen (1978, 1979, 1985a). The basic principles to interpret the meaning of $\delta^{34}\text{S}$ -values in sulfidic ores were elucidated by Sakai (1968), which have been subsequently extended and clarified by Ohmoto (1972).

The major factors which control the sulfur isotope composition in hydrothermal ore deposits are:

1. Temperature which determines the fractionations between sulfur-bearing minerals. This point has been already discussed on p. 54 and is not further elucidated here.
2. The source of the sulfur, which can only be traced on the basis of the isotopic composition of the *total* sulfur in an ore deposit. $\delta^{34}\text{S}_{\Sigma\text{S}}$ can be grouped into three categories:
 - a) deposits with $\delta^{34}\text{S}$ -values near zero should derive their sulfur from igneous sources, including sulfur released from magmas and sulfur leached from sulfides in igneous rocks;
 - b) deposits with $\delta^{34}\text{S}$ -values near 20‰ should derive their sulfur from ocean water;
 - c) deposits with $\delta^{34}\text{S}$ -values between 5 and 15‰ may receive their sulfur from local country rocks or from mixtures of (a) and (b).
3. Ohmoto (1972) has demonstrated that the p_{H} -value of the ore-forming fluid and the proportions of oxidized and reduced sulfur species may be of crucial importance when interpreting $\delta^{34}\text{S}$ -values in hydrothermal ore deposits.

Let us first consider the effect of p_{H} increase due to the reaction of an acidic fluid with carbonatic host rocks. At $p_{\text{H}} = 5$ practically all of the dissolved sulfur is undissociated H_2S , whereas at $p_{\text{H}} = 9$ the dissolved sulfide is almost entirely dissociated. Since H_2S concentrates ^{34}S relative to the dissolved sulfide ion, a p_{H} increase means an increase in the $\delta^{34}\text{S}$ of precipitated sulfides. Thus, when the p_{H} of an ore fluid increases from 5 to 9 during migration through the site of ore deposition, an increase in $\delta^{34}\text{S}$ should be observed between early precipitated and later precipitated sulfide minerals. At 250 °C the

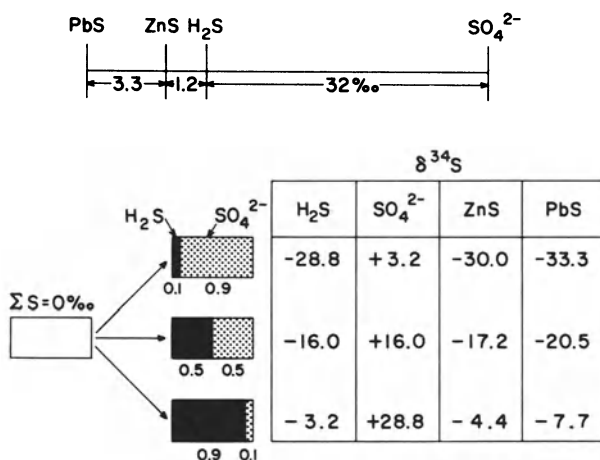


Fig. 33. Variation of $\delta^{34}\text{S}$ of H_2S , sulfate, and sulfide minerals with variation in the $\text{H}_2\text{S}/\text{SO}_4^{2-}$ ratio of the hydrothermal solution ($T = 200^\circ\text{C}$, $\delta^{34}\text{S}_{\Sigma\text{S}} = 0\text{‰}$) (Rye and Ohmoto 1974)

H_2S , $\text{HS}^-/\text{S}^{2-}$ ratios at pH values of 6, 7, and 8 are approximately 80:20:0, 35:35:30, and 5:25:70, respectively, and the corresponding $\delta^{34}\text{S}$ -increase is $\sim 1\text{‰}$, $\sim 3.5\text{‰}$, and $\sim 5\text{‰}$.

An increase in oxygen fugacities has a much stronger effect on the $\delta^{34}\text{S}$ -values than a pH change, because of the large isotope fractionation between sulfate and sulfide. An illustration of how the sulfur isotopic composition of sulfur-containing phases are affected by the chemistry of fluids is given in Fig. 33. It is assumed that the isotopic composition of the total sulfur is 0‰ , the temperature 200°C , and that the ratio of H_2S to SO_4^{2-} changes from 1/9 to 9/1. $\delta^{34}\text{S}$ -values of each aqueous sulfur species varies as a function of the $\text{H}_2\text{S}/\text{SO}_4^{2-}$ ratio (e.g., $\delta^{34}\text{S}_{\text{H}_2\text{S}}$ from -28.8‰ to -3.2‰), but differences between $\delta^{34}\text{S}$ -values of coexisting sulfur phases remain constant.

Figure 34a summarizes the stability fields of some important sulfur species at 250°C in a $\text{pH}-f_{\text{O}_2}$ diagram. The transition field between the predominance of reduced and oxidized sulfur species is restricted to one decade of the f_{O_2} value. The $\delta^{34}\text{S}$ -values at points A, B, C, and D are presented in Fig. 34b which indicates that changes of f_{O_2} have drastic effects on the sulfur isotopic composition. Magmatic sulfur with a total sulfur isotope composition of zero may yield very light sulfides, which are otherwise typical for biogenic sulfur (situation A), whereas a hydrothermal fluid with sulfur of seawater origin may yield

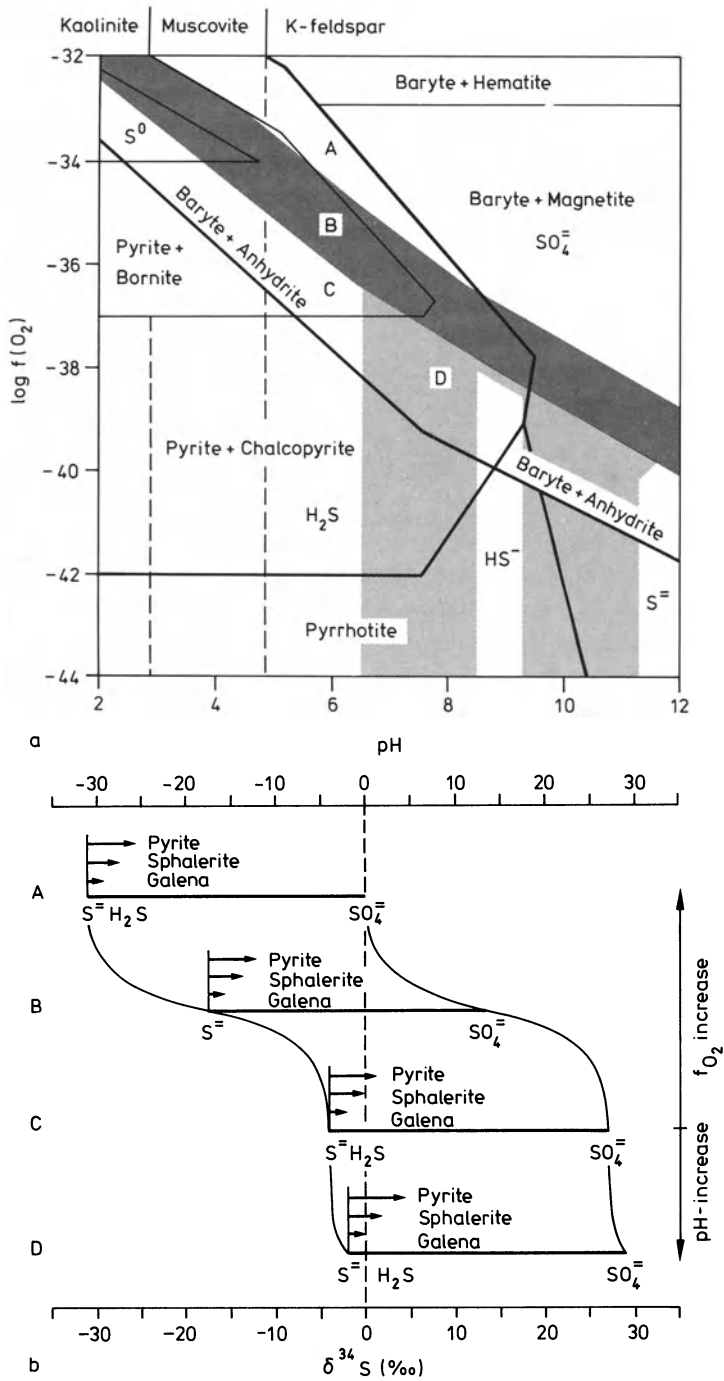


Fig. 34. a Stability fields of sulfur phases in a pH- $\log f_{O_2}$ diagram at 250 °C for $\Sigma S = 0.1$ and $Ba^{2+} = 10^{-3}$ mol kg $^{-1}$ (Nielsen 1985a). b $\delta^{34}S$ -values of sulfides and sulfate at 250 °C. Letters refer to those in a (Nielsen 1985a)

sulfides typical for magmatic sulfur (situation C and D). Figure 34 indicates clearly that the source of sulfur in hydrothermal fluids can only be traced when one has a knowledge of the $p_H-f_{O_2}$ relationships in an ore deposit.

Up to this point chemical and isotopic equilibrium among the ore-forming fluid and the precipitating sulfides and sulfate has been tacitly assumed. However, there is increasing evidence that isotopic disequilibrium is more common than originally assumed (Shelton and Rye 1982). Under such conditions of isotopic disequilibrium $\delta^{34}\text{S}$ -values do not respond to changes in the chemical environment of ore deposition as described above.

It is a well-known fact that at temperatures below $\sim 350^\circ\text{C}$ sulfide-sulfate mineral pairs do not attain isotopic equilibrium during the coprecipitation of sulfate and sulfide minerals (Ohmoto and Lasaga 1982; Shelton and Rye 1982). Obviously, sulfide minerals approach isotopic equilibrium with an H_2S -bearing fluid more quickly than aqueous sulfate and H_2S equilibrate. A similar relationship is commonly observed for aqueous sulfate-sulfide pairs in geothermal fluids (Robinson 1978). Ohmoto and Lasaga (1982) have computed the rate constants from experimental data and demonstrated that they are strongly dependent on temperature and p_H , but in a very complex manner. They suggested that mixing of sulfide-rich solutions with sulfate-rich solutions at or near the depositional sites may explain many of the observed fractionations.

In the following section a few examples of hydrothermal sulfide ore deposits of general interest are discussed.

Recent Sulfide Deposits at Mid-ocean Ridges. Recent sulfide deposits have been identified on the East Pacific Rise off Mexico at 21°N and at the Galapagos Rift at 86°W . There are two possible primary sources for the sulfur in these vents: reduction of seawater sulfate and a mantle source, either as a direct magmatic contribution or indirectly during the leaching of the basaltic host rocks in the hydrothermal system. Studies by Styr et al. (1981), Arnold and Sheppard (1981), Skirrow and Coleman (1982), Kerridge et al. (1983), and Zierenberg et al. (1984) show that the $\delta^{34}\text{S}$ -values are enriched in ^{34}S relative to a mantle source, implying the addition of sulfide derived from seawater. $\delta^{34}\text{S}$ -values from the East Pacific Rise deposits range from 1.3 to 4.1‰, which may be interpreted to indicate that the sulfides received a 10% seawater sulfate contribution to 90% derived from the leaching of basalt.

At the Galapagos Rift Skirrow and Coleman (1982) found somewhat higher $\delta^{34}\text{S}$ -values between 5.4 and 6.3‰ implying that the seawater contribution was more dominant than at the East Pacific Rise. Thus, there is agreement that both sources must be involved in the formation of these deposits, however, the relative importance of the two sources is still under debate.

Porphyry Copper Deposits. From δD - and $\delta^{18}\text{O}$ -measurements it has been concluded that porphyry copper deposits show the clearest affinity of a magmatic water imprint (Taylor 1974a). Many porphyry type copper deposits have been investigated for their sulfur isotope composition, but only Field and Gustafson (1976) and Shelton and Rye (1982) have taken a detailed look at the relationship between the sulfur isotopic composition of coexisting sulfates and sulfides. The majority of the $\delta^{34}\text{S}$ -values of the sulfides and sulfates in porphyry deposits fall between -3 and +1‰ and between +8 and +15‰, respectively. The calculated sulfate-sulfide equilibrium isotope temperatures lie typically between 450° and 650 °C and agree with temperatures estimated from other methods. Thus, the sulfur isotope data and temperatures seem to support the magmatic origin of the sulfur in porphyry deposits. This view was, however, questioned by Shelton and Rye (1982) who argued that sulfur isotope disequilibria between aqueous sulfate and H_2S may be an important feature of porphyry copper ore formation and may reveal remobilization of earlier precipitated ores as well as record changes in the chemistry of the ore-forming fluid.

Vein-Type Deposits. A wide spectrum of ore deposits of a different nature occurs in this category. Rye and Ohmoto (1974) have demonstrated the difficulty in interpreting the genesis of an ore body from the observed $\delta^{34}\text{S}$ -ranges. The only meaningful classification seems to be related to the temperature of the ore deposition. Vein deposits, due to their vertical extent, frequently exhibit a pronounced isotope zoning. Differences in $^{34}\text{S}/^{32}\text{S}$ ratios may result from temperature differences and from an increase in f_{O_2} or p_{H} toward the upper level. In many of these deposits the sulfur appears to have been derived from igneous sources and the sulfides were precipitated under $p_{\text{H}}-f_{\text{O}_2}$ conditions where H_2S was the dominant sulfur species.

Stratabound Deposits. Stratabound deposits are those confined to a single or a small number of stratigraphic units. They can be divided into

two main categories, those enclosed in predominantly marine sedimentary rocks (carbonates and shales) and those enclosed in predominantly marine volcanic rocks or volcanoclastic sediments. Stratabound deposits in volcanic rocks are generally thought to be related to submarine volcanism and formed at or near the ocean water-rock interface. Reviews by Sangster (1968, 1976) and Nielsen (1985b) showed that the $\delta^{34}\text{S}$ -values of sulfides in these volcanic deposits are typically positive with a relatively narrow spread and that generally sulfide is depleted by about 15‰ in ^{34}S relative to the contemporaneous seawater sulfate.

The sulfur isotope data for most volcanic stratabound deposits are best explained by a mechanism in which ocean water became an ore-forming fluid by various degrees of reduction of its sulfate while in contact with hot volcanic rocks. The $\delta^{34}\text{S}$ -values of sulfate minerals, when present in the volcanic stratabound ores, are larger than those of contemporaneous seawater, as would be expected when seawater sulfate is partially reduced at temperatures above 250 °C in equilibrium with sulfides.

Biogenic Deposits. The discrimination between bacterial and inorganic sulfur in ore deposits on the basis of $\delta^{34}\text{S}$ -values is rather complex. The best criterion to distinguish between both types is the internal spread of δ -values. If individual sulfide grains at a distance of only a few millimeters or centimeters exhibit large and nonsystematic differences in δ -values, then it seems to be safe to assume an origin involving bacterial sulfate reduction. Irregular δ -variations are obviously due to bacteria growing in reducing microenvironments around individual particles of organic matter. In contrast, inorganic sulfate reduction would need a considerable supply of thermal energy by an ascending hot fluid. Such an environment is not consistent with bacterial reduction in a small-scale, closed system.

Unfortunately, this discrimination can only be successfully applied in deposits that have not been overprinted by later metamorphic events, which tend to homogenize the nonequilibrium δ -differences over very short distances. Two types of deposits, where the internal S-isotope variations fit the expected scheme of bacterial reduction, but where the biogenic nature was already known earlier from conventional geological analysis, are the "sandstone-type" uranium mineralization in the Colorado Plateau (Warren 1972) and the Kupferschiefer in Central Europe (Marowsky 1969).

Metamorphosed Deposits. It is generally assumed that metamorphism reduces the isotopic variations in a sulfide ore deposit. Recrystallization, liberation of sulfur in fluid and vapor phases, such as the breakdown of pyrite into pyrrhotite and sulfur, and diffusion at elevated temperatures should tend to reduce initial isotopic heterogeneities. However, Willan and Coleman (1983) were able to demonstrate that sulfide and sulfate minerals have not reequilibrated over distances of ~ 1 cm during greenschist or amphibolite facies metamorphism. They concluded that the variations found in sulfide deposits of the Dalradian metamorphic terrain, Scotland represent primary variations of the sulfur source.

3.5.4 Hydrothermal Carbonates


Similar to sulfur, the isotopic composition of carbon in hydrothermal carbonates depends not only on the $\delta^{13}\text{C}$ -value of the total carbon in the ore-forming fluid, but also on the oxygen fugacity, the pH, the temperature, the ionic strength of the fluid, and on the total concentration of carbon (Ohmoto 1972; Rye and Ohmoto 1974). The oxygen fugacity affects the oxidation states of the carbon species. If the oxygen fugacity is about 10^{-38} atm, most of the carbon is oxidized and the reduced carbon is negligible. However, at lower oxygen fugacities the reduced carbon increases in abundance and has a dramatic effect on the $\delta^{13}\text{C}$ -values of the coexisting carbonate species because the reduced carbon is strongly enriched in ^{12}C . Similarly, at a fixed f_{O_2} value, the $\delta^{13}\text{C}$ of the oxidized carbon varies with p_{H} because of the changing abundances of the HCO_3^- and CO_3^{2-} ions in aqueous solution.

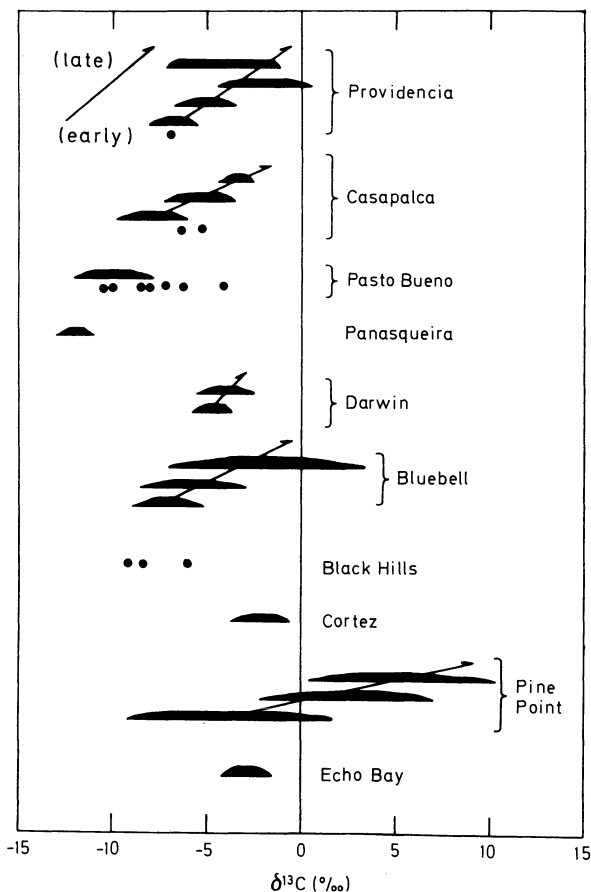
Carbon in hydrothermal systems could originate from three different sources:

1. marine limestones which have average $\delta^{13}\text{C}$ -values near zero;
2. deep-seated carbon with a range in $\delta^{13}\text{C}$ -values between -8‰ and -5‰ (see p. 82);
3. organic carbon from sedimentary rocks with $\delta^{13}\text{C}$ -values typically lower than -20‰ .

Considering the carbon isotope composition in more detail, Fig. 35 shows the variation of $\delta^{13}\text{C}$ -values of carbonate gangue minerals for a number of hydrothermal ore deposits. The different generations of carbonates are arranged from early to late as shown by arrows in Fig. 35. Most early carbonates have $\delta^{13}\text{C}$ -values between -7 and -5‰ which

Fig. 35. $\delta^{13}\text{C}$ -values of carbonates from various hydrothermal ore deposits. Different generations of carbonate are arranged from early to late (Rye and Ohmoto 1974)


 Carbonates
 • Fluid inclusion



may indicate a deep-seated origin of the carbon. However, such δ -values can also be generated by simple mixing between carbonate-derived and organically-derived CO_2 . Late-stage carbonates may show an enrichment in the heavy isotope relative to the main-stage carbonates as a result of (1) cooling of the ore fluid, (2) decreasing CO_2/CH_4 ratios in the fluid, and/or (3) increasing contribution of CO_2 from other sources.

3.6 Hydrosphere

First, some definitions concerning water of different origin are given.

The term “*meteoric*” applies to water that has gone through the meteorological cycle, i.e., evaporation, condensation, and finally pre-

precipitation. All continental surface waters, such as rivers, lakes, and glaciers, fall into this general category. Because meteoric water may seep into the underlying rock strata, it will also be found at various depths of the lithosphere. The *ocean*, although it continuously receives the continental run-off of meteoric waters as well as rain, is not regarded as being of meteoric nature. *Connate* water is “fossil” water, which has been trapped in the sediments at the time of burial. *Formation* water is present in rocks immediately before drilling and may be a useful nongenetic term for waters of unknown age and origin.

3.6.1 Meteoric Water

The natural water cycle has been compared to a multiple-stage distillation column with reflux of the condensate to the reservoir (Epstein and Mayeda 1953; Siegenthaler 1979). The oceans correspond to the reservoir, and the ice fields at the poles correspond to the highest stages of the column. In all processes concerning the evaporation and condensation of water the hydrogen isotopes are fractionated in proportion to the oxygen isotopes, because a corresponding difference in vapor pressures exists between H_2O and HDO in one case and H_2^{16}O and H_2^{18}O in the other. Therefore, the hydrogen and oxygen isotope distributions are correlated in meteoric waters. Craig (1961a) first defined the following relationship:

$$\delta D = 8 \delta^{18}\text{O} + 10,$$

which describes the interdependence of H- and O-isotope ratios in meteoric waters.

This relationship, shown in Fig. 36, is generally described as the “Meteoric Water Line”. Neither the numerical coefficient 8 nor the constant 10, also called the deuterium excess “d”, are really constant. Both vary with the conditions of evaporation, vapor transport, and precipitation and thus offer insight into climatic processes. Based on the “deuterium excess”, Leguy et al. (1983) were able to separate rain waters from the Negev desert into three groups. These authors postulated that the two extreme groups, one has “deuterium excess” values above 22, the other has values less than 10‰, have quite different origins. The intermediate group, to which the majority of cases belong, seem to represent some combination of the two extreme groups.

Thus, the study of the deuterium excess “d”, introduced originally by Dansgaard (1964), promises to be a source of additional climatic

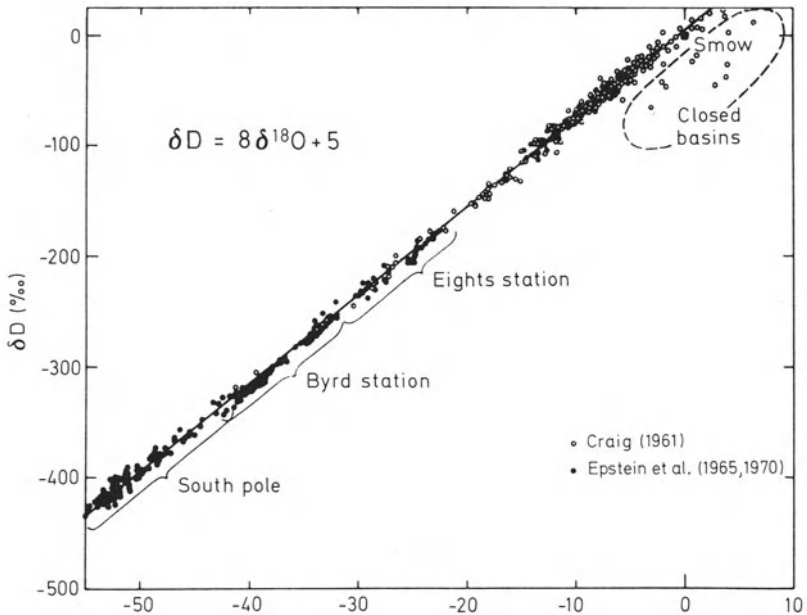


Fig. 36. δD versus $\delta^{18}O$ for various meteoric surface waters (Taylor 1974a)

information. Harmon and Schwarcz (1981) noted a shift of about 10‰ in the “d” value for meteoric waters in North-Central North America between interglacial and glacial times and Jouzel et al. (1982) interpreted the decrease of “d” in an Antarctic ice core from about 9‰ in the recent interglacial to 4.5‰ during full glacial conditions as indicating a 10% increase in relative humidity during glacial times.

Atmospheric precipitation generally follows a Rayleigh process at liquid-vapor equilibrium. The atmospheric Rayleigh process also explains why, at higher altitudes and latitudes, fresh waters become progressively lighter isotopically, whereas tropical waters show very small depletions relative to ocean water. Gat (1980) has pointed out some serious problems with this simple Rayleigh distillation model, namely that:

1. the meteorological pattern of air movement is not consistent with a gradual poleward movement of low-latitude air masses;
2. the latitudinal “distillation column” is certainly not closed, additional evaporation over middle- and high-latitude oceans, as well as over continents occurs;

3. the mathematical solution of a simple Rayleigh-type process does not predict a straight line, such as the meteoric water line, especially in its terminal stages (i.e., polar snow);
4. according to the Rayleigh model, the isotopic composition of precipitation depends only on the composition of the vapor and the temperature of condensation. However, evaporation and isotope exchange with water vapor *after* condensation also affects the isotopic composition.

Nevertheless, the distillation model describes the isotopic composition of rain water in qualitative terms, if not in quantitative terms.

As already mentioned several times, when water evaporates from the surface of the ocean, the water vapor is enriched in H and ^{16}O because $\text{H}_2\ ^{16}\text{O}$ has a higher vapor pressure than HDO and $\text{H}_2\ ^{18}\text{O}$. Under equilibrium conditions at $25\ ^\circ\text{C}$ the fractionation factors for evaporating water are 1.0092 for ^{18}O and 1.074 for D (Craig and Gordon 1965). However, under natural conditions, the actual isotopic composition of water vapor is significantly more negative than the predicted equilibrium values, which is due to kinetic effects (Craig and Gordon 1965). Vapor leaving the surface of the ocean cools as it rises and rain forms when the dew point is reached. During the outraining of the moist air mass, the vapor is continuously depleted in the heavy isotopes, because the rain leaving the system is enriched in ^{18}O and D. If the air mass moves poleward and becomes cooler, additional rain will form having less ^{18}O than the first rain. This relationship is schematically shown in Fig. 37.

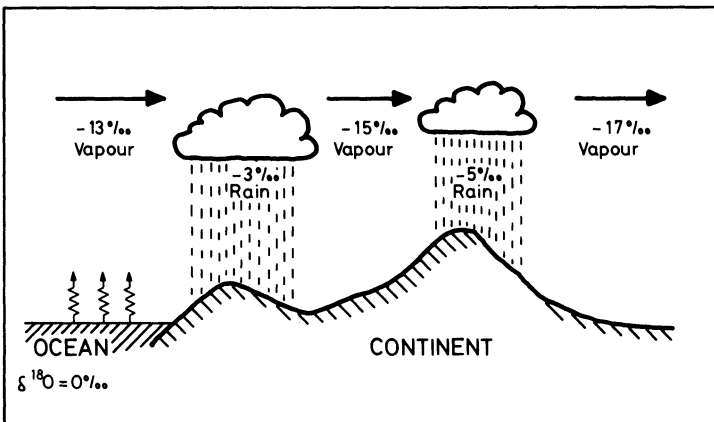


Fig. 37. Schematic fractionation in the atmospheric water cycle (Siegenthaler 1979)

The global distribution of D and ^{18}O in rain has been monitored since 1961 through a network of stations (Yurtsever 1975). From this extensive data base it can be deduced how geographic factors influence the isotopic composition of precipitation. Besides the dominant temperature effect, a latitude, an altitude, and an amount effect can be distinguished (Dansgaard 1964).

Marine precipitation at any given latitude is more ^{18}O -rich than continental precipitation. In the absence of any land masses, $\delta^{18}\text{O}$ -values of precipitation can be expected to be near -1‰ at the equator and to diminish to about -5‰ at about 30°N or S latitude. At latitudes greater than 30° the rate of ^{18}O -exchange with latitudes increases by about a factor of 4. In continental areas, the latitude effect is roughly 0.5‰ per degree latitude (Dansgaard 1964). The altitude effect, which also favors the light isotopes, depends on local climate and topography, but gradients of $0.15\text{--}0.5\text{‰}$ $\delta^{18}\text{O}/100\text{ m}$ are typical (Gat 1980).

Besides a latitude and an altitude effect there is an “amount effect” in areas of high rainfall. Dansgaard (1964) observed that for each 100 mm increase in rainfall the value of $\delta^{18}\text{O}$ decreased by about 1.5‰ . This “amount effect” is ascribed by Dansgaard (1964) to deep cooling of the air in heavy rainfall with only slight enrichments possible in later evaporation.

Our knowledge of the isotopic variations in precipitation will certainly be increased when short-term variations are analyzed from local stations. Especially under midlatitudinal weather conditions such short-term variations arise from varying contributions of tropical, polar, marine, and continental air masses and these in conjunction with other weather data should provide important climatic information.

Isotope variations in discrete meteorological events can be studied by analyzing hailstones, because they keep a record on the internal structure of a cloud. Jouzel et al. (1975) concluded that hailstones grow during a succession of upward and downward movements in a cloud.

Deviations from the Meteoric Water Line tend to lie on the right-hand side of the line, i.e., toward low δD and/or high $\delta^{18}\text{O}$ values (Craig 1961a; Clayton et al. 1966). These deviations are typically observed in lakes and other water bodies subjected to intense evaporation. In contrast to condensation, evaporation mostly takes place under kinetic conditions, especially when the relative humidity is significantly less than 100%. Thus, in dry climates such as in the Sahara Desert, $\delta^{18}\text{O}$ -values as high as $+31\text{‰}$ and δD -values as high as $+129\text{‰}$ have been measured (Fontes and Gonfiantini 1967).

Snow and Ice Stratigraphy. The isotopic composition of snow and ice deposited in the polar regions and at high elevations in mountains depends primarily on the temperature. Snow deposited during the summer has less negative $\delta^{18}\text{O}$ - and δD -values than snow deposited during the winter. A good example of the seasonal dependence has been given by Deutsch et al. (1966) on an Austrian glacier, where the mean δD -difference between winter and summer snow was observed to be -14‰ . Systematic ^{18}O - and D-measurements have been used to study flow patterns of glaciers, snow accumulation rates, and climatic variations. Isotope profiles through a glacier should give lighter isotopic compositions at depth than near the surface, because deep ice may have originated from locations upstream of the ice-core site, where temperatures may be colder.

Annual accumulation rates of snow and firn have been also determined. For example, Epstein et al. (1965) found an average annual accumulation rate of 7 cm water at the South Pole during the time interval from 1958–1963. This estimate is in good agreement with results obtained by conventional stratigraphic methods and by radioactive dating methods. The isotopic composition of snow and firn at one site may record changing climatic conditions. Detailed studies over a time scale of 1000 years at different sites show considerable diversity in the records (Johnson et al. 1972; Dansgaard et al. 1975; Paterson et al. 1977). Because the isotopic record is based on distinct snowfall events, these isotopic differences between the different sites may result from storms of varying trajectories and may not be affected by changes in the mean temperature. Whether the different sites correlate or not, it can also be that each site records its own paleotemperature history.

The seasonal fluctuations of $\delta^{18}\text{O}$ and δD in snow and ice are gradually eliminated due to homogenization processes, such as melting and refreezing of water percolating downward through snow or firn. Judy et al. (1970) demonstrated, for example, that δD -values of individual snowfalls ranged from -230 to -106‰ , whereas the δD -range in the snowpack some months later was reduced to only -182 to -158‰ . They attributed this homogenization to recrystallization by vapor transport within the snowpack.

Although the seasonal variations of the annual layers are gradually obliterated, the absolute values record climatic conditions primarily in terms of the mean air temperatures. Therefore, continuous ice cores drilled from the continental ice sheets in Greenland and Antarctica contain a climatic record over more than the last 100000 years (Dans-

gaard et al. 1969, 1982; Johnson et al. 1972; Lorius et al. 1985). In Fig. 38 the $\delta^{18}\text{O}$ -record of two cores from Greenland and Antarctica are compared. Because of the difficulty in establishing absolute time scales for these cores, detailed comparisons between the $\delta^{18}\text{O}$ -records of the ice sheets in Greenland and Antarctica are unreliable. Nevertheless, there are remarkable similarities in both cores. The upper portions in both cores are rather constant and then at around 10000 years $\delta^{18}\text{O}$ -values decrease to about -40‰ , suggesting significantly lower

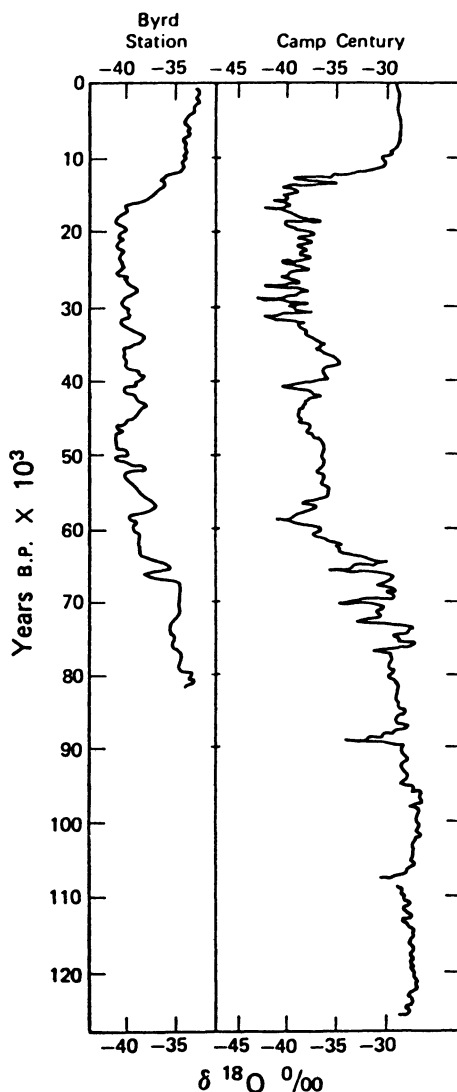


Fig. 38. Variations of $\delta^{18}\text{O}$ in ice cores from Byrd Station, Antarctica and Camp Century, Greenland. (The more negative $\delta^{18}\text{O}$ -values from about 70000 to 12000 years before present reflect colder climatic conditions during the last ice age) (Faure 1977)

average air temperatures. Towards the bottom of the core the $\delta^{18}\text{O}$ -values increase again, implying a warmer climate.

3.6.2 Groundwater

In temperate and humid climates the isotopic composition of groundwater is similar to that of the precipitation in the area of recharge (Gat 1971). This is strong evidence of direct recharge to an aquifer. The variation of $\delta^{18}\text{O}$ and δD with altitude can be used for estimating the altitude of unknown recharge areas of artesian waters (Stahl et al. 1974).

According to Gat (1971) the main mechanism which can cause variations between precipitation and recharged groundwater are:

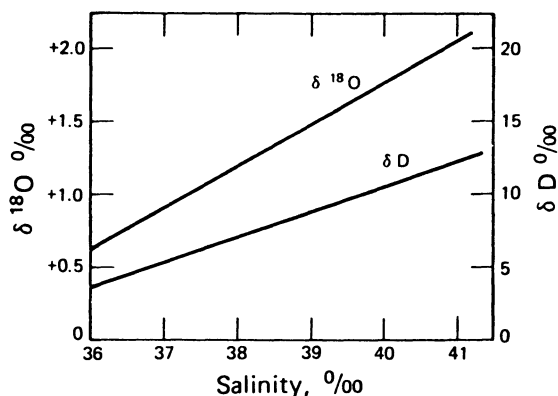
1. recharge from partially evaporated surface water bodies;
2. recharge that occurred in past periods of different climate when the isotopic composition of precipitation was different from that at present;
3. isotope fractionation processes resulting from differential water movement through the soil or the aquifer or due to exchange reactions with geologic formations.

In semiarid or arid regions, evaporation losses before and during recharge shift the isotopic composition of groundwater towards heavier values. Furthermore, transpiration of shallow groundwater through plant leaves may also be an important evaporation process. In deserts, evaporation becomes the dominant process in influencing isotopic composition. Gat and Dansgaard (1972) and Gat and Issar (1974) have demonstrated clearly that the isotopic composition of paleowaters (remnants of meteoric waters of past cooler climatic periods) can be distinguished from more recently recharged groundwaters which have been evaporated. Because rain is scarce and irregular in deserts, direct recharge to groundwaters appears to be negligible. However, in groundwaters of the Sinai desert, Gat and Issar (1974) demonstrated that direct rain recharge to aquifers is widespread.

3.6.3 Ocean Water

The isotopic composition of ocean water has been discussed in detail by Redfield and Friedman (1965), Craig and Gordon (1965), and

Fig. 39. Relationship between $\delta^{18}\text{O}$, δD , and salinity of water in the Red Sea due to preferential loss of H_2^{16}O during evaporation (Faure 1977)



Broecker (1974). Ocean water with 35‰ salinity exhibits a very narrow range in isotopic composition, less than 10‰ for D/H ratios and 1‰ for $^{18}\text{O}/^{16}\text{O}$ ratios. However, evaporation processes strongly affect the isotopic composition, because they cause a preferential depletion in the lighter isotopes, which become enriched in the vapor phase. Consequently, the remaining water will be isotopically enriched so that highly saline waters generally have the highest D and ^{18}O contents. This effect is well illustrated by water from the Red Sea (Craig 1966) shown in Fig. 39. Low salinities, which are caused by fresh water and melt water dilution, correlate with low D and ^{18}O concentrations (Epstein and Mayeda 1953; Redfield and Friedman 1965).

One very important fact concerns the circulation of deep water masses in the oceans. At least half of all the water currently entering the deep ocean is generated in the Norwegian Sea at the northern end of the Atlantic Ocean. This water flows down the Atlantic basins around Africa, through the Indian Ocean, and finally up into the Pacific Ocean. Joining this North Atlantic Deep Water flow toward the Deep Pacific is water which has been recooled in the Antarctic Ocean.

A $\delta^{18}\text{O}$ versus salinity diagram for North Atlantic ocean water samples is shown in Fig. 40 (after Broecker 1974). Those samples with salinities of about 36‰ have $\delta^{18}\text{O}$ -values about 1‰ higher than samples of SMOW. Waters taken close to Greenland with a salinity of 16‰ have an isotopic composition of -11‰. As can be seen in Fig. 40, all the North Atlantic surface waters (NASW) fall along one line, suggesting that these waters are mixtures of normal ocean water with fresh water. The same holds true for North Atlantic deep water samples (NADW), taken from 3000 m depth. However, deep Pacific and Antarctic waters

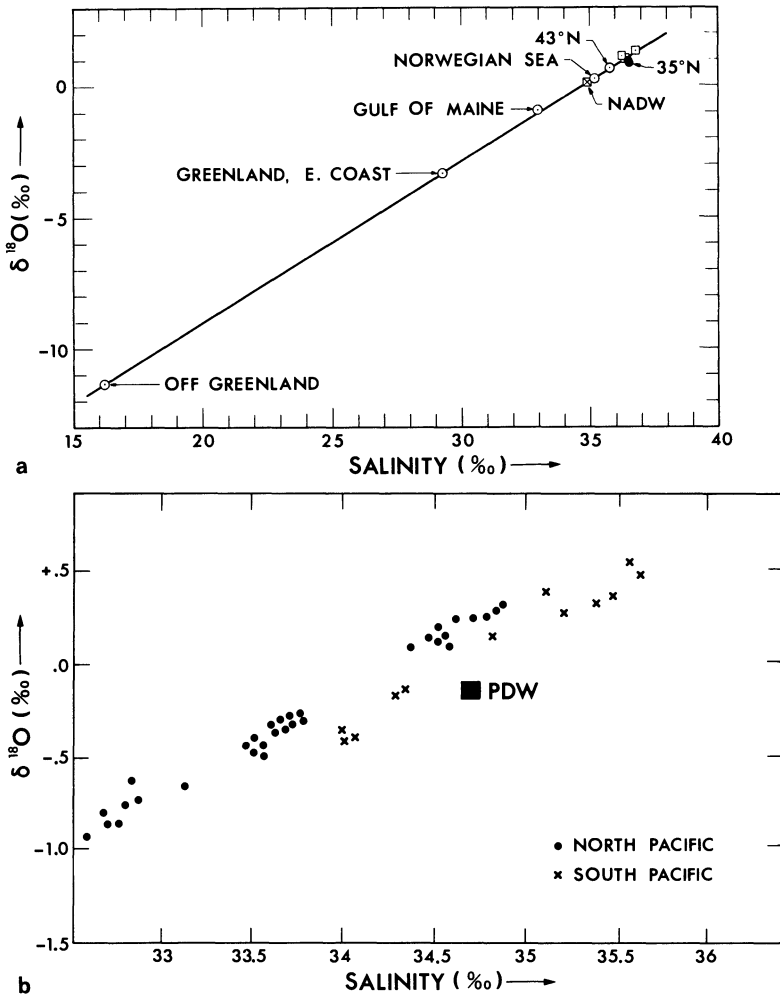


Fig. 40a,b. Plots of $\delta^{18}\text{O}$ versus salinity. **a** Samples from the North Atlantic, suggesting that North Atlantic Deep Water (NADW) consists dominantly of water sinking at the northern end of the Atlantic. **b** Samples throughout the Pacific Ocean (deep water in the Pacific cannot be generated from any mixture of these waters) (Broecker 1974)

differ from NADW (see Fig. 41). Thus, one may conclude that NADW consists almost entirely of surface water from the North Atlantic, because, if more than 30% of Antarctic water or Mediterranean water were mixed with it, NADW would not fall on the Atlantic ^{18}O -salinity line.

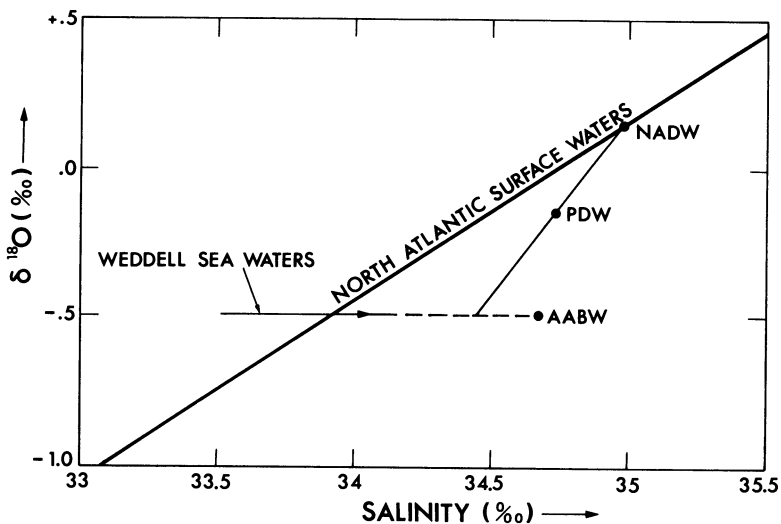


Fig. 41. Relationship between the salinity and ^{18}O of major deep waters: NADW, AABW, and PDW. Pacific Deep Water (PDW) can only be generated by mixing roughly equal amounts of water originating in the Northern Atlantic (NADW) and water originating along the edge of the Antarctic continent (AABW) (Broecker 1974)

Figure 40b shows the relationship for Pacific surface waters. Note that the Pacific Deep Water point (PDW) does not fall on the North or South Pacific water surface water line. Actually, the deep ocean points of PDW, NADW, and AABW (Antarctic Bottom Water) in Fig. 41 are almost on a line, suggesting that PDW could be produced by mixing NADW with water sinking in the Antarctic.

Two surface sources account for the bulk of deep water in the ocean:

1. NADW falls along a line that defines the water found at the surface of the North Atlantic, and
2. Antarctic Bottom Water (AABW) falls along an extension of the Weddell Sea Line.

Each of the known sources of deep water, the water sinking in the Norwegian Sea and the water sinking along the Antarctic coast, have isotopic composition-salinity relationships consistent with that in the Deep Pacific. A 50/50 mixture of these two would be identical to PDW.

One important question concerning the isotopic composition of ocean water is how constant its isotopic composition has been throughout geologic history. If all the ice sheets in the world were melted, the

$\delta^{18}\text{O}$ -value of the ocean would be lowered by about 1‰ and the δD -value by about 10‰. Estimates for the maximum enrichment of the ocean in ^{18}O during the Pleistocene glaciation range from 0.5‰ (Emiliani 1966) to 1.8‰ (Craig 1965; Shackleton 1968). At least throughout Phanerozoic time, the isotopic composition of ocean water has probably fluctuated within those limits. There are major uncertainties about the Precambrian. Whereas Becker and Clayton (1976) argued that the Precambrian ocean had a $\delta^{18}\text{O}$ -value at least as light as -3.5 ‰, Knauth and Epstein (1976) and Kolodny and Epstein (1976) believed that these oceans were roughly similar in isotopic composition to the modern ocean.

As has already been demonstrated magmatic waters have $\delta^{18}\text{O}$ -values between +6 to +8‰ and δD -values between -80 ‰ and -50 ‰. If the oceans originate from such waters, why are they now at 0‰? The apparent shift in isotopic compositions is probably due to the sedimentation of authigenic minerals rich in ^{18}O and poor in D relative to ocean water. For instance, much oxygen enriched in ^{18}O is bound in the form of cherts, carbonates, and clay minerals. Savin and Epstein (1970b) estimated on the basis of material balance calculations that the volume of ^{18}O -rich sediments can account for an ^{18}O -depletion of about 6‰ in the oceans. If the oceans have grown progressively with time, they could have remained more or less constant in ^{18}O . If the volume of the oceans has remained constant for the last 3 billion years, this model would require a progressive shift in the $\delta^{18}\text{O}$ -value of about 1‰ every 500 million years. Kokubu et al. (1961) suggested that the apparent enrichment of ocean water in deuterium relative to the magmatic water is due to preferential loss of dissociated H-atoms or ions to the exosphere over geologic time. Murozumi (1961) calculated the amounts of water photochemically decomposed in the upper atmosphere in order to account for this isotope enrichment. He estimated more than 10^{23} g water, representing some 10% of the present ocean, to have been lost by this effect.

3.6.4 Pore Water

Knowledge of the chemical composition of sedimentary pore waters has increased considerably since the beginning of the Deep-Sea Drilling Program. From numerous drill sites it has been found that significant variations exist in the chemical and isotopic composition of pore waters relative to ocean water.

Lawrence et al. (1975) and Perry et al. (1976) noted a decrease in $\delta^{18}\text{O}$ of the pore waters from an initial value very near 0‰ (Atlantic Deep Water) to about -2‰ at depths around 200 m. This decrease in ^{18}O of the pore water is due to the formation of authigenic clay minerals such as smectite and sepiolite from complete alteration of basaltic material and volcanic ash. In all cases where significant isotopic gradients have been found in the pore waters, they have been accompanied by increases in the Ca^{2+} concentration and decreases in the Mg^{2+} concentration of the pore water. The alteration reactions least effective in causing ^{18}O -depletion in the pore waters are the recrystallization of fossil carbonate to limestones and of biogenic silica to chert. In fact, at temperatures above 20 °C, these reactions will act to increase the $\delta^{18}\text{O}$ of the pore water (Lawrence et al. 1975).

3.6.5 Formation Waters and Oil Field Brines

Oil field brines are the best-known examples of subsurface saline waters. The processes involved in the development of saline formation waters are complicated by the extensive changes that have taken place in the brines after sediment deposition. Clayton et al. (1966), Hitchon and Friedman (1969), and Kharaka et al. (1974) have shown convincingly that the water now present in the formation brines is largely meteoric in origin. Formation waters show a wide range in δD , $\delta^{18}\text{O}$, and salinity, but the waters within a sedimentary basin are usually isotopically distinct. Just as with the surface meteoric waters, there is a general decrease in isotopic composition as one moves to higher latitudes (see Fig. 42).

The oxygen isotopic composition of the water is affected by exchange with carbonate minerals and by isotope fractionation across membranes. It is well known that shales and compacted clays can act as semipermeable membranes which prevent passage of ions in solution while allowing passage of water (ultrafiltration or salt filtration). Coplen and Hanshaw (1973) have shown experimentally that ultrafiltration may be accompanied by hydrogen and oxygen isotope fractionation. The ultrafiltrates were depleted in D and in ^{18}O relative to the residual solution.

Somewhat unusual isotopic compositions have been observed in highly saline deep waters from Precambrian crystalline rocks, which plot above or to the left of the Meteoric Water Line (Frape et al. 1984;

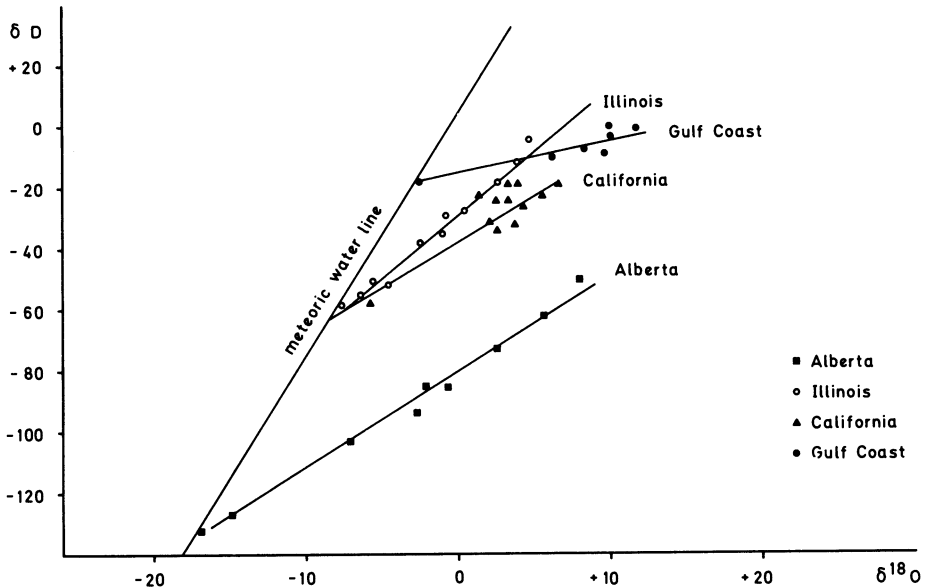


Fig. 42. Plot of δD versus $\delta^{18}O$ for oil field brines (formation waters) from the midcontinent region of the United States. (After Taylor 1974a)

Kelly et al. 1986). How to explain the unusual isotopic composition of these brines is not at all clear. Kelly et al. (1986) advocated a multi-step model, in which the formation waters evolve in Paleozoic sediments, then deeply infiltrate the crystalline basement under high temperature conditions and water/rock ratios. Later on, as the sedimentary cover was removed, the waters “back-react” under the new conditions of low temperatures and low water/rock ratios. In a final stage these waters have been contaminated to varying degrees by fresh meteoric waters.

3.6.6 Water in Hydrated Salt Minerals

Very little data exist on the isotopic composition of water in hydrated minerals (Matsuo et al. 1972; Matsubaya and Sakai 1973; Stewart 1974; Sofer 1978). To interpret such isotopic data it is necessary to know the equilibrium fractionation factors between the hydration water and the solution from which they are deposited. If the isotopic compositions of the parent water and the crystalline water are known, the tem-

perature of precipitation may be obtained. From the fractionation factor and a temperature estimate, the isotopic composition of the water from which the hydrated salt minerals were precipitated can be determined. This may yield information about the environmental conditions of depositions such as whether deposition occurred from fresh or marine water and whether such water had undergone evaporation. Sofer (1978) showed that the isotopic composition of the hydration water of gypsum may be used to specify the mechanisms of its formation, either from an evaporating brine, by hydration of anhydrite, or through oxidation of sulfides in groundwaters. Since the isotopic record in primary gypsum is destroyed both by dehydration and exchange processes with water, one cannot expect to find ancient marine gypsum samples which have retained their original water composition. Only under arid conditions may the primary isotopic record be preserved (Sofer 1978).

3.7 The Isotopic Composition of Dissolved and Suspended Compounds in Ocean and Fresh Waters

3.7.1 Nitrogen

The major sources of nitrogen in the ocean are river runoff, rain, and fixation of molecular nitrogen by organisms. Sinks originate by burial on the sediments and especially by denitrification, which is the dominant process producing large N-isotope fractionations. Denitrification seems to be the principal mechanism that keeps marine nitrogen at higher $\delta^{15}\text{N}$ -values than atmospheric nitrogen.

Due to the transient nature of marine nitrate, $\delta^{15}\text{N}$ -values of dissolved nitrate vary considerably. Cline and Kaplan (1975) observed in the North Pacific Ocean a $\delta^{15}\text{N}$ -range from +6.5‰ in the surface region to +18.8‰ in the active denitrification zone. Saino and Hattori (1980) presented a vertical ^{15}N -profile on particulate organic matter in the Indian Ocean. $\delta^{15}\text{N}$ -values decrease near the surface and reach a minimum near 30-m water depth and then increase through the 30–500 m depth by 10‰. Below 500 m the $\delta^{15}\text{N}$ -value remained constant around 13‰. The ^{15}N -enrichment with depth may result from isotope fractionations during oxidative degradation of particulate organic matter. The minimum $\delta^{15}\text{N}$ -values near the surface may be due to preferential ^{14}N -incorporation during nitrate uptake by phytoplankton.

Altabet and Deuser (1985) observed seasonal ^{15}N -variations in particles sinking to the ocean bottom. They suggested that the $\delta^{15}\text{N}$ -values

of sinking particles represent a monitor for nitrate flux in the euphotic zone. If the sediments preserve this $\delta^{15}\text{N}$ -record it may represent a means by which primary production in the oceans of the past can be studied.

Sweeney et al. (1978) have shown that nitrogen in suspended marine organic matter is significantly heavier than nitrogen in suspended terrestrial organic matter. In near-shore environments $\delta^{15}\text{N}$ -values can, therefore, act as a tracer to determine the source of nitrogen (Mariotti et al. 1984).

3.7.2 Oxygen

As early as 1951 Rakestraw et al. demonstrated that dissolved oxygen in the oceans is enriched in ^{18}O relative to atmospheric oxygen. Extreme enrichments, up to 14‰ (Kroopnick and Craig 1976), occur in the oxygen minimum region of the deep ocean due to preferential consumption of ^{16}O by bacteria in abyssal ocean waters, which is evidence for a “deep metabolism” (see also Fig. 43).

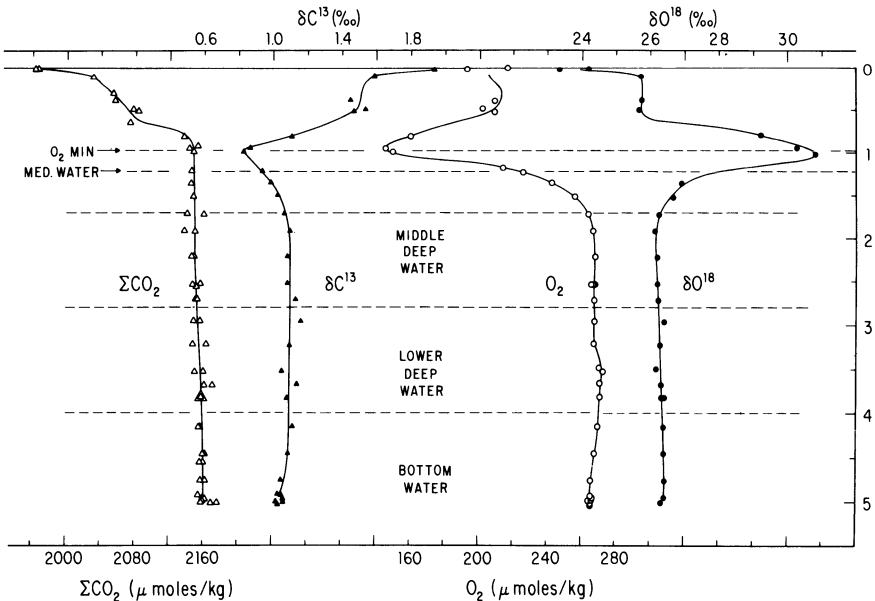


Fig. 43. Vertical profiles of CO_2 , $\delta^{13}\text{C}$, dissolved O_2 , and $\delta^{18}\text{O}$ in the dissolved O_2 in the North Atlantic (Kroopnick et al. 1972)

3.7.3 Carbon Species in Water

3.7.3.1 Bicarbonate in Ocean Water

In addition to organic carbon, four other carbon species exist in natural water: dissolved CO_2 , H_2CO_3 , HCO_3^- , and CO_3^{2-} , all of which tend to equilibrate as a function of temperature. As previously mentioned, the concentration and the isotopic composition of the individual species also vary with pH.

HCO_3^- is the dominant C-bearing species in ocean water. The C-isotope composition in a vertical profile is shown in Fig. 43. Most surface waters in the central ocean basins have $\delta^{13}\text{C}$ -values of about +2.2‰ (Deuser and Hunt 1969; Kroopnick 1985). However, this value changes downward into deeper water masses due to continuous flux of organic and skeletal detritus into the deep water (see Fig. 43). In a very detailed study Kroopnick (1985) analyzed 2252 samples from 107 hydrographic stations and demonstrated that the distribution of $\delta^{13}\text{C}$ is controlled mainly by the input of organically produced material and its subsequent oxidations as it falls through the water column. Other factors which influence the $\delta^{13}\text{C}$ -value are the dissolution of inorganic carbonate and the addition of anthropogenic CO_2 . It is estimated that from a preindustrial value of 2.5‰ the $\delta^{13}\text{C}$ -value of the total dissolved CO_2 in the ocean has decreased by 0.5‰.

3.7.3.2 POM

Particulate organic matter (POM) in the ocean originates in large parts from the detrital remains of plankton in the euphotic zone and reflects living plankton populations. As POM sinks, biological reworking changes its chemical composition, with labile compounds such as amino acids and sugars being degraded in preference to the more refractory lipid components. The extent of biological degradation depends on residence time in the water column. Most reported POM profiles exhibit a general trend of surface isotopic values comparable to those for living plankton towards increasingly lower $\delta^{13}\text{C}$ -values with depth. Eadie and Jeffrey (1973) and Jeffrey et al. (1983) interpreted this trend as the loss of labile, isotopically enriched amino acids and sugars through biological reworking, leaving the more refractory, isotopically light lipid components.

C/N ratios of POM increase with depth of the water column. This implies that nitrogen is more rapidly lost than carbon during degradation of POM. This is the reason for the much greater variation in $\delta^{15}\text{N}$ -values than in $\delta^{13}\text{C}$ -values (Saino and Hattori 1980; Altabet and McCarthy 1985).

3.7.3.3 Carbon Isotope Composition of Pore Waters

Initially, the pore water at the sediment/water interface has a $\delta^{13}\text{C}$ -value near that of seawater. In oxic environments with little organic matter no major change in $\delta^{13}\text{C}$ with depth should occur. In more organic carbon-rich sediments a decrease in the pore water $\delta^{13}\text{C}$ is observed. The decomposition of organic matter in sediments consumes oxygen and releases isotopically light CO_2 to the pore water, while the dissolution of CaCO_3 adds CO_2 which is isotopically heavy. The carbon isotope composition of pore waters at a given locality reflects modification by these two processes. The net result of these two sources is to make pore waters isotopically lighter than the overlying bottom water. Nissenbaum et al. (1972) and Grossman (1984a) have documented a strong negative $\delta^{13}\text{C}$ -signal in several reducing marine environments. McCorkle et al. (1985) have shown that steep gradients in pore water $\delta^{13}\text{C}$ exist in the first few centimeters below the sediment-water inter-

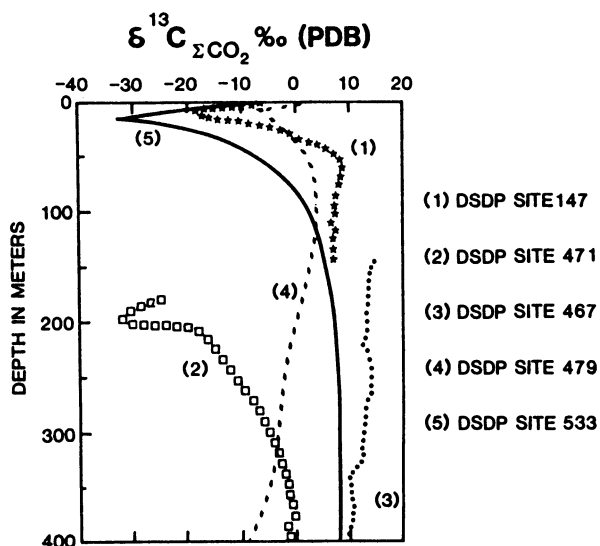


Fig. 44. $\delta^{13}\text{C}$ -profiles of total CO_2 (dissolved inorganic carbon) from pore waters of anoxic sediments recovered in various Deep Sea Drilling Project Sites (Anderson and Arthur 1983)

face. The observed $\delta^{13}\text{C}$ -profiles vary systematically with the rain of organic matter to the seafloor, with higher carbon rain rates resulting in isotopically lighter $\delta^{13}\text{C}$ -values.

One would expect that pore waters have $\delta^{13}\text{C}$ -values no more negative than organic matter. However, a more complex situation is actually observed due to bacterial methanogenesis (see Fig. 44). Bacterial methane production generally follows sulfate reduction in anaerobic carbon-rich sediments, the two microbiological environments being distinct from one another. Since methane-producing bacteria produce very ^{12}C -rich methane, the residual pore water becomes enriched in ^{13}C . As bacterial methane production continues, the pore waters evolve to higher $\delta^{13}\text{C}$ -values (see Fig. 44). The observed trends cannot simply be interpreted in terms of amounts of sulfate reduction and methane formation, rather carbon losses and gains from the pore water systems must also be taken into account.

3.7.3.4 *Bicarbonate in Fresh Waters*

Dissolved carbonate in fresh water exhibits an extremely variable isotopic composition, because it represents varying mixtures of carbonate species derived from weathering of carbonates and that originating from biogenic sources like freshwater plankton or CO_2 from organic matter in soils (Hitchon and Krouse 1972; Longinelli and Edmond 1983). Comparison of the data from the Mackenzie River (Hitchon and Krouse 1972) with those from the Amazon basin (Longinelli and Edmond 1983) reveals an interesting difference. The Mackenzie River data have a major $\delta^{13}\text{C}$ -peak at about -9‰ with a "tail" to lower values. The Amazon River data are displaced to about -20‰ with a broad distribution range. These differences are consistent with a dominance of carbonate weathering in the Mackenzie River drainage system, whereas in the tropical environment of the Amazon River biological CO_2 predominates.

3.7.4 Sulfate in Ocean and Fresh Water

3.7.4.1 *Sulfur Isotope Composition of Ocean Water*

Modern ocean water with its large sulfate reservoir has a fairly constant isotopic sulfur composition of $+21\text{‰}$ (Rees et al. 1978). An interesting

question is whether an isotope fractionation occurs in the sulfate during evaporation of seawater. Nielsen and Ricke (1964) showed that later evaporites within the different evaporation cycles are depleted in ^{34}S by about 2‰ relative to earlier precipitates. Nevertheless, the difference that might occur in the late stages may be neglected if we consider the gypsum-brine relationship. Assuming that calcium sulfates preserve the $\delta^{34}\text{S}$ -value of the ancient oceans, then it may be concluded that gypsum, anhydrite, and other sulfate-containing evaporite minerals provide information about the isotopic composition of oceanic sulfate during the geologic past. This topic will be discussed in more detail in the following chapter.

3.7.4.2 Sulfur Isotope Composition of Fresh Water

A compilation of river water $\delta^{34}\text{S}$ -values is shown in Fig. 45. The data of Hitchon and Krouse (1972) for water samples from the Mackenzie

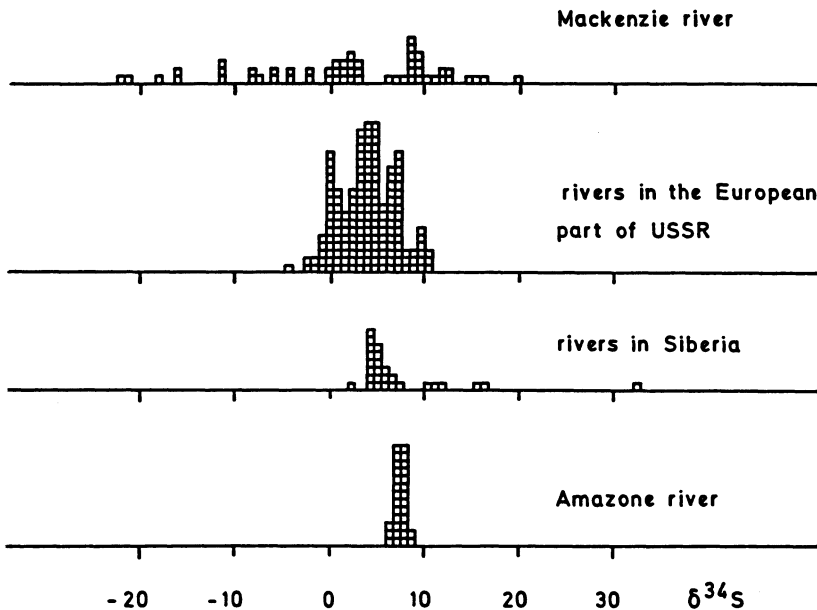


Fig. 45. Frequency distribution of $\delta^{34}\text{S}$ -values in river sulfate. (Data source: Amazon, Longinelli and Edmond 1983; Mackenzie River, Hitchon and Krouse 1972; rivers in Siberia and in the European part of the USSR, Rabinovich and Grinenko 1979)

River drainage systems exhibit a wide range of $\delta^{34}\text{S}$ -values reflecting contributions from marine evaporites and shales. Surprisingly, Longinelli and Edmond (1983) found a very narrow range for the Amazon River which was interpreted as representing a dominant Andean source of Permian evaporites with a lesser admixture of sulfide sulfur.

Rabinowitch and Grinenko (1979) reported time-series measurements for the large European and Asian rivers in the Soviet Union. The European river systems are approximately normally distributed with a mean value of +6‰, while in the Asian systems $\delta^{34}\text{S}$ -values below 4‰ are, with one exception, lacking. Rabinowitch and Grinenko (1979) found a mean value of 8.2‰ for the 22 largest rivers in the USSR, which coincides with the average isotopic composition of sediments.

3.7.4.3 Oxygen Isotope Composition of Ocean Water Sulfate

Oceanic sulfate has a very constant oxygen isotope composition of 9.6‰ (Lloyd 1967, 1968; Longinelli and Craig 1967). From the theoretical calculations of Urey (1947) it is quite clear that this value does not represent equilibrium with the $\delta^{18}\text{O}$ -value of the ocean water, but how this value has been achieved in the world's ocean is still controversial. Lloyd (1967, 1968) proposed a model in which the fast bacterial turnover of sulfate at the sea bottom determines the oxygen isotope composition of dissolved sulfate. This conclusion was questioned by Holser et al. (1979), who argued that the oxygen isotope composition of seawater sulfate should be controlled by a dynamic balance of sulfate inputs (mainly from weathering of sulfides and sulfates) and sulfate outputs (mainly through evaporite formation and sulfate reduction). When considering the oxygen isotopic variations of evaporite minerals through geologic time, one has to consider the fractionation of around 3.5‰ (Lloyd 1968) between the crystallized evaporite mineral and ocean water. Cortecchi and Longinelli (1971, 1973) have observed that the ^{18}O -content of sulfate in living shells is close to that of the dissolved oceanic sulfate. Fossil shells, however, exhibit a wide range in sulfate ^{18}O -content, which they interpret as the product of postdepositional changes. Thus, the ^{18}O -content of fossil shells apparently gives no information on the past ocean sulfate $\delta^{18}\text{O}$ -values.

3.7.4.4 *Oxygen Isotope Composition of Fresh Water Sulfate*

The oxygen isotope composition of rainfall sulfate is highly variable with $\delta^{18}\text{O}$ -values ranging from +5 to +17‰ (Cortecci and Longinelli 1970). From the $\delta^{34}\text{S}$ -values of the samples analyzed by these authors, it appears that most of their rainfall sulfate is not oceanic, but is produced by oxidation of sulfur produced during the burning of fossil fuels. Because the isotopic composition of sulfate in rivers reflects the isotopic composition of the sulfate sources, it is not surprising that sulfates from nonmarine environments range over a wide spectrum (Longinelli and Cortecci 1970; Longinelli and Edmond 1983). Longinelli and Edmond (1983) argued that the variations in the sulfate oxygen of the Amazon River require exchange with the water and dissolved oxygen via partial redox processes.

3.8 Changes in the Isotopic Composition of the Ocean During Geologic History

The question of whether or not the chemical and isotopic composition of the ocean has remained constant throughout geologic history, has been discussed quite frequently in the literature. Hoefs (1981) has summarized current thinking on this controversial topic.

3.8.1 Sulfur

Perhaps the best documented trend of isotope variation is that for the sulfur isotope distribution in marine sulfate. In 1964 Nielsen and Ricke and Thode and Monster published independently the first two “age curves” which showed that the isotopic composition of gypsum and anhydrite in marine evaporites was different at different times in the geologic past. Since then, this curve has been updated with many more analyses (see Holser and Kaplan 1966; Nielsen 1972; Holser 1977; Claypool et al. 1980), demonstrating that especially during the Phanerozoic several pronounced maxima and minima in $\delta^{34}\text{S}$ exist, the extremes lying close to +10‰ (Permian) and +30‰ (Cambrian) (see Fig. 46). Because the isotope fractionation between the sulfate-containing evaporite and the sulfate in ocean water is almost negligible, the observed trend in evaporite sulfate should closely reflect fluctu-

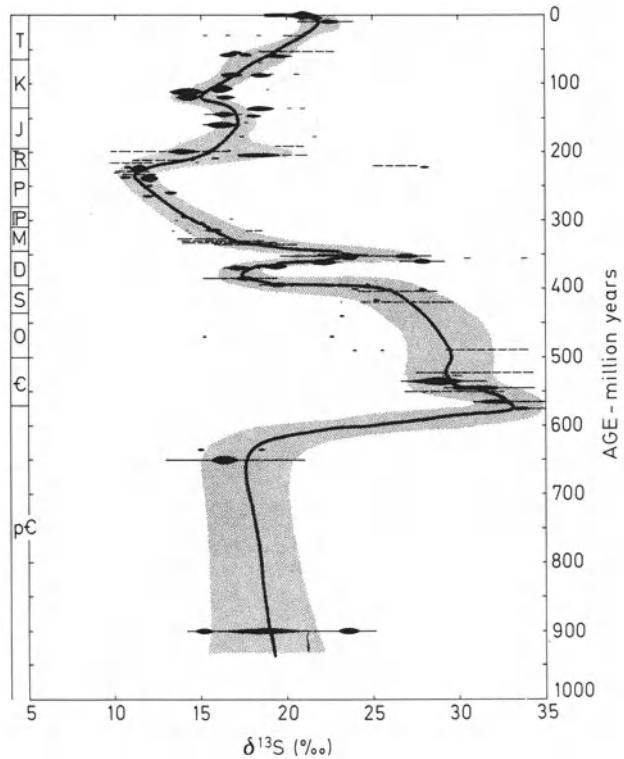


Fig. 46. $\delta^{34}\text{S}$ age curve of oceanic sulfate (Holser 1977)

ations in the sulfur isotope composition of marine sulfate through geologic time. The present $\delta^{34}\text{S}$ -value of marine sulfate is primarily the result of the activity of sulfate-reducing microorganisms.

Changes in the $\delta^{34}\text{S}$ of marine sulfate during the geologic past may be caused by major changes in the budget between the individual reservoirs: during periods of high biological sulfate reduction, which should take place under favorable paleogeographic conditions, the $\delta^{34}\text{S}$ of ocean water should increase. In contrast, periods of extended weathering introduce additional light continental sulfur into the ocean which decreases the $\delta^{34}\text{S}$ -value of ocean sulfate. Such periods of extended weathering are geologically plausible in periods of high tectonic, mountain-building activity.

Early models of Nielsen (1965) and Holser and Kaplan (1966) discussed quantitatively the consequences of such changes in the weathering rate and bacterial reduction rate. These earlier models did not,

however, consider the possible influence of varying rates of evaporite formation on the $\delta^{34}\text{S}$ -values of marine sulfate. Rees (1970) was the first to point to the importance of sulfur extraction by evaporite formation and postulated that the $\delta^{34}\text{S}$ of the ocean "should have tended to high values in periods when evaporite formation was of minor importance and to low values in periods of major evaporite formation. This is qualitatively the case for the Cambrian and the Permian ..."

Recently, a further mechanism of sulfate extraction became quite evident, i.e., the annual cycling of large quantities of seawater through midocean ridges which can have a remarkable effect on the chemistry of ocean water. Claypool et al. (1980) investigated the oxygen isotope together with the sulfur isotope composition of evaporites. Their model approximates each of the flux pairs of sulfide in and sulfide out of the ocean and sulfate in and sulfate out of the ocean by a single net flux of sulfide or sulfate.

Whatever the actual causes may be for the fluctuations of the $\delta^{34}\text{S}$ -values of oceanic sulfate during the geologic past, it is obvious that this behavior of oceanic sulfate deviates strongly from that expected from an extreme concept of a steady-state ocean. In such a steady-state view the partition into reduced and oxidized reservoirs would be at a fixed ratio. According to Garrels and Perry (1974) the range of $\delta^{34}\text{S}$ from +30‰ to +10‰ corresponds to a variation of $\pm 30\%$ in the average total amount of sulfate stored in sedimentary rocks and in the ocean. In addition, it is obvious that fluctuations in the three major mechanisms for sulfate removal (1) evaporite formation; (2) bacterial reduction; and (3) cycling through midocean ridges; all have occurred largely in response to changes in the geography of the ocean basins and/or of the adjacent seas.

While the partial cycle between ocean and evaporites only involves sulfate transfer from one reservoir to the other, bacterial sulfate reduction, as well as the weathering of sulfides from argillaceous sediments, change the valence state of the sulfur. Therefore, during a period with increased rate of one of these two processes, appreciable amounts either of organic compounds or of free atmospheric oxygen are needed. Especially in the latter case, oxygen consumption during weathering is appreciable.

3.8.2 Carbon

In the system ocean-atmosphere-biosphere the ocean contains approximately 90% exchangeable carbon, whereas the biosphere contains only 8% and the atmosphere 2%. The ocean is thus the major long-term regulator for the atmospheric CO₂ concentration. Secular variations in the oceanic, dissolved bicarbonate reservoir are generally interpreted as representing changes in the output of carbon from the oceans. At present, a C_{org}/C_{carbonate} output ratio of about 1:4 maintains a steady state δ¹³C of about 0‰ in the oceanic, total dissolved carbon reservoir. Shifts towards higher δ¹³C-values in limestones of a given age may be due to an increase of organic carbon burial relative to carbonate carbon burial. Negative δ¹³C-shifts may accordingly indicate a decrease in the rate of carbon burial. Unusually heavy δ¹³C-values in Cretaceous carbonates have been thus related to unusually high burial rates of organic carbon (Scholle and Arthur 1980; Hilbrecht and Hoefs 1986; Jenkyns and Clayton 1986).

Such periods have been called “anoxic oceanic events” and the best documented example is the Cenomanian/Turonian boundary. The present stratigraphic resolution of the different sections is not sufficient to establish whether or not the “δ¹³C-anomaly” is isochronous worldwide.

Similar drastic ¹³C-changes of carbonates have been reported for other geologic time periods (for the Permian/Triassic boundary by Magaritz et al. 1983 and for the Upper Proterozoic by Knoll et al. 1986). It is still debatable whether these changes represent worldwide phenomena which characterize the ocean water at those specific time intervals or represent more local phenomena. Furthermore, it is also possible that in some cases the observed ¹³C-patterns are partially due to secondary diagenetic processes. However, in thick beds of more or less pure limestones with minor amounts of organic carbon diagenetic reactions should have only a negligible effect on the primary isotopic composition.

Because of the 1:4 ratio of organic carbon to carbonate carbon withdrawal from the ocean, the organic carbon reservoir is much more sensitive to such secular variations. However, diagenetic reactions during burial and maturation of organic matter may change the isotopic composition by several ‰ (see p. 158) which complicates the use of organic carbon in the search for secular isotope variations. Nevertheless, as Knoll et al. (1986) suggested measurement of both organic and carbonate carbon greatly reduces the chance of misinterpretations.

Due to the relatively rapid exchange in the ocean-atmosphere-biosphere system, an increase in photosynthetic activity may also lead to secular changes in the system. The larger the amount of carbon accumulated in the biosphere, the more positive is the $\delta^{13}\text{C}$ of the oceanic carbon reservoir. A decrease in photosynthetic activity should, of course, lead to a shift in the opposite direction. Attempts to relate differences in photosynthetic activity with $\delta^{13}\text{C}$ -values have been made by Welte et al. (1975) and Arneeth et al. (1985).

Such $\delta^{13}\text{C}$ -excursions can be modelled quantitatively in order to estimate changes of C_{org} both forward and backward in time (Garrels and Lerman 1984). Finally, it should be mentioned that because the geochemical cycles of carbon and sulfur are coupled, the observed changes in the sulfur isotope composition of evaporites should lead to a concomitant change in the carbon isotope composition. And, indeed, careful inspection of the literature data led Veizer et al. (1980) to conclude that a negative correlation between the $\delta^{13}\text{C}$ -values of sedimentary carbonates and $\delta^{34}\text{S}$ -values of the sulfates does exist.

3.8.3 Oxygen

To alter the oxygen isotope composition of ocean water demands huge amounts of water being isotopically very different from the ocean water composition. Short-term variations of $\delta^{18}\text{O}$ occur during the ice ages. When continental glaciers grow, ^{16}O is preferentially removed from the ocean, the reverse occurs when glaciers melt. Thus, the advance and retreat of glaciation during the ice ages must have changed the $\delta^{18}\text{O}$ of seawater.

Besides these short-term fluctuations, long-term unidirectional processes also have to be considered. As is known for many years the $\delta^{18}\text{O}$ -values of marine cherts and limestones tend to decrease with increasing geologic age (Knauth and Lowe 1978; Veizer and Hoefs 1976). The significance of these trends is still not settled; continuous postdepositional exchange with interstitial solutions was the first explanation for these trends and undoubtedly many of the samples which define trends have been subjected to diagenesis. Nevertheless, this hypothesis appears to be contradictory to several important observations. The $\delta^{18}\text{O}$ versus age trends for cherts and carbonates are nearly parallel despite the fact that the susceptibility of quartz and calcite to isotope exchange with fluids is quite different. Shemesh et al. (1983)

reported a similar trend for phosphorites and concluded that the stability of the phosphate ion and its inertness of phosphate-water isotope exchange excludes meteoric water diagenesis as an explanation for the trend. These phosphorite data suggest that the trend towards lower $\delta^{18}\text{O}$ -values reflect changes in temperatures and/or changes in the isotopic composition of the ocean.

This interpretation again is in conflict with data from altered ocean crust. Muehlenbachs and Clayton (1976) presented a model in which the isotopic composition of ocean water is held constant by two different processes: (1) low-temperature weathering of oceanic crust which depletes ocean water in ^{18}O because ^{18}O is preferentially bound in the weathering products, whereas (2) high-temperature hydrothermal alteration of MORB basalts enriches ocean water in ^{18}O because ^{16}O is consumed by the hydrothermal alteration reactions. These two processes, being opposite in sense and roughly equal in magnitude, thus buffer the isotopic composition of ocean water. Similar conclusions have been drawn by Gregory and Taylor (1981) who postulated that ocean water had a constant $\delta^{18}\text{O}$ -value during almost all of earth history. In summary, various strong arguments contradict each other, which leaves the issue far from being resolved.

3.9 Atmosphere

The basic chemical composition of the atmosphere is quite simple, being made up almost entirely of three elements: nitrogen, oxygen, and argon. Other elements and compounds are present in amounts that, although small, are nevertheless significant in terms of important properties of the atmosphere, such as the ozone content. The atmosphere is moderately homogeneous in season as well as at elevation except for water and ozone; the former is continually derived from and returned to the hydrosphere and the latter is largely concentrated in the stratosphere. Other interchanges between the ocean and the atmosphere take place within the carbon, nitrogen, and sulfur cycles. The average abundances of some important atmospheric constituents are shown in Table 22. There is increasing awareness that isotope techniques can be very useful in evaluating the sources of anthropogenic pollution of the atmosphere, such as CO_2 , SO_2 , and nitrogen oxides.

The constituents of the atmosphere have been derived largely from degassing of the earth's mantle. From observations of volcanic and cos-

Table 22. Average contents of some important constituents in the atmosphere (on a water-free basis)

Gas	Abundance by volume (%)
N ₂	78.09
O ₂	20.95
Ar	0.93
CO ₂	0.032
CH ₄	0.00002
H ₂	0.00005
N ₂ O	0.00005
O ₃	0.000007 (Summer)
	0.000002 (Winter)

mic gases it has been concluded that the primeval atmosphere was free of oxygen and that reducing conditions prevailed. The first free oxygen was probably produced through photochemical dissociation of water vapor in the upper atmosphere, which would produce oxygen and hydrogen, with the hydrogen escaping into outer space. However, this free oxygen probably did not initially accumulate in the atmosphere, but was used up in oxidizing the more reduced constituents of the atmosphere. This stage came to an end when oxygen production exceeded oxygen use, which probably occurred when photosynthesis reached a certain level of oxygen production.

The amount of argon in the atmosphere, which is 99.69% ⁴⁰Ar, is anomalously high when compared with that of the other inert gases. This is evidently due to the production of ⁴⁰Ar by the radioactive decay of ⁴⁰K throughout geologic time.

3.9.1 Nitrogen

Atmospheric nitrogen collected from many altitudes shows a constant isotopic composition (Dole et al. 1954; Sweeney et al. 1978). Air samples collected over a 6-month period at several locations had a constant ¹⁵N/¹⁴N ratio, within 0.2‰ (Hoering 1956).

Besides the overwhelming predominance of elemental nitrogen, there are various other nitrogen compounds in the atmosphere as trace compounds. Of these, nitrous oxide (N₂O) is an important greenhouse gas, which thus influences the energy budget of the atmosphere. Nitrous

oxide is mainly produced by bacterial processes of nitrification and denitrification in soils and oceans. It is destroyed photochemically in the stratosphere. $\delta^{15}\text{N}$ - and $\delta^{18}\text{O}$ -measurements (Yoshida and Matsuo 1983; Yoshida et al. 1984; Whalen and Yoshinara 1985) have shown that N_2O is isotopically variable in the atmosphere depending upon its specific source.

Besides its natural occurrence, N_2O plays a special role in stable isotope investigations, because it condenses when CO_2 is extracted from air in a liquid nitrogen trap. Because the masses of the isotopic N_2O molecules equal those of CO_2 , N_2O interferes with the $^{13}\text{C}/^{12}\text{C}$ and $^{18}\text{O}/^{16}\text{O}$ ratios of CO_2 and thus a correction for the N_2O atmosphere concentration is required (Craig and Keeling 1963; Mook and van der Hoek 1983).

3.9.2 Oxygen

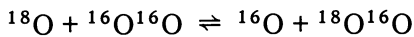
Atmospheric oxygen has a rather constant isotopic composition with a $\delta^{18}\text{O}$ -value of +23‰ (Dole et al. 1954; Kroopnick and Craig 1972; Horibe et al. 1973). Urey (1947) calculated that if equilibrium was obtained between atmospheric oxygen and water, then atmospheric oxygen should be enriched in ^{18}O by 6‰ at 25 °C. This means that atmospheric oxygen cannot be in equilibrium with the hydrosphere and thus, enrichment of free O_2 in ^{18}O , the so-called Dole effect, must have another explanation.

It was originally believed that photosynthesis of green plants might control the $^{18}\text{O}/^{16}\text{O}$ ratio in the atmosphere. It is commonly accepted that molecular oxygen produced during photosynthesis arises from the splitting of H_2O molecules and not from the splitting of CO_2 . Dole and Jenks (1944) determined that the liberated oxygen was enriched in ^{18}O by about 5‰ relative to the water from which it was derived. Thus, photosynthetic oxygen has an $^{18}\text{O}/^{16}\text{O}$ ratio approximately expected for isotopic equilibrium between water and free oxygen. Therefore, photosynthesis cannot account for the Dole effect. To solve the problem, Rabinowitch (1945) suggested that the cause of the Dole effect might be isotope fractionation caused by the preferential uptake of ^{16}O during respiration. This is supported by the observation of Lane and Dole (1956), who found that oxygen isotope enrichment during respiration in several plants, bacteria, and in man varied from 7‰ to 25‰. Kroopnick (1975) measured the oxygen isotope fractionation

during respiration on natural populations in ocean water and found that respiration can cause an enrichment of about 21‰. It is, therefore, reasonable to assume that the $\delta^{18}\text{O}$ -value of atmospheric oxygen is balanced between input from photosynthesis and output by respiration.

The analysis of fossil air in ice cores yields information about the isotope composition during the past tens of thousands years. When snow transforms into ice, atmospheric air is trapped in the form of bubbles. Fireman and Norris (1982), Horibe et al. (1985), and Bender et al. (1985) demonstrated that the $\delta^{18}\text{O}$ -value of this atmospheric oxygen was ^{18}O -enriched and varied along with that of seawater (during the ice ages, seawater is ^{18}O -enriched).

Ozone. In situ mass spectrometric measurements of stratospheric ozone by Mauersberger (1981) have shown large ^{18}O -enrichments, as much as 40% above tropospheric values. He explained this enrichment as being due to preferential dissociation of $^{18}\text{O}^{16}\text{O}$ leading to an overabundance of ^{18}O -atoms. However, as pointed out by Kaye and Strobel (1983) the problem is that isotope exchange of the exchange reaction:



is much faster than ozone formation, which should prevent any enhancement of heavy ozone in the stratosphere.

As has been shown recently by Thiemens and Heidenreich (1983), photochemical reactions may produce anomalous isotopic patterns. These authors reported equal enrichment of ^{17}O and ^{18}O in ozone produced by an electric discharge in oxygen and interpreted their results by self-shielding of $^{16}\text{O}_2$. Navon and Wasserburg (1985) analyzed the oxygen isotope shifts during photodissociation of oxygen and found that the remaining O_2 is enriched in ^{16}O . However, it is necessary to separate the anomalous oxygen from the gas reservoir in order to preserve the isotope shifts. Furthermore, Navon and Wasserburg (1985) demonstrated that the effects found by Thiemens and Heidenreich (1983) cannot be explained by self-shielding of UV radiation as the pressure is below the minimum needed for self-shielding to occur.

3.9.3 Carbon

3.9.3.1 Carbon Dioxide

$\delta^{13}\text{C}$. The CO_2 content of the atmosphere controls many processes of geologic importance (e.g., pH of ocean water and the “greenhouse effect” of shielding solar energy). Daily, seasonal, secular, local, and regional changes in atmospheric content have been observed as regular fluctuations. Careful determinations by Keeling (1958, 1960, 1961) have shown that daily variations, which depend on respiration, exist over continents. Respiration of plants reaches a distinct maximum around midnight or in the early morning hours. Respiratory plant CO_2 has a $\delta^{13}\text{C}$ -value between -26‰ and -21‰ . At night, when respiration of plants reaches maximum values, there is a measurable contribution of respiratory CO_2 . This relation between CO_2 content and $\delta^{13}\text{C}$ is demonstrated in Fig. 47.

The burning of fossil fuel has significantly increased the CO_2 content of the atmosphere. Farmer and Baxter (1974) noted an increase from about 290 ppm CO_2 in 1900 to 320 ppm in 1970. Freyer and Wiesberg (1973) and Farmer and Baxter (1974) suggested that the carbon isotope composition of tree rings is, in fact, a record of atmospheric carbon isotopic variations. Besides the burning of fossil fuel, other factors such as increased oxidation of plant debris caused by increased

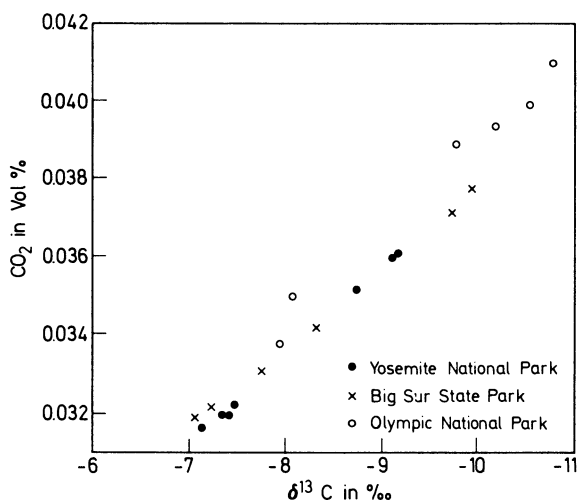


Fig. 47. Relationship between atmospheric CO_2 concentration and $\delta^{13}\text{C}(\text{CO}_2)$. (After Keeling 1958)

cultivation of arable land could have influenced the carbon isotopic composition of atmospheric CO_2 .

The annual combustion of 10^{15} g fossil fuel with an average $\delta^{13}\text{C}$ -value of -27‰ would change $\delta^{13}\text{C}$ of the atmospheric CO_2 by -0.2‰ yr^{-1} . The observed change is about ten times as small (Mook et al. 1983). There are two reasons for this apparent discrepancy:

1. only about 60% of the injected CO_2 remains airborne, the other part is mainly dissolved in the oceans;
2. oceanic, dissolved carbon exchanges isotopically with atmospheric CO_2 .

One of the most promising methods of reconstructing atmospheric CO_2 concentrations of earlier times are measurements on air trapped in polar ice. Such measurements have revealed that at the end of the last glaciation, the atmospheric CO_2 concentration was about 30% lower than during the Holocene. Friedli et al. (1984) made $\delta^{13}\text{C}$ -measurements on CO_2 separated from air extracted from South Pole ice which yielded a 1.1‰ higher $\delta^{13}\text{C}$ -value than air- CO_2 in 1980. This is consistent with the measured CO_2 concentration in these samples and with model-based estimations.

By measuring the ^{13}C -content of planktonic and benthic foraminifera, Shackleton et al. (1983) reached very similar conclusions and postulated low CO_2 concentrations during the last glacial ages (see also discussion on p. 175).

$\delta^{18}\text{O}$. Atmospheric CO_2 has a $\delta^{18}\text{O}$ -value of $+41\text{‰}$, which means that atmospheric CO_2 is in approximate equilibrium with ocean water at 25°C . Bottinga and Craig (1969) showed that exchange with ocean water regulates the average composition of atmospheric CO_2 , although exchange with atmospheric water may cause small perturbations.

3.9.3.2 Other Carbon Compounds

Stevens et al. (1972) reported regular seasonal variations in the carbon and oxygen isotopic composition of atmospheric carbon monoxide. They estimated the worldwide average $\delta^{13}\text{C}$ -value for engine CO to be $-27.4\text{‰} \pm 0.3\text{‰}$. Bainbridge et al. (1961) determined one $\delta^{13}\text{C}$ -value of atmospheric methane of -39‰ .

3.9.4 Hydrogen

Free atmospheric hydrogen is present to approximately five parts in 10^7 in tropospheric air. The deuterium concentration is in the vicinity of $+70\text{‰} \pm 30\text{‰}$ (Friedman and Scholz 1974). Gonsior et al. (1966) found δD -values from -600 to -200‰ for industrial hydrogen, which was mainly ascribed to hydrogen released from automobile exhausts. The δD -values of atmospheric hydrogen are higher than in any natural material found on earth. Because all equilibrium isotope exchange reactions that are known concentrate hydrogen in H_2 relative to the other reacting phase, kinetic effects seem to account for this heavy hydrogen.

3.9.5 Sulfur

Sulfur is found in trace compounds in the atmosphere where it occurs in aerosols as sulfate and in the gaseous state as H_2S and SO_2 . The major contributions to atmospheric sulfur are: (1) industrial sulfur, (2) ocean spray sulfate, (3) bacterial sulfur, mostly from tidal flats, and (4) volcanic sulfur. Mizutani and Rafter (1969) concluded that seawater spray was one of the main sources of sulfate in the rain studies, the other main source being industrial activity, which produces SO_2 . The contribution of each source varied widely, depending mainly upon meteorological conditions. However, about one-half of the samples studied showed a dominant contribution of seawater sulfate.

Anthropogenic vs Natural Sources. Sulfur compounds arising from anthropogenic and natural sources are mixed in the atmosphere and hydrosphere. The complexities involved in the isotopic composition of atmospheric sulfur have been discussed by Nielsen (1974). Grey and Jensen (1972) argued that, in the Salt Lake City Region of Utah, the atmospheric sulfur comes from automobile exhausts, from biological H_2S production, and from the plume of a large copper smelter. During their investigation, an extended strike brought the smelter to a standstill and thus enabled the determination of δ -values with and without the smelter exhaust. The results are shown graphically in Fig. 48. Normally, the premises are much more complicated, which limits the "fingerprint" character of the S-isotope composition of atmospheric sulfur to such rare cases as described above.

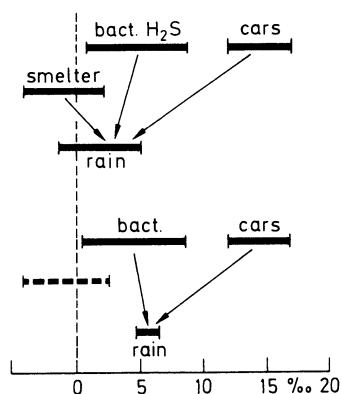


Fig. 48. $\delta^{34}\text{S}$ -values in rain water in the Salt Lake area (USA) with and without contribution from copper smelter (Nielsen 1974)

For another very unique situation in Alberta (Canada) where the industrial SO_2 had a $\delta^{34}\text{S}$ -value near 20‰, while the $\delta^{34}\text{S}$ of uncontaminated soil was near 0‰, Krouse (1980) was able to give semiquantitative estimates. However, it must be clearly stated that these data cannot be transferred to other localities. The isotopic composition of the industrial sources are generally so variable that the assessment of anthropogenic contributions to the atmosphere is extremely difficult.

3.10 Biosphere

As used here, the term “biosphere” includes the total sum of living matter, plants, animals, and microorganisms, and the residues of living matter in the geologic environment, such as coal and petroleum. A fairly close balance exists between photosynthesis and respiration, although over the whole of geologic time respiration has been exceeded by photosynthesis, and the energy thus derived was stored mostly in disseminated organic matter and, of course, in coal and petroleum.

Questions concerning the origin of coal and petroleum center around three topics: the nature and composition of the parent organisms, the mode of accumulation of the organic material, and the reactions whereby it was transformed into the end products.

Petroleum (frequently also called crude oil) is a naturally occurring complex mixture, composed mainly of hydrocarbons, but also with varying amounts of heterocompounds containing S, N, O, and metal-organic molecules, such as vanadium and nickel porphyrins. Although there are, without any doubt, numerous compounds that have been formed more or less directly from biologically produced molecules,

the majority of petroleum components are of secondary origin, either decomposition products or products of condensation and polymerization reactions.

3.10.1 Living Organic Matter

3.10.1.1 Carbon

The complexities involved in the photosynthetic fixation of carbon have already been discussed briefly on p. 34. Wickman (1952) and Craig (1953) were the first to demonstrate that marine plants are about 10‰ enriched in ^{13}C relative to terrestrial plants. Since then, numerous studies have broadened this view and provided a much more detailed picture of isotope variations in the biosphere. The reasons for the large C-isotope differences found in plants were only satisfactorily explained after the discovery of new photosynthetic pathways in the late 1960's. The bulk of the plant kingdom fixes CO_2 during the pathway described by Calvin (also called C_3 -pathway). The two new pathways are known as Hatch-Slack (or C_4 -pathway) and CAM (Crassulacean Acid Metabolism, diurnal process of acidification and deacidification). The differences in isotopic composition characteristic for each of the pathways are due to different enzymatic processes and the different sizes of the metabolic pools of carbon.

Figure 49 summarizes the variability of $\delta^{13}\text{C}$ -values exhibited by some major groups of higher plants, algae, and microorganisms. Especially noteworthy is that the $\delta^{13}\text{C}$ -ranges of C_3 and C_4 plants virtually do not overlap and that the methanogenic bacteria show an extremely large variation range.

One of the most important groups of all living matter is marine phytoplankton. Natural oceanic phytoplankton populations vary in $\delta^{13}\text{C}$ -values by about 15‰ (Sackett et al. 1973; Wong and Sackett 1978). Rau et al. (1982) showed that latitudinal trends in the $^{13}\text{C}/^{12}\text{C}$ ratio of plankton differ significantly between the northern and the southern oceans: south of the equator the correlation between latitude and the plankton $\delta^{13}\text{C}$ -value is significant, whereas a much weaker relationship exists in the northern oceans. This is strong evidence against a simple temperature-plankton $\delta^{13}\text{C}$ -relationship as originally proposed by Sackett et al. (1973). Therefore, factors other than temperature must also play an important role in determining plankton $\delta^{13}\text{C}$.

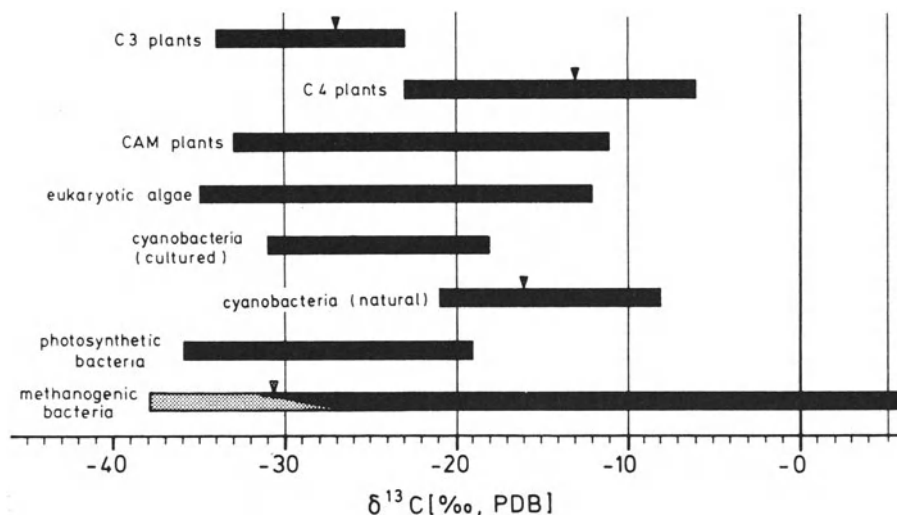
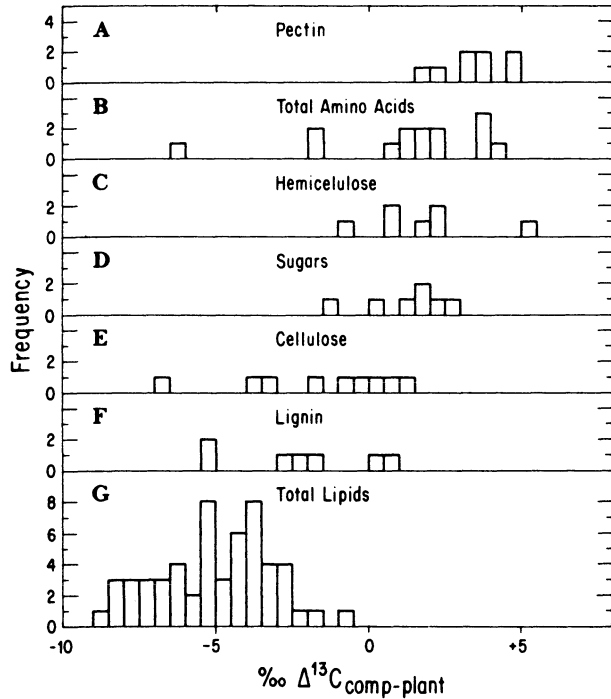


Fig. 49. Carbon isotope composition of extant higher plants, algae, and autotrophic prokaryotes. Means for some groups are indicated by *triangles*. Note the virtual absence of overlap in the ranges of C3 and C4 plants (Schidlowski et al. 1983)

Chemical Components of Plant Material. A number of investigators have studied the isotopic composition of the major biochemical constituents of plants (Park and Epstein 1960; Abelson and Hoering 1961; Parker 1964; Degens et al. 1968b; Smith and Epstein 1970; DeNiro and Epstein 1977). Figure 50 demonstrates that differences in ^{13}C -contents exist between different chemical plant components: sugar, cellulose, and hemicellulose exhibit values close to the mean plant carbon isotopic composition, whereas pectin appears to be enriched in ^{13}C and lignin and lipids are depleted in ^{13}C relative to the total plant. In the latter class the size of the isotopic difference is especially pronounced (see Fig. 50). This is not surprising because the lipid fraction includes a wide variety of organic compounds. For example, Degens et al. (1968b) found that the CHCl_3 extractable lipids had lighter $\delta^{13}\text{C}$ -values than the $\text{C}_2\text{H}_5\text{OH}$ extractable lipids.

Amino acids as a whole exhibit a general ^{13}C -enrichment with respect to the total plant. By separating different amino acids Abelson and Hoering (1961) were able to demonstrate that there are large variations among individual amino acids. In the case of *Chlorella*, for example, some typical values are: glutamic acid -18.7% , aspartic acid

Fig. 50. Differences in ^{13}C -contents of chemical constituents and the bulk plant material (Deines 1980b)



-6.6‰, serine -5.7‰, alanine -10.3‰, leucine -22.7‰, and tyrosine -19.8‰. Thus, any approach to isotope fractionations of amino acids as a whole must fail. However, the situation is even more complex. By using a similar method to that of Abelson and Hoering (1961), Macko et al. (1983) observed a wide range in $\delta^{13}\text{C}$ - and $\delta^{15}\text{N}$ -values of individual amino acids, many appear to be associated with kinetic fractionations that follow the metabolic pathways of amino acids. These results illustrate the diversity of isotope fractionations that occur within the cells of a single organism.

Respiratory Processes. Although plants fix CO_2 in the form of organic compounds, a certain amount of CO_2 is also released as the result of respiration. Measurements made by trapping the CO_2 in a CO_2 -free atmosphere indicate that there is little difference between respired CO_2 and total plant for both C_3 and C_4 plants. However, not all of the CO_2 , formed as a result of respiration and other CO_2 -forming processes is actually released to the environment. Some of this CO_2 is re-fixed with some isotope fractionation (O'Leary 1981). Consequently,

the isotopic composition measured for respired carbon may differ from that of total carbon formed by respiratory processes.

Soil CO₂. Soil CO₂ originates from the decomposition of organic material and from plant root respiration. Available $\delta^{13}\text{C}$ -measurements of soil CO₂ have been compiled by Deines (1980b) and reveal the same bimodality observed for C₃ and C₄ plants. Long-term observations on the isotope variation in soil CO₂ by Parada et al. (1983) have shown seasonal variations of $\sim\pm 5\%$. Some variations might be due to mixing with atmospheric CO₂, which is more noticeable in winter, when soil CO₂ concentrations are lowered. Other variations could be caused by decomposition of organic matter with different isotopic composition and different decay rates.

Animals. Already Craig (1953) noted that $\delta^{13}\text{C}$ -values for animal tissues fall in the same range as their food supply. DeNiro and Epstein (1978) demonstrated clearly that the carbon isotope composition of an animal greatly depends on its diet. Studies by Haines (1976) and Minson et al. (1975) have shown that the large differences in the ^{13}C -value between plants possessing either the C₃ or C₄ photosynthetic pathways are reflected in animals which derive their carbon predominantly from C₃ or C₄ plants. Furthermore, animals feeding on marine organisms have different isotopic compositions from those feeding on terrestrial organisms (Schoeninger and DeNiro 1984).

3.10.1.2 Hydrogen

During photosynthesis, plants remove hydrogen from water and transfer it to organic compounds. The fixation of CO₂ and H₂O to organic matter leads to a deuterium depletion in the plants relative to the environmental water (Schiegl and Vogel 1970; Smith and Epstein 1970). After the formation of the organic matter the oxygen-bound hydrogen atoms are readily exchangeable, while the carbon-bound hydrogen seems to be nonexchangeable (Epstein et al. 1976). This has to be taken into account when correlations between the D/H ratio in plants and the environmental water are attempted (see also Sect. 3.10.2).

There are systematic differences in the hydrogen-isotope ratios among classes of compounds in plants. Lipids usually contain less deuterium than the protein and the carbohydrate of the extracted plant

(Hoering 1975; Estep and Hoering 1980). The lipids may be subdivided into two different groups having greatly different deuterium contents. The first contains the fatty acid-saturated hydrocarbons which have a common biosynthetic pathway involving synthesis from two carbon fragments. The second group contains the pythol, sterols, and carotenes which synthesized via the five-carbon isoprenoid pathway (Hoering 1975).

3.10.1.3 Oxygen

The experimental difficulties in determining the oxygen isotope composition of biological materials lie in the rapid exchange between organically bound oxygen, in particular the oxygen of carbonyl and carboxyl functional groups with water. Thus, it is not surprising that studies on the oxygen isotope fractionation within living systems have been limited to that associated with the biosynthesis of cellulose, the oxygen of which is only very slowly exchangeable at physiological pH (Epstein et al. 1977; DeNiro and Epstein 1979, 1981). Epstein et al. (1977) analyzed the ^{18}O -content of cellulose from aquatic and terrestrial plants and compared the $\delta^{18}\text{O}$ -values obtained to those of the water used by the plants ($\delta^{18}\text{O}$ -values range from +14 to +33‰). For aquatic plants the fractionation factor between the oxygen in the cellulose and that in the water medium is about 1.027. A model which accounts for this fractionation factor is that two-thirds of the cellulose oxygen comes from the dissolved CO_2 and one-third from the oxygen of the water.

The relationship between ^{18}O in cellulose and in water from terrestrial plants is more complicated because evaporative transpiration of water takes place through their leaves. In cases in which an aquatic and a terrestrial plant have similar δD -values, making a comparison possible, the $\delta^{18}\text{O}$ -values of the terrestrial plants are higher by 4 to 16‰. DeNiro and Epstein (1979) investigated the relationship between the oxygen isotope ratios of plant cellulose, carbon dioxide, and water. They argued that the oxygen derived from CO_2 undergoes complete exchange with the water oxygen in the plant during the synthesis of cellulose. This equilibration implies that the $\delta^{18}\text{O}$ -value of cellulose is primarily a function of the ^{18}O -content of the water in the plant.

3.10.1.4 Sulfur

Sulfur is a key element of life constituting on average between 0.5 and 1.5% (dry weight) of plant and animal matter. It occurs mainly in proteins that typically display a C/S ratio of about 50. The processes responsible for the direct primary production of organically combined sulfur are the direct assimilation of sulfate by living plants and microbiological assimilatory processes in which organic sulfur compounds are synthesized. During these processes, sulfate is first phosphorylated to give "activated" sulfate species which in turn are reduced via sulfite and other intermediates to the sulfide level. At present, only a limited number of measurements of $^{34}\text{S}/^{32}\text{S}$ ratios of biological material are available. Mekhtiyeva and Pankina (1968) and Mekhtiyeva et al. (1976) have demonstrated that sulfur of aquatic plants from a given water is slightly lighter than the sulfur of the dissolved sulfate. The same results have been obtained by Kaplan et al. (1963) for marine organisms, plants, and animals.

3.10.1.5 Nitrogen

Nitrogen uptake in terrestrial plants is primarily implemented by the fixation of atmospheric N_2 mediated by soil bacteria. Since this process is not related with an appreciable isotope effect (Hoering and Ford 1960; Delwiche and Steyn 1970), the organic matter in terrestrial plants should have a $\delta^{15}\text{N}$ -value near that of atmospheric nitrogen.

3.10.2 Tree Rings

3.10.2.1 Deuterium and Oxygen

The approach to such studies is to compare the δD - and $\delta^{18}\text{O}$ -values in organic material from growth rings which represent various ages and stages in the development of the tree. A depletion in D and ^{18}O in growth rings from numerous specimens of the same tree species growing in the same location could be an indication of lower temperature, while an enrichment in D and ^{18}O may then reflect a higher temperature.

Because of an intracellular heterogeneity in the δD -distribution of plant organic matter, Epstein et al. (1976) suggested that those studies

which attempted to determine climatic changes based upon analyses of whole wood samples may be erroneous due to the presence of a mixture of cellulose, starch, lignins, and lipids within the wood tissues and that D/H ratios of only single, specified components should be compared. Epstein et al. (1976) chose cellulose as that component of wood which could be isolated in the purest form, by first replacing the exchangeable OH groups of the polymer with nitrate.

Burk and Stuiver (1981) have shown that the oxygen isotope composition of cellulose can be used as a temperature indicator in specific West Coast areas of the United States where humidity values are fairly constant. These authors suggested that the $\delta^{18}\text{O}$ -values of the source water, humidity, leaf boundary-layer dynamics and the $\delta^{18}\text{O}$ -composition of atmospheric water vapor must be considered when evaluating the temperature dependence of oxygen isotope ratios in tree rings.

3.10.2.2 Carbon

There is debate about the meaning of $^{13}\text{C}/^{12}\text{C}$ variations in tree rings. Two different interpretations are frequently discussed: one relates the decrease in $^{13}\text{C}/^{12}\text{C}$ ratios over the period 1850 to 1950 to an increase in fossil fuel combustion (Freyer 1979), whereas the other explains the $^{13}\text{C}/^{12}\text{C}$ variations with climatic temperature changes (Mazany et al. 1980). Further work must be done to identify and eliminate sources of "noise" in the tree ring record. The recent model of Francey and Farquhar (1982), in which carbon isotope variations are related to physiological properties of a leaf, is an important step forward in understanding the meaning of $^{13}\text{C}/^{12}\text{C}$ variations in tree rings.

3.10.3 Organic Matter in Sediments

Immediately after burial of the biological organic material into the sediments, complex diagenetic changes occur in the organic matter. The biopolymers, e.g., polysaccharides and proteins, are attacked by microorganisms and are partly broken down to soluble components, while other parts polymerize and react to high molecular weight polycondensation products, i.e., humic substances. With these diagenetic changes carbon isotope shifts of a few or several per mil are connected. They include isotope effects during bacterial degradation of the bio-

polymers which preferentially eliminate ^{13}C -enriched carbohydrates and proteins and preserve ^{12}C -enriched lipids. Decarboxylation reactions remove ^{13}C -enriched carboxyl groups leading to ^{13}C -depletion in the residue. As has been mentioned above, humic substances are considered to represent the first transformation products of the organic matter. They are defined as dark-brown polymers that are divided into alkali soluble, but acid insoluble, humic acids and into alkali- and acid-soluble fulvic acids. Nissenbaum and Kaplan (1972) demonstrated that humic acids are generally depleted in ^{13}C relative to fulvic acids. Thus, fulvic acids are closer in $\delta^{13}\text{C}$ to plant carbon and are considered by Nissenbaum and Schallinger (1974) to be an intermediate in the humification process.

Considered as a whole, recent marine sediments show a mean $\delta^{13}\text{C}$ -value of -25‰ (Deines 1980b). With transformation to kerogen some ^{13}C -loss occurs, leading to an average $\delta^{13}\text{C}$ -value of -27.5‰ (Hayes et al. 1983). This ^{13}C -depletion might be best explained by the large losses of CO_2 that occur during the transformation to kerogen and which are especially pronounced during the decarboxylation of some ^{13}C -rich carboxyl groups.

With further thermal maturation the opposite effect of an ^{13}C -enrichment is observed. Experimental studies of Chung and Sackett (1979), Peters et al. (1981), and Lewan (1983) indicate that thermal alteration produces a maximum ^{13}C -change of about $+2\text{‰}$ in kerogens. Changes of more than $2\text{--}3\text{‰}$ are most probably not due to isotope fractionation during normal thermal degradation of kerogen, but due to isotope exchange reactions between kerogen and carbonates.

Recent marine organic carbon is ^{13}C -enriched relative to terrestrial organic carbon (Deines 1980b). This distinction has been used to differentiate between these two sources in sediments (Brown et al. 1972). However, Dean et al. (1986) and Arthur et al. (1985) failed to observe a consistent relationship between $\delta^{13}\text{C}$ -values of organic carbon and independent geochemical indicators of marine and terrestrial organic matter for samples older than Miocene in age. On the contrary, just the opposite is apparently observed: those samples with the highest $\delta^{13}\text{C}$ -values had chemical compositions indicating the greatest contributions of marine organic matter. Arthur et al. (1985) concluded that marine organic carbon in sediments that are Cretaceous or older have $\delta^{13}\text{C}$ -values that are 5 to 7‰ more negative than marine organic carbon in Holocene sediments. The reasons for this inverse relationship are not fully understood. Arthur et al. (1985) and Dean et al. (1986)

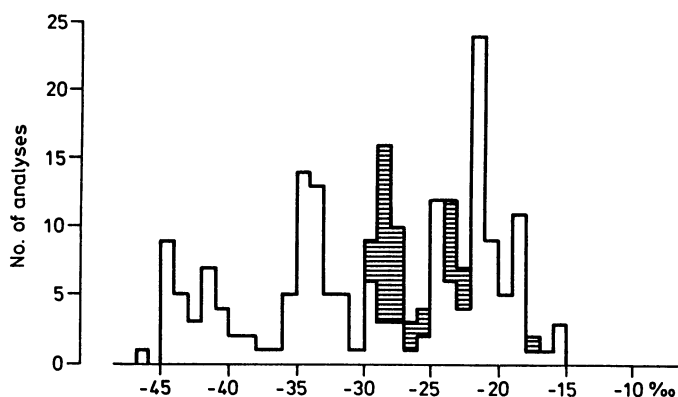


Fig. 51. Frequency distribution of $\delta^{13}\text{C}$ -values of Precambrian graphites. \square Archean, \blacksquare Proterozoic (Strauss 1986)

postulated that marine photosynthesis in Mid-Cretaceous or earlier oceans resulted in larger fractionation producing organic carbon with lighter $\delta^{13}\text{C}$ -values.

Extremely low $\delta^{13}\text{C}$ -values have been observed in Archean organic matter. About 25% of around 250 samples analyzed are anomalously depleted in ^{13}C with $\delta^{13}\text{C}$ -values between -47 and -35‰ (Strauss 1986), while the remaining 75% cover a “normal” spread between -35 and -15‰ (see Fig. 51). As far as it is known, such low $\delta^{13}\text{C}$ -values have to be attributed to methanogenic bacteria and their metabolic processes. Such extremely ^{13}C -depleted organic matter seems to be restricted to the Archean and may represent special conditions during the evolution of life.

3.10.4 Oil

In recent years the combination of stable isotope data ($\delta^{13}\text{C}$, δD , $\delta^{34}\text{S}$, $\delta^{15}\text{N}$) on crude oils and natural gas has become a powerful tool in petroleum exploration. The papers of Fuex (1977), Stahl (1977), Schoell (1984a,b), and Sofer (1984) summarize recent work in this area.

The isotopic composition of crude oil is mainly determined by the isotopic composition of its source material, more specifically the type of kerogen and the sedimentary environment in which it has been formed. Secondary effects like biodegradation and water washing have

only little effect on its isotopic composition. Because the isotopically lightest fractions are preferentially consumed during secondary alteration processes, biodegradation and water washing lead to a small ^{13}C -enrichment. In laboratory experiments of bacterial oxidation Stahl (1980) was able to demonstrate a small ^{13}C -enrichment in the remaining saturated hydrocarbons, while the asphaltene fraction showed a tendency to become isotopically lighter.

As far as it is known today, very small changes in the $^{13}\text{C}/^{12}\text{C}$ ratio do occur during migration. Silverman (1965) observed a shift of 0.4‰ during secondary migration of 6 km in the Quriquru field in Venezuela. Heterocompounds, being the most polar petroleum constituents, tend to be absorbed on mineral surfaces. Aromatics are more polar and water soluble than saturates and, therefore, preferentially removed during migration. This leads to a small ^{13}C -decrease in the crude oil with increasing migration paths.

Sofer (1984) could not support earlier reports stating that marine oils are isotopically heavier than terrigenous oils and that the difference can be utilized to distinguish between them. However, isotopic differences between oils derived from terrigenous and marine organic matter manifest in the isotopic relationship between the saturate and aromatic hydrocarbon fractions.

The various classes of chemical compounds in crude oils show small, but characteristic, differences in their carbon isotope composition. With increasing polarity the ^{13}C -content increases from the saturated hydrocarbons to the aromatic hydrocarbons, to the heterocomponents (N, S, O compounds) to the asphaltene fractions. As recently demonstrated by Schoell (1984a,b), the same relationship is also true for hydrogen. Thus, the combination of carbon and hydrogen isotope ratio determinations effectively increases the importance of this method for oil-oil and oil-source rock correlations.

Figure 52 schematically demonstrates the changes in isotopic compositions of extracts in relation to kerogens for various maturities (after Schoell 1984b). From comparison of the type patterns it becomes evident that an isotopic relationship between extract and kerogen can only be expected in the mature stage of kerogens. This has been supported by Johns and Hoefs (1985) on immature extracts from the Vienna Basin. How these "petroleum-type curves" can be successfully applied for exploration questions is shown in Fig. 53, which shows a positive oil-oil correlation and a negative crude-oil-source rock correlation. The Tertiary and Jurassic oils are isotopically more or less identical,

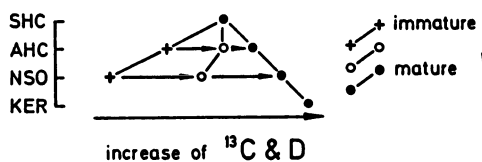


Fig. 52. Changes in isotopic composition of extracts in relation to kerogen. From comparison of the type patterns of immature and mature stages, it is evident that an isotopic relationship between extract and kerogen can only be expected in the mature stage of kerogen (*SHC* saturated hydrocarbons; *AHC* aromatic hydrocarbons; *NSO* components; *KER* kerogen) (Schoell 1984b)

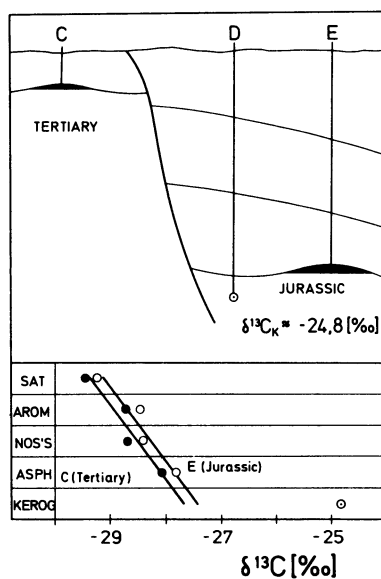


Fig. 53. "Petroleum-type curves" of different oil components from the North Sea. The diagram shows a positive oil-oil correlation and a negative source rock-oil correlation (*SAT* saturated hydrocarbons; *AROM* aromatic hydrocarbons; *NOS's* heterocomponents; *ASPH* asphaltenes) (Stahl et al. 1977)

which points to an origin from the same source rocks. The $\delta^{13}\text{C}$ -value of the kerogen is not in line with the type line, thus indicating a migration from elsewhere into both reservoirs.

Yeh and Epstein (1981) and Schoell (1984a,b) investigated the hydrogen isotope composition of crude oils. Because there are considerable variations in deuterium concentrations in the biological precursor materials and in kerogens, it is not surprising that there is a considerable range in δD -values (between -200 and -80‰ , Yeh and Epstein 1981). As far as it is known, D/H exchange processes with pore waters have no major effect on the D-composition of crude oils, at least at temperatures below $160\text{ }^\circ\text{C}$.

Since the pioneering studies of Silverman and Epstein (1958) and Silverman (1964, 1967) it is generally agreed that crude oil is isotopically lighter than the kerogen from which it is derived, but it is similar in isotopic composition to the lipid fraction. However, comparison of the deuterium variations in oils and kerogens (Schoell 1984a,b) shows that many oils have similar deuterium concentrations to the kerogens. This suggests that possibly not only lipidic compounds are responsible for the formation of oils, but the restructuring of the kerogen as a whole leads to the formation of extractable compounds.

Sulfur in Oil. Recently, Krouse (1977) and Thode (1981) reviewed the use of sulfur isotopes in petroleum exploration. Sulfur isotope studies in crude oil may be useful in several respects: (1) to identify crude oil from specific source beds, (2) to group oils into genetic families, (3) to follow their migration, and (4) under favorable conditions to identify oil alteration processes. Oils from widely distributed pools in the same reservoir rocks have similar $\delta^{34}\text{S}$ -values despite marked differences in sulfur contents, whereas oils from different source beds have variable sulfur isotope compositions because of different environmental conditions during source rock deposition. In the Williston Basin Thode (1981) was able to correlate crude oils with their source rocks and to distinguish three major types of crude oil on the basis of their sulfur isotope composition.

Although the reduced sulfur in crude oil is present in a large number of aliphatic and aromatic compounds with various degrees of complexity and stability, Monster (1972) demonstrated that the sulfur isotope composition in a particular compound class is principally the same as that of the bulk oil. In oil-source rock correlation studies Monster and Thode (unpubl. results) demonstrated that the sulfur in the crude oil is slightly more ^{34}S -rich than the kerogen sulfur, but nearly identical in $\delta^{34}\text{S}$ -value to that of the solvent-extractable organic sulfur in the source rock.

During thermal maturation, oils maintain their characteristic $\delta^{34}\text{S}$ -values (Harrison and Thode 1958; Thode et al. 1958), even though sulfur is lost. However, during the very mature stages of thermal alteration Orr (1974) found that $\delta^{34}\text{S}$ -values in the light fractions of the crude oil change considerably, whereas the heavy asphaltenes tend to retain their original $\delta^{34}\text{S}$ -values. According to Thode (1981), long distance secondary migration over some 150 km results in little or no change in $\delta^{34}\text{S}$ -value. However, crude oil alteration, such as water washing and biodegradation, may change sulfur isotope ratios of the bulk oil.

3.10.5 Coal

Carbon and hydrogen isotope compositions of coals are rather variable (Schiegl and Vogel 1970; Redding et al. 1980; Smith et al. 1982). Different plant communities and climates may account for these variations. Several studies, summarized by Maass et al. (1978), have indicated that with increasing grade of coalification very little change in the carbon isotope composition occurs. This may be due to the fact that during coalification the amount of methane and other higher hydrocarbons liberated is small compared to the total carbon reservoir in coals. With respect to hydrogen the reservoir is smaller, which may explain why δD -differences up to 50‰ have been observed by Redding et al. (1980). Schwarzkopf (cited in Schoell 1984b) found systematic δD -differences among different coal macerals, which they explained to represent primary differences within the plant constituents. On the other hand Smith et al. (1982) argued that the complex reactions taking place during the conversion of land plant debris into coals lead to a homogenization of the isotopic differences that initially characterized contributing plant materials.

Because of the problems associated with the combustion of coals, the origin and distribution of sulfur in coals is of special significance. Sulfur in coals usually occurs in different forms, as organic sulfur, as pyrite, sulfates, and elemental sulfur. Pyrite and organic sulfur are the most abundant forms. Organic sulfur is primarily derived from two sources: the original organically bound plant sulfur preserved during the coalification process and biogenic sulfides which reacted with organic compounds during the biochemical alteration of plant debris.

Studies by Smith and Batts (1974), Smith et al. (1982), Price and Shieh (1979), and Hackley and Anderson (1986) have shown that organic sulfur in coal exhibits rather characteristic isotope variations which correlate with sulfur contents. In low-sulfur coals $\delta^{34}\text{S}$ -values of organic sulfur are rather homogeneous and reflect the primary plant sulfur. In contrast, high-sulfur coals are more variable and typically more negative in $\delta^{34}\text{S}$ -values, suggesting a significant contribution from bacteriogenic sulfides. The range of $\delta^{34}\text{S}$ -values in massive pyrite is even more variable and shows no systematic correlation with organic sulfur. This is possibly due to the occurrence of several pyrite generations (Price and Shieh 1979; Hackley and Anderson 1986).

3.10.6 Natural Gas

Natural gases have been found in a wide variety of environments. While methane is always a major constituent of the gas, other components are higher hydrocarbons (ethane, propane, butane), CO_2 , H_2S , N_2 , H_2 , and rare gases. Two different processes are responsible for the formation of the major methane occurrences. The most useful parameters in distinguishing the two different types are their $^{13}\text{C}/^{12}\text{C}$ and D/H ratios.

Biogenic Gas. According to Rice and Claypool (1981), over 20% of the world's natural gas accumulations are of biogenic origin. Biogenic methane commonly occurs in recent anoxic sediments and is well documented in freshwater environments, such as lakes and swamps and in marine environments, such as estuaries and shelf regions. Two primary metabolic pathways are generally recognized for methanogenesis: fermentation of acetate and reduction of CO_2 . Although both pathways may occur in both marine and freshwater environments, CO_2 reduction is dominant in the sulfate-free zone of marine sediments, while acetate fermentation is dominant in freshwater sediments.

During the microbial action kinetic isotope fractionations on the organic material by methanogenic bacteria result in methane very much enriched in ^{12}C , typically with $\delta^{13}\text{C}$ -values between -110 to -50‰ (Schoell 1980, 1984b; Rice and Claypool 1981; Whiticar et al. 1986). In marine sediments the methane formed by CO_2 reduction is often more depleted in ^{13}C than methane formed by acetate fermentation in freshwater sediments. Thus, typical ranges for marine sediments are between -110 and -60‰ , while methane from freshwater sediments ranges from -65 to -50‰ (Whiticar et al. 1986).

The distribution between methane of freshwater and of marine origin is even more pronounced on the basis of hydrogen isotopes. Marine bacterial methane has δD -values between -250 to -170‰ , while biogenic methane in freshwater sediments is strongly depleted in D with δD -values between -400 to -250‰ (Whiticar et al. 1986).

Different sources of hydrogen in biogenic methanes can be accounted for these large differences in hydrogen isotope composition. Formation water supplies the hydrogen during CO_2 reduction, whereas during fermentation three-quarters of the hydrogen come directly from the methyl group, being extremely depleted in D.

Thermogenic Gas. Thermogenic gas is produced when organic matter is buried to greater depths. Increasing temperatures modify the organic matter due to various chemical variations, such as cracking and hydrogen disproportionation in the kerogen. ^{12}C – ^{12}C bonds are preferentially broken during the first stages of organic matter maturation. As this results in an ^{13}C -enrichment of the residue, more ^{13}C – ^{12}C bonds are broken with increasing temperatures, producing higher $\delta^{13}\text{C}$ -values. Thermal cracking experiments carried out by Sackett (1978) have confirmed this view and showed that the resulting methane is 4 to 25‰ lower than the parent material. Thus, thermogenic gas typically has $\delta^{13}\text{C}$ -values between -50 and -20 ‰ (Rice 1983; Schoell 1980, 1984b). Gases generated from nonmarine (humic) source rocks are isotopically heavier than those generated from marine (sapropelic) source rocks at equivalent levels of maturity.

In contrast to the $\delta^{13}\text{C}$ -values, δD -values are independent of the composition of the precursor material, but solely depend on the maturity of kerogen. The combination of $\delta^{13}\text{C}$ - and δD -determinations on natural gases is one of the most promising tools for gas-gas correlations. In a $\delta^{13}\text{C}$ - versus δD -diagram (see Fig. 54) not only can a clear distinction of biogenic and thermogenic gases from different environ-

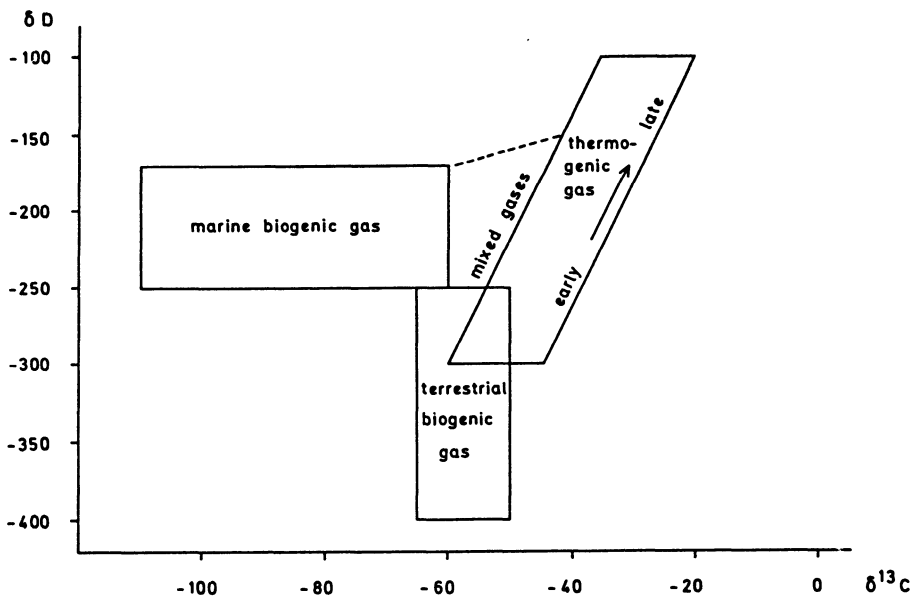


Fig. 54. Natural gas genetic classification diagram using $\delta^{13}\text{C}$ and δD of methane. (After Whiticar et al. 1986)

ments be made, but it is also possible to delineate mixtures between the different types.

A well-defined correlation is observed between the $\delta^{13}\text{C}$ -values of natural gases and the vitrinite reflectance of the sedimentary organic matter from which the gas is derived. The vitrinite reflectance is a measure of the maturity of the organic matter, it changes from about $R_0 \approx 0.3\%$ to $R_0 \approx 3.5\%$ in mature kerogen.

This relationship can be successfully applied for gas-source rock correlations (see Fig. 55). Figure 55 gives an example from the Arctic. A gas was discovered in a Jurassic sand, which could have originated in the relatively immature Lower Cretaceous-Jurassic section (R_0 of 0.5 to 0.65%) or from thermally overcooked Triassic black shale (R_0 of 1.0 to 2.0%). The $\delta^{13}\text{C}_1$ -value of the gas was -37.2‰ and the vitrinite reflectance R_0 1.9%, and thus the gas could only have originated in the Triassic black shales at a considerable depth below the horizon. It was apparent to the exploration geologists that any search for similar-type deposits was dependent on the existence of the Triassic black shale beneath the reservoir rock.

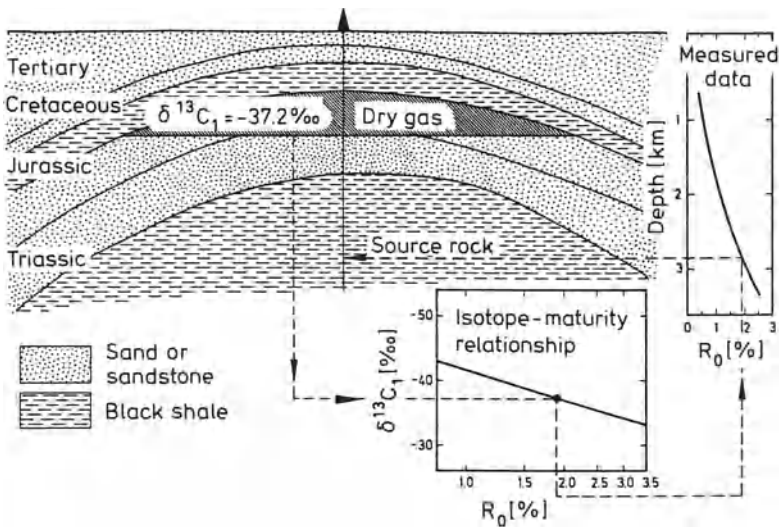


Fig. 55. Correlation between the isotopic composition of methane and the maturity of kerogen as indicated by the vitrinite reflectance. The diagram shows a positive gas-source rock correlation from the Canadian Arctic (Stahl 1979)

3.11 Sedimentary Rocks

Sediments are the weathering products and residues of magmatic, metamorphic, and sedimentary rocks after transport and accumulation in water and air. Classification of sedimentary rocks is based on easily recognizable characteristics that reflect something of the mode of transport and the environment of deposition. It is customary to consider sedimentary rocks in two categories: clastic and chemical. Transported fragmental debris of all kinds – sands, gravel, shell fragments – make up the clastic component of the rock. Inorganic precipitates from water obviously belong to the chemical category. But the chemical components also include biogenic material extracted from waters and secreted as skeletons of living organisms. According to their very different mode of formation, sedimentary rocks may be quite variable in isotopic composition. Thus, the $\delta^{18}\text{O}$ -values of sedimentary rocks span a large range from about +10 (certain sandstones) to about +44‰ (cherts).

3.11.1 Clay Minerals

The major processes that produce clays are the weathering of rocks in contact with ocean and fresh water, the diagenesis of sediments at low temperatures, and the alteration of country rocks by hydrothermal fluids at elevated temperatures. Clays from these sources are usually distinguishable isotopically (Savin and Epstein 1970a; Lawrence and Taylor 1971; Sheppard et al. 1971).

Because weathering normally involves large amounts of water relative to the amount of parent rock, the isotopic composition of the parent rock should have little influence on the isotopic composition of the weathering products. Lawrence and Taylor (1971) confirmed that the isotopic composition of weathered rocks mainly reflects the isotopic variations of meteoric waters. It follows that clay minerals which originated from fresh waters or have undergone diagenetic, isotopic exchange have more negative δ -values than those for minerals whose isotopic compositions have been established in a marine environment. Thus, clay minerals formed in contact with meteoric waters should have δD - and $\delta^{18}\text{O}$ -values which depend on the meteoric water relationship $\delta\text{D} = 8 \delta^{18}\text{O} + 10$. Therefore, on a δD - versus $\delta^{18}\text{O}$ -diagram (shown in Fig. 56) sedimentary clay minerals plot on lines which are parallel to the meteoric water line. Many clay-rich soils analyzed

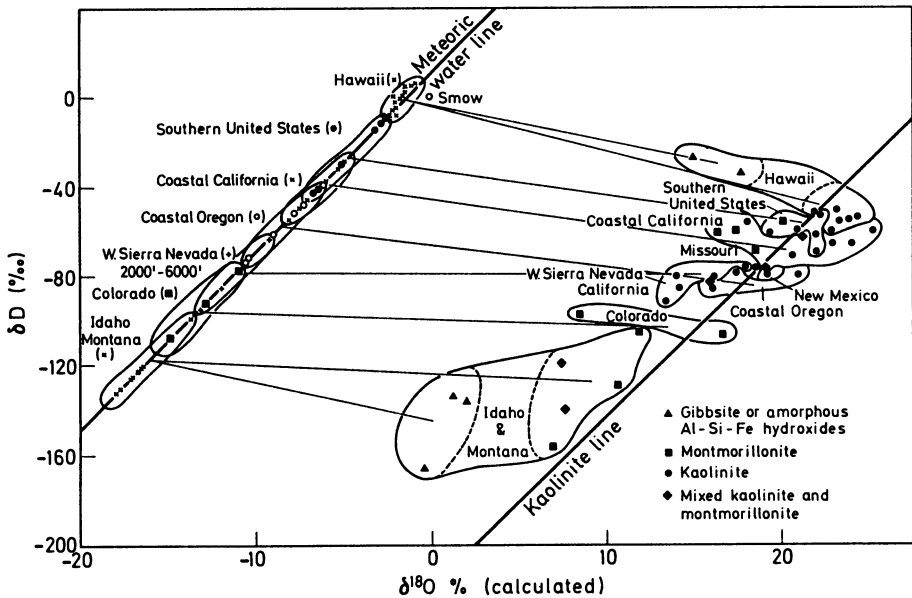


Fig. 56. Plot of δD versus $\delta^{18}O$ of clay minerals and hydroxides from Quaternary soil zones (Lawrence and Taylor 1971)

by Lawrence and Taylor (1971, 1972) lie close to the kaolinite line and obviously reflect the climatic conditions at the time of formation.

Generally, authigenic components may be distinguished from detrital components. $^{18}O/^{16}O$ ratios of detrital minerals appear to reflect the provenance and mode of origin. Detrital quartz, for instance, seems to be resistant to weathering, and it will retain its original ^{18}O -content as established in the parent rock. Rex et al. (1969) found that the $^{18}O/^{16}O$ ratio of quartz isolated from Hawaiian soils, Pacific sediments, and tropospheric dusts are remarkably uniform. The authors suggested a common eolian origin of this quartz from continental land masses. The question remains: If authigenic minerals form under equilibrium conditions, do they retain their original composition or is there a subsequent isotope exchange with pore fluids? Clay minerals can exchange isotopes with water depending upon the temperature, and the chemistry and grain size of the mineral. While interlayer water isotopically equilibrates with water vapor at room temperatures within a few days, structural water normally does not at temperatures typical of sedimentary environments (James and Baker 1976; O'Neil and Kharaka 1976; Yeh and Savin 1976; Eslinger and Yeh 1981). As temperatures

rise, the rate of isotope exchange increases with notable exchange of hydrogen at temperatures near 100 °C and of oxygen near 300 °C (O'Neil and Kharaka 1976). These experimental findings have gained support from natural systems, where Yeh and Savin (1976) and Eslinger and Yeh (1981) were able to show that oxygen isotope exchange is significant for only the very finest size fractions ($< 0.2 \mu\text{m}$).

Whole-Rock Composition of Sediments. The isotopic composition of whole-rock ocean sediments cannot be interpreted without knowledge of their chemical and mineralogical composition. Ocean sediments are complex mixtures of many minerals and generally consist of illite, smectite, mixed-layer clays, chlorite, kaolinite, quartz, and feldspar. Commonly, the relative proportions of these minerals change as a function of particle size.

Knowing the isotopic composition of the pure phases, the average composition of marine shales relatively similar in mineralogy and chemistry to recent ocean sediments can be calculated. Savin and Epstein (1970b) found a variation range of +14 to 19‰ for the oxygen isotope composition of shales. Yeh and Savin (1977) determined $\delta^{18}\text{O}$ -values for shales from wells drilled through argillaceous sediments in the Gulf of Mexico. The $\delta^{18}\text{O}$ -variations observed indicate that the rocks are not isotopically equilibrated systems. In comparison with the coarser fractions, the finer fractions of clay minerals are always richer in ^{18}O . The disequilibrium among clay fractions becomes less pronounced as the temperatures of diagenesis increase.

δD -values of shales range from -73 to -33‰ (Yeh 1980). The δD -variation among different size fractions of a shale is about 15 to 20‰ in the upper parts of the sedimentary column and decreases with depth of burial. The large range is mostly due to the variations in proportion of clays of different origins. The differences in δD -values among different size fractions indicate isotopic disequilibrium between clays of different sizes. Yeh (1980) concluded that significant fractionations occurred between residual and expelled pore water and that the conversion of montmorillonite to illite during burial diagenesis of shales is the most important mechanism of late-stage dehydration.

3.11.2 Cherts

Cherts have the highest $^{18}\text{O}/^{16}\text{O}$ ratios found in rocks. This is due to the large oxygen isotope fractionation factor between quartz and water

at low temperatures. Cherts are very similar in chemical and mineralogical composition, however, their oxygen isotope composition may vary by as much as 25‰.

Cherts, like carbonates, show temporal isotopic variations, the older cherts having lower $\delta^{18}\text{O}$ -values (Degens and Epstein 1962). Cherts of different geologic ages may contain a record of temperature, isotopic composition of ocean water, and the diagenetic history. There has been some discussion as to which factor is more important, the temperature (Knauth and Epstein 1976), the isotopic composition of ocean water (Perry 1967; Perry and Tan 1972), or the diagenetic history (Kolodny and Epstein 1976).

Knauth and Epstein (1975) and Murata et al. (1977) analyzed the various forms of silica with increasing sedimentary burial. Murata et al. (1977) found that the oxygen isotope ratios in different silica phases from three different diagenetic zones decrease abruptly at the transition from biogenic opal into disordered cristobalite and again at the transition from ordered cristobalite into microquartz (quartzose chert). These stepwise changes indicate that each phase retains its original composition during progressive burial until some limiting depth where it is transformed into another phase. This decrease in $\delta^{18}\text{O}$ with increasing burial seems to reflect a rise in temperature or an isotope exchange with some kind of isotopically light water.

There is strong evidence that most cherts of Paleozoic and younger age originate from biogenic amorphous silica. However, a purely inorganic origin has been found for cherts in sodium carbonate lakes of East Africa. O'Neil and Hay (1973) concluded from oxygen isotope analyses that such East-African cherts formed from their precursors in lake waters of widely varying salinity.

3.11.3 Carbonates

3.11.3.1 *Marine Organisms and "Paleotemperatures"*

In 1946 Urey presented a paper concerning the thermodynamics of isotopic systems and suggested that variations in the temperature of precipitation of calcium carbonate from water should lead to measurable variations in the $^{18}\text{O}/^{16}\text{O}$ ratio of the calcium carbonate. He postulated that the determination of temperatures of the ancient oceans should be possible, in principle, by measuring the ^{18}O -content of fossil calcite shells. The first paleotemperature scale was introduced by

McCrea (1950) and refined by Epstein et al. (1953), who obtained the following empirical relationship, slightly modified by Craig (1965):

$$T (^{\circ}\text{C}) = 16.9 - 4.2 \Delta + 0.13 \Delta^2 ,$$

where Δ is the per mil difference between CO_2 derived from carbonate by reaction with H_3PO_4 at 25°C and CO_2 equilibrated at 25°C with the water from which the carbonate was deposited.

Three problems make the interpretation of paleotemperature determinations rather complicated:

1. the unknown ^{18}O -content of the ancient oceans;
2. metabolic effects on carbonate precipitation;
3. the isotopic preservation of primary oxygen in the carbonates.

1. We have to assume that ancient ocean water has had a more or less constant isotopic composition, similar to that at present. However, a crucial point is the question of "paleosalinities". We must know if the organism to be analyzed has lived in ocean water of 35‰ salinity. Ocean water of higher salinities has a higher ^{18}O -content, because ^{16}O is preferentially concentrated in the vapor phase during evaporation. Ocean water of lower salinity has a lower ^{18}O -content, because it is diluted by fresh waters. Epstein and Mayeda (1953) estimated that a variation in salinity of 1‰ would be accompanied by 1°C error in temperature determinations in a nonglacial period of the history of the Earth.

2. Some organisms, such as many foraminifera species, which apparently deposit calcite or aragonite in isotope equilibrium with ocean water and other organisms (e.g., echinoderms, asterioida, ophiuroidea, and crinoidea) do not precipitate their carbonates in equilibrium with their environment (Weber and Raup 1966a,b; Weber 1968). These so-called vital effects are accounted for by an isotope exchange reaction between respiratory CO_2 and dissolved bicarbonate at or near the site of skeletal deposition.

Knowledge of the ecologic behavior of shell-secreting organisms is also essential. If nonextinct species are used for thermometry the assumption must be made that their depth habitats have not changed with time. Another important point is the question of whether the CaCO_3 -secreting organisms grow shells only during a portion of the local temperature range or throughout the entire range. Epstein and Lowenstam (1953) have shown that growth of skeletons of most species does not take place during the entire year. The majority of the

pelecypods, for instance, seem to grow primarily in the warm temperature range, whereas the gastropods show winter as well as summer growth. Some forms retain shell growth at low temperatures.

3. The isotopic composition of oxygen in an aragonite or calcite shell will remain unchanged until the shell material dissolves and re-crystallizes during diagenesis. Some of the criteria by which unaltered samples might be recognized have been discussed by Lowenstam (1961). But the problem of how to prove the preservation is still unsolved.

Mineralogy can also play a role in the isotopic composition of carbonates (Sharma and Clayton 1965). For instance, the $\delta^{18}\text{O}$ -value of aragonite at 25 °C is 0.6‰ higher than in coexisting calcite and the ^{13}C -content of aragonite is enriched by 1.8‰ relative to calcite (Rubinson and Clayton 1969).

In recent years most "paleoclimate" studies have concentrated on foraminifera. Since the first pioneering paper of Emiliani (1955) numerous cores from the Atlantic, Caribbean, and equatorial Pacific have been analyzed and, when correlated accurately, produced a well established oxygen isotopic curve for the past hundred thousands of years (Emiliani 1972; Shackleton and Opdyke 1973; Emiliani and Shackleton 1974; Emiliani 1978).

$\delta^{18}\text{O}$ -values exist from both planktonic and benthic species. From these core studies it is quite obvious that similar $\delta^{18}\text{O}$ -variations are observed in all areas. With independently dated time scales on hand, these $\delta^{18}\text{O}$ -variations result in synchronous isotope signals in the sedimentary record because the mixing time of the oceans is relatively short ($\sim 10^3$ years). These synchronous signals provide stratigraphic markers enabling correlations between cores which may be thousands of kilometers apart.

Differences in oxygen isotope composition of foraminifera can be caused by both glacially controlled changes in the isotopic composition of ocean water and variations in the temperature of the ocean. There has been some controversy concerning the extent of the "temperature factor" as opposed to the "ice volume factor". While Emiliani (1955, 1966) originally favored the temperature factor, Shackleton and Opdyke (1973), and later many others, favored the ice volume factor. Although the resolution of the $\delta^{18}\text{O}$ -values into these two effects cannot yet be adequately done for all times and all ocean areas, the problem can be partly resolved by separately analyzing planktonic and benthic foraminifera. Recall that bottom water in the oceans (see p. 125f.) is produced at high latitudes. It could be expected that the

temperature of this water is more or less constant, as long as ice caps exist at the Poles. Thus, the oxygen isotope composition of benthic dwelling organisms should preferentially reflect the change in the isotopic composition of the water, while the $\delta^{18}\text{O}$ -values of planktonic foraminifera should be affected by both temperature and isotopic water composition.

Most species of benthic foraminifera have been shown to precipitate carbonate slightly out of isotopic equilibrium with ambient seawater. Adjustments of these species to equilibrium have been proposed by Shackleton and Opdyke (1973), Shackleton (1977a), Belanger et al. (1981), and Graham et al. (1980). However, for several species, there is considerable range in the estimates of the adjustments. As suggested by Vincent et al. (1981) the degree of disequilibrium might be even variable in space and time.

Oxygen isotope variations in foraminifera have been very successful when applied in the Pleistocene regardless of the exact proportion of the temperature, ice-volume effect, and species-specific factors. One such example is a very detailed record of sea level variation, another the global synchronicity of a biostratigraphic marker (Thierstein et al. 1977). As shown in Fig. 57 there are several striking features of the Pleistocene record: the most obvious one is the cyclicity, secondly the fluctuations never go beyond a certain maximum value on either side of the range. This seems to imply that very effective feedback mechanisms are at work stopping the cooling and warming trends at some maximum level. Furthermore, the curve shown in Fig. 57 is characterized by a "sawtooth" slope, resulting from maximum warm periods followed immediately by maximum cold periods. This may mean the maximum ice cover is abruptly melted by rapid warming when a certain critical maximum ice cover is reached.

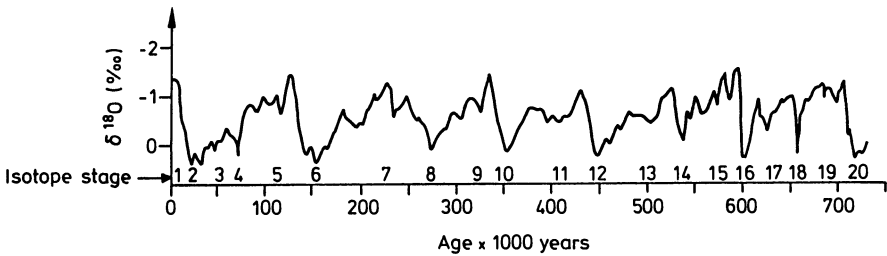


Fig. 57. Composite $\delta^{18}\text{O}$ -fluctuations in the foraminifera species *G. sacculifer* from Caribbean cores showing constancy of ^{18}O -maxima and minima (Emiliani 1978)

Broecker (1982) summarized the Pleistocene $\delta^{18}\text{O}$ -records of planktonic and benthic foraminifera from deep-sea cores and showed that there is no significant difference between the average amplitudes for both records. This similarity demands that the glacial to interglacial change in surface ocean temperature be quite small. He further demonstrated that only a small portion of the observed ^{18}O -change from glacial to interglacial conditions for benthic shells can be attributed to temperature change, by far the larger portion must be due to the change in ice volume.

Savin (1977) tried to trace the oxygen isotope record back throughout the Tertiary. In addition to the problems mentioned above, other questions such as the importance of diagenetic recrystallization complicate the record (Killingley 1983). Nevertheless, the evidence for a global cooling throughout the Tertiary is well established. Figure 58 presents the oxygen isotope record from foraminifera at the DSDP Site 167 in the Pacific Ocean (Savin 1977). A gradual, although several steplike events are clearly evident, deep water temperature decrease from nearly 12°C during Late Cretaceous to present values of $1^\circ\text{--}2^\circ\text{C}$ is observed.

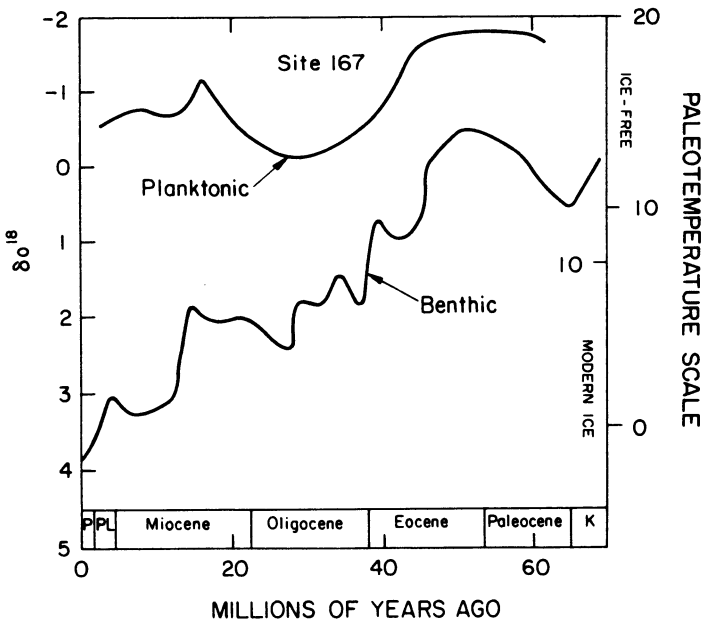


Fig. 58. Oxygen isotopic values from benthic and planktonic foraminifera from DSDP Site 167 from the Pacific Ocean. Interpreted paleotemperatures with two scales, with polar ice and without polar ice. (After Savin 1977)

3.11.3.2 *Carbon in Foraminifera*

In recent years, a large number of investigations have been undertaken to use the $\delta^{13}\text{C}$ -values of foraminifera as a paleoceanographic tracer (Shackleton and Kennett 1975; Williams et al. 1977, 1981; Bender and Keigwin 1979; Broecker 1982; Shackleton et al. 1983). The carbon isotope composition in foraminifera is, however, influenced by many factors and, therefore, more difficult to interpret than the oxygen isotope record. The first good record of carbon isotope variations in Cenozoic deep-sea carbonates was given by Shackleton and Kennett (1975). They clearly demonstrated that planktonic and benthic foraminifera yield consistent differences in $\delta^{13}\text{C}$ -values, the former being enriched in ^{13}C by about 1‰ relative to the latter.

This ^{13}C -enrichment in planktonic foraminifera is due to photosynthesis which removes ^{12}C preferentially from the surficial layer. A portion of this precipitated organic matter settles into deeper water where it is reoxidized, which causes a slight ^{12}C -enrichment in the deeper water masses. Besides these internal oceanographic processes, external factors may also influence the carbon isotope composition, which act on a much slower time scale than the internal processes. One very important external factor is obviously the sea level change: periods of high sea level coincide with times of ^{13}C -enrichment. During times of transgression, higher rates of organic carbon are buried into marginal sediments. For instance, the excess removal of 1% of the ocean's carbon into marine sediments results in an ^{13}C -increase of 0.2‰ (assuming a $\delta^{13}\text{C}$ -value of -20‰ for the organic carbon).

A further complication results from the fact that, in general, the $\delta^{13}\text{C}$ -value of foraminifera is not equal to dissolved bicarbonate, which is interpreted as indicating disequilibrium due to vital effects. Grossman (1984b), however, by analyzing live benthic foraminifera, demonstrated that when mineralogy, temperature, and dissolved inorganic carbon are considered, foraminiferal carbonate- HCO_3^- fractionation may not be very different from inorganic precipitated carbonate. Assuming that vital effects are either nonexistent or on the average invariant with time, then systematic variations in C-isotope composition may reflect variations in bottom water $\delta^{13}\text{C}$. With these prerequisites Bender and Keigwin (1979) attempted to trace the age and movement of deep water masses. Shackleton et al. (1983) used $\delta^{13}\text{C}$ -data to confirm reduced CO_2 concentrations in the ice age atmosphere, which has also been verified by directly measuring the CO_2 content of air bubbles in ice cores.

3.11.3.3 *Fresh Water Carbonates*

Since fresh water is, in general, depleted in ^{18}O relative to ocean water and more variable in the $^{13}\text{C}/^{12}\text{C}$ ratio due to a relatively high contribution of soil-derived organic CO_2 , fresh water carbonates are generally lighter and show a much broader variation range in carbon and oxygen isotope composition than marine carbonates (Clayton and Degens 1959; Keith and Weber 1964; Keith et al. 1964). This very general distinction has been used to determine paleoenvironmental conditions. However, decisive in this connection is the degree of evaporation of the fresh water body.

Carbonates deposited from highly evaporated fresh water lakes may not only have higher $\delta^{18}\text{O}$ -values than marine carbonates, but also have even more pronounced higher $\delta^{13}\text{C}$ -values (Rothe and Hoefs 1977). The ^{13}C -enrichment may be interpreted as reflecting an increased CO_2 exchange between the atmosphere and the shallowing water body.

A further complication may arise from stratification of fresh water bodies either intermittently (i.e., seasonally) or permanently (thermal or salinity). During stratification, ^{12}C is transferred from the surface to deeper waters by sinking of dead organic matter. Degradation in deeper water masses leads to relatively ^{12}C -enriched dissolved carbon dioxide, while the surface waters exhibit a ^{13}C -enrichment. McKenzie (1982) observed a maximum gradient of 5 to 6‰ during summer thermal stratification, while during winter-spring mixing there is no $\delta^{13}\text{C}$ -gradient.

There have been several attempts to use the isotopic composition of fresh water shells as a paleoclimatic indicator. Objects of studies have been mollusks (Fritz and Poplawski 1974), gastropods (Abell 1986), and land snails (Yapp 1979; Magaritz and Heller 1980). However, since fresh waters are highly variable in isotopic composition and can be easily altered by evaporative processes, quantitative interpretations of climatic changes are nearly impossible. Nevertheless, qualitative changes of environmental conditions are clearly indicated. Thus, Magaritz and Heller (1980) found that snails from an arid zone are enriched by 2‰ in ^{18}O compared to the same species from a moderate climate zone.

3.11.3.4 *Dolomites*

The “dolomite problem”, i.e., the origin of dolomite and the conditions promoting the dolomitization of limestones, is still being debated.

Although many claims of primary dolomite have been made, the preferred view now is that most dolomites are of replacement origin. Land (1980) concluded that there is no unique environment of dolomitization. Aside from the basic chemical constraint that a solution must be oversaturated with dolomite in order to crystallize it, dolomite may form in a variety of chemical environments. Within the last few thousand years dolomite has formed from hypersaline, subtidal waters of marine derivation. McKenzie (1984), studying dolomitization in coastal sabkhas from the Persian Gulf, postulated that aragonite and perhaps high Mg-calcite serve as intermediates in the formation of dolomite via a dissolution-precipitation process. At the other end of the salinity spectrum, dolomite forms in the mixing zone between meteoric and ocean waters (Land 1980). Such a model has also been favored for very old Precambrian deposits (Tucker 1983).

Two problems complicate the interpretation of isotope data to delineate the origin and diagenesis of dolomites. First, it has not been possible to determine directly the equilibrium oxygen isotope fractionations between dolomite and water at sedimentary temperatures, because the laboratory synthesis of dolomite at these low temperatures is still problematic. Furthermore, the fractionation may depend partly on the crystal structure, more specifically on the composition and the degree of crystalline order and, in this respect, it is well known that dolomite is a very complex mineral. Secondly, dolomitization on a massive scale appears to occur under open-system conditions, simply because large quantities of magnesium have to be supplied. Extrapolations of high-temperature, experimental, dolomite-water fractionations to low temperatures suggest that at 25 °C dolomite should be enriched in ^{18}O relative to calcite by 4 to 7‰. In contrast, the oxygen isotope fractionation observed between Holocene calcite and dolomite is somewhat lower, namely in the range between 2 and 4‰ (Land 1980; McKenzie 1981).

A very important site of dolomite formation is the deep-sea environment (Pisciotti and Mahoney 1981; Kelts and McKenzie 1982). Along continental margins and in small ocean basins dolomite forms as cement, layers, and concretionary zones in associations with rapidly deposited, fine-grained, organic-rich sediments. As shown by Deuser (1970), among others, these dolomites can be extremely variable in C-isotope composition with $\delta^{13}\text{C}$ -values ranging from -60 to +20‰. In contrast to this very large variation for deep-sea dolomites, most platform dolomites fall in the relatively small $\delta^{13}\text{C}$ -range between -2 to +4‰ (Land

1980). The low $\delta^{13}\text{C}$ -values of deep-sea dolomites are characteristic of formation at shallow depths from organic matter via microbial reduction of sulfate, whereas the high $\delta^{13}\text{C}$ -values are typical of dolomites formed below this zone where dissolved $\text{H}^{12}\text{CO}_3^-$ is preferentially removed by reduction of CO_2 to methane during methanogenesis. Thus, in the sequence of diagenetic alteration of organic matter, carbonate is continuously precipitated and each alteration reaction carries a distinct C-isotope signature which is preserved in the diagenetic carbonate. Differences in the sedimentation rate, the amount of organic matter available, and the geothermal gradient will affect these reactions and the extent of $\delta^{13}\text{C}$ -variation (Pisciotti and Mahoney 1981; Kelts and McKenzie 1982).

3.11.4 Diagenesis of Limestones

Isotope data on several thousand limestone samples have been reported in the literature to date. The tendency toward lower $^{18}\text{O}/^{16}\text{O}$ ratios with their increasing age is a well-documented fact (Keith and Weber 1964; Veizer and Hoefs 1976), although the reasons for this isotope shift are still under debate (see discussion on the isotopic evolution of ocean water). The majority of isotope analyses of limestones have involved whole-rock samples, but in recent years individual components such as different generations of cements have been analyzed (Hudson 1977; Dickson and Coleman 1980; Moldovanyi and Lohmann 1984; Given and Lohmann 1985).

The original marine carbonate assemblage of aragonite, Mg-calcite, and low-Mg-calcite is converted into stable diagenetic low-Mg-calcite through a process of dissolution and reprecipitation during which isotopes from the dissolving phases mix with the intervening water. This diagenetic, mineralogical stabilization usually proceeds in discrete microenvironments which often preserve original textures. Once stabilized, carbonates are normally not subject to perpetual dissolution-precipitation and isotopic reequilibrium with younger diagenetic fluids. This is supported by results of Given and Lohmann (1985), who found that two distinct secondary calcite phases, representing a fine-scale intermixture, have maintained isotopic integrity despite intimate association.

The diagenetic process can proceed in waters of meteoric or marine derivation, the former are typical for shallow marine sequences, while

the latter are common for deep-sea carbonates. Several studies have reported a general decrease of the ^{18}O -content in pelagic carbonate sediments with increasing age and depth of burial (cf. Matter et al. 1975; McKenzie et al. 1978). The progressive decrease of $\delta^{18}\text{O}$ appears to reflect precipitation of cement at progressively higher temperatures. In contrast, the $\delta^{13}\text{C}$ -values are little altered and obviously reflect the composition in the original sediment. A special case is carbonate diagenesis in carbonates closely associated with basalts. Many oceanic limestones lying above basalt or interbedded with them show alteration which is commonly attributed to contact thermal metamorphism. However, isotope studies show that the alteration frequently occurred at relatively low temperatures (Bernoulli et al. 1978; McKenzie and Kelts 1979).

Clear trends in the isotopic composition of cements can be established for near-surface diagenesis (Allan and Matthews (1982) and burial diagenesis (Milliken et al. 1981). Allan and Matthews (1973, 1982) determined the effects of subaerial diagenesis on the isotopic composition of carbonates. These studies showed that subaerial carbonate sediments can be recognized from characteristic isotope patterns preserved in vertical stratigraphic sections. In particular, they observed $\delta^{13}\text{C}$ -depleted carbonates at the exposure surface which are interpreted as representing soil-derived CO_2 from the vegetation on the exposure surface. Beeunas and Knauth (1985) observed equivalent isotope trends in the 1.2 Ga Mescal Limestone of central Arizona and suggested that a vegetative land cover existed on the Precambrian exposure surface.

Studies of sequential cement generations by Dickson and Coleman (1980) suggest that early cements exhibit higher $\delta^{18}\text{O}$ - and $\delta^{13}\text{C}$ -values with successive cements becoming more depleted in both ^{13}C and ^{18}O . This ^{18}O -trend is attributed to increasing temperatures and to isotopic evolution of pore waters during burial. The $\delta^{13}\text{C}$ -trend is interpreted as an increase of organic-derived CO_2 during burial. A more unusual effect of diagenesis is the formation of carbonate concretions in essentially uniform argillaceous sediments. Isotope studies of Hoefs (1970), Sass and Kolodny (1972), Irwin et al. (1977), Hudson (1977), and Gautier (1982) suggest that microbiological activity created localized supersaturation of calcite in which dissolved carbonate species were produced more rapidly than they could be dispersed by diffusion. Extremely variable $\delta^{13}\text{C}$ -values in these concretions indicate that different microbiological processes participated in concretionary growth. Irwin et al. (1977) presented a model in which organic matter is diagenetically

modified by (1) sulfate reduction, (2) fermentation, and (3) thermally-induced, abiotic CO₂ formation which can be distinguished by their $\delta^{13}\text{C}$ -values; (1) $\sim -25\text{‰}$; (2) $\sim +15\text{‰}$; and (3) $\sim -20\text{‰}$.

3.11.5 Diagenesis of Clastic Rocks

A very detailed study of Milliken et al. (1981) constrained the diagenetic history for the Frio sandstone, Gulf Coast area. Quartz is most commonly the first cement and constitutes around 2.5% of the average sandstone volume. The average $\delta^{18}\text{O}$ of quartz cement is $31\text{‰} \pm 1.5$, indicating precipitation at considerably cooler temperatures than that at which most clay mineral transformations take place. Calcite is the dominant cement in Frio sandstone, constituting about 5% of the total sandstone volume and generally postdates quartz precipitation. Its isotopic composition is relatively constant around $23 \pm 2\text{‰}$. The volume of water required to precipitate quartz and calcite cements far exceeds the volume of pore water deposited with, near, or beneath the sands. Thus, an external water source is required.

Longstaffe (1983) summarized case studies of the application of stable isotope research in clastic diagenesis. One set of case studies estimates the crystallization temperature of authigenic minerals from experimentally determined oxygen isotope mineral-water fractionations (such as kaolinite-water, Land and Dutton 1978; and smectite-water, Yeh and Savin 1977). The calculated temperatures can be used to determine the sequence of authigenic mineral formation and to estimate geothermal gradients and maximum depths of burial. Another group of examples concerns studies of shale diagenesis. Oxygen isotope geothermometry using quartz-illite/smectite can provide estimates of the maximum temperature to which the shale has been heated. Examples have been reported from the Precambrian Belt Supergroup, the Texas Gulf Coast, and the Great Valley Sequence (Eslinger and Savin 1973a,b; Yeh and Savin 1977; SuchECKI and Land 1983). The latter authors demonstrated that illite/smectite reactions during burial can control the geochemical evolution of formation fluids. A final example presented by Longstaffe (1983) discusses the control that meteoric water can exert upon diagenesis. He concluded that isotope signatures of authigenic minerals precipitated from an isotopically characteristic fluid may provide a method by which the paleohydrology of a sandstone can be inferred.

3.11.6 Phosphates

As was pointed out by Urey et al. (1951), the development of a temperature scale using calcium carbonate and another oxygen compound precipitated by marine organisms (e.g., phosphates) would permit a temperature scale independent of the oxygen isotope composition of ocean waters. This was originally presented by Longinelli (1965, 1966). However, Longinelli and Nuti (1973) gave a revised phosphate-water isotope temperature scale and showed that the slope of the calculated equation is practically identical to that of the carbonate equation. This means that the difference in the δ -values of carbonate and phosphate in equilibrium with ocean water is constant and independent of the temperature and of the $\delta^{18}\text{O}$ -value of the water.

The major advantage of the phosphate thermometer is that it is a system which is insensitive towards diagenetic reactions (Shemesh et al. 1983). As shown by Kolodny et al. (1983) only in enzyme-catalyzed reactions is phosphate oxygen readily exchangeable with environmental water. This inertness towards postdepositional recrystallization is illustrated in Fig. 59, where the isotopic composition of cherts, limestones, and phosphorites from a single area in the Negev, Israel is compared. The $\delta^{18}\text{O}$ -values of carbonates and cherts vary widely, with probably only the highest values indicative of marine conditions. In contrast, the phosphorites are very uniform in isotopic composition. The small spread in phosphorite $\delta^{18}\text{O}$ -values is strong evidence for the resistance of PO_4 to dissolution-reprecipitation processes.

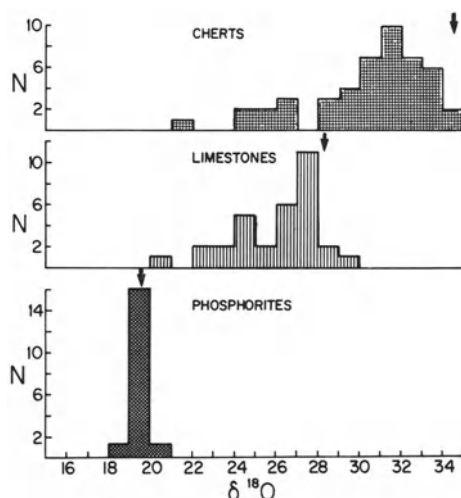


Fig. 59. Histogram of $\delta^{18}\text{O}$ -values for cherts, limestones, and phosphorites of the Mishash Formation of Campanian age in Israel. *Arrows* mark expected composition of cherts and carbonates in equilibrium with phosphate of $\delta^{18}\text{O} = 19.5\text{‰}$ (Shemesh et al. 1983)

Another interesting observation made by Shemesh et al. (1983) is that the $\delta^{18}\text{O}$ -values of phosphorites decrease with increasing geologic age, a similar trend is also observed for limestones and cherts. Because this trend cannot be explained by postdepositional exchange with ^{18}O -depleted meteoric water, the $\delta^{18}\text{O}$ -change implies either higher temperatures of phosphorite formation in the past or the progressive depletion of the ocean in ^{18}O through time.

3.11.7 Sedimentary Sulfides

Due to the activity of sulfate-reducing bacteria (producing isotopically light sulfide and isotopically heavy residual sulfate), most sulfur isotope fractionation takes place in the uppermost layers of the muds of shallow sea basins and tidal flats. Thode et al. (1960), Vinogradov et al. (1962), Kaplan et al. (1963), Nakai and Jensen (1964), Hartmann and Nielsen (1969), and others have observed that depletions occurred in ^{34}S from 15 to 62‰ for sulfides relative to associated sulfates in various natural environments. Normally, sedimentary sulfides should have a $\delta^{34}\text{S}$ -value between -30 and -10‰, although numerous examples exist where the sedimentary sulfides show a ^{34}S -enrichment.

Unconsolidated mud remains slightly permeable to dissolved marine sulfate and, therefore, the availability of sulfate within the uppermost centimeters of the sediment is unlimited. With increasing sediment depths, a gradual transition from the open system of the free water column toward an almost completely closed system at depth takes place. If the bottom water above a sediment is poorly aerated, then the sediment may be reduced almost to the sediment-water interface and very large amounts of isotopically light sulfide can accumulate within this transition zone. Such an example, shown in Fig. 60, has been described by Hartmann and Nielsen (1969) in the Baltic Sea. Here, the sulfide concentration increases progressively from zero at the sediment surface to about ten times the original sulfate concentration in the interstitial water at a depth of 5 cm. Because the open-system condition is restricted to the uppermost few centimeters of the sediment, the production rate of isotopically light biogenic sulfide is inversely correlated with the rate of sediment accumulation.

$\delta^{34}\text{S}$ of pyrite may depend on its texture (Raiswell 1982). Predominantly framboidal pyrites have lighter $\delta^{34}\text{S}$ -values than euhedral pyrites. The former have evolved in an open system relative to seawater sulfate, the latter at greater depths under closed-system conditions.

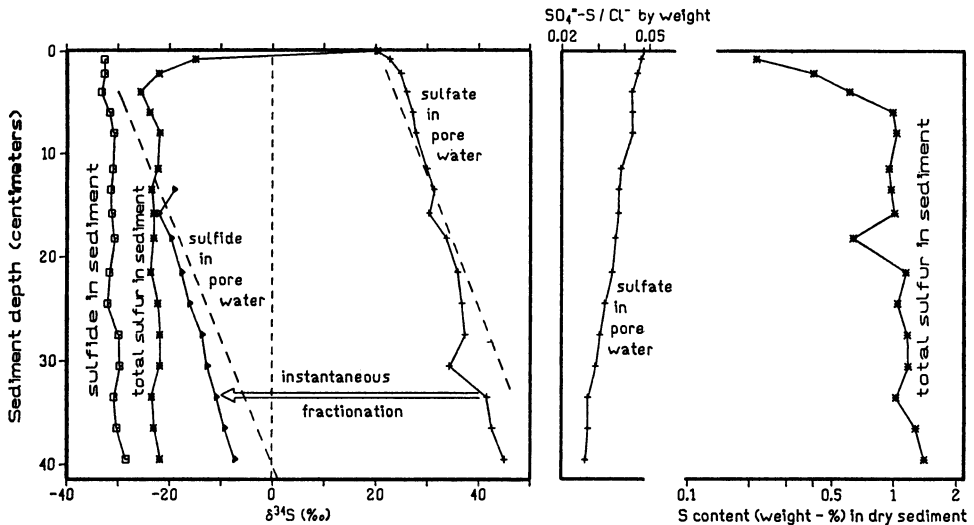


Fig. 60. Variation in sulfur content (*right*) and in $\delta^{34}\text{S}$ (*left*) from Kiel Bay, Baltic Sea. Dotted lines indicate theoretical Rayleigh fractionation curves (Nielsen 1978)

Berner (1972, 1984) has discussed the factors governing the formation of sedimentary pyrite in detail. Pyrite is formed in those marine sediments where organic matter accumulates faster than it can be destroyed, pore waters become anaerobic, and the process of bacterial sulfate reduction begins. As H_2S is formed, some of it reacts with detrital iron minerals to form black iron sulfide. The primary limitations upon how much sulfate can be transformed and fixed as pyrite are:

1. the availability of bacterially metabolizable organic matter;
2. the concentration and rate of deposition of detrital iron compounds which can react with H_2S ;
3. the rate of replenishment of sulfate in the sediment via diffusion from the overlying water.

Laboratory studies (Harrison and Thode 1958; Kemp and Thode 1968) have demonstrated that the rate of sulfate reduction is much more strongly dependent upon the concentration of bacterially metabolizable organic compounds than on the concentration of sulfate. The population of sulfate reducers in marine sediments decreases rapidly with depth, most likely as a result of the loss of organic matter. The readily decomposable material rapidly disappears so that the sulfate reducers become dependent upon fermentative microorganisms

to break down long-chain polymers and other macromolecules which are otherwise not available to the sulfate reducers. No matter how much H_2S is produced in a sediment, no more pyrite can form than the amount of iron available for reaction with H_2S .

Accepting that a difference in $\delta^{34}\text{S}$ -values of -30 to -50‰ between bacteriogenic sulfide and marine sulfate exists in present-day sedimentary environments, similar fractionations in ancient sedimentary rocks may be interpreted as evidence for the activity of sulfate-reducing bacteria. The presence or absence of such fractionations in sedimentary sulfur may thus constrain the time of emergence of sulfate-reducing microorganisms.

In early Archaean sedimentary rocks (> 3.0 Ga) most sulfides and the rare sulfates have isotopic compositions near 0‰ (Monster et al. 1979; Cameron 1982), indicating an absence of bacterial reduction in oceanic sulfate. According to Cameron (1982) and Hattori et al. (1983), the onset of bacterial reduction was at around 2.3 Ga. Pyrites in strata older than 2.3 Ga have $\delta^{34}\text{S}$ -values of $\sim 0\text{‰}$, while younger pyrites are depleted in ^{34}S and have a wide range in sulfur isotope composition. Thode and Goodwin (1983) and Goodwin et al. (1985) presented evidence for an even earlier development of bacterial sulfate reduction. However, the criteria which are used to distinguish sulfide of biogenic and of hydrothermal origin are not unequivocal, therefore, the exact beginning of bacterial sulfate reduction is still debatable.

3.12 Metamorphic Rocks

The application of stable isotopes to metamorphic rocks has concentrated primarily (1) on the nature of fluid-rock interactions and (2) on the determination of metamorphic or equilibration temperatures.

3.12.1 Metamorphic Fluids: Their Flow, Sources, and Water/Rock Ratios

The problem addressed here is the extent to which the isotopic characteristic of the metamorphic system was modified by a fluid phase (see also the recent review by Valley 1986). Two end-member situations can be postulated in which coexisting minerals would reequilibrate during metamorphism.

1. In the case of equilibration of minerals with a *pervasive* fluid of uniform composition a pervasive fluid moves independently of structural and lithologic control and each mineral becomes isotopically homogeneous despite whatever differences in isotopic composition may have existed prior to metamorphism.

2. Local equilibration between adjacent mineral grains by *channelized* fluids, which move along vein systems, shear zones, or other channel-ways, such as rock contacts or more permeable lithologic units. This fluid flow leads to equilibration on the scale of individual beds or units, but will not result in isotopic homogenization of different rock types. Channelized flow favors chemical heterogeneity, allowing some rocks to remain unaffected. Most C–O–H studies have demonstrated that fluid flow is channelized along structural weaknesses or more permeable lithologies (Rumble et al. 1982; Graham et al. 1983; Rumble and Spear 1983; Tracy et al. 1983; Valley and O'Neil 1984; Nabelek et al. 1984; Bebout and Carlson 1986).

Fluid involvement in fault and shear zones is an established phenomenon. Kerrick et al. (1984) demonstrated that, in general, flow regimes follow a sequence of events: during initiation of the structures, locally-derived fluids at low water/rock ratios predominate which, as the structures propagate, change to metamorphic fluids with high water/rock ratios along conduits. Later in the tectonic evolution and at shallower crustal levels there is often invasion of surface waters into the faults.

Prograde metamorphism of sediments causes the liberation of volatiles. Dehydration is most common, decarbonation occurs in carbonate-bearing rocks, desulfidation can be locally important. The liberation of volatiles can be described by two end-member processes (Rumble 1982; Valley 1986):

1. Rayleigh volatilization during which rocks interact only with fluids generated internally by devolatilization reactions between the rocks' minerals. The conditions of Rayleigh distillation require that once fluid is generated it is isolated immediately from the rock.
2. Batch volatilization, where all fluid is evolved before any is permitted to escape. Most natural processes actually fall between these extremes, but these two end-member situations provide useful limits.

Dehydration is the best known and most common example of metamorphic volatilization. The effect of dehydration reactions on the $\delta^{18}\text{O}$ value of a rock will always be small, less than a 1‰. The temperature effect is the most important due to the crossover in the sign of

fractionations. At temperatures below 400°–500 °C, H₂O is isotopically lighter than an average rock and dehydration will cause ¹⁸O-enrichment. At temperatures above 500 °C oxygen in H₂O is heavier and dehydration causes ¹⁸O-depletion. Thus, reactions tend to cancel each other, depending on the details of the reaction path. Even with conservatively made assumptions to maximize the isotope effect, it will be under all circumstances less than 1‰ (Valley 1986).

In contrast to $\delta^{18}\text{O}$, the effect of dehydration on δD may be much larger because the amount of hydrogen in the rock is much smaller. Because the isotopic composition of the fluids will be buffered at high temperatures by the isotopic composition of the surrounding rocks from which they were derived or passed through, oxygen isotope ratios often do not provide clear constraints on the origin of the fluids, whereas H-isotope ratios in many cases may do so. Possible sources for metamorphic fluids are:

1. magmatic water derived from deep levels in the crust or even in the upper mantle;
2. water liberated during metamorphic dehydration reactions;
3. meteoric water derived from the earth's surface;
4. connate formation waters (brines) trapped at deep levels in the sedimentary pile;
5. seawater derived from the ocean, possibly in a rift zone (Wickham and Taylor 1985).

On the basis of their δD -value, fluids (1) and (2) are not necessarily distinguishable from each other, but fluids (3) and (5) are. In order to calculate the isotopic composition of the fluid it is necessary to know the fractionation factors between the minerals and water as a function of temperature and composition.

Studies of prograde regional metamorphic mineral assemblages have suggested the preservation of hydrogen isotope equilibrium amongst coexisting hydrous minerals (Rye et al. 1976; Hoernes and Friedrichsen 1978, 1980). Much of the available literature pertains to muscovite and biotite δD -values, the latter being always more negative than the former. However, Graham (1981) has argued that this apparent preservation of hydrogen isotope equilibrium may be a consequence of the similarity of grain size and diffusion parameters. Describing methods of calculating diffusion coefficients Graham (1981) presented experimental evidence that in the absence of a fluid phase, H-isotope exchange is slower by at least two orders of magnitude than in the pre-

sence of a fluid phase. Rapid diffusion of hydrogen implies that in slowly cooling regional metamorphic terranes closure temperatures for cessation of H-isotope exchange may be far below the temperature of formation. Thus, it is often difficult to establish whether hydrogen isotope equilibrium is commonly preserved between hydrous minerals in metamorphic rocks.

Decarbonation is a very important process that effects the isotopic composition of carbonate rocks during metamorphism (e.g., Shieh and Taylor 1969b; Taylor and O'Neil 1977; Matthews and Kolodny 1978; Rumble 1982; Nabelek et al. 1984). Both equilibrium and kinetic fractionations may be operative during the process, but in any event, the CO₂ leaving the system is relatively enriched in both ¹⁸O and ¹³C. Consequently, decarbonation results in a lowering of both δ¹³C- and δ¹⁸O-values of the metamorphosed carbonates. Significant shifts in both ¹³C and ¹⁸O may occur at isograd boundaries, where large amounts of volatile-producing reactions take place (Lattanzi et al. 1980). The magnitude of ¹⁸O- and ¹³C-depletions are directly linked and can be calculated if the reaction stoichiometry is known.

Since prograde reactions in carbonate rocks are dependent on H₂O/CO₂ ratios in the fluid phase and the carbonates themselves generate only CO₂, it is very likely that the observed reactions occur because of H₂O infiltration. Rumble et al. (1982), Graham et al. (1983) and others have demonstrated from both phase equilibrium and isotopic data that greenschist and amphibolite facies metacarbonates were infiltrated by between 1 and 5 rock volumes of H₂O. These are the volumes of H₂O that have reacted with the rock and therefore represent lower limits of the water that actually passed through the rocks. Such high fluid-rock ratios have only been well documented in metacarbonate units. Their implication for the more common pelitic and psammitic units is difficult to establish, because these rocks produce a water-rich fluid, and the effects of externally derived waters are thus difficult to document.

Nitrogen in metamorphic rocks is mainly fixed as ammonium within the crystal lattice of micas and other silicate minerals and, to a lesser amount, in fluid inclusions as molecular nitrogen. Haendel et al. (1986) determined the content and isotopic composition of ammonium-nitrogen in metasedimentary rocks with increasing metamorphic grade and found a decrease in nitrogen content and an increase in δ¹⁵N-values (see Fig. 61).

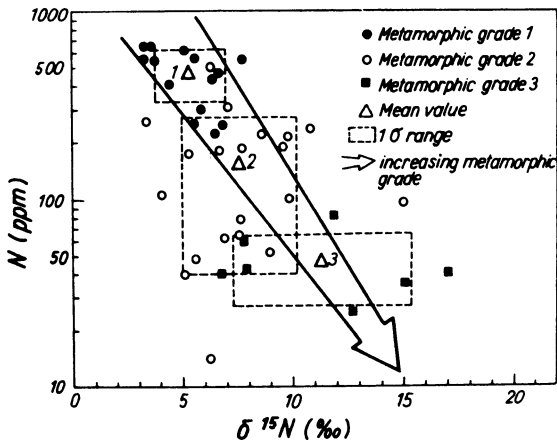


Fig. 61. Correlation between $\delta^{15}\text{N}$ -values and nitrogen concentrations in regional metamorphic rocks (Haendel et al. 1986)

From model experiments they concluded that isotope exchange mainly takes place between ammonium and molecular nitrogen, which is fast enough to reach isotopic equilibrium even at temperatures around 400 °C.

3.12.2 Temperature Determination in Metamorphic Rocks

Although most attempts to apply stable isotope geothermometers to metamorphic rocks have utilized oxygen isotope fractionations, in recent years carbon isotope fractionations between carbonates and graphite have also been successfully applied (see below). In this context the problems of choosing suitable temperature calibrations have been already discussed on p. 16f. and will not be elucidated here.

It is common belief that the metamorphic assemblage observed at the earth's surface represents the peak grade of metamorphism. However, with respect to oxygen isotope temperatures this is not necessarily the case. The detailed summary of O-isotope relationships in mineral triplets by Deines (1977) demonstrated clearly that concordant temperatures indicative of maximum metamorphic temperatures do occur, but not as a rule. Oxygen isotope temperatures comparable to maximum temperatures of metamorphism will only be preserved if water is lost from the assemblage at this temperature or if oxygen diffusion in a mineral pair in the presence of water is sufficiently slow. In addition to diffusion coefficients, the degree of isotope discordancy also depends upon grain size, role and nature of the fluid phase, rock and

grain permeabilities, rate of cooling, and other factors. For example, Hoefs et al. (1982) demonstrated on iron ores from the Iron Quadrangle, Brazil, that temperatures obtained from quartz-iron oxide fractionations depend upon the deformation history. Iron ores which have been overprinted by later deformation events are selectively reset to lower "isotopic" temperatures. In these rocks the qualitative relationship exists such that the more closely spaced the schistosity planes, the larger the extent of temperature lowering.

Inspection of the literature data (Deines 1977; Javoy 1977; Hoernes and Friedrichsen 1978, 1980; Hoernes and Hoffer 1979; Matthews and Schliestedt 1984) indicates the following general pattern of apparent temperatures:

1. "high" temperatures: quartz-rutile, quartz-garnet, quartz-iron oxides, quartz-pyroxene, and
2. "low" temperatures: quartz-muscovite, quartz-biotite, quartz-feldspar, quartz-calcite.

The preferred interpretation of this subdivision is that, due to different diffusion rates, some minerals exchange their oxygen isotopes with a fluid phase down to relatively low temperatures during retrograde cooling of a metamorphic event. Some retrograde temperatures may even represent a distinctly younger metamorphic event in a poly-phase metamorphic rock. However, this cannot be differentiated by oxygen isotope determinations alone. A different interpretation has been proposed by Hoernes and Hoffer (1978), who argued that the $^{18}\text{O}/^{16}\text{O}$ ratio of biotite, for instance, is fixed at the time of crystallization and its initial composition is preserved when the temperature increases. In a later paper Hoernes and Hoffer (1985) argued that at relatively high temperatures the initiation of specific dehydration reactions, their production, and their escape rates from the metamorphic system are so fast as to inhibit a complete reequilibration of the solids with the fluid. The oxygen isotope disequilibria frequently discussed in the literature may result from this kinetic effect rather than from retrograde exchange.

Very informative are temperature studies of low-grade metamorphic rocks, because isotope fractionations are large at these low temperatures and temperature information hard to receive. However, because of the fine-grained nature of such rocks, mineral separations are much more difficult. Furthermore, oxygen isotope geothermometry relies on the assumption that fine-grained diagenetic quartz and mixed-layer

illite/smectite continuously equilibrate with one another during burial. Eslinger et al. (1979) demonstrated that there is no well-established example of mineral pair thermometry at temperatures below 100 °C and this may well be true up to 200 °C. However, studies on such very low-grade metamorphic rocks can be used to provide a measure of the extent of isotope exchange toward the equilibrium value. Analyzing the Precambrian Belt Series Eslinger and Savin (1973b) showed that extensive oxygen isotope exchange can occur at relatively low temperatures (225° to 310 °C) in rocks that appear lithologically to be ordinary shale and carbonate. Their data indicate some degree of disequilibrium between carbonate and quartz, because carbonate may have been more affected by retrograde effects than silicate. Eslinger and Yeh (1986) estimated maximum burial temperatures for carbonates and shales to be 160° to 250 °C, which agreed with other petrologic estimates.

Becker and Clayton (1976) studied the banded iron formation from the Hamersley Range, Western Australia and concluded that chert and iron oxide had undergone burial metamorphism at a temperature of 270° to 310 °C. Similar temperatures have been obtained by Hoefs et al. (in press) on the much younger Urucum deposits in Brazil.

Other low-temperature metamorphic reactions are serpentinization processes which have been investigated by Barnes and O'Neil (1969), Wenner and Taylor (1974), Magaritz and Taylor (1974), and Ikin and Harmon (1983). Magaritz and Taylor (1974) demonstrated that antigorites typically have very uniform δD - and $\delta^{18}O$ -values identical to those of most metamorphic chlorites. Thus, the antigorites seem to form by reaction with metamorphic fluids. The δD -values of lizardite-chrysotile serpentines, on the other hand, show a latitudinal dependence as a result of interactions with meteoric groundwaters at relatively low temperatures (≈ 100 °C or less). Wenner and Taylor (1973) demonstrated that oceanic serpentines have higher δD - and lower $\delta^{18}O$ -values than the serpentines of the continental ophiolite complexes, and concluded that heated ocean water was involved in submarine serpentinization.

Carbon Isotope Fractionation Between Calcite and Graphite. Recently, carbon isotope fractionations between calcite and graphite in marble have been applied as geothermometers by Valley and O'Neil (1981), Wada and Suzuki (1983), and Morikiyo (1984). Valley and O'Neil (1981) calibrated their temperature scale empirically against the potas-

sium feldspar-plagioclase and magnetite-ilmenite thermometers, while Wada and Suzuki (1983) calibrated it against the calcite-dolomite solvus thermometer. Although the slope of all temperature scales is slightly different, geologically meaningful temperatures are only obtained in the high temperature range at temperatures above 500 °C. At temperatures below 500 °C kinetics of the isotope exchange reaction may become so important that a general application of the thermometer at lower temperatures is hazardous.

In terranes where organic carbonaceous matter can be traced from low to high grade, a progressive increase in $\delta^{13}\text{C}$ -values is commonly observed (Hoefs and Frey 1976; Barker and Friedman 1969). This increase is partly due to progressive loss of isotopically light methane and partly due to exchange with isotopically heavy carbonates. At high metamorphic temperatures, the low $\delta^{13}\text{C}$ -values that are characteristic of sedimentary organic matter should not be preserved in the presence of high $\delta^{13}\text{C}$ -carbonates. Thus, high $\delta^{13}\text{C}$ -values in graphite are not a sufficient criterion to infer an abiogenic origin in high-grade marbles.

3.12.3 Contact Metamorphism

Because the oxygen isotope composition of igneous rocks is quite different from that of sedimentary and low-grade metamorphic rocks, studies of the variation of oxygen isotopes in the vicinity of an intrusive contact offers the possibility of investigating the extent of isotope exchange between the intrusive and its country rock. Typically, exchange between the igneous intrusion and the adjacent pelitic country rock takes place within a short distance of the intrusive contact. The width of the exchanged zone correlates well with the size of the intrusions, the presumed intrusive temperatures, the length of heating time, and the availability of fluids. Figure 62 shows the percent oxygen isotope exchange between intrusive and country rock as a function of distance from the contact for several contact zones (Shieh and Taylor 1969a). The narrowness and steepness of an isotope gradient (see Fig. 62) in the exchanged zones suggest that such small-scale isotope exchange occurred essentially in the solid state by a diffusion-controlled recrystallization process.

In many contact metamorphic aureoles values of $\delta^{18}\text{O}$ and $\delta^{13}\text{C}$ vary systematically. Table 23 summarizes 16 studies, mostly of contact aureoles, that show coupled O–C trends. In all cases $\delta^{18}\text{O}$ -

Table 23. Studies demonstrating coupled O-C depletion trends in metamorphosed carbonates (Valley 1986)

	Width of aureole or traverse	Pressure/depth	Maximum temperature (°C)	X(CO ₂)	Range in $\delta^{18}\text{O}$	Range in $\delta^{13}\text{C}$	Pluton	Rock types, comments
1. Trenton limestone Mount Royal, Quebec	100 m				14	6	Essexite, nepheline- syenite	Limestone, marble, calcite from intrusion
2. Marysville, Montana	1-3 km	1 kbar	525	0.95	18	6	Grano- diorite	Marble, hydrothermal assemblages Depletion attributed to Rayleigh volatilization Largest isotope shift at diop- side isograd
3. Pine Creek, California W-skarn	Roof pendant	<2 kbar	600	<0.25	22	14	Quartz- monzonite	Marble, calc-silicate, skarn in pendant Gradients in $\delta^{18}\text{O}$ up to 10‰ per 10 cm across skarn Depletion attributed to mixing with magmatic O + C
4. Osgood Mts., Nevada	<1 km	<2 kbar	>550	<0.15	9	9	Grano- diorite	Marble, calc-silicate hornfels, skarn 3 Stages of skarn formation
5. Skye, Scotland				20	7	7	Granite	Marble, skarn Some depletion due to meteoric water
6. Elkhorn, Montana	Marble 240 m Skarn 21 m	1 kbar	525	<0.25	15	7	Quartz- diorite	Dolostone, marble, skarn
7. Notch Peak Stock, Utah	3 km	1.5 kbar	600	<0.2	12	12	Quartz- monzonite	Metamorphosed calcareous argillite, marble
8. Weolag W-Mo Deposit, Korea	2.5 km	1.0-2.4 km	>400	15	11	11	Granite	Limestone, calc-silicate, skarn

9. Tauern Area, Austria	3 m	>4 kbar	450-600	8	2	-	Traverse across a 3 m-thick marble layer
10. Birch Creek, California	750 m		540	13	4	Granite	Marble, skarn
11. McArthur R. Pb-Zn Deposits, Australia			350	7	2.5	-	Dolomite, values change in relation to distance to the Emu Fault Range in values attributed to variable T=350°-150 °C and constant fluid composition
12. Providencia Pb-Zn Deposits, Mexico			365	10	10		Limestone, late-stage hydrothermal calcites Variable T=365°-200 °C
13. Gaspé Cu Deposits, Quebec			350	17	14		13a = Drill hole GMS4, limestone, marble, vein calcite, skarn 13b = Drill hole GMS2, limestone, marble Variable T=350°-150 °C
14. CanTung W-skarn, N.W. Territories			500	9	9	Monzogranite	Limestone, marble, calc-silicate, skarn Variable T=350°-270 °C
15. Mottled Zone, Israel		<25 atm	1300	13	25	None	Natural combustion of bituminous marl
16. Bergell Aureole, Italy	<20 cm	2 kbar	400	0.1-0.25	15.3	8	Metasomatic zone around veins in marble Sharp isotopic gradients, 5-14 per mil cm ⁻¹ at infiltration fronts

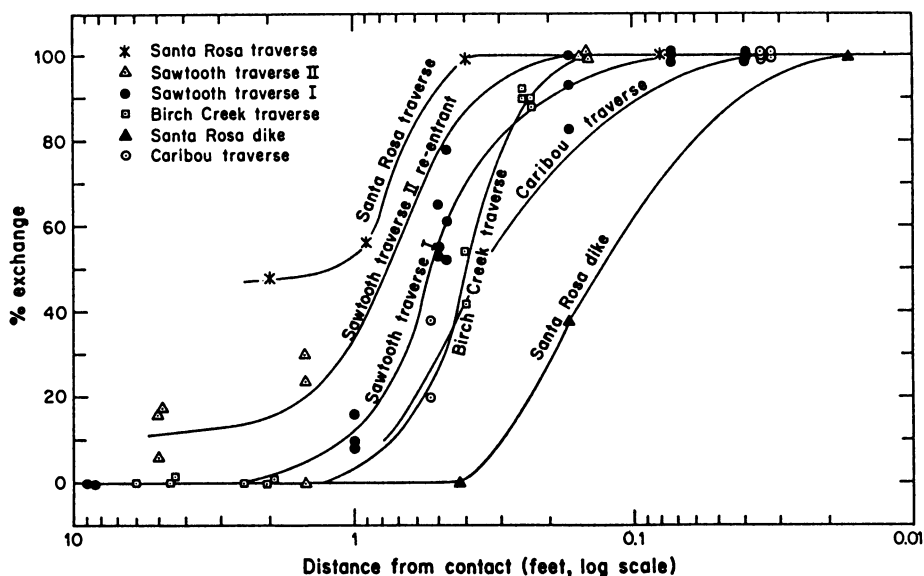


Fig. 62. Percent oxygen isotope exchange between intrusive and country rock as a function of distance from the intrusive contacts (Shieh and Taylor 1969a)

scales from 3 m to 3 km. Important questions to be answered are to what extent these depletion trends are affected by volatilization, by infiltration, and mixing or by changing p-T-X conditions. In general, the effects of volatilization, infiltration, and disequilibrium all tend towards lower $\delta^{13}\text{C}$ - and $\delta^{18}\text{O}$ -values in calc-silicates and marbles with increasing metamorphic grade. However, detailed analysis shows that volatilization, although always leading to a depletion in heavy isotopes, is not the dominant cause of large shifts. Most contact aureoles studied have been infiltrated by fluids and O-C-H isotope ratios frequently enable identification of fluid sources. For example, Taylor and O'Neil (1977) presented evidence that magmatic water moved out from the pluton during the first stage of development of a skarn, then, at a later stage, meteoric water constituted between 20 and 50% of the fluid volume and in the final stage, meteoric water was the predominant component.

Many of the large isotopic changes documented in Table 23 have previously been misinterpreted to result largely from volatilization. However, as already mentioned, volatilization is not a sufficient process to cause the large isotope shifts seen in Table 23; these must result largely from exchange with infiltrating fluids. The effect of infiltration

is greatest when sufficient fluids are available, when contrasts in isotopic composition are great, and when permeability is high (Valley 1986).

One important factor in determining the permeability of a metamorphic rock is the transient effect of volatilization itself (Rumble and Spear 1983; Nabelek et al. 1984; Valley and O'Neil 1984; Valley 1986). During volatilization reactions, small fluid overpressures are created. At the same time, the volume of the solid rock is reduced by the removal of material. Both of these effects may lead to an enhancement of permeability that will be short-lived in the ductile environment.

The infiltration of surface derived fluids into a contact aureole requires that fluid pressures be approximately hydrostatic or less. Thus, if stable isotope ratios indicate exchange with large amounts of surface waters, then $p_{\text{H}_2\text{O}}$ must have been much less than $p_{\text{lithostatic}}$. Perhaps the deepest known penetration of surface-derived fluids is the Trois Seigneurs Massif, Pyrenees where seawater infiltration may have contributed to partial melting of migmatites at a depth of around 11 to 12 km (Wickham and Taylor 1985).

3.12.4 Regional Metamorphism

There have been extensive debates whether metamorphic fluids and the rocks with which they interact form "open" or "closed" systems. If metamorphism occurs under closed-system conditions with respect to externally derived fluids, then evolved fluids must leave their rock of origin without interacting with other rocks which are also closed systems. This would represent a perfectly channelized system. If metamorphism occurs under open-system conditions, then fluid flow must be pervasive such that all rocks interact with the homogenizing fluid. Because in many rocks steep isotope gradients have been observed, indicating that homogenization has not occurred, most rocks fall somewhere between these end-member conditions.

The processes that determine isotopic compositions in systems with large amounts of pervasive fluids are very different from those in the presence of small amounts of fluids or highly channelized fluid movement. In the former case, some studies propose isotopic homogenization which would require convective circulation of fluids during regional metamorphism. This is supported by the general observation that low-grade metamorphic pelites have $\delta^{18}\text{O}$ -values between 15 and

18‰, whereas high-grade gneisses often have $\delta^{18}\text{O}$ -values between 6 and 10‰ (Shieh and Schwarcz 1974; Longstaffe and Schwarcz 1977). In the latter case, other studies report fine-scale gradients which would suggest that isotope exchange was very limited and took place without large amounts of fluid (Rumble et al. 1982; Graham et al. 1983; Valley and O'Neil 1984; Bebout and Carlson 1986).

The results of these studies and many others indicate that the exact nature of fluid migration is highly variable among metamorphic rocks. For example, Hoernes and Hoffer (1985) observed a 5‰ difference between quartzes from very low-grade and quartzes formed under greenschist conditions, but a further increase in metamorphic grade did not result in any further systematic decrease in $\delta^{18}\text{O}$ -values. These authors argued that a free-fluid phase is only present during the low-grade transformations, while at high grades the fluid phase had already escaped from the system and left behind a "dry" system, which had no effect on the overall oxygen isotope composition with increasing temperatures.

3.12.5 Granulite Facies Metamorphism

Since the pioneering work of Touret (1971), it is well known that lower crustal rocks are characterized by the presence of an H_2O -poor, CO_2 -rich fluid phase. Although the source of this CO_2 is still a matter of debate, many workers have suggested mantle outgassing as the most feasible CO_2 source (Newton et al. 1980). One of the main arguments for this assumption is that the volume of the lower continental crust is so great and the required $\text{CO}_2/\text{H}_2\text{O}$ ratio so high that only a mantle source can deliver sufficient quantities of CO_2 .

Three possible sources must be considered for the CO_2 present in granulite facies rocks:

1. CO_2 may be generated by decarbonation reactions in siliceous dolomite and other impure carbonate rocks. Both equilibrium and kinetic fractionation effects may be operative during this process, but in any event the liberated CO_2 should be slightly enriched in ^{13}C relative to the carbonate.
2. CO_2 may be produced by oxidation of carbonaceous matter (graphite) during metamorphism. Since most of this graphite is depleted in ^{13}C , the resulting CO_2 should, therefore, have low $\delta^{13}\text{C}$ -values.

3. CO₂ may be of deep-seated origin, possibly derived from degassing of the upper mantle. This deep-seated CO₂ should have $\delta^{13}\text{C}$ -values between -8 and -5‰.

Preliminary $\delta^{13}\text{C}$ -values from fluid inclusions in quartzes (Hoefs and Touret 1975) and from scapolite-rich granulites (Hoefs et al. 1981) show variable, but rather low $\delta^{13}\text{C}$ -values between -20 and -10‰. Such low $\delta^{13}\text{C}$ -values do not support a simple, mantle-degassing process, but rather favor the idea that a substantial portion of the CO₂ may be derived from a graphitic source within the crust.

Many granulites have rather low $\delta^{18}\text{O}$ -values between 6 and 8‰ (Wilson et al. 1970; Fourcade and Javoy 1973; Longstaffe 1979). Even more depleted $\delta^{18}\text{O}$ -values (down to 0.1‰) have been reported by Wilson and Baksi (1983). The normal range of $\delta^{18}\text{O}$ -values between 6-8‰ requires that the precursor rocks have similar low $\delta^{18}\text{O}$ -values and/or that extensive oxygen isotope exchange with a low ¹⁸O-reservoir occurred. It is likely that the unusually low $\delta^{18}\text{O}$ -values below 6 record pre-granulitic facies events. The Australian rocks analyzed by Wilson and Baksi (1983) may be explained by pre-granulitic exchange with heated seawater. Similarly, the low ¹⁸O-eclogites reported by Vogel and Garlick (1970) may have preserved their premetamorphic values and may be interpreted as representing altered oceanic crust.

References

- Abell PI (1986) Oxygen isotope ratios in modern African gastropod shells: a data base for paleoclimatology. *Chem Geol* 58:183–193
- Abelson PH, Hoering TC (1961) Carbon isotope fractionation in formation of amino acids by photosynthetic organism. *Proc Natl Acad Sci USA* 47:623
- Allan JR, Matthews RK (1973) Carbon and oxygen isotopes as diagenetic and stratigraphic tools: Surface and subsurface data, Barbados, West Indies. *Geology* 5:16–20
- Allan JR, Matthews RK (1982) Isotope signature associated with early meteoric diagenesis. *Sedimentology* 29:797–817
- Allard P (1979) $^{13}\text{C}/^{12}\text{C}$ and $^{34}\text{S}/^{32}\text{S}$ ratios in magmatic gases from ridge volcanism in Afar. *Nature (London)* 282:56–58
- Altabet MA, Deuser WG (1985) Seasonal variations in natural abundance of ^{15}N in particles sinking to the deep Sargossa Sea. *Nature (London)* 315:218–219
- Altabet MA, McCarthy JJ (1985) Temporal and spatial variations in the natural abundance of ^{15}N in POM from a warm-core ring. *Deep Sea Res* 32:755–772
- Anderson AT (1967) The dimensions of oxygen isotope equilibrium attainment during prograde metamorphism. *J Geol* 75:323–332
- Anderson AT (1975) Some basaltic and andesitic gases. *Rev Geophys Space Phys* 13:37–55
- Anderson AT, Clayton RN, Mayeda TK (1971) Oxygen isotope thermometry of mafic igneous rocks. *J Geol* 79:715–729
- Anderson TF, Arthur MA (1983) Stable isotopes of oxygen and carbon and their application to sedimentologic and paleoenvironmental problems. In: *Stable isotopes in sedimentary geology*. SEPM Short Course No 10, Dallas, 1983, p 1-1–1-151
- Arnason B (1977) The hydrogen and water isotope thermometer applied to geothermal areas in Iceland. *Geothermics* 5:75–80
- Arnason B, Sigurgeirsson T (1968) Deuterium content of water vapour and hydrogen in volcanic gas at Surtsey, Iceland. *Geochim Cosmochim Acta* 32:807–813
- Arnth JD, Matzigkeit U, Boos A (1985) Carbon isotope geochemistry of the Cretaceous-Tertiary section of the Wasserfallgraben, Lattengebirge, Southeast Germany. *Earth Planet Sci Lett* 75:50–58
- Arnold M, Sheppard SMF (1981) East Pacific Rise at 21°N : isotopic composition and origin of the hydrothermal sulfur. *Earth Planet Sci Lett* 56:148–156
- Arthur MA (1984) Carbon isotope anomalies? *Nature (London)* 310:450–451
- Arthur MA, Dean WE, Claypool GE (1985) Anomalous ^{13}C enrichment in modern marine organic carbon. *Nature (London)* 315:216–218
- Bachinski DJ (1969) Bond strength and sulfur isotope fractionation in coexisting sulfides. *Econ Geol* 64:56–65
- Baertschi P (1976) Absolute ^{18}O content of standard mean ocean water. *Earth Planet Sci Lett* 31:341–344

- Bainbridge KT, Nier AO (1950) Relative isotopic abundances of the elements. Preliminary Rep No 9. Nuclear Sciences Ser, Natl Res Council USA, Washington DC
- Bainbridge AE, Suess HE, Friedman I (1961) Isotopic composition of atmospheric hydrogen and methane. *Nature* (London) 192:648–649
- Barker F, Friedman I (1969) Carbon isotopes and pelites of the Precambrian Uncompahgre formation, Needle, Colorado. *Bull Geol Soc Am* 80:1403–1408
- Barnes I, O'Neil JR (1969) The relationship between fluids in some fresh Alpine type ultramafics and possible modern serpentinization, western United States, *Bull Geol Soc Am* 80:1947–1960
- Barnes IL, Garner EL, Gramlich JW, Machlan LA, Moody JR, Moore JR, Murphy TJ, Shields WR (1973) Isotopic abundance ratios and concentrations of selected elements in some Apollo 15 and 16 samples. *Proc 4th Lunar Sci Conf*, pp 1197–1207
- Barrer RM, Denny AF (1964) Water in hydrates. I Fractionation of hydrogen isotopes by crystallization of salt hydrates. *J Chem Soc* 1964:4677–4684
- Beaty DW, Taylor HP (1982) Some petrologic and oxygen isotopic relationships in the Amulet Mine, Noranda, Quebec, and their bearing on the origin of Archaean massive sulfide deposits. *Econ Geol* 77:95–108
- Bebout GE, Carlson WD (1986) Fluid evolution and transport during metamorphism: evidence from the Llano Uplift, Texas. *Contrib Mineral Petrol* 92:518–529
- Becker RH (1982) Nitrogen isotopic ratios of individual diamond samples. In: 5th Int Conf Geochronology, Cosmochronology, Isotope Geology, Jpn 1982, Abstr pp 21–22
- Becker RH, Clayton RN (1975) Nitrogen abundances and isotopic compositions in lunar samples. *Proc 6th Lunar Sci Conf* 2:2131–2149
- Becker RH, Clayton RN (1976) Oxygen isotope study of a Precambrian banded-iron-formation, Hamersley Range, Western Australia. *Geochim Cosmochim Acta* 40:1153–1165
- Becker RH, Clayton RN (1977) Nitrogen isotopes in igneous rocks. *EOS Trans Am Geophys Union* 58:536
- Becker RH, Epstein S (1982) Carbon, hydrogen and nitrogen isotopes in solvent-extractable organic matter from carbonaceous chondrites. *Geochim Cosmochim Acta* 46:97–103
- Becker RH, Pepin RO (1984) The case for a martian origin of the shergottites: nitrogen and noble gases in EETA 79001. *Earth Planet Sci Lett* 69:225–242
- Beeunas MA, Knauth LP (1985) Preserved stable isotopic signature of subaerial diagenesis in the 1.2 b.y. Mescal Limestone, central Arizona. Implications for the timing and development of a terrestrial plant cover. *Geol Soc Am Bull* 96:737–745
- Belanger PE, Curry WB, Matthews RK (1981) Core-top evaluation of benthic foraminiferal isotopic ratios for paleo-oceanographic interpretation. *Palaeogeogr-climatol-eol* 33:205–220
- Bender ML, Keigwin LD (1979) Speculations about upper Miocene changes in abyssal Pacific dissolved bicarbonate $\delta^{13}\text{C}$. *Earth Planet Sci Lett* 45:383–393
- Bender ML, Labeyrie LD, Raynaud D, Lorius C (1985) Isotopic composition of atmospheric O_2 in ice linked with deglaciation and global primary productivity. *Nature* (London) 318:344–352
- Bentor YK (1986) A new approach to the problem of tektite genesis. *Earth Planet Sci Lett* 77:1–13
- Berger WH (1979) Stable isotopes in foraminifera. In: SEPM short course No. 6, Houston, 1979, pp 156–198

- Berger WH, Vincent E (1986) Deep-sea carbonates: reading the carbon isotope signal. *Geol Rundsch* 75:249–269
- Berner RA (1972) Sulfate reduction, pyrite formation and the oceanic sulfur budget. In: Dryssen D, Jagner D (eds) *The changing chemistry of the oceans*. Interscience, New York, pp 347–361
- Berner RA (1984) Sedimentary pyrite formation: an update. *Geochim Cosmochim Acta* 48:605–615
- Bernoulli D, Garrison RE, McKenzie J (1978) Petrology, isotope geochemistry and origin of limestone and dolomite associated with basaltic breccia, Hole 373A, Tyrrhenian Basin. *Initial Rep DSDP* 42:541–553
- Berthenrath R, Friedrichsen H, Hellner E (1973) Die Fraktionierung der Sauerstoffisotope $^{18}\text{O}/^{16}\text{O}$ im System Eisenoxid-Wasser. *Fortschr Mineral* 50:32–33
- Biemann K, Owen T, Rushneck DR, Lafleur AL, Howarth DW (1976) The atmosphere of Mars near the surface: Isotope ratios and upper limits on noble gases. *Science* 194:76–78
- Bigeleisen J (1965) Chemistry of isotopes. *Science* 147:463–471
- Bigeleisen J, Mayer MG (1947) Calculation of equilibrium constants for isotopic exchange reactions. *J Chem Phys* 15:261–267
- Bigeleisen J, Wolfsberg M (1958) Theoretical and experimental aspects of isotope effects in chemical kinetics. *Adv Chem Phys* 1:15–76
- Bigeleisen J, Perlman ML, Prosser HC (1952) Conversion of hydrogenic materials for isotopic analysis. *Anal Chem* 24:1356
- Blattner P, Bird GW (1974) Oxygen isotope fractionation between quartz and K-feldspar at 600 °C. *Earth Planet Sci Lett* 23:21–27
- Blattner P, Hulston JR (1978) Proportional variations of geochemical $\delta^{18}\text{O}$ scales – an interlaboratory comparison. *Geochim Cosmochim Acta* 42:59–62
- Blattner P, Dietrich V, Gansser A (1983) Contrasting ^{18}O enrichment and origins of High Himalayan and Transhimalayan intrusives. *Earth Planet Sci Lett* 65:276–286
- Boettcher AL, O'Neil JR (1980) Stable isotope, chemical and petrographic studies of high-pressure amphiboles and micas: evidence for metasomatism in the mantle source regions of alkali basalts and kimberlites. *Am J Sci* 280A (Jackson Vol): 594–621
- Böhlke JK, Kistler RW (1986) Rb–Sr, K–Ar and stable isotope evidence for the ages and sources of fluid components of gold-bearing quartz veins in the Northern Sierra Nevada Foothills Metamorphic Belt, California. *Econ Geol* 81:296–322
- Borthwick J, Harmon RS (1982) A note regarding ClF_3 as an alternative to BrF_5 for oxygen isotope analysis. *Geochim Cosmochim Acta* 46:1665–1668
- Bottinga Y (1969a) Calculated fractionation factors for carbon and hydrogen isotope exchange in the system calcite-carbon dioxide-graphite-methane-hydrogen-water-vapor. *Geochim Cosmochim Acta* 33:49–64
- Bottinga Y (1969b) Carbon isotope fractionation between graphite, diamond and carbon dioxide. *Earth Planet Sci Lett* 5:301–307
- Bottinga Y, Craig H (1969) Oxygen isotope fractionation between CO_2 and water and the isotopic composition of marine atmospheric CO_2 . *Earth Planet Sci Lett* 5:285–295
- Bottinga Y, Javoy M (1973) Comments on oxygen isotope geothermometry. *Earth Planet Sci Lett* 20:250–265
- Bottinga Y, Javoy M (1975) Oxygen isotope partitioning among the minerals in igneous and metamorphic rocks. *Rev Geophys Space Phys* 13:401–418

- Bowers TS, Taylor HP (1985) An integrated chemical and isotope model of the origin of mid-ocean ridge hot spring systems. *J Geophys Res* 90:12583–12606
- Bowman JR, O'Neil JR, Essene EJ (1985) Contact skarn formation at Elkhorn, Montana. II. Origin and evolution of C–O–H skarn fluids. *Am J Sci* 285:621–660
- Boyd AW, Brown F, Lounsbury M (1955) Mass spectrometric study of natural and neutron-irradiated chlorine. *Can J Phys* 33:35
- Bremner JM, Keeney DR (1966) Determination and isotope ratio analysis of different forms of nitrogen in soils, III. *Soil Sci Soc Am Proc* 30:577–582
- Brenninkmeijer CAM, Kraft P, Mook WG (1983) Oxygen isotope fractionation between CO₂ and H₂O. *Isotope Geosci* 1:181–190
- Broecker WS (1974) *Chemical oceanography*. Harcourt Brace Jovanovich, New York
- Broecker WS (1982) Ocean chemistry during glacial time. *Geochim Cosmochim Acta* 46:1689–1705
- Brown FS, Baedeker MJ, Nissenbaum A, Kaplan IR (1972) Early diagenesis in a reducing fjord, Saanich Inlet, British Columbia. III. Changes in organic constituents of a sediment. *Geochim Cosmochim Acta* 36:1185–1203
- Brown PE, Bowman JR, Kelly WC (1985) Petrologic and stable isotope constraints on the source and evolution of skarn-forming fluids at Pine Creek, California. *Econ Geol* 80:72–95
- Burk RL, Stuiver M (1981) Oxygen isotope ratios in trees reflect mean annual temperature and humidity. *Science* 211:1414–1419
- Cameron EM (1982) Sulphate and sulphate reduction in early Precambrian oceans. *Nature (London)* 296:145–148
- Carr LP, Grady MM, Wright IP, Fallick AE, Pillinger CT (1983) Carbon, nitrogen and hydrogen in enstatite chondrites. *Meteoritics* 18:270
- Cerling TE, Brown FH, Bowman JR (1985) Low-temperature alteration of volcanic glass: hydration, Na, K, ¹⁸O and Ar mobility. *Chem Geol Isotope Geosci Sect* 52:281–293
- Chambers LA, Trudinger PA (1979) Microbiological fractionation of stable sulfur isotopes. *Geomicrobiology J* 1:249–293
- Charef A, Sheppard SMF (1986) Pb–Zn mineralization associated with diapirism: fluid inclusion and stable isotope evidence (H, C, O) for the origin of the fluids at Fedj-El-Adoun. *Chem Geol* (in press)
- Chivas AR, Andrew AS, Sinha AK, O'Neil JR (1982) Geochemistry of Pliocene–Pleistocene oceanic arc plutonic complex, Guadalcanal. *Nature (London)* 300:139–143
- Chung HM, Sackett WM (1979) Use of stable carbon isotope compositions of pyrolytically derived methane as maturity indices for carbonaceous materials. *Geochim Cosmochim Acta* 43:1979–1988
- Claypool GE, Holser WT, Kaplan IR, Sakai H, Zak I (1980) The age curves of sulfur and oxygen isotopes in marine sulfate and their mutual interpretation. *Chem Geol* 28:199–260
- Clayton RN (1959) Oxygen isotope fractionation in the system calcium carbonate–water. *J Chem Phys* 30:1246–1250
- Clayton RN (1981) Isotopic thermometry. In: Newton RC, Navrotsky A, Wood BJ (eds) *Thermodynamics of minerals and melts*. Springer, Berlin Heidelberg New York, pp 85–109
- Clayton RN, Degens ET (1959) Use of carbon isotope analyses of carbonates for differentiating freshwater and marine sediments. *Bull Am Assoc Petrol Geol* 43:890–897

- Clayton RN, Epstein S (1958) The relationship between O^{18}/O^{16} ratios in coexisting quartz, carbonate and iron oxides from various geological deposits. *J Geol* 66:352–373
- Clayton RN, Mayeda TK (1963) The use of bromine pentafluoride in the extraction of oxygen from oxides and silicates for isotopic analysis. *Geochim Cosmochim Acta* 27:43–52
- Clayton RN, Mayeda TK (1978) Genetic relations between iron and stony meteorites. *Earth Planet Sci Lett* 40:168–174
- Clayton RN, Mayeda TK (1983) Oxygen isotopes in eucrites, shergottites, nakhlites and chassignites. *Earth Planet Sci Lett* 62:1–6
- Clayton RN, Mayeda TK (1984) The oxygen isotope record in Murchison and other carbonaceous chondrites. *Earth Planet Sci Lett* 67:151–161
- Clayton RN, Steiner A (1975) Oxygen isotope studies of the geothermal system at Wairakei, New Zealand. *Geochim Cosmochim Acta* 39:1179–1186
- Clayton RN, Friedman I, Graf DL, Mayeda TK, Meents WF, Shimp NF (1966) The origin of saline formation waters. 1. Isotopic composition. *J Geophys Res* 71:3869–3882
- Clayton RN, Muffler LJP, White (1968) Oxygen isotope study of calcite and silicates of the River Branch No. 1 well, Salton Sea Geothermal Field, California. *Am J Sci* 266:968–979
- Clayton RN, O'Neil JR, Mayeda TK (1972) Oxygen isotope exchange between quartz and water. *J Geophys Res* 77:3057–3067
- Clayton RN, Grossman L, Mayeda TK (1973a) A component of primitive nuclear composition in carbonaceous meteorites. *Science* 182:485–488
- Clayton RN, Hurd JM, Mayeda TK (1973b) Oxygen isotopic compositions of Apollo 15, 16 and 17 samples and their bearing on lunar origin and petrogenesis. *Proc 4th Lunar Sci Conf Geochim Cosmochim Acta Suppl* 2:1535–1542
- Clayton RN, Goldsmith JR, Karel KJ, Mayeda TK, Newton RC (1975) Limits on the effect of pressure in isotopic fractionation. *Geochim Cosmochim Acta* 39:1197–1201
- Clayton RN, Onuma N, Mayeda TK (1976) A classification of meteorites based on oxygen isotopes. *Earth Planet Sci Lett* 30:10–18
- Clayton RN, Onuma N, Grossman C, Mayeda TK (1977) Distribution of the pre-solar component in Allende and other carbonaceous chondrites. *Earth Planet Sci Lett* 34:209–224
- Cline JD, Kaplan IR (1975) Isotopic fractionation of dissolved nitrate during denitrification in the eastern tropical North Pacific Ocean. *Mar Chem* 3:271–299
- Cloud PE, Friedman I, Sisler FD (1958) Microbiological fractionation of the hydrogen isotopes. *Science* 127:1394–1395
- Cole DR, Ohmoto H, Lasaga AC (1983) Isotopic exchange in mineral fluid systems. I. Theoretical evaluation of oxygen isotopic reactions and diffusion. *Geochim Cosmochim Acta* 47:1681–1693
- Coplen TB, Hanshaw BB (1973) Ultrafiltration by a compacted clay membrane. I. Oxygen and hydrogen isotopic fractionation. *Geochim Cosmochim Acta* 37:2295–2310
- Coplen TB, Kendall C (1982) Preparation and stable isotope determination of NBS-16 and NBS-17 carbon dioxide reference samples. *Anal Chem* 1982:2611–2612
- Coplen TB, Kendall C, Hopple J (1983) Comparison of stable isotope reference samples. *Nature (London)* 302:236–238
- Correns CW (1950) Zur Geochemie der Diagenese. I. Das Verhalten von $CaCO_3$ and SiO_2 . *Geochim Cosmochim Acta* 1:49–54

- Cortecci G, Longinelli A (1970) Isotopic composition of sulfate in rain water, Pisa, Italy. *Earth Planet Sci Lett* 8:36–40
- Cortecci G, Longinelli A (1971) $^{18}\text{O}/^{16}\text{O}$ ratios in sulfate from living marine organisms. *Earth Planet Sci Lett* 11:273–276
- Cortecci G, Longinelli A (1973) $^{18}\text{O}/^{16}\text{O}$ ratios in sulfate from fossil shells. *Earth Planet Sci Lett* 19:410–412
- Craig H (1953) The geochemistry of the stable carbon isotopes. *Geochim Cosmochim Acta* 3:53–92
- Craig H (1957) Isotopic standards for carbon and oxygen and correction factors for mass-spectrometric analysis of carbon dioxide. *Geochim Cosmochim Acta* 12:133–149
- Craig H (1961a) Isotopic variations in meteoric waters. *Science* 133:1702–1703
- Craig H (1961b) Standard for reporting concentration of deuterium and oxygen-18 in natural waters. *Science* 133:1833–1834
- Craig H (1963) The isotopic geochemistry of water and carbon in geothermal areas. In: *Nuclear geology of geothermal areas*, p 17–53. Spoleto, Sept 9–13, 1963
- Craig H (1965) The measurement of oxygen isotope paleotemperatures. *Proc Spoleto Conf Stable Isotopes Oceanogr Stud Paleotemp* 3
- Craig H (1966) Isotopic composition and origin of the Red Sea and Salton Sea geothermal brines. *Science* 154:1544–1548
- Craig H, Gordon L (1965) Deuterium and oxygen-18 variations in the ocean and the marine atmosphere. In: *Symposium on marine geochemistry*. Graduate School of Oceanography, Univ Rhode Island, Occ Publ No 3:277
- Craig H, Keeling CD (1963) The effects of atmospheric N_2O on the measured isotopic composition of atmospheric CO_2 . *Geochim Cosmochim Acta* 27:549–551
- Craig H, Lupton JE (1976) Primordial neon, helium and hydrogen in oceanic basalts. *Earth Planet Sci Lett* 31:369–385
- Craig H, Boato G, White DE (1956) Isotopic geochemistry of thermal waters. *Proc 2nd Conf Nucl Process Geol Settings*, p 29
- Criss RE, Taylor HP (1983) An $^{18}\text{O}/^{16}\text{O}$ and D/H study of Tertiary hydrothermal systems in the Southern half of the Idaho batholith. *Geol Soc Am Bull* 94:640–653
- Criss RE, Ekren EB, Hardyman RF (1984) Casto Ring Zone: A 4500 km² fossil hydrothermal system in the Challis Volcanic Field, Central Idaho. *Geology* 12:331–334
- Criss RE, Champion DE, McIntyre DH (1985) Oxygen isotope, aeromagnetic and gravity anomalies associated with hydrothermally altered zones in the Yankee Fork Mining District, Custer County, Idaho. *Econ Geol* 80:1277–1296
- Curry WB, Lohmann GP (1982) Carbon isotopic changes in benthic foraminifera from the western South Atlantic: reconstruction of glacial abyssal circulation patterns. *Quat Res* 18:218–235
- Czamanske GK, Rye RO (1974) Experimentally determined sulfur isotope fractionations between sphalerite and galena in the temperature range 600 °C to 275 °C. *Econ Geol* 69:17–25
- Dansgaard W (1964) Stable isotopes in precipitation. *Tellus* 16:436–468
- Dansgaard W, Johnsen SJ, Moller J, Langway CC (1969) One thousand centuries of climatic record from Camp Century on the Greenland ice sheet. *Science* 166:377–381
- Dansgaard W, Johnsen SF, Reeh N, Gundestrup N, Clausen HB, Hammer CU (1975) Climatic changes, Norsemen and modern man. *Nature (London)* 255:24–28
- Dansgaard W, Clausen HB, Gundestrup N, Hammer CU, Johnsen SF, Kristindottir PM, Reeh N (1982) A new Greenland deep ice core. *Science* 218:1273–1277

- Davidson J (1985) Mechanisms of contamination in Lesser Antilles island arc magmas from radiogenic and oxygen isotope relationships. *Earth Planet Sci Lett* 72:163–174
- Dean WE, Arthur MA, Claypool GE (1986) Depletion of ^{13}C in Cretaceous marine organic matter: source, diagenetic or environmental signal? *Mar Geol* 70:119–158
- Degens ET, Epstein S (1962) Relationship between $^{18}\text{O}/^{16}\text{O}$ ratios in coexisting carbonates, cherts and diatomites. *Bull Am Assoc Pet Geol* 46:534–542
- Degens ET, Guillard RRL, Sackett WM, Hellebust JA (1968a) Metabolic fractionation of carbon isotopes in marine plankton. I. Temperature and respiration experiments. *Deep Sea Res* 15:1–9
- Degens ET, Behrendt M, Gotthardt B, Reppmann E (1968b) Metabolic fractionation of carbon isotopes in marine plankton. II. Data on samples collected off the coasts of Peru and Ecuador. *Deep Sea Res* 15:11–20
- Deines P (1977) On the oxygen isotope distribution among mineral triplets in igneous and metamorphic rocks. *Geochim Cosmochim Acta* 41:1709–1730
- Deines P (1980a) The carbon isotopic composition of diamonds: relationship to diamond shape, color, occurrence and vapor composition. *Geochim Cosmochim Acta* 44:943–962
- Deines P (1980b) The isotopic composition of reduced organic carbon. In: Fritz P, Fontes JCh (eds) *Handbook of environmental geochemistry*, vol I. Elsevier, New York Amsterdam, pp 239–406
- Deines P, Gold DP (1973) The isotopic composition of carbonatite and kimberlite carbonates and their bearing on the isotopic composition of deep-seated carbon. *Geochim Cosmochim Acta* 37:1709–1733
- Deines P, Gurney JJ, Harris JW (1984) Associated chemical and carbon isotopic composition variations in diamonds from Finsch and Premier Kimberlite, South Africa. *Geochim Cosmochim Acta* 48:325–342
- Delwiche CC, Steyn PL (1970) Nitrogen isotope fractionation in soils and microbial reactions. *Environ Sci Technol* 4:929
- DeNiro MJ, Epstein S (1977) Mechanism of carbon isotope fractionation associated with lipid synthesis. *Science* 197:261–263
- DeNiro MJ, Epstein S (1978) Influence of diet on the distribution of carbon isotopes in animals. *Geochim Cosmochim Acta* 42:495–506
- DeNiro MJ, Epstein S (1979) Relationship between the oxygen isotope ratios of terrestrial plant cellulose, carbon dioxide and water. *Science* 204:51–53
- DeNiro MJ, Epstein S (1981) Isotopic composition of cellulose from aquatic organisms. *Geochim Cosmochim Acta* 45:1885–1894
- Dennis PF (1984) Oxygen self-diffusion in quartz under hydrothermal conditions. *J Geophys Res* 89:4047–4058
- Desaulniers DE, Kaufmann RS, Cherry JO, Bentley HW (1986) ^{37}Cl – ^{35}Cl variations in a diffusion-controlled groundwater system. *Geochim Cosmochim Acta* 50:1757–1764
- Des Marais DJ (1983) Light element geochemistry and spallogeneis in lunar rocks. *Geochim Cosmochim Acta* 47:1769–1781
- Des Marais DJ, Moore JG (1984) Carbon and its isotopes in mid-oceanic basaltic glasses. *Earth Planet Sci Lett* 69:43–57
- Deuser WG (1970) Extreme $^{13}\text{C}/^{12}\text{C}$ variations in Quaternary dolomites from the continental shelf. *Earth Planet. Sci Letters* 8:118–124
- Deuser WG, Hunt JM (1969) Stable isotope ratios of dissolved inorganic carbon in the Atlantic. *Deep Sea Res* 16:221–225
- Deutsch S, Ambach W, Eisner H (1966) Oxygen isotope study of snow and firn of an Alpine glacier. *Earth Planet Sci Lett* 1:197–201

- Dickson JAD, Coleman ML (1980) Changes in carbon and oxygen isotope composition during limestone diagenesis. *Sedimentology* 27:107–118
- Dole M, Jenks G (1944) Isotopic composition of photosynthetic oxygen. *Science* 100:409
- Dole M, Lange GA, Rudd DP, Zaukelies DA (1954) Isotopic composition of atmospheric oxygen and nitrogen. *Geochim Cosmochim Acta* 6:65–78
- Donahue TM, Hoffman JH, Hodges RD, Watson AJ (1982) Venus was wet: a measurement of the ratio of deuterium to hydrogen. *Science* 216:630–633
- Douthitt CB (1982) The geochemistry of the stable isotopes of silicon. *Geochim Cosmochim Acta* 46:1449–1458
- Downs WF, Touyinhthiphonexay Y, Deines P (1981) A direct determination of the oxygen isotope fractionation between quartz and magnetite at 600° and 800 °C and 5 kbar. *Geochim Cosmochim Acta* 45:2065–2072
- Dugan JP, Borthwick J, Harmon RS, Gagnier MA, Glahn JE, Kinsel EP, McLeod S, Viglino JA (1985) Guadinine hydrochloride method for determination of water oxygen isotope ratios and the oxygen-18 fractionation between carbon dioxide and water at 25 °C. *Anal Chem* 57:1734–1736
- Dungan MA, Lindstrom MM, McMillan NJ, Moorbath S, Hoefs J, Haskin LA (1986) Open system magmatic evolution of the Taos Plateau Volcanic Field, Northern New Mexico. I. The petrology and geochemistry of the Servilleta basalts. *J Geophys Res* 91:5999–6028
- Eadie BJ, Jeffrey LM (1973) $\delta^{13}\text{C}$ analyses of oceanic particulate organic matter. *Mar Chem* 1:199–209
- Eggler DH, Wendlandt RF (1979) Experimental studies on the relationship between kimberlite magmas and partial melting of peridotites. In: Boyd FR, Meyer HOA (eds) *Kimberlites, diatremes and diamonds: their geology, petrology and geochemistry*. *Am Geophys Union* 1:330–338
- Ellis AJ (1979) Chemical geothermometry in geothermal systems. *Chem Geol* 25: 219–226
- Elphick SC, Dennis PF, Graham CM (1986) An experimental study of the diffusion of oxygen in quartz and albite using an overgrowth technique. *Contrib Min Petrol* 92:322–330
- Emiliani C (1955) Pleistocene temperatures. *J Geol* 63:538–578
- Emiliani C (1966) Isotopic paleotemperatures. *Science* 154:851–857
- Emiliani C (1972) Quaternary paleotemperatures and the duration of the high-temperature intervals. *Science* 178:398–401
- Emiliani C (1978) The cause of the ice ages. *Earth Planet Sci Lett* 37:349–354
- Emiliani C, Shackleton NJ (1974) The Brunhes epoch: Isotopic paleotemperatures and geochronology. *Science* 183:511–514
- Epstein S, Lowenstam HA (1953) Temperature-shell-growth relations of recent and interglacial Pleistocene shoal-water biota from Bermuda. *J Geol* 61:424–438
- Epstein S, Mayeda TK (1953) Variations of O^{18} content of waters from natural sources. *Geochim Cosmochim Acta* 4:213–224
- Epstein S, Taylor HP (1970) $^{18}\text{O}/^{16}\text{O}$, $^{30}\text{Si}/^{28}\text{Si}$, D/H and $^{13}\text{C}/^{12}\text{C}$ studies of lunar rocks and minerals. *Science* 167:533–535
- Epstein S, Taylor HP (1971) $\text{O}^{18}/\text{O}^{16}$, $\text{Si}^{30}/\text{Si}^{28}$, D/H and $\text{C}^{13}/\text{C}^{12}$ ratios in lunar samples. *Proc 2nd Lunar Sci Conf* 2:1421–1441
- Epstein S, Taylor HP (1972) $\text{O}^{18}/\text{O}^{16}$, $\text{Si}^{30}/\text{Si}^{28}$, $\text{C}^{13}/\text{C}^{12}$ and D/H studies of Apollo 14 and 15 samples. *Proc 3rd Lunar Sci Conf* 2:1429–1454
- Epstein S, Buchsbaum HA, Lowenstam HA, Urey HC (1953) Revised carbonate-water isotopic temperature scale. *Bull Geol Soc Am* 64:1315–1326

- Epstein S, Sharp RP, Dow AJ (1965) Six-year record of oxygen and hydrogen isotope variations in South Pole firn. *J Geophys Res* 70:1809–1814
- Epstein S, Yapp CJ, Hall JH (1976) The determination of the D/H ratio of non-exchangeable hydrogen in cellulose extracted from aquatic and land plants. *Earth Planet Sci Lett* 30:241–251
- Epstein S, Thompson P, Yapp CJ (1977) Oxygen and hydrogen isotopic ratios in plant cellulose. *Science* 198:1209–1215
- Eslinger EV, Savin SM (1973a) Mineralogy and oxygen isotope geochemistry of the hydrothermally altered rocks of the Ohaki-Broadlands, New Zealand geothermal area. *Am J Sci* 273:240
- Eslinger EV, Savin SM (1973b) Oxygen isotope geothermometry of the burial metamorphic rocks of the Precambrian Belt Supergroup, Glacier National Park, Montana. *Bull Geol Soc Am* 84:2549–2560
- Eslinger EV, Yeh HW (1981) Mineralogy, $^{18}\text{O}/^{16}\text{O}$ and D/H ratios of clay-rich sediments from Deep Sea Drilling Project site 180, Aleutian Trench: Clays Clay Minerals 29:309–315
- Eslinger EV, Yeh HW (1986) Oxygen and hydrogen isotope geochemistry of Cretaceous bentonites and shales from the Disturbed Belt, Montana. *Geochim Cosmochim Acta* 50:59–68
- Eslinger EV, Savin SM, Yeh HW (1979) Oxygen isotope geothermometry of diagenetically altered shales. *Soc Econ Paleontol Mineral Spec Publ* 26:113–124
- Estep MF, Hoering TC (1980) Biogeochemistry of the stable hydrogen isotopes. *Geochim Cosmochim Acta* 44:1197–1206
- Exley RA, Matthey DP, Clague DA, Pillinger CT (1986a) Carbon isotope systematics of a mantle “hot spot”: a comparison of Loihi seamount and MORB glasses. *Earth Planet Sci Lett* 78:189–199
- Exley RA, Matthey DP, Boyd SR, Pillinger CT (1986b) Nitrogen isotope geochemistry of basaltic glasses. *Terra Cognita* 6:191
- Fallick AE, Hinton RW, McNaughton NJ, Pillinger CT (1983) D/H ratios in meteorites: some results and implications. *Ann Geophys* 1:129–134
- Farmer JG, Baxter MS (1974) Atmospheric carbon dioxide levels as indicated by the stable isotope record in wood. *Nature (London)* 247:273–275
- Faure G (1977) Principles of isotope geology. John Wiley & Son, New York
- Faure G, Hoefs J, Mensing TM (1984) Effects of oxygen fugacity on sulfur isotope compositions and magnetite concentrations in the Kirkpatrick basalt, Mount Falla, Queen Alexandra Range, Antarctica. *Isotope Geosci* 2:301–311
- Ferrara G, Laurenzi MA, Taylor HP, Tonarini S, Turi B (1985) Oxygen and strontium isotope studies of K-rich volcanic rocks from the Alban Hills, Italy. *Earth Planet Sci Lett* 75:13–28
- Ferrara G, Preite-Martinez M, Taylor HP, Tonarini S, Turi B (1986) Evidence for crustal assimilation, mixing of magmas, and a ^{87}S -rich upper mantle. An oxygen and strontium isotope study of the M. Vulsini volcanic area, Central Italy. *Contrib Mineral Petrol* 92:269–280
- Feder HM, Taube H (1952) Ionic hydration, an isotopic fractionation technique. *J Chem Phys* 20:1335
- Ferry JM (1985a) Hydrothermal alteration of Tertiary igneous rocks from the Isle of Skye, northwest Scotland. I. Gabbros. *Contr Mineral Petrol* 91:264–282
- Ferry JM (1985b) Hydrothermal alteration of Tertiary igneous rocks from the Isle of Skye, northwest Scotland. II. Granites. *Contr Mineral Petrol* 91:283–304
- Field CW, Gustafson LB (1976) Sulfur isotopes in the porphyry copper deposit at El Salvador, Chile. *Econ Geol* 71:1533–1548
- Fireman EL, Norris TL (1982) Ages and composition of gas trapped on Allan Hills and Byrd core ice. *Earth Planet Sci Lett* 60:339–350

- Fontes JC, Gonfiantini R (1967) Comportement isotopique au cours de l'évaporation de deux bassins Sahariens. *Earth Planet Sci Lett* 3:258–266
- Forester RW, Taylor HP (1977) $^{18}\text{O}/^{16}\text{O}$, D/H, and $^{13}\text{C}/^{12}\text{C}$ studies of the Tertiary igneous complex of Skye, Scotland. *Am J Sci* 277:136–177
- Fourcade S, Javoy M (1973) Rapports $^{18}\text{O}/^{16}\text{O}$ dans les roches du vieux socle catazonal d'In Ouzal (Sahara algérien). *Contrib Mineral Petrol* 42:235–244
- Francey RJ, Farquhar GD (1982) An explanation of the $^{13}\text{C}/^{12}\text{C}$ variations in tree rings. *Nature (London)* 297:28–31
- Frape SK, Fritz P, McNutt RH (1984) Water-rock interaction and chemistry of groundwaters from the Canadian Shield. *Geochim Cosmochim Acta* 48:1617–1627
- Freer R, Dennis PF (1982) Oxygen diffusion studies. I: A preliminary ion microprobe investigation of oxygen diffusion in some rock-forming minerals. *Min Mag* 45:179–192
- Freyer HD (1979) On the ^{13}C -record in tree rings. I. ^{13}C variations in northern hemisphere trees during the last 150 years. *Tellus* 31:124–137
- Freyer HD, Wiesberg L (1973) ^{13}C -decrease in modern wood due to the large scale combustion of fossil fuels. *Naturwissenschaften* 60:517–518
- Friedli H, Moor E, Oeschger H, Siegenthaler U, Stauffer B (1984) $^{13}\text{C}/^{12}\text{C}$ ratios in CO_2 extracted from Antarctic Ice. *Geophys Res Lett* 11:1145–1148
- Friedman I (1953) Deuterium content of natural waters and other substances. *Geochim Cosmochim Acta* 4:89–103
- Friedman I, O'Neil JR (1977) Compilation of stable isotope fractionation factors of geochemical interest. In: *Data Geochem*, 6th edn Geol Suvr Prof Pap 440KK
- Friedman I, O'Neil JR (1978) Hydrogen. In: Wedepohl KH (ed) *Handbook of geochemistry*. Springer, Berlin Heidelberg New York
- Friedman I, Scholz TG (1974) Isotopic composition of atmospheric hydrogen (1967–1969). *J Geophys Res* 79:785–788
- Friedman I, O'Neil JR, Adami LH, Gleason JD, Hardcastle KG (1970) Water, hydrogen, deuterium, carbon-13, and oxygen-18 content of selected lunar material. *Science* 167:538–540
- Friedman I, Hardcastle KG, Gleason JD (1974) Water and carbon in rusty lunar rock 66095. *Science* 185:346–349
- Fritz P, Poplawski S (1974) ^{18}O and ^{13}C in the shells of freshwater molluscs and their environment. *Earth Planet Sci Lett* 24:91–98
- Fry B, Cox J, Gest H, Hayes JM (1986) Discrimination between ^{34}S and ^{32}S during bacterial metabolism of inorganic sulfur compounds. *J Bacteriol* 165:328–330
- Fuchs G, Thauer R, Ziegler H, Stiehler W (1979) Carbon isotope fractionation by *Methanobacterium thermoautotrophicum*. *Arch Microbiol* 120:135–139
- Fuex AN (1977) The use of stable carbon isotopes in hydrocarbon exploration. *J Geochem Explor* 7:155–188
- Fuex AN, Baker DR (1973) Stable carbon isotopes in selected granitic, mafic and ultramafic rocks. *Geochim Cosmochim Acta* 37:2509–2521
- Galimov EM (1973) Carbon isotopes in oil-gas geology. Nedra, Moscow, p 384 (in Russian)
- Galimov EM (1985) The relation between formation conditions and variations in isotope compositions of diamonds. *Geochem Int* 22, 1:118–141
- Gardiner LR, Pillinger CT (1979) Static mass spectrometric analysis of active gases. *Anal Chem* 51:1230–1236
- Garlick GD (1969) The stable isotopes of oxygen. In: Wedepohl KH (ed) *Handbook of geochemistry*, 8B. Springer, Berlin Heidelberg New York
- Garlick GD, Dymond JR (1970) Oxygen isotope exchange between volcanic materials and ocean water. *Geol Soc Am Bull* 81:2137–2142

- Garlick GD, MacGregor ID, Vogel DE (1971) Oxygen isotope ratios in eclogites from kimberlites. *Science* 172:1025–1027
- Garrels RM, Lerman A (1984) Coupling of the sedimentary sulfur and carbon cycles – an improved model. *Am J Sci* 284:989–1007
- Garrels RM, Perry EA (1974) Cycling of carbon, sulfur and oxygen through geologic time. In: Goldberg ED (ed) *The sea*, vol 5. Wiley and Son, New York, p 303
- Gat JR (1971) Comments on the stable isotope method in regional groundwater investigation. *Water Resource Res* 7:980
- Gat JR (1980) The isotopes of hydrogen and oxygen in precipitation. In: *Handbook of environmental isotope geochemistry*, vol 1. Elsevier, New York Amsterdam, pp 21–47
- Gat JR, Dansgaard W (1972) Stable isotope survey of the fresh water occurrences in Israel and the northern Jordan Rift Valley. *J Hydrol* 16:177
- Gat JR, Issar A (1974) Desert isotope hydrology: water sources of the Sinai desert. *Geochim Cosmochim Acta* 38:1117–1131
- Gautier DL (1982) Siderite concretions: indicators of early diagenesis in the Ganimon Shale (Cretaceous). *J Sediment Petrol* 52:859–871
- Gerlach TM, Thomas DM (1986) Carbon and sulphur isotopic composition of Kilauea parental magma. *Nature (London)* 319:480–483
- Giggenbach W (1982) Carbon-13 exchange between CO₂ and CH₄ under geothermal conditions. *Geochim Cosmochim Acta* 46:159–165
- Giggenbach W, Robinson BW (1976) Sulfur isotope geochemistry of White Island volcanic discharges. *Abstr Int Conf Stable Isotopes, Lower Hutt, N Z*, p 23
- Giletti BJ (1986) Diffusion effect on oxygen isotope temperatures of slowly cooled igneous and metamorphic rocks. *Earth Planet Sci Lett* 77:218–228
- Giletti BJ, Anderson TE (1975) Studies in diffusion. II. Oxygen in phlogopite mica. *Earth Planet Sci Lett* 28:225–233
- Giletti BJ, Yund RA (1984) Oxygen diffusion in quartz. *J Geophys Res* 89:4039–4046
- Giletti BJ, Semet MP, Yund RA (1978) Studies in diffusion. III. Oxygen in feldspars: an ion microprobe determination. *Geochim Cosmochim Acta* 42:45–57
- Gilmour I, Pillinger CT (1983) The carbon isotopic composition of individual high molecular weight alkanes in the Murchison carbonaceous chondrite. *Meteoritics* 18:302
- Given RK, Lohmann KC (1985) Derivation of the original isotopic composition of Permian marine cements. *J Sediment Petrol* 55:430–439
- Godfrey JD (1962) The deuterium content of hydrous minerals from the East-Central Sierra Nevada and Yosemite National Park. *Geochim Cosmochim Acta* 26:1215–1245
- Goldhaber MB, Kaplan IR (1974) The sedimentary sulfur cycle. In: Goldberg EB (ed) *The sea*, vol IV. Wiley and Son, New York
- Gonfiantini R (1978) Standards for stable isotope measurements in natural compounds. *Nature (London)* 271:534–536
- Gonfiantini R (1984) Advisory group meeting on stable isotope reference samples for geochemical and hydrological investigations. Rep Director General IAEA Vienna
- Gonsior B, Friedman I, Lindenmayr G (1966) New tritium and deuterium measurements in atmospheric hydrogen. *Tellus* 18:256
- Goodwin AM, Thode HG, Chou CL, Karkhansis SN (1985) Chemostratigraphy and origin of the late Archaen siderite-pyrite-rich Helen Iron Formation, Michipicoten belt, Canada. *Can J Earth Sci* 22:72–84

- Grady MM, Wright IP, Fallick AE, Pillinger CT (1983) The stable isotope composition of carbon, nitrogen and hydrogen in some Yamato meteorites. *Proc 8th Symp Antarctic Meteorites 1983*, pp 289–302
- Grady MM, Wright IP, Swart PK, Pillinger CT (1985) The carbon and nitrogen isotopic composition of ureilites: implications for their genesis. *Geochim Cosmochim Acta* 49:903–915
- Graham AM, Graham CM, Harmon RS (1982) Origins of mantle waters: stable isotope evidence from amphibole-bearing plutonic cumulate blocks in calc-alkaline volcanics, Grenada, Lesser Antilles. *Abstr 5th Int Conf Geochronology, Cosmochronology, Isotope Geology*, pp 119–120
- Graham CM (1981) Experimental hydrogen isotope studies. III. Diffusion of hydrogen in hydrous minerals and stable isotope exchange in metamorphic rocks. *Contrib Mineral Petrol* 76:216–228
- Graham CM, Harmon RS (1983) Stable isotope evidence on the nature of crust-mantle interactions. In: Hawkesworth CJ, Norry MJ (eds) *Continental basalts and mantle xenoliths*. Shiva, pp 20–45
- Graham CM, Sheppard SMF, Heaton THE (1980) Experimental hydrogen isotope studies. I. Systematics of hydrogen isotope fractionation in the systems epidote-H₂O, zoisite-H₂O and AlO(OH)-H₂O. *Geochim Cosmochim Acta* 44:353–364
- Graham CM, Greig KM, Sheppard SMF, Turi B (1983) Genesis and mobility of the H₂O-CO₂ fluid phase during regional greenschist and epidote amphibolite facies metamorphism: a petrological and stable isotope study in the Scottish Dalradian. *J Geol Soc London* 140:577–599
- Graham CM, Harmon RS, Sheppard SMF (1984) Experimental hydrogen isotope studies: hydrogen isotope exchange between amphibole and water. *Am Mineral* 69:128–138
- Graham DW, Corliss BH, Bender ML, Keigwin LD (1981) Carbon and oxygen isotopic disequilibrium of recent deep-sea benthic foraminifera. *Mar Micropaleontol* 6:483–497
- Green GR, Ohmoto D, Date J, Takahashi T (1983) Whole-rock oxygen isotope distribution in the Fukazawa-Kosaka Area, Hokuroko District, Japan and its potential application to mineral exploration. *Econ Geol Monogr* 5:395–411
- Gregory RT, Taylor HP (1981) An oxygen isotope profile in a section of Cretaceous oceanic crust, Samail Ophiolite, Oman: evidence for $\delta^{18}\text{O}$ buffering of the oceans by deep (> 5 km) seawater-hydrothermal circulation at Mid-Ocean Ridges. *J Geophys Res* 86:2737–2755
- Gregory RT, Taylor HP (1986) Non-equilibrium, metasomatic $^{18}\text{O}/^{16}\text{O}$ effects in upper mantle mineral assemblages. *Contr Mineral Petrol* 93:124–135
- Grey DC, Jensen ML (1972) Bacteriogenic sulfur in air pollution. *Science* 177:1099–1100
- Grinenko LN, Ukhanov AV (1977) Sulfur levels and isotopic compositions in upper mantle xenoliths from the Obnazhennaya Kimberlite pipe. *Geochemistry* 14, 6:169–171
- Grinenko VA, Dimitriev LV, Migdisov AA, Sharas'Kin AY (1975) Sulfur contents and isotope composition for igneous and metamorphic rocks from mid-ocean ridges. *Geochem Int* 12, 1:132
- Grootenboer J, Schwarcz HP (1969) Experimentally determined sulfur isotope fractionations between sulfide minerals. *Earth Planet Sci Lett* 7:162–166
- Grossman EL (1984a) Carbon isotopic fractionation in live benthic foraminifera – comparison with inorganic precipitate studies. *Geochim Cosmochim Acta* 48:1505–1512

- Grossman EL (1984b) Stable isotope fractionation in live benthic foraminifera from the Southern California borderland. *Paleogeogr Paleoclimatol Paleoecol* 47:301–327
- Haack U, Hoefs J, Gohn E (1982) Constraints on the origin of Damaran granites by Rb/Sr and $\delta^{18}\text{O}$ data. *Contrib Mineral Petrol* 79:279–289
- Hackley KC, Anderson TF (1986) Sulfur isotopic variations in low-sulfur coals from the Rocky Mountain region. *Geochim Cosmochim Acta* 50:1703–1713
- Haendel D, Mühle K, Nitzsche HM, Stiehl G, Wand U (1986) Isotopic variations of the fixed nitrogen in metamorphic rocks. *Geochim Cosmochim Acta* 50:749–758
- Hagemann R, Nief G, Roth E (1970) Absolute isotopic scale for deuterium analysis of natural waters. Absolute D/H ratio for SMOW. *Tellus* 22:712–715
- Haimson M, Knauth LP (1983) Stepwise fluorination – a useful approach for the isotopic analysis of hydrous minerals. *Geochim Cosmochim Acta* 47:1589–1595
- Haines EB (1976) Relation between the stable carbon isotope composition of fiddler crabs, plants and soils in a salt marsh. *Limnol Oceanogr* 21:880–883
- Halliday AN, Stephens WE, Harmon RS (1980) Rb–Sr and O isotopic relationships in 3 zoned Caledonian granitic plutons, Southern Uplands, Scotland: evidence for varied sources and hybridization of magmas. *J Geol Soc London* 137:329–348
- Hamza MS, Epstein S (1980) Oxygen isotopic fractionation between oxygen of different sites in hydroxylbearing silicate minerals. *Geochim Cosmochim Acta* 44:173–182
- Harmon RS, Hoefs J (1984) O-isotope relationships in Cenozoic volcanic rocks: Evidence for a heterogeneous mantle source and open-system magmagenesis. In: *Proc ISEM Field Conf Open Magmatic System*, pp 69–71
- Harmon RS, Hoefs J (1986) S-isotope relationships in Late Cenozoic destructive plate margin and continental intraplate volcanic rocks. *Terra Cognita* 6:182
- Harmon RS, Schwarcz HP (1981) Changes of ^2H and ^{18}O enrichment of meteoric water and Pleistocene glaciation. *Nature (London)* 290:125–127
- Harmon RS, Barreiro BA, Moorbath S, Hoefs J, Francis PW, Thorpe RS, Déruelle B, McHugh J, Viglino JA (1984) Regional O-, Sr- and Pb-isotope relationships in late Cenozoic calc-alkaline lavas of the Andean Cordillera. *J Geol Soc* 141:803–822
- Harmon RS, Hoefs J, Wedepohl KH (1987) Stable isotope (O, H, S) relationships in Tertiary basalts and their mantle xenoliths from the northern Hessian Depression. *Contr Mineral Petrol* (in press)
- Harrison AG, Thode HG (1957a) Kinetic isotope effect in chemical reduction of sulphate. *Faraday Soc Trans* 53:1648–1651
- Harrison AG, Thode HG (1957b) Mechanism of the bacterial reduction of sulphate from isotope fractionation studies. *Faraday Soc Trans* 54:84–92
- Harrison AG, Thode HG (1958) Sulphur isotope abundances in hydrocarbons and source rocks of Uinta Basin, Utah. *Bull Am Assoc Petrol Geol* 42:2642–2649
- Hartmann M, Nielsen H (1969) $\delta^{34}\text{S}$ -Werte in rezenten Meeressedimenten und ihre Deutung am Beispiel einiger Sedimentprofile aus der westlichen Ostsee. *Geol Rundsch* 58:621–655
- Hattori K, Muehlenbachs K (1982) Oxygen isotope ratios in the Icelandic crust. *J Geophys Res* 87:6559–6565
- Hattori K, Krouse HR, Campbell FA (1983) The start of sulfur oxidation in continental environments: about 2.2×10^9 years ago. *Science* 221:549–551

- Hayes JM (1983) Practice and principles of isotopic measurements in organic geochemistry. In: *Organic geochemistry of contemporaneous and ancient sediments*, Great Lakes Section, SEPM, Bloomington, Ind, pp 5-1–5-31
- Heidenreich JE, Thiemens MH (1983) A non-mass-dependent isotope effect in the production of ozone from molecular oxygen. *J Chem Phys* 78:892–895
- Heidenreich JE, Thiemens MH (1985) The non-mass-dependent oxygen isotope effect in the electro dissociation of carbon dioxide: a step toward understanding NoMaD chemistry. *Geochim Cosmochim Acta* 49:1303–1306
- Heinzinger K (1969) Ein Wasserstoffisotopieeffekt in $\text{CuSO}_4 \cdot 5 \text{H}_2\text{O}$. *Z Naturforsch* 24:1502
- Heilmann H, Lensch G (1977) Sulfur isotope investigations of sulfides and rocks from the Main Basic Series of the Ivrea Zone. *Schweiz Mineral Petrogr Mitt* 57: 349–360
- Heyl AV, Landis GR, Zartman RE (1974) Isotopic evidence for the origin of Mississippi-Valley-type mineral deposits: A review. *Econ Geol* 69:992–1006
- Hilbrecht H, Hoefs J (1986) Geochemical and palaeontological studies of the $\delta^{13}\text{C}$ -anomaly in Boreal and North Tethyan Cenomanian-Turonian sediments in Germany and adjacent areas. *Palaeogeogr-climatol-ecol* 53:169–189
- Hildreth W, Christiansen RL, O'Neil JR (1984) Catastrophic isotopic modification of rhyolitic magma at times of caldera subsidence, Yellowstone Plateau Volcanic Field. *J Geophys Res* 89:8339–8369
- Hitchon B, Friedman I (1969) Geochemistry and origin of formation waters in the western Canada sedimentary basin. I. Stable isotopes of hydrogen and oxygen. *Geochim Cosmochim Acta* 33:1321–1349
- Hitchon B, Krouse HR (1972) Hydrogeochemistry of the surface waters of the Mackenzie River drainage basin, Canada. III. Stable isotopes of oxygen, carbon and sulfur. *Geochim Cosmochim Acta* 36:1337–1357
- Hoefs J (1970) Kohlenstoff- und Sauerstoff-Isotopenuntersuchungen an Karbonatkonkretionen und umgebendem Gestein. *Contrib Mineral Petrol* 27:66–79
- Hoefs J (1973) Ein Beitrag zur Isotopengeochemie des Kohlenstoffs in magmatischen Gesteinen. *Contrib Mineral Petrol* 41:277–300
- Hoefs J (1981) Isotopic composition of the ocean-atmospheric system in the geologic past. In: O'Connell RJ, Fyfe WS (eds) *Evolution of the earth*. Geodynamic Series, vol 5. American Geophys. Union, Washington, DC, pp 110–119
- Hoefs J, Emmermann R (1983) The oxygen isotope composition of Hercynian granites and pre-Hercynian gneisses from the Schwarzwald, SW Germany. *Contrib Mineral Petrol* 83:320–329
- Hoefs J, Frey M (1976) The isotopic composition of carbonaceous matter in a metamorphic profile from the Swiss Alps. *Geochim Cosmochim Acta* 40:945–951
- Hoefs J, Touret J (1975) Fluid inclusion and carbon isotope study from Bamble granulites (South Norway). *Contrib Mineral Petrol* 52:165–174
- Hoefs J, Faure G, Elliot DH (1980) Correlation of $\delta^{18}\text{O}$ and initial $^{87}\text{Sr}/^{86}\text{Sr}$ ratios in Kirkpatrick basalt on Mt Falla, Transantarctic Mountains. *Contrib Mineral Petrol* 75:199–203
- Hoefs J, Coolen JJM, Touret J (1981) The sulfur and carbon isotope composition of scapolite-rich granulites. *Contrib Mineral Petrol* 78:332–336
- Hoefs J, Müller G, Schuster AK (1982) Polymetamorphic relations in iron ores from the Iron Quadrangle, Brazil: The correlation of oxygen isotope variations with deformation history. *Contrib Mineral Petrol* 79:241–251
- Hoering T (1956) Variations in the nitrogen isotope abundance. *Proc 2nd Conf Nucl Process Geol Settings*, p 85

- Hoering T (1975) The biochemistry of the stable hydrogen isotopes. *Carnegie Inst Washington Yearb* 74:598
- Hoering T, Ford HT (1960) The isotope effect in the fixation of nitrogen by azotobacter. *Am Chem J* 82:376
- Hoering T, Parker PL (1961) The geochemistry of the stable isotopes of chlorine. *Geochim Cosmochim Acta* 23:186–199
- Hoernes S, Friedrichsen HT (1978) Oxygen and hydrogen isotope study of the polymetamorphic area of the Northern Ötztal-Stubai Alps (Tyrol). *Contrib Mineral Petrol* 67:305–315
- Hoernes S, Friedrichsen HT (1980) Oxygen and hydrogen isotopic composition of Alpine and Pre-Alpine minerals of the Swiss Central Alps. *Contrib Mineral Petrol* 72:19–32
- Hoernes S, Hoffer E (1979) Equilibrium relations of prograde metamorphic mineral assemblages. A stable isotope study of rocks of the Damara Orogen, Namibia. *Contrib Mineral Petrol* 68:377–389
- Hoernes S, Hoffer E (1985) Stable isotope evidence for fluid-present and fluid-absent metamorphism in metapelites from the Damara Orogen, Namibia. *Contrib Mineral Petrol* 90:322–330
- Hoffman JH, Hodges RR, McElroy MB, Donahue TM, Kolpin M (1979) Composition and structure of the Venus atmosphere: results from Pioneer Venus. *Science* 205:49–52
- Holm PM, Munksgaard NC (1982) Evidence for mantle metasomatism: an oxygen and strontium isotope study of the Vulsinian district, Central Italy. *Earth Planet Sci Lett* 60:376–389
- Holser WT (1977) Catastrophic chemical events in the history of the ocean. *Nature (London)* 267:403–408
- Holser WT, Kaplan IR (1966) Isotope geochemistry of sedimentary sulfates. *Chem Geol* 1:93–135
- Holser WT, Kaplan IR, Sakai H, Zak I (1979) Isotope geochemistry of oxygen in the sedimentary sulfate cycle. *Chem Geol* 25:1–17
- Horibe Y, Shigehara K, Takakuwa Y (1973) Isotope separation factor of carbon dioxide-water system and isotopic composition of atmospheric oxygen. *J Geophys Res* 78:2625–2629
- Horibe Y, Shigehara K, Langway CJ (1985) Chemical and isotopic composition of air inclusions in a Greenland ice core. *Earth Planet Sci Lett* 73:207–210
- Hubberten HW (1980) Sulfur isotope fractionation in the systems Pb–S, Cu–S and Ag–S. *Geochem J* 14:177–184
- Hubberten HW (1984) Die Fraktionierung der Schwefelisotope bei der Entstehung und Veränderung der ozeanischen Kruste. *Habil Univ Karlsruhe*
- Hubberten HW, Puchelt H (1980) Zur Schwefelisotopengeochemie basaltischer Gesteine. *ZFI Mitt Leipzig* 30:80–90
- Hubberten HW, Nielsen H, Puchelt H (1975) The enrichment of ^{34}S in the solfataras of the Nea Kameni volcano, Santorini archipelago, Greece. *Chem Geol* 16:197–205
- Hudson JD (1977) Stable isotopes and limestone lithification. *J Geol Soc London* 133:637–660
- Hulston JR (1977) Isotope work applied to geothermal systems at the Institute of Nuclear Sciences, New Zealand. *Geothermics* 5:89–96
- Hulston JR (1978) Methods of calculating isotopic fractionation in minerals. In: *Stable isotopes in the earth sciences*. DSIR Bull 220:211–219
- Hulston JR, McCabe WJ (1962) Mass spectrometer measurements in the thermal areas of New Zealand, Part II. Carbon isotopic ratios. *Geochim Cosmochim Acta* 26:398–410

- Hulston JR, Thode HG (1965) Variations in the S^{33} , S^{34} and S^{36} contents of meteorites and their relations to chemical and nuclear effects. *J Geophys Res* 70: 3475–3484
- Ikin NP, Harmon RS (1983) A stable isotope study of serpentinization and metamorphism in the Highland Border Suite Scotland, U.K. *Geochim Cosmochim Acta* 47:153–167
- Irwin H, Coleman M, Curtis C (1977) Isotopic evidence for the source of diagenetic carbonate during burial of organic-rich sediments. *Nature (London)* 269:209–213
- Ivanov MV, Gogotova GI, Matrosov AG, Zyakun AM (1976) Fractionation of sulfur isotopes by phototrophic sulfur bacteria, *Ectothiorhodospira slaposhnikovii* *Microbiology (English translation)* 45:655–659
- James AT, Baker DR (1976) Oxygen isotope exchange between illite and water at 22 °C. *Geochim Cosmochim Acta* 40:235–239
- James DE (1981) The combined use of oxygen and radiogenic isotopes as indicators of crustal contamination. *Annu Rev Earth Planet Sci* 9:311–344
- Javoy M (1977) Stable isotopes and geothermometry. *J Geol Soc* 133:609–636
- Javoy M (1980) $^{18}O/^{16}O$ and D/H ratios in high temperature peridotites. *Coll Int CNRS* 272:279–287
- Javoy M, Pineau F (1986) Nitrogen isotopes in mantle materials. *Terra Cognita* 6: 103
- Javoy M, Pineau F, Iiyama I (1978) Experimental determination of the isotopic fractionation between gaseous CO_2 and carbon dissolved in the tholeiitic magma. *Contrib Mineral Petrol* 67:35–39
- Javoy M, Pineau F, Demaiffe D (1984) Nitrogen and carbon isotopic composition in the diamonds of Mbuji Mayi (Zaire). *Earth Planet Sci Lett* 68:399–412
- Jeffrey AWA, Pflaum RC, Brooks JM, Sackett WM (1983) Vertical trends in particulate organic carbon $^{13}C/^{12}C$ ratios in the upper water column. *Deep Sea Res* 30:971–983
- Jenkyns HC, Clayton CJ (1986) Black shales and carbon isotopes in pelagic sediments from the Tethyan Lower Jurassic. *Sedimentology* 33:87–106
- Jensen ML, Nakai N (1962) Sulfur isotope meteorite standards, results and recommendations. In: Jensen ML (ed) *Biogeochemistry of sulfur isotopes*. NSF Symp Vol, p 31
- Johns WD, Hoefs J (1985) Maturation of organic matter in Neogene sediments from the Aderklaa Oilfield, Vienna Basin, Austria. *TMPM Tschermaks Mineralog Petrogr Mitt* 34:143–158
- Johnson SJ, Dansgaard W, Clausen HB, Langway CL (1972) Oxygen isotope profiles through the Antarctica and Greenland ice sheets. *Nature (London)* 235: 429–434
- Jouzel J, Merlivat L, Roth E (1975) Isotopic study of hail. *J Geophys Res* 80: 5015–5030
- Jouzel J, Merlivat L, Lorius C (1982) Deuterium excess in an East Antarctic ice core suggests higher relative humidity at the oceanic surface during the last glacial maximum. *Nature (London)* 299:688–691
- Judy C, Meiman JR, Friedman I (1970) Deuterium variations in an annual snowpack. *Water Resource Res* 6:125
- Junk G, Svec H (1958) The absolute abundance of the nitrogen isotopes in the atmosphere and compressed gas from various sources. *Geochim Cosmochim Acta* 14:234–243
- Kajiwaraya Y, Krouse HR (1971) Sulfur isotope partitioning in metallic sulfide systems. *Can J Earth Sci* 8:1397–1408

- Kanehira K, Yui S, Sakai H, Sasaki A (1973) Sulphide globules and sulphur isotopic ratios in the abyssal tholeiite from the Mid-Atlantic Ridge near 30°N latitude. *Geochem J* 7:89–96
- Kanzaki T, Yoshida M, Momura M, Kakihana H, Ozawa T (1979) Boron isotopic composition of fumarolic condensates and sassolites from Satsuma Iwo-jima, Japan. *Geochim Cosmochim Acta* 43:1859–1863
- Kaplan IR (1975) Stable isotopes as a guide to biogeochemical processes. *Proc R Soc London Ser B* 189:183–211
- Kaplan IR (1983) Stable isotopes of sulfur, nitrogen and deuterium in recent marine environments. In: *Stable isotopes in sedimentary geology*. SEPM Short Course 10, Dallas
- Kaplan IR, Hulston JR (1966) The isotopic abundance and content of sulfur in meteorites. *Geochim Cosmochim Acta* 30:479–496
- Kaplan IR, Rafter TA, Hulston JR (1960) Sulphur isotope variations in nature: Application to some biogeochemical problems. *N Z J Sci* 3:338
- Kaplan IR, Emery KO, Rittenberg SC (1963) The distribution and isotopic abundance of sulphur in recent marine sediments off Southern California. *Geochim Cosmochim Acta* 27:297–332
- Kaufmann RS, Long A, Bentley H, Davis S (1984) Natural chlorine isotope variations. *Nature (London)* 309:338–340
- Kaufmann RS, Long A, Bentley H, Campbell DJ (1986) Chlorine isotope distribution of formation water in Texas and Louisiana. *Bull Am Assoc Petrol Geol* (in press)
- Kaye JA, Strobel DF (1983) Enhancement of heavy ozone in the earth's atmosphere? *J Geophys Res* 88:8447–8452
- Keeling CD (1958) The concentration and isotopic abundance of atmospheric carbon dioxide in rural areas. *Geochim Cosmochim Acta* 13:322–334
- Keeling CD (1960) The concentration and isotopic abundances of CO₂ in the atmosphere. *Tellus* 2:200
- Keeling CD (1961) The concentration and isotopic abundances of carbon dioxide in rural and marine air. *Geochim Cosmochim Acta* 24:277–298
- Keith ML, Weber JN (1964) Carbon and oxygen isotopic composition of selected limestones and fossils. *Geochim Cosmochim Acta* 28:1787–1816
- Kneith ML, Anderson GM, Eichler R (1964) Carbon and oxygen isotopic composition of mollusk shells from marine and fresh-water environment. *Geochim Cosmochim Acta* 28:1757–1786
- Kelly WC, Rye RO, Livnat A (1986) Saline minewaters of the Keweenaw Peninsula, Northern Michigan: their nature, origin and relation to similar deep waters in Precambrian crystalline rocks of the Canadian Shield. *Am J Sci* 286:281–308
- Kelts K, McKenzie JA (1982) Diagenetic dolomite formation in Quaternary anoxic diatomaceous muds of DSDP Leg 64, Gulf of California. *Initial Rep DSDP 64*: 553–569
- Kemp ALW, Thode HG (1968) The mechanism of the bacterial reduction of sulphate and of sulphite from isotopic fractionation studies. *Geochim Cosmochim Acta* 32:71–91
- Kerrick R (1980) Archaen gold-bearing chemical sedimentary rocks and veins: A synthesis of stable isotope and geochemical relations. *Ontario Geol Survey Misc Pap* 97:144–175
- Kerrick R, Latour TE, Willmore L (1984) Fluid participation in deep fault zones: evidence from geological, geochemical and ¹⁸O/¹⁶O relations. *J Geophys Res* 89:4331–4343

- Kerridge JF (1983) Isotopic composition of carbonaceous-chondrite kerogen: evidence for an interstellar origin of organic matter in meteorites. *Earth Planet Sci Lett* 64:186–200
- Kerridge JF (1985) Carbon, hydrogen and nitrogen in carbonaceous chondrites: abundances and isotopic compositions in bulk samples. *Geochim Cosmochim Acta* 49:1707–1714
- Kerridge JF, Haymon RM, Kastner M (1983) Sulfur isotope systematics at the 21°N site, East Pacific Rise. *Earth Planet Sci Lett* 66:91–100
- Kharaka YK, Berry FAF, Friedman I (1974) Isotopic composition of oil-field brines from Kettleman North Dome, California and their geologic implications. *Geochim Cosmochim Acta* 37:1899–1908
- Kieffer SW (1982) Thermodynamic and lattice vibrations of minerals: 5. Application to phase equilibria, isotopic fractionation and high-pressure thermodynamic properties. *Rev Geophys Space Phys* 20:827–849
- Killingley JS (1983) Effects of diagenetic recrystallization on $^{18}\text{O}/^{16}\text{O}$ values of deep-sea sediments. *Nature (London)* 301:594–597
- Kirschenbaum I, Smith JS, Crowell T, Graff J, McKee R (1947) Separation of the nitrogen isotopes by the exchange reaction between ammonia and solutions of ammonium nitrate. *J Chem Phys* 15:440–446
- Kiyosu Y (1973) Sulfur isotopic fractionation among sphalerite, galena and sulfide ions. *Geochem J* 7:191–199
- Kiyosu Y (1983) Hydrogen isotopic compositions of hydrogen and methane from some volcanic areas in northeastern Japan. *Earth Planet Sci Lett* 62:41–52
- Klots CE, Benson BB (1963) Isotope effect in solution of oxygen and nitrogen in distilled water. *J Chem Phys* 38:890–892
- Knauth LP, Epstein S (1975) Hydrogen and oxygen isotope ratios in silica from the JOIDES Deep Sea Drilling Project. *Earth Planet Sci Lett* 25:1–10
- Knauth LP, Epstein S (1976) Hydrogen and oxygen isotope ratios in nodular and bedded cherts. *Geochim Cosmochim Acta* 40:1095–1108
- Knauth LP, Lowe DR (1978) Oxygen isotope geochemistry of cherts from the Onverwacht group (3.4 billion years), Transvaal, South Africa, with implications for secular variations in the isotopic composition of chert. *Earth Planet Sci Lett* 41:209–222
- Knoll AH, Hayes JM, Kaufman AJ, Swett K, Lambert IB (1986) Secular variation in carbon isotope ratios from Upper Proterozoic successions of Svalbard and East Greenland. *Nature (London)* 321:832–838
- Kokubu N, Mayeda TK, Urey HC (1961) Deuterium content of minerals, rocks and liquid inclusions from rocks. *Geochim Cosmochim Acta* 21:247–256
- Kolodny Y, Epstein S (1976) Stable isotope geochemistry of deep sea cherts. *Geochim Cosmochim Acta* 40:1195–1209
- Kolodny Y, Gross S (1974) Thermal metamorphism by combustion of organic matter: Isotopic and petrological evidence. *J Geol* 82:489–506
- Kolodny Y, Kerridge JF, Kaplan IR (1980) Deuterium in carbonaceous chondrites. *Earth Planet Sci Lett* 46:149–153
- Kolodny Y, Luz B, Navon O (1983) Oxygen isotope variations in phosphate of biogenic apatites, I Fish bone apatite – rechecking the rules of the game. *Earth Planet Sci Lett* 64:393–404
- Krichevsky MI, Sesler FD, Friedman I, Newell M (1961) Deuterium fractionation during molecular H_2 formation in a marine pseudomonad. *J Biol Chem* 236:2520
- Kroopnick P (1974a) Correlations between ^{13}C and ΣCO_2 in surface waters and atmospheric CO_2 . *Earth Planet Sci Lett* 22:397–403

- Kroopnick P (1974b) The dissolved O_2 - CO_2 - ^{13}C system in the eastern equatorial Pacific. *Deep Sea Res* 21:211-227
- Kroopnick P (1975) Respiration, photosynthesis, and oxygen isotope fractionation in oceanic surface water. *Limnol Oceanogr* 20:988-992
- Kroopnick P (1985) The distribution of ^{13}C of ΣCO_2 in the world oceans. *Deep Sea Res* 32:57-84
- Kroopnick P, Craig H (1972) Atmospheric oxygen: isotopic composition and solubility fractionation. *Science* 175:54-55
- Kroopnick P, Craig H (1976) Oxygen isotope fractionation in dissolved oxygen in the deep sea. *Earth Planet Sci Lett* 32:375-388
- Kroopnick P, Weiss RF, Craig H (1972) Total CO_2 , ^{13}C and dissolved oxygen- ^{18}O at Geosecs II in the North Atlantic. *Earth Planet Sci Lett* 16:103-110
- Krouse HR (1977) Sulfur isotope studies and their role in petroleum exploration. *J Geochem Explor* 7:189-211
- Krouse HR (1980) Sulphur isotopes in our environment. In: Fritz P, Fontes JCh (eds) *Handbook of environmental isotope geochemistry*, vol 1. Elsevier Sci Publ Co, Amsterdam, pp 435-471
- Krouse HR, Thode HG (1962) Thermodynamic properties and geochemistry of isotopic compounds of selenium. *Can J Chem* 40:367
- Kung CC, Clayton RN (1978) Nitrogen abundances and isotopic compositions in stony meteorites. *Earth Planet Sci Lett* 38:421-435
- Kuroda Y, Suzuoki T, Matuo S, Kanisawa S (1974) D/H fractionation of coexisting biotite and hornblende in some granitic rock masses. *J Jpn Assoc Mineral Petrol Econ Geol* 69:95
- Kuroda Y, Suzuoki T, Matsuo S, Aoki K (1975) D/H ratios of the coexisting phlogopite and richterite from mica nodules and a peridotite in South African kimberlites. *Contrib Mineral Petrol* 52:315-318
- Kuroda Y, Suzuoki T, Matsuo S (1977) Hydrogen isotope composition of deep-seated water. *Contrib Mineral Petrol* 60:311-315
- Kyser TK, O'Neil JR (1984) Hydrogen isotope systematics of submarine basalts. *Geochim Cosmochim Acta* 48:2123-2134
- Kyser TK, O'Neil JR, Carmichael ISE (1981) Oxygen isotope thermometry of basic lavas and mantle nodules. *Contrib Mineral Petrol* 77:11-23
- Kyser TK, O'Neil JR, Carmichael ISE (1982) Genetic relations among basic lavas and mantle nodules. *Contrib Mineral Petrol* 81:88-102
- Lambert SJ, Epstein S (1980) Stable isotope investigations of an active geothermal system in Valles Caldera, Jemez Mountains, New Mexico. *J Volcanol Geotherm Res* 8:111-129
- Lancet MS, Anders E (1970) Carbon isotope fractionation in the Fischer-Tropsch synthesis and in meteorites. *Science* 170:980-982
- Land LS (1980) The isotopic and trace element geochemistry of dolomite: the state of the art. In: *Concepts and models of dolomitization*. *Soc Econ Paleontol Min Spec Publ* 28:87-110
- Land LS, Dutton SP (1978) Cementation of a Pennsylvanian deltaic sandstone: isotope data. *J Sediment Petrol* 48:1167-1176
- Lane GA, Dole M (1956) Fractionation of oxygen isotopes during respiration. *Science* 123:574-576
- Lattanzi P, Rye OM, Rice JM (1980) Behavior of ^{13}C and ^{18}O in carbonates during contact metamorphism at Marysville, Montana. *Am J Sci* 280:890-906
- Lawrence JR, Taylor HP (1971) Deuterium and oxygen-18 correlation: Clay minerals and hydroxides in Quaternary soils compared to meteoric waters. *Geochim Cosmochim Acta* 35:993-1003

- Lawrence JR, Taylor HP (1972) Hydrogen and oxygen isotope systematics in weathering profiles. *Geochim Cosmochim Acta* 36:1377–1393
- Lawrence JR, Gieskes JM, Broecker WS (1975) Oxygen isotope and cation composition of DSDP pore waters and the alteration of layer II basalts. *Earth Planet Sci Lett* 27:1–10
- Leguy C, Rindsberger M, Zangwil A, Issar A, Gat J (1983) The relation between the ^{18}O and deuterium contents of rain water in the Negev desert and air mass trajectories. *Isotope Geosci* 1:205–218
- Letolle R (1980) Nitrogen-15 in the natural environment. In: Fritz P, Fontes JCh (eds) *Handbook of environmental isotope geochemistry*. Elsevier, Amsterdam, pp 407–433
- Lewan MD (1983) Effects of thermal maturation on stable carbon isotopes as determined by hydrous pyrolysis of Woodford shale. *Geochim Cosmochim Acta* 47:1471–1480
- Lewis RS, Anders E, Wright IP, Norris SJ, Pillinger CT (1983) Isotopically anomalous nitrogen in primitive meteorites. *Nature (London)* 305:767–771
- Lipman PW, Friedman I (1975) Interaction of meteoric water with magma: An oxygen isotope study of ash-flow sheets from Southern Nevada. *Geol Soc Am Bull* 86:695–702
- Liu KK, Epstein S (1984) The hydrogen isotope fractionation between kaolinite and water. *Isotope Geosci* 2:335–350
- Lloyd MR (1967) Oxygen-18 composition of oceanic sulfate. *Science* 156:1228–1231
- Lloyd MR (1968) Oxygen isotope behavior in the sulfate-water system. *J Geophys Res* 73:6099–6110
- Longinelli A (1965) Oxygen isotopic composition of orthophosphate from shells of living marine organisms. *Nature (London)* 207:716–719
- Longinelli A (1966) Ratios of O-18/O-16 in phosphate and carbonate from living and fossil marine organisms. *Nature (London)* 211:923–927
- Longinelli A, Cortecci G (1970) Isotopic abundance of oxygen and sulfur in sulfate ions from river water. *Earth Planet Sci Lett* 7:376–380
- Longinelli A, Craig H (1967) Oxygen-18 variations in sulfate ions in sea-water and saline lakes. *Science* 156:56–59
- Longinelli A, Edmond JM (1983) Isotope geochemistry of the Amazon basin. A reconnaissance. *J Geophys Res* 88:3703–3717
- Longinelli A, Nuti S (1973) Revised phosphate-water isotopic temperature scale. *Earth Planet Sci Lett* 19:373–376
- Longstaffe FJ (1979) The oxygen-isotope geochemistry of Archaean granitoids. In: Barker F (ed) *Trondhjemites, dacites and related rocks*. Elsevier, New York Amsterdam
- Longstaffe FJ (1982) Stable isotopes in the study of granitic pegmatites and related rocks. *Mineral Assoc Can Short Course Handb* 8:373–404
- Longstaffe FJ (1983) Diagenesis 4. Stable isotope studies of diagenesis in clastic rocks. *Geosci Can* 10:43–58
- Longstaffe FJ, Schwarcz HP (1977) $^{18}\text{O}/^{16}\text{O}$ of Archean clastic metasedimentary rocks: a petrogenetic indicator for Archean gneisses? *Geochim Cosmochim Acta* 41:1303–1312
- Lorius C, Jouzel J, Ritz C, Merlivat L, Barkov NI, Korotkevich YS, Kotlyakov VM (1985) A 150,000 year climatic record from Antarctic ice. *Nature (London)* 316:591–596
- Lowenstam HA (1961) Mineralogy, O-18/O-16 ratios and strontium and magnesium contents of recent and fossil brachiopods and their bearing on the history of the oceans. *J Geol* 69:241–260

- Lyon GL (1974a) Isotopic analyses of gas from the Carico Trench sediments. In: Kaplan IR (ed) *Natural gases in marine sediments*. Plenum, New York, pp 91–97
- Lyon GL (1974b) Geothermal gases. In: Kaplan IR (ed) *Natural gases in marine sediments*. Plenum, New York, p 41
- Maass I, Wand U, Kaemmel T (1978) Die Kohlenstoff-Isotopenzusammensetzung hochinkohlter organischer Substanzen. *Z Angew Geol* 24:109–120
- Macko SE, Estep MLF, Hare PE, Hoering TC (1983) Stable nitrogen and carbon isotopic composition of individual amino acids isolated from cultured microorganisms. *Carnegie Inst Washington Yearb* 82:404–410
- Macnamara J, Thode HG (1950) Comparison of the isotopic constitution of terrestrial and meteoritic sulphur. *Phys Rev* 78:307
- Magaritz M, Heller J (1980) A desert migration indicator – oxygen isotopic composition of land snail shells. *Paleogeogr Paleoclimatol Paleoecol* 32:153–162
- Magaritz M, Taylor HP (1974) Oxygen and hydrogen isotope studies of serpentinization in the Troodos ophiolite complex, Cyprus. *Earth Planet Sci Lett* 23:8–14
- Magaritz M, Taylor HP (1976) $^{18}\text{O}/^{16}\text{O}$ and D/H along a 500 km traverse across the Coast Range batholith and its country rocks, Central British Columbia. *Can J Earth Sci* 13:1514–1536
- Magaritz M, Taylor HP (1986) Oxygen 18/Oxygen 16 and D/H studies of plutonic granitic and metamorphic rocks across the Cordilleran batholiths of Southern British Columbia. *J Geophys Res* 91:2193–2217
- Magaritz M, Anderson RY, Holser WT, Saltzman ES, Garber J (1983) Isotope shifts in the Late Permian of the Delaware basin, Texas, precisely timed by warped sediments. *Earth Planet Sci Lett* 66:111–124
- Mariotti A (1983) Atmospheric nitrogen is a reliable standard for natural abundance measurements. *Nature (London)* 303:685–687
- Mariotti A, Germon JC, Hubert P, Kaiser P, Letolle R, Tardieux P (1981) Experimental determination of nitrogen kinetic isotope fractionation: some principles, illustration for the denitrification and nitrification processes. *Plant Soil* 62:413–430
- Mariotti A, Germon JC, Leclerc A, Catroux G, Letolle R (1982) Experimental determination of kinetic isotope fractionation of nitrogen isotopes during denitrification. In: Schmidt HL, Förster H, Heinzinger K (eds) *Stable isotopes*. Elsevier, New York Amsterdam
- Mariotti A, Lancelot C, Billen G (1984) Natural isotopic composition of nitrogen as a tracer of origin for suspended organic matter in the Scheldt estuary. *Geochim Cosmochim Acta* 48:549–555
- Marowsky G (1969) Schwefel-, Kohlenstoff- und Sauerstoffisotopenuntersuchungen am Kupferschiefer als Beitrag zur genetischen Deutung. *Contrib Mineral Petrol* 22:290–334
- Marshall B, Taylor BE (1981) Origin of hydrothermal fluids responsible for gold deposition, Alleghany district, Sierra County, California. *U S Geol Surv Open-File Rep* 81-355:280–293
- Marumo K, Nagasawa K, Kuroda Y (1980) Mineralogy and hydrogen isotope geochemistry of clay minerals in Ohnuma geothermal area, northeastern Japan. *Earth Planet Sci Lett* 47:255–262
- Matsubaya O, Sakai H (1973) Oxygen and hydrogen isotopic study on the water of crystallization of gypsum from the Kuroko-type mineralization. *Geochem J* 7:153–165

- Matsuhisa Y (1979) Oxygen isotopic compositions of volcanic rocks from the east Japan island arcs and their bearing on petrogenesis. *J Volcanic Geotherm Res* 5:271–296
- Matsuhisa Y, Goldsmith JR, Clayton RN (1979) Oxygen isotope fractionation in the systems quartz-albite-anorthite-water. *Geochim Cosmochim Acta* 43:1131–1140
- Matsuo S, Friedman I, Smith GI (1972) Studies of Quaternary saline lakes. I. Hydrogen isotope fractionation in saline minerals. *Geochim Cosmochim Acta* 36:427–435
- Matter A, Douglas RG, Perch-Nielsen K (1975) Fossil preservation, geochemistry and diagenesis of pelagic carbonates from Shatsky Rise, northeast Pacific. *Initial Rep DSDP* 32:891–922
- Mattey DP, Carr RH, Wright IP, Pillinger CT (1984) Carbon isotopes in submarine basalts. *Earth Planet Sci Lett* 70:196–206
- Matthews A, Beckinsale RD (1979) Oxygen isotope equilibration systematics between quartz and water. *Am Mineral* 64:232–240
- Matthews A, Katz A (1977) Oxygen isotope fractionation during the dolomitization of calcium carbonate. *Geochim Cosmochim Acta* 41:1431–1438
- Matthews A, Kolodny Y (1978) Oxygen isotope fractionation in decarbonation metamorphism: the Mottled Zone event. *Earth Planet Sci Lett* 39:179–192
- Matthews A, Schliestedt M (1984) Evolution of the blueschist and greenschist facies rocks of Sifnos, Cyclades, Greece. A stable isotope study of subduction-related metamorphism. *Contrib Mineral Petrol* 88:150–163
- Matthews A, Goldsmith JR, Clayton RN (1983a) Oxygen isotope fractionation involving pyroxenes: the calibration of mineral-pair geothermometers. *Geochim Cosmochim Acta* 47:631–644
- Matthews A, Goldsmith JR, Clayton RN (1983b) Oxygen isotope fractionation between zoisite and water. *Geochim Cosmochim Acta* 47:645–654
- Matthews A, Goldsmith JR, Clayton RN (1983c) On the mechanics and kinetics of oxygen isotope exchange in quartz and feldspars at elevated temperatures and pressures. *Geol Soc Am Bull* 94:396–412
- Mauersberger K (1981) Measurement of heavy ozone in the stratosphere. *Geophys Res Lett* 8:935–937
- Mayeda TK, Goldsmith JR, Clayton RN (1986) Oxygen isotope fractionation at high temperature. *Terra Cognita* 6:261
- Mazany T, Lerman JC, Long A (1980) Carbon-13 in tree-ring cellulose as an indicator of past climates. *Nature (London)* 287:432–435
- McCorkle DC, Emerson SR, Quay P (1985) Carbon isotopes in marine porewaters. *Earth Planet Sci Lett* 74:13–26
- McCrea JM (1950) The isotopic chemistry of carbonates and a paleotemperature scale. *J Chem Phys* 18:849–857
- McCready RGL (1975) Sulphur isotope fractionation by *Desulfovibrio* and *Desulfotomaculum* species. *Geochim Cosmochim Acta* 39:1395–1401
- McCready RGL, Kaplan IR, Din GA (1974) Fractionation of sulfur isotopes by the yeast *Saccharomyces cerevisiae*. *Geochim Cosmochim Acta* 38:1239–1253
- McEwing CF, Rees CE, Thode HG (1983) Sulphur isotope ratios in the Canyon Diablo metal spheroids. *Meteoritics* 18:185–198
- McKeegan KD, Walker RM, Zinner E (1985) Ion microprobe isotopic measurements of individual interplanetary dust particles. *Geochim Cosmochim Acta* 49:1971–1987
- McKenzie J (1984) Holocene dolomitization of calcium carbonate sediments from the coastal sabkhas of Abu Dhabi, U.A.E.: A stable isotope study. *J Geol* 89:185–198

- McKenzie J, Kelts KR (1979) A study of interpillow limestones from the M-zero anomaly, DSDP Leg 51, Site 417 D. Initial Rep DSDP 51-53, 2:753-769
- McKenzie J, Bernoulli D, Garrison RE (1978) Lithification of pelagic-hemipelagic sediments at DSDP Site 372: oxygen isotope alteration with diagenesis. Initial Rep DSDP 41:473-478
- McKenzie WF, Truesdell AH (1977) Geothermal reservoir temperatures estimated from the oxygen isotope compositions of dissolved sulfate and water from hot springs and shallow drillholes. *Geothermics* 5:51
- McKinney CR, McCrea JM, Epstein S, Allen HA, Urey HC (1950) Improvements in mass spectrometers for the measurement of small differences in isotope abundance ratios. *Rev Sci Instrum* 21:724
- McNaughton NJ, Borthwick J, Fallick AE, Pillinger CT (1981) Deuterium/hydrogen ratios in unequilibrated ordinary chondrites. *Nature (London)* 294:639-641
- McNaughton NJ, Fallick AE, Pillinger CT (1982) Deuterium enrichments in type 3 ordinary chondrites. *Proc 13th Lunar Planet Sci Conf, J Geophys Res* 87:A297-A302 (Suppl)
- Mekhtiyeva VL, Pankina GR (1968) Isotopic composition of sulfur in aquatic plants and dissolved sulfates. *Geochemistry* 5:624
- Mekhtiyeva VL, Pankina GR, Gavrillov EYa (1976) Distribution and isotopic composition of forms of sulfur in water animals and plants. *Geochem Int* 13:82
- Melander L (1960) Isotope effects on reaction rates. Ronald, New York
- Melander L, Saunders WH (1980) Reaction rates of isotopic molecules. Wiley and Sons, New York
- Melton CE, Giardini AA (1974) The composition and significance of gas released from natural diamonds from Africa and Brazil. *Am Mineral* 59:775-782
- Mensing TM, Faure G, Jones LM, Bowman JR, Hoefs J (1984) Petrogenesis of the Kirkpatrick basalt, Solo Nunatak, Northern Victoria Land, Antarctica based on isotopic composition of strontium, oxygen and sulfur. *Contrib Mineral Petrol* 87:101-108
- Michaelis J, Usdowski E, Menschel G (1985) Partitioning of ^{13}C and ^{12}C on the degassing of CO_2 and the precipitation of calcite: Rayleigh-type fractionation and a kinetic model. *Am J Sci* 285:318-327
- Michard-Vitrac A, Albarede F, Dupuis C, Taylor HP (1980) The genesis of Variscan (Hercynian) plutonic rocks. Inferences from Sr, Pb and O studies on the Maladeta igneous complex, Central Pyrenees, Spain. *Contrib Mineral Petrol* 72:57-72
- Milliken KL, Land LS, Loucks RG (1981) History of burial diagenesis determined from isotopic geochemistry, Frio Formation, Brazoria County, Texas. *Am Assoc Petrol Geol Bull* 65:1397-1413
- Mills GA, Urey HC (1940) The kinetics of isotopic exchange between carbon dioxide, bicarbonate ion, carbonate ion and water. *J Am Chem Soc* 62:1019
- Minson DJ, Ludlow MM, Throughton JH (1975) Differences in natural carbon isotope ratios of milk and hair from cattle grazing tropical and temperate pastures. *Nature (London)* 256:602
- Miyake Y, Wada E (1971) The isotope effect on the nitrogen in biochemical oxidation-reduction reactions. *Res Oceanogr Works Jpn* 11:1
- Mizutani Y, Rafter TA (1969) Isotopic composition of sulphate in rain water, Gracefield, New Zealand. *N Z J Sci* 12:69
- Moldovanyi EP, Lohmann KC (1984) Isotopic and petrographic record of phreatic diagenesis: Lower Cretaceous Sligo and Cupido Formations. *J Sediment Petrol* 54:972-985
- Monson KD, Hayes JM (1982) Carbon isotopic fractionation in the biosynthesis of bacterial fatty acids. Ozonolysis of unsaturated fatty acids as a means of de-

- termining the intramolecular distribution of carbon isotopes. *Geochim Cosmochim Acta* 46:139–149
- Monster J (1972) Homogeneity of sulfur and carbon isotope ratios, $^{34}\text{S}/^{32}\text{S}$ and $^{13}\text{C}/^{12}\text{C}$, in petroleum. *Bull Am Assoc Petrol Geol* 56:941–949
- Monster J, Anders E, Thode HG (1965) $^{34}\text{S}/^{32}\text{S}$ ratios for the different forms of sulphur in the Orgueil meteorite and their mode of formation. *Geochim Cosmochim Acta* 29:773–779
- Monster J, Appel PWU, Thode HG, Schidlowski M, Carmichael CM, Bridgwater D (1979) Sulfur isotope studies in early Archean sediments from Isua, West Greenland: implications for the antiquity of bacterial sulfate reduction. *Geochim Cosmochim Acta* 43:405–413
- Mook WG, van der Hoek S (1983) The N_2O correction in the carbon and oxygen isotopic analyses of atmospheric CO_2 . *Isotope Geosci* 1:237–242
- Mook WG, Bommerson JC, Staverman WH (1974) Carbon isotope fractionation between dissolved bicarbonate and gaseous carbon dioxide. *Earth Planet Sci Lett* 22:169–176
- Mook WG, Koopman M, Carter AF, Keeling CD (1983) Seasonal, latitudinal and secular variations in the abundance and isotopic ratios of atmospheric carbon dioxide. I. Results from land stations. *J Geophys Res* 88:10915–10933
- Moore JG (1970) Water content of basalt erupted on the ocean floor. *Contr Mineral Petrol* 28:272–279
- Moore JG, Bachelder JN, Cunningham CG (1977) CO_2 -filled vesicles in mid-ocean basalt. *J Volcanol Geotherm Res* 2:309–327
- Morikiyo T (1984) Carbon isotopic study on coexisting calcite and graphite in the Ryoke metamorphic rocks, northern Kiso district, central Japan. *Contrib Mineral Petrol* 87:251–259
- Muehlenbachs K, Byerly G (1982) ^{18}O enrichment of silicic magmas caused by crystal fractionation at the Galapagos Spreading Center. *Contrib Mineral Petrol* 79:76–79
- Muehlenbachs K, Clayton RN (1972a) Oxygen isotope studies of fresh and weathered submarine basalts. *Can J Earth Sci* 8:1591–1594
- Muehlenbachs K, Clayton RN (1972b) Oxygen isotope geochemistry of submarine greenstones. *Can J Earth Sci* 9:471–478
- Muehlenbachs K, Clayton RN (1976) Oxygen isotope composition of the oceanic crust and its bearing on seawater. *J Geophys Res* 81:4365–4369
- Muehlenbachs K, Kushiro I (1974) Oxygen isotope exchange and equilibrium of silicates with CO_2 or O_2 . *Geophys Lab Yearb* 73:232
- Murata KJ, Friedman I, Gleason JD (1977) Oxygen isotope relations between diagenetic silica minerals in Monterey Shale, Temblor Range, California. *Am J Sci* 277:259–272
- Murozumi M (1961) *Bull Geol Surv Jpn* 12:183
- Nabelek PI, O'Neil JR, Papike JJ (1983) Vapor phase exsolution as a controlling factor in hydrogen isotope variation in granitic rocks. The Notch Peak granitic stock, Utah. *Earth Planet Sci Letters* 66:137–150
- Nabelek PI, Labotka TC, O'Neil JR, Papike JJ (1984) Contrasting fluid/rock interaction between the Notch Peak granitic intrusion and argillites and limestones in western Utah: evidence from stable isotopes and phase assemblages. *Contrib Mineral Petrol* 86:25–43
- Nagy KL, Parmentier EM (1982) Oxygen isotope exchange at an igneous intrusive contact. *Earth Planet Sci Lett* 59:1–10
- Nakai N, Jensen ML (1964) The kinetic isotope effect in the bacterial reduction and oxidation of sulfur. *Geochim Cosmochim Acta* 28:1893–1912

- Navon O, Wasserburg GJ (1985) Self-shielding in O_2 – a possible explanation for oxygen isotope anomalies in meteorites. *Earth Planet Sci Lett* 73:1–16
- Newton RC, Smith JV, Windley BF (1980) Carbonic metamorphism, granulites and crustal growth. *Nature* (London) 288:45–50
- Nielsen H (1965) S-Isotope im marinen Kreislauf und das $\delta^{34}S$ der früheren Meere. *Geol Rundsch* 55:160–172
- Nielsen H (1972) Sulphur isotopes and the formation of evaporite deposits. In: *Geology of saline deposits, Proc Hannover Symp 1968, Earth Sci* 7:91, UNESCO 1972
- Nielsen H (1974) Isotopic composition of the major contributors to atmospheric sulfur. *Tellus* 26:213
- Nielsen H (1978) Sulfur isotopes. In: Wedepohl KH (ed) *Handbook of geochemistry*. Springer, Berlin Heidelberg New York
- Nielsen H (1979) Sulfur isotopes. In: Jäger E, Hunziker J (eds) *Lectures in isotope geology*. Springer, Berlin Heidelberg New York, pp 283–312
- Nielsen H (1985a) Isotope in der Lagerstättenforschung. In: Bender F (ed) *Ange wandte Geowissenschaften*. Enke, Stuttgart
- Nielsen H (1985b) Sulfur isotopes in stratabound mineralizations of Central Europe. *Geol Jahrb D70*:225–262
- Nielsen H, Rieke W (1964) S-Isotopenverhältnisse von Evaporiten aus Deutschland. Ein Beitrag zur Kenntnis von $\delta^{34}S$ im Meerwasser Sulfat. *Geochim Cosmochim Acta* 28:577–591
- Nier AO (1950) A redetermination of the relative abundances of the isotopes of carbon, nitrogen, oxygen, argon and potassium. *Phys Rev* 77:789
- Nier AO, Ney EP, Inghram MG (1947) A null method for the comparison of two ion currents in a mass spectrometer. *Rev Sci Instrum* 18:294
- Nier AO, McElroy MB, Yung YL (1976) Isotopic composition of the Martian atmosphere. *Science* 194:68–70
- Nissenbaum A (1974) Deuterium content of humic acids from marine and non-marine environments. *Mar Chem* 2:59
- Nissenbaum A, Kaplan IR (1972) Chemical and isotopic evidence for the in situ origin of marine humic substances. *Limnol Oceanogr* 17:570–582
- Nissenbaum A, Schallinger KM (1974) The distribution of stable carbon isotopes ($^{13}C/^{12}C$) in fractions of soil organic matter. *Geoderma* 11:137–145
- Nissenbaum A, Presley BJ, Kaplan IR (1972) Early diagenesis in a reducing Fjord, Saanich Inlet, British Columbia. I: Chemical and isotopic changes in major components of interstitial water. *Geochim Cosmochim Acta* 36:1007–1027
- Nitzsche HM, Stiehl G (1984) Untersuchungen zur Isotopenfraktionierung des Stickstoffs in den Systemen Ammonium/Ammoniak und Nitrid/Stickstoff. *ZFI Mitt* 84:283–291
- Nomura M, Kanzaki T, Ozawa T, Okamoto M, Kakihana H (1982) Boron isotopic composition of fumarolic condensates from some volcanoes in Japanese island arcs. *Geochim Cosmochim Acta* 46:2403–2406
- Northrop DA, Clayton RN (1966) Oxygen isotope fractionations in systems containing dolomite. *J Geol* 74:174–196
- Nriagu J (1974) Fractionation of sulfur isotopes by sediment adsorption of sulfate. *Earth Planet Sci Lett* 22:366–370
- Ohmoto H (1972) Systematics of sulfur and carbon isotopes in hydrothermal ore deposits. *Econ Geol* 67:551–578
- Ohmoto H, Lasaga AC (1982) Kinetics of reactions between aqueous sulfates and sulfides in hydrothermal systems. *Geochim Cosmochim Acta* 46:1727–1745
- Ohmoto H, Rye RO (1979) Isotopes of sulfur and carbon. In: *Geochemistry of hydrothermal ore deposits*, 2nd edn. Holt Rinehart and Winston, New York

- Ohmoto H, Skinner BJ (1983) The Kuroko and related deposits. *Econ Geol Monograph* 5
- O'Leary MH (1981) Carbon isotope fractionation in plants. *Phytochemistry* 20: 553–567
- O'Neil JR (1968) Hydrogen and oxygen isotopic fractionation between ice and water. *J Phys Chem* 72:3683
- O'Neil JR (1977) Stable isotopes in mineralogy. *Phys Chem Mineral* 2:105
- O'Neil JR, Clayton RN (1964) Oxygen isotope thermometry. In: Craig H, Miller SL, Wasserburg GJ (eds) *Isotopic and cosmic chemistry*. North Holland Publ Co, Amsterdam, pp 157–168
- O'Neil JR, Epstein S (1966) A method for oxygen isotope analysis of milligram quantities of water and some of its applications. *J Geophys Res* 71:4955–4961
- O'Neil JR, Hay RL (1973) $^{18}\text{O}/^{16}\text{O}$ ratios in cherts associated with the saline lake deposits of East Africa. *Earth Planet Sci Lett* 19:257–266
- O'Neil JR, Kharaka YK (1976) Hydrogen and oxygen isotope exchange reactions between clay minerals and water. *Geochim Cosmochim Acta* 40:241–246
- O'Neil JR, Silberman ML (1974) Stable isotope relations in epithermal Au–Ag deposits. *Econ Geol* 69:902–909
- O'Neil JR, Taylor HP (1967) The oxygen isotope and cation exchange chemistry of feldspars. *Am Mineral* 52:1414–1437
- O'Neil JR, Taylor HP (1969) Oxygen isotope equilibrium between muscovite and water. *J Geophys Res* 74:6012–6022
- O'Neil JR, Clayton RN, Mayeda TK (1969) Oxygen isotope fractionation in divalent metal carbonates. *J Chem Phys* 51:5547
- O'Neil JR, Adami LH, Epstein S (1975) Revised value for the ^{18}O fractionation between CO_2 and H_2O at 25 °C. *J Res US Geol Surv* 3:623
- Onuma N, Clayton RN, Mayeda TK (1970a) Apollo 11 rocks: Oxygen isotope fractionation between minerals and an estimate of the temperature of formation. *Proc Apollo 11 Lunar Sci Conf Geochim Cosmochim Acta Suppl* 2:1429–1434
- Onuma N, Clayton RN, Mayeda TK (1970b) Oxygen isotope fractionation between minerals and an estimate of the temperature of formation. *Science* 167: 536–538
- Orr WL (1974) Changes in sulfur content and isotopic ratios of sulfur during petroleum maturation. Study of Big Horn Basin Paleozoic oils. *Am Assoc Petrol Geol Bull* 58:2295–2318
- Osmond CB, Ziegler H (1975) Schwere Pflanzen und leichte Pflanzen: Stabile Isotope im Photosynthesestoffwechsel und in der biochemischen Ökologie. *Naturwiss Rundsch* 28:323
- Owen T, Biemann K, Rushneck DR, Biller JE, Howarth DW, Lafleur AL (1977) The composition of the atmosphere at the surface of Mars. *J Geophys Res* 82: 4635–4639
- Panichi C, Gonfiantini R (1978) Environmental isotopes in geothermal studies. *Geothermics* 6:143–161
- Panichi C, Ferrara GC, Gonfiantini R (1977) Isotope geochemistry in the Lardarello geothermal fields. *Geothermics* 5:81–88
- Parada CB, Long A, Davis SN (1983) Stable isotopic composition of soil carbon dioxide in the Tuscon basin, Arizona, USA. *Isotope Geosci* 1:219–236
- Pardue JW, Scalan RS, van Baalen C, Parker PL (1976) Maximum carbon isotope fractionation in photosynthesis by blue-green algae and a green alga. *Geochim Cosmochim Acta* 40:309–312
- Park R, Epstein S (1960) Carbon isotope fractionation during photosynthesis. *Geochim Cosmochim Acta* 21:110–126

- Parker PL (1964) The biogeochemistry of the stable isotopes of carbon in a marine bay. *Geochim Cosmochim Acta* 28:1155–1164
- Paterson WSB, Koerner RM, Fisher D, Johnsen SJ, Clausen HB, Dansgaard W, Bucher P, Oeschger H (1977) An oxygen isotope climatic record from the Devon Island Ice Cap, Arctic Canada. *Nature (London)* 266:508–511
- Penzias AA (1980) Nuclear processing and isotopes in the galaxy. *Science* 208: 663–669
- Perry EA, Gieskes JM, Lawrence JR (1976) Mg, Ca and $^{18}\text{O}/^{16}\text{O}$ exchange in the sediment-pore water system, Hole 149, DSDP. *Geochim Cosmochim Acta* 40: 413–423
- Perry EC (1967) The oxygen isotope chemistry of ancient cherts. *Earth Planet Sci Lett* 3:62–66
- Perry EC, Tan FC (1972) Significance of oxygen and carbon isotope variations in early Precambrian cherts and carbonate rocks of Southern Africa. *Bull Geol Soc Am* 83:647–664
- Peters KE, Rohrback BG, Kaplan IR (1981) Carbon and hydrogen stable isotope variations in kerogen during laboratory-simulated thermal maturation. *Am Assoc Petrol Geol Bull* 65:501–508
- Pillinger CT (1984) Light element stable isotopes in meteorites – from grams to picograms. *Geochim Cosmochim Acta* 48:2739–2768
- Pinckney DM, Rye RO (1972) Variation of $^{18}\text{O}/^{16}\text{O}$, $^{13}\text{C}/^{12}\text{C}$, texture and mineralogy in altered limestone in the Hill Mine, Cave-in-District, Illinois. *Econ Geol* 67:1–18
- Pineau F, Javoy M (1983) Carbon isotopes and concentrations in mid-ocean ridge basalts. *Earth Planet Sci Lett* 62:239–257
- Pineau F, Javoy M, Bottinga Y (1976a) $^{13}\text{C}/^{12}\text{C}$ ratios of rocks and inclusions in popping rocks of the Mid-Atlantic Ridge and their bearing on the problem of isotopic composition of deep-seated carbon. *Earth Planet Sci Lett* 29:413–421
- Pineau F, Javoy M, Hawkins JW, Craig H (1976b) Oxygen isotope variations in marginal basin and ocean-ridge basalts. *Earth Planet Sci Lett* 28:299–307
- Pisciotti KA, Mahoney JJ (1981) Isotopic survey of diagenetic carbonates, DSDP Leg 63. *Initial Rep DSDP* 63:595–609
- Presley BJ, Kaplan IR (1968) Changes in dissolved sulfate, calcium and carbonate from interstitial water of near-shore sediments. *Geochim Cosmochim Acta* 32: 1037–1048
- Price FT, Shieh YN (1979) The distribution and isotopic composition of sulfur in coals from the Illinois Basin. *Econ Geol* 74:1445–1461
- Prombo CA, Clayton RN (1985) A striking nitrogen isotope anomaly in the Ben-cubbin and Weatherford meteorites. *Science* 230:935–937
- Puchelt H, Hubberten HW (1980) Preliminary results of sulfur isotope investigations on deep sea drilling project cores from legs 52 and 53. *Initial Rep DSDP* 51, 52, 53, Part 2:1145–1148
- Puchelt H, Sabels BR, Hoering TC (1971) Preparation of sulfur hexafluoride for isotope geochemical analysis. *Geochim Cosmochim Acta* 35:625–628
- Rabinowitch EI (1945) *Photosynthesis and related processes*, vol I. Interscience, New York, p 10
- Rabinovitch AL, Grinenko VA (1979) Sulfate sulfur isotope ratios for USSR river water. *Geochemistry* 16, 2:68–79
- Rafter TA (1957) Sulphur isotopic variations in nature, P 1: The preparation of sulphur dioxide for mass spectrometer examination. *N Z J Sci Tech* B38:849
- Raiswell R (1982) Pyrite texture, isotopic composition and the availability of iron. *Am J Sci* 282:1244–1236

- Rakestraw NM, Rudd DP, Dole M (1951) Isotopic composition of oxygen in air dissolved in Pacific Ocean water as a function of depth. *J Am Chem Soc* 73: 2976
- Rashid K, Krouse HR, McCready RGL (1978) Selenium isotope fractionation during bacterial selenite reduction. In: Short Pap 4th Int Conf Geochronol Cosmochronol Isotope Geol, p 347
- Rau GH, Sweeney RE, Kaplan IR (1982) Plankton $^{13}\text{C}/^{12}\text{C}$ ratio changes with latitude: differences between northern and southern oceans. *Deep Sea Res* 29: 1035–1039
- Rayleigh JWS (1896) Theoretical considerations respecting the separation of gases by diffusion and similar processes. *Philos Mag* 42:493
- Redding CE, Schoell M, Monin JC, Durand B (1980) Hydrogen and carbon isotopic composition of coals and kerogen. In: Douglas AG, Maxwell JR (eds) *Phys Chem Earth* 12:711–723
- Redfield AC, Friedman I (1965) Factors affecting the distribution of deuterium in the ocean. In: *Symp Rhode Island Occ Publ* 3:149
- Rees CE (1970) The sulphur isotope balance of the ocean: an improved model. *Earth Planet Sci Lett* 7:366–370
- Rees CE (1978) Sulphur isotope measurements using SO_2 and SF_6 . *Geochim Cosmochim Acta* 42:383–389
- Rees CE, Thode HG (1966) Selenium isotope effects in the reduction of sodium selenite and of sodium selenate. *Can J Chem* 44:419
- Rees CE, Jenkins WJ, Monster J (1978) The sulphur isotopic composition of ocean water sulphate. *Geochim Cosmochim Acta* 42:377–381
- Reibach PH, Benedict CR (1977) Fractionation of stable carbon isotopes by PEP carboxylase from C_4 plants. *Plant Physiol* 59:564–568
- Rex RW, Syers JK, Jackson JK, Clayton RN (1969) Eolian origin of quartz in soils of Hawaiian Islands and in Pacific pelagic sediments. *Science* 163:277–279
- Rice CM, Harmon RS, Shepherd TJ (1985) Central City, Colorado: The upper part of an alkaline porphyry molybdenum system. *Econ Geol* 80:1769–1796
- Rice DD (1983) Relation of natural gas composition to thermal maturity and source rock type in San Juan Basin, northwestern New Mexico and southwestern Colorado. *Am Assoc Petrol Geol Bull* 67:1199–1218
- Rice DD, Claypool GE (1981) Generation, accumulation and resource potential of biogenic gas. *Am Assoc Petrol Geol Bull* 65:5–25
- Richet P, Bottinga Y, Javoy M (1977) A review of H, C, N, O, S, and Cl stable isotope fractionation among gaseous molecules. *Annu Rev Earth Planet Sci* 5:65–110
- Ricke W (1964) Präparation von Schwefeldioxid zur massenspektrometrischen Bestimmung des S-Isotopenverhältnisses in natürlichen S-Verbindungen. *Z Anal Chemie* 199:401
- Robert F, Epstein S (1980) Carbon, hydrogen and nitrogen isotopic composition of the Renazzo and Orgeuil organic components. *Meteoritics* 15:351
- Robert F, Epstein S (1982) The concentration and isotopic composition of hydrogen, carbon and nitrogen carbonaceous meteorites. *Geochim Cosmochim Acta* 46:81–95
- Robert F, Merlivat L, Javoy M (1978) Water and deuterium content in ordinary chondrites. *Meteoritics* 12:349–354
- Robert F, Merlivat L, Javoy M (1979a) Water and deuterium content in the Chainpur meteorite. *Meteoritics* 13:613–615
- Robert F, Merlivat L, Javoy M (1979b) Deuterium concentration in the early solar system: a hydrogen and oxygen isotope study. *Nature (London)* 282:785–789

- Robinson BW (1973) Sulphur isotope equilibrium during sulphur hydrolysis at high temperatures. *Earth Planet Sci Lett* 18:443–450
- Robinson BW (1975) Carbon and oxygen isotopic equilibria in hydrothermal calcites. *Geochem J* 9:43–46
- Robinson BW (1978) Sulfate-water and H₂S isotopic thermometry in the New Zealand geothermal systems. In: Short Pap 4th Int Con Geochronol Cosmochronol Isotope Geol, p 354–356
- Robinson BW, Kusakabe M (1975) Quantitative preparation of sulphur dioxide for ³⁴S/³²S analyses from sulphides by combustion with cuprous oxide. *Anal Chem* 47:1179
- Roginsky SS (1962) *Theoretische Grundlagen der Isotopenchemie*. Deutscher Verlag der Wissenschaften, Berlin
- Rosenbaum J, Sheppard SMF (1986) An isotopic study of siderites, dolomites and ankerites at high temperatures. *Geochim Cosmochim Acta* 50:1147–1150
- Ross PJ, Martin EA (1970) Rapid procedure for preparing gas samples for nitrogen-15 determinations. *Analyst* 95:817–822
- Rothe P, Hoefs J (1977) Isotopengeochemische Untersuchungen an Karbonaten der Ries-See-Sedimente der Forschungsbohrung Nördlingen 1973. *Geol Bavaria* 75:59–66
- Rubinson M, Clayton RN (1969) Carbon-13 fractionation between aragonite and calcite. *Geochim Cosmochim Acta* 33:997–1002
- Rumble D III (1978) Mineralogy, petrology and oxygen isotope geochemistry of the Clough Formation, Black Mountain, western New Hampshire, USA. *J Petrol* 19:317–340
- Rumble D III (1982) Stable isotope fractionation during metamorphic devolatilization reactions. In: *Characterization of metamorphism through mineral equilibria*. *Rev Mineral* 10:327–353
- Rumble D III, Spear FS (1983) Oxygen-isotope equilibration and permeability enhancement during regional metamorphism. *J Geol Soc London* 140:619–628
- Rumble D III, Ferry JM, Hoering TC, Boucot AJ (1982) Fluid flow during metamorphism at the Beaver Brook fossil locality. *Am J Sci* 282:886–919
- Russell WA, Papanastassiou DA, Tombrello TA (1978) Ca isotope fractionation on the Earth and other solar system materials. *Geochim Cosmochim Acta* 42:1075–1090
- Rye RO (1974) A comparison of sphalerite-galena sulfur isotope temperatures with filling-temperatures of fluid inclusions. *Econ Geol* 69:26–32
- Rye RO, Ohmoto H (1974) Sulfur and carbon isotopes and ore genesis. A review. *Econ Geol* 69:826–842
- Rye RO, O'Neil JR (1968) The ¹⁸O-content of water in primary fluid inclusions from Providencia, North Central Mexico. *Econ Geol* 63:232–238
- Rye RO, Sawkins FJ (1974) Fluid inclusion and stable isotope studies on the Casapalca Ag–Pb–Zn–Cu deposit, central Andes, Peru. *Econ Geol* 69:181–205
- Rye RO, Hall WE, Ohmoto H (1974) Carbon, hydrogen, oxygen and sulfur isotope study of the Darwin lead-silver-zinc deposit, southern California. *Econ Geol* 69:468–481
- Rye RO, Schilling RD, Rye DM, Jansen JBH (1976) Carbon, hydrogen and oxygen isotope studies of the regional metamorphic complex at Naxos, Greece. *Geochim Cosmochim Acta* 40:1031–1049
- Sackett WM (1978) Carbon and hydrogen isotope effects during the thermocatalytic production of hydrocarbons in laboratory simulation experiments. *Geochim Cosmochim Acta* 42:571–580
- Sackett WM, Eadie BJ, Exner ME (1973) Stable isotope composition of organic carbon in Recent Antarctic sediments. *Adv Org Geochem* 1973:661

- Saino T, Hattori A (1980) ^{15}N natural abundance in oceanic suspended particulate organic matter. *Nature (London)* 283:752–754
- Sakai H (1957) Fractionation of sulphur isotopes in nature. *Geochim Cosmochim Acta* 12:150–169
- Sakai H (1968) Isotopic properties of sulfur compounds in hydrothermal processes. *Geochem J* 2:29–49
- Sakai H (1977) Sulfate-water isotope thermometry applied to geothermal systems. *Geothermics* 5:67–74
- Sakai H, Krouse HR (1971) Elimination of memory effect in $^{18}\text{O}/^{16}\text{O}$ determinations in sulfates. *Earth Planet Sci Lett* 11:369–373
- Sakai H, Matsubaya O (1974) Isotopic geochemistry of the thermal waters of Japan and its bearing on the Kuroko ore solutions. *Econ Geol* 69:974–991
- Sakai H, Tsutsumi M (1978) D/H fractionation factors between serpentine and water at 100 to 500 °C and 2000 bar water pressure and the D/H ratios of natural serpentines. *Earth Planet Sci Lett* 40:231–242
- Sakai H, Ueda A, Field CW (1978) $\delta^{34}\text{S}$ and concentration of sulfide and sulfate sulfurs in some ocean-floor basalts and serpentinites. Short Pap 4th Int Conf Geochronol Cosmochromol Isotope Geol, Geol Surv Open-File Rep 78-701, p 371
- Sakai H, Gunnlaugson E, Tomasson J, Rouse JE (1980) Sulfur isotope systematics in Icelandic geothermal systems and influence of seawater circulation at Reykjanes. *Geochim Cosmochim Acta* 44:1223–1231
- Sakai H, Casadevall TJ, Moore JG (1982) Chemistry and isotope ratios of sulfur in basalts and volcanic gases at Kilauea volcano, Hawaii. *Geochim Cosmochim Acta* 46:729–738
- Sakai H, DesMarais DJ, Ueda A, Moore JG (1984) Concentrations and isotope ratios of carbon, nitrogen and sulfur in ocean-floor basalts. *Geochim Cosmochim Acta* 48:2433–2441
- Sangster DF (1968) Relative sulphur isotope abundances of ancient seas and stratabound sulphide deposits. *Geol Assoc Can Proc* 19:79
- Sangster DF (1976) Sulphur and lead isotopes in stratabound deposits. In: Wolf KH (ed) *Handbook of stratabound and stratiform ore deposits*, vol 2, pp 219–266
- Sasaki A, Arikawa Y, Folinsbee RE (1979) Kiba reagent method of sulfur extraction applied to isotopic work. *Bull Geol Surv Jpn* 30:241
- Sass E, Kolodny Y (1972) Stable isotopes, chemistry and petrology of carbonate concretions (Mishash formation, Israel). *Chem Geol* 10:261–286
- Satake H, Matsuo S (1984) Hydrogen isotopic fractionation factor between brucite and water in the temperature range from 100 to 510 °C. *Contrib Mineral Petrol* 86:19–24
- Savin SM (1977) The history of the earth's surface temperature during the past 100 million years. *Annu Rev Earth Planet Sci* 5:319–355
- Savin SM, Epstein S (1970a) The oxygen and hydrogen isotope geochemistry of clay minerals. *Geochim Cosmochim Acta* 34:25–42
- Savin SM, Epstein S (1970b) The oxygen and hydrogen isotope geochemistry of ocean sediments and shales. *Geochim Cosmochim Acta* 34:43–63
- Savin SM, Epstein S (1970c) The oxygen isotopic composition of coarse grained sedimentary rocks and minerals. *Geochim Cosmochim Acta* 34:323–329
- Savin SM, Yeh HW (1981) Stable isotopes in ocean sediments. In: Emiliani C (ed) *The sea*, vol 7. Wiley-Interscience, New York, pp 1521–1554
- Schidlowski M, Hayes JM, Kaplan IR (1983) Isotopic inferences of ancient biochemistries: carbon, sulfur, hydrogen and nitrogen. In: Schopf JW (ed) *Earth's earliest biosphere: Its origin and evolution*. Princeton Univ Press, pp 149–186

- Schiegl WE, Vogel JV (1970) Deuterium content of organic matter. *Earth Planet Sci Lett* 7:307–313
- Schneider A (1970) The sulfur isotope composition of basaltic rocks. *Contrib Mineral Petrol* 25:95–124
- Schoell M (1980) The hydrogen and carbon isotopic composition of methane from natural gases of various origins. *Geochim Cosmochim Acta* 44:649–661
- Schoell M (1984a) Recent advances in petroleum isotope geochemistry. *Organ Geochem* 6:645–663
- Schoell M (1984b) Wasserstoff- und Kohlenstoffisotope in organischen Substanzen, Erdölen und Erdgasen. *Geol Jahrb R D, H* 67
- Schoell M, Faber E, Coleman ML (1983) Carbon and hydrogen isotopic compositions of the NBS 22 and NBS 21 stable isotope reference materials: An interlaboratory comparison. *Organ Geochem* 5:3–6
- Schoeller DA, Peterson DW, Hayes JM (1983) Double-comparison method for mass spectrometric determination of hydrogen isotopic abundances. *Anal Chem* 55:827–832
- Schoeninger MJ, DeNiro MJ (1984) Nitrogen and carbon isotopic composition of bone collagen from marine and terrestrial animals. *Geochim Cosmochim Acta* 48:625–639
- Scholle PA, Arthur MA (1980) Carbon isotope fluctuations in Cretaceous pelagic limestones: potential stratigraphic and petroleum exploration tool. *Am Assoc Petrol Geol Bull* 64:67–87
- Schwarcz HP, Ageyi EK, McCullen CC (1969) Boron isotopic fractionation during clay adsorption from seawater. *Earth Planet Sci Lett* 6:1–5
- Seckbach J, Kaplan IR (1973) Growth pattern and $^{13}\text{C}/^{12}\text{C}$ isotope fractionation of *Cyanidium calcarium* and hot spring algal mats. *Chem Geol* 12:161–169
- Shackleton N (1968) Depth of pelagic foraminifera and isotopic changes in Pleistocene Oceans. *Nature (London)* 218:79–80
- Shackleton NJ (1977a) The oxygen isotope stratigraphic record of the late Pleistocene. *Philos Trans R Soc London Ser B* 280:169–182
- Shackleton NJ (1977b) Carbon-13 in *Uvigerina*: tropical rainforest history and the equatorial Pacific carbonate dissolution cycles. In: *The fate of fossil fuel CO₂ in the oceans*. Plenum, New York, pp 401–428
- Shackleton NJ, Kennett JP (1975) Paleotemperature history of the Cenozoic and initiation of Antarctic glaciation: oxygen and carbon isotope analyses in DSDP sites 277, 279 and 281. *Initial Rep DSDP* 29:743–755
- Shackleton NJ, Opdyke ND (1973) Oxygen isotope and paleomagnetic stratigraphy of equatorial Pacific core V 28–V39: Oxygen isotope temperatures and ice volumes on a 10^5 and 10^6 year scale. *Q Res* 3:39
- Shackleton NJ, Hall MA, Line J, Shuxi C (1983) Carbon isotope data in core V19-30 confirm reduced carbon dioxide concentrations in the ice age atmosphere. *Nature (London)* 306:319–322
- Sharma T, Clayton RN (1965) Measurement of $\text{O}^{18}/\text{O}^{16}$ ratios of total oxygen of carbonates. *Geochim Cosmochim Acta* 29:1347–1353
- Shelton KL, Rye DM (1982) Sulfur isotopic compositions of ores from Mines Gaspé, Quebec: An example of sulfate-sulfide isotopic disequilibria in ore-forming fluids with applications to other porphyry-type deposits. *Econ Geol* 77:1688–1709
- Shemesh A, Kolodny Y, Luz B (1983) Oxygen isotope variations in phosphate of biogenic apatites, II. Phosphorite rocks. *Earth Planet Sci Lett* 64:405–416
- Sheppard SMF (1984) Isotopic geothermometry. In: Lagache M (ed) *Thermométrie et barométrie géologiques*. Soc Fr Mineral Cristallogr, pp 349–412

- Sheppard SMF, Epstein S (1970) D/H and O^{18}/O^{16} ratios of minerals of possible mantle or lower crustal origin. *Earth Planet Sci Lett* 9:232–239
- Sheppard SMF, Harris C (1985) Hydrogen and oxygen isotope geochemistry of Ascension Island lavas and granites: variation with crystal fractionation and interaction with sea water. *Contrib Mineral Petrol* 91:74–81
- Sheppard SMF, Nielsen RL, Taylor HP (1969) Oxygen and hydrogen isotope ratios of clay minerals from Porphyry Copper Deposits. *Econ Geol* 64:755–777
- Sheppard SMF, Nielsen RL, Taylor HP (1971) Hydrogen and oxygen isotope ratios in minerals from Porphyry Copper Deposits. *Econ Geol* 66:515–542
- Shieh YN, Schwarcz HP (1974) Oxygen isotope studies of granite and migmatite, Grenville province of Ontario, Canada. *Geochim Cosmochim Acta* 38:21–45
- Shieh YN, Taylor HP (1969a) Oxygen and hydrogen isotope studies of contact metamorphism in the Santa Rosa Range, Nevada and other areas. *Contrib Mineral Petrol* 20:306–356
- Shieh YN, Taylor HP (1969b) Oxygen and carbon isotope studies of contact metamorphism of carbonate rocks. *J Petrol* 10:307–331
- Shima M (1986) A summary of extremes of isotopic variations in extra-terrestrial materials. *Geochim Cosmochim Acta* 50:577–584
- Siegenthaler U (1979) Stable hydrogen and oxygen isotopes in the water cycle. In: Jäger E, Hunziker JC (eds) *Lectures in isotope geology*. Springer, Berlin Heidelberg New York, pp 264–273
- Silverman SR (1964) Investigations of petroleum origin and evolution mechanisms by carbon isotope studies. In: *Isotopic and cosmic chemistry*. Elsevier/North Holland Biomedical Press, Amsterdam, p 92
- Silverman SR (1965) Migration and segregation of oil and gas. In: *Fluids in subsurface environments*. AAPG Mem 4:53
- Silverman SR (1967) Carbon isotopic evidence for the role of lipids in petroleum. *J Am Oil Chem Soc* 44:691
- Silverman SR, Epstein S (1958) Carbon isotopic compositions of petroleum and other sedimentary organic materials. *Bull Am Assoc Petrol Geol* 42:998
- Skirrow R, Coleman ML (1982) Origin of sulfur and geothermometry of hydrothermal sulfides from the Galapagos Rift, 86°W. *Nature (London)* 249:142–144
- Smith BN, Epstein S (1970) Biochemistry of the stable isotopes of hydrogen and carbon in salt marsh biota. *Plant Physiol* 46:738
- Smith BN, Epstein S (1971) Two categories of $^{13}C/^{12}C$ ratios for higher plants. *Plant Physiol* 47:380
- Smith JW, Batts BD (1974) The distribution and isotopic composition of sulfur in coal. *Geochim Cosmochim Acta* 38:121–123
- Smith JW, Gould KW, Rigby D (1982) The stable isotope geochemistry of Australian coals. *Org Geochem* 3:111–131
- Sofer Z (1978) Isotopic composition of hydration water in gypsum. *Geochim Cosmochim Acta* 42:1141–1149
- Sofer Z (1984) Stable carbon isotope compositions of crude oils: Application to source depositional environments and petroleum alteration. *Am Assoc Petrol Geol Bull* 68:31–49
- Sofer Z, Gat JR (1972) Activities and concentrations of oxygen-18 in concentrated aqueous salt solutions: Analytical and geophysical implications. *Earth Planet Sci Lett* 15:232–238
- Spivack AJ (1985) Boron isotope marine geochemistry (Abstr.). *Conf Int Les isotopes dans le cycle sedimentaire, Obernai, Fr 1–5 July 1985*

- Spivack AJ, Edmond JM (1986) Determination of boron isotope ratios by thermal ionization mass spectrometry of the dicesium metaborate cation. *Anal Chem* 58:31–35
- Spooner ETC, Beckinsale RD, Fyfe WS, Snewing JD (1974) O¹⁸-enriched ophiolitic metabasic rocks from E. Liguria (Italy), Pindos (Greece) and Troodos (Cyprus). *Contrib Mineral Petrol* 47:41–62
- Stahl W (1977) Carbon and nitrogen isotopes in hydrocarbon research and exploration. *Chem Geol* 20:121–149
- Stahl W (1979) Carbon isotopes in petroleum geochemistry. In: Jäger E, Hunziker JC (eds) *Lectures in isotope geology*. Springer, Berlin Heidelberg New York
- Stahl W (1980) Compositional changes and ¹³C/¹²C fractionations during the degradation of hydrocarbons by bacteria. *Geochem Cosmochim Acta* 44:1903–1907
- Stahl W, Aust H, Dounas A (1974) Origin of artesian and thermal waters determined by oxygen, hydrogen and carbon isotope analyses of water samples from the Sperkios Valley, Greece. In: *Isotope techniques in groundwater hydrology*, IAEA Vienna, 1:317
- Stahl W, Wollanke G, Boigk H (1977) Carbon and nitrogen isotope data of Upper Carboniferous and Rotliegend natural gases from North Germany and their relationship to the maturity of the organic source material. In: Campos R, Goni J (eds) *Advances in organic geochemistry*. Madrid, p 539
- Stern MJ, Spindel W, Monse EU (1968) Temperature dependence of isotope effects. *J Chem Phys* 48:2908
- Stevens LM, Krout L, Walling D, Venters A, Engelkemeir A, Ross LE (1972) The isotopic composition of atmospheric carbon monoxide. *Earth Planet Sci Lett* 16:147–165
- Stewart MK (1974) Hydrogen and oxygen isotope fractionation during crystallization of mirabilite and ice. *Geochim Cosmochim Acta* 38:167–172
- Strauss H (1986) Carbon and sulfur isotopes in Precambrian sediments from the Canadian Shield. *Geochim Cosmochim Acta* 50:2653–2662
- Styrt MM, Brackmann AJ, Holland HD, Clark BC, Pisutha-Arnold U, Eldridge CS, Ohmoto H (1981) The mineralogy and the isotopic composition of sulfur in hydrothermal sulfide/sulfate deposits on the East Pacific Rise, 21°N latitude. *Earth Planet Sci Lett* 53:382–390
- Suhecki RK, Land LS (1983) Isotopic geochemistry of burial metamorphosed volcanogenic sediments, Great Valley sequence, northern California. *Geochim Cosmochim Acta* 47:1487–1500
- Suzuoki T, Epstein S (1976) Hydrogen isotope fractionation between OH-bearing minerals and water. *Geochim Cosmochim Acta* 40:1229–1240
- Swart PK, Grady MM, Pillinger CT (1982) Isotopically distinguishable carbon phases in the Allende meteorite. *Nature (London)* 297:381–383
- Swart PK, Grady MM, Pillinger CT, Lewis RS, Anders E (1983) Interstellar carbon in meteorites. *Science* 220:406–410
- Sweeney RE, Liu KK, Kaplan IR (1978) Oceanic nitrogen isotopes and their use in determining the source of sedimentary nitrogen. In: Robinson BW (ed) *DSIR Bull* 220:9–26
- Swihart GH, Moore PB, Callis EL (1986) Boron isotopic composition of marine and non-marine evaporite borates. *Geochim Cosmochim Acta* 50:1297–1301
- Tarutani T, Clayton RN, Mayeda TK (1969) The effect of polymorphism and magnesium substitution on oxygen isotope fractionation between calcium carbonate and water. *Geochim Cosmochim Acta* 33:987–996
- Taube H (1954) Use of oxygen isotope effects in the study of hydration ions. *J Phys Chem* 58:523

- Taylor BE, Friedrichsen H (1983) Light stable isotope systematics of granitic pegmatites from North America and Norway. *Isotope Geosci* 1:127–167
- Taylor BE, O'Neil JR (1977) Stable isotope studies of metasomatic Ca–Fe–Al–Si skarns and associated metamorphic and igneous rocks, Osgood Mountains, Nevada. *Contrib Mineral Petrol* 63:1–49
- Taylor BE, Foord EE, Friedrichsen H (1979) Stable isotope and fluid inclusion studies of gem-bearing granitic pegmatite aplite dikes, San Diego Co., California. *Contrib Mineral Petrol* 68:187–205
- Taylor BE, Eichelberger JC, Westrich HR (1983) Hydrogen isotopic evidence of rhyolitic magma degassing during shallow intrusion and eruption. *Nature (London)* 306:541–545
- Taylor HP (1967) Oxygen isotope studies of hydrothermal mineral deposits. In: Barnes HL (ed) *Geochemistry of hydrothermal ore deposits*. Holt Rinehart and Winston, New York
- Taylor HP (1968) The oxygen isotope geochemistry of igneous rocks. *Contrib Mineral Petrol* 19:1–71
- Taylor HP (1974a) The application of oxygen and hydrogen isotope studies to problems of hydrothermal alteration and ore deposition. *Econ Geol* 69:843–883
- Taylor HP (1974b) Oxygen and hydrogen isotope evidence for large-scale circulation and interaction between groundwaters and igneous intrusions with particular reference to the San Juan volcanic field, Colorado. In: *Geochemical transport and kinetics*. Carnegie Inst Washington 634:299–323
- Taylor HP (1977) Water/rock interactions and the origin of H₂O in granitic batholiths. *J Geol Soc* 133:509–558
- Taylor HP (1978) Oxygen and hydrogen isotope studies of plutonic granitic rocks. *Earth Planet Sci Lett* 38:177–210
- Taylor HP (1980) The effects of assimilation of country rocks by magmas on ¹⁸O/¹⁶O and ⁸⁷Sr/⁸⁶Sr systematics in igneous rocks. *Earth Planet Sci Lett* 47:243–254
- Taylor HP, Epstein S (1961) ¹⁸O/¹⁶O ratios of feldspars and quartz in zoned granitic pegmatites. *Geol Soc Am Spec Pap* 68:183
- Taylor HP, Epstein S (1962) Relationship between ¹⁸O/¹⁶O ratios in coexisting minerals of igneous and metamorphic rocks, Part I: Principles and experimental results. *Bull Geol Soc Am* 73:461–480
- Taylor HP, Epstein S (1964) Comparison of oxygen isotope analyses of tektites, soils and impactite glasses. In: *Cosmic and isotopic chemistry*. Elsevier/North Holland Biomedical Press, Amsterdam
- Taylor HP, Epstein S (1966) Oxygen isotope studies of Ivory Coast tektites and impactite glass from the Bosumtwi crater, Ghana. *Science* 153:173–175
- Taylor HP, Epstein S (1969) Correlations between O¹⁸/O¹⁶ ratios and chemical composition of tektites. *J Geophys Res* 74:6834–6844
- Taylor HP, Forester RW (1971) Low-¹⁸O igneous rocks from the intrusive complexes of Skye, Mull and Ardnamurchan, Western Scotland. *J Petrol* 12:465–497
- Taylor HP, Forester RW (1979) An oxygen and hydrogen isotope study of the Skaergaard Intrusion and its country rocks: a description of a 55 M.Y. old fossil hydrothermal system. *J Petrol* 20:355–419
- Taylor HP, Silver LT (1978) Oxygen isotope relationships in plutonic igneous rocks of the Peninsular Ranges Batholith, Southern and Baja California. Short papers of the 4th Intern Conf Geochronology, Cosmochronology, Isotope Geology. U.S. Geological Survey Open-File Report 78-701, pp 423–426

- Taylor HP, Albee AL, Epstein S (1963) O^{18}/O^{16} ratios of coexisting minerals in three assemblages of kyanite zone pelitic schists. *J Geol* 71:513–522
- Taylor HP, Gianetti B, Turi B (1979) Oxygen isotope geochemistry of the potassic igneous rocks from Roccamonfina volcano, Roman comagmatic region. *Earth Planet Sci Lett* 46:81–106
- Taylor HP, Turi B, Cundari A (1984) $^{18}O/^{16}O$ and chemical relationships in K-rich volcanic rocks from Australia, East Africa, Antarctica and San Venanzo-Cupaello, Italy. *Earth Planet Sci Lett* 69:263–276
- Thiemens MH, Heidenreich JE (1983) The mass independent fractionation of oxygen – A novel isotope effect and its cosmochemical implications. *Science* 219:1073–1075
- Thierstein HR, Geizzenauer KR, Molfino B, Shackleton NJ (1977) Global synchronicity of late Quaternary coccolith datum levels: validation by oxygen isotopes. *Geology* 5:400–404
- Thode HG (1970) Sulphur isotope geochemistry and fractionation between coexisting sulphide minerals. *Mineral Soc Am Spec Pap* 3:133
- Thode HG (1981) Sulfur isotope ratios in petroleum research and exploration: Williston Basin. *Am Assoc Petrol Geol Bull* 65:1527–1535
- Thode HG, Goodwin AM (1983) Further sulfur and carbon isotope studies of late Archean iron-formations of the Canadian Shield and the rise of sulfate reducing bacteria. *Precambrian Res* 20:337–356
- Thode HG, Monster J (1964) The sulfur isotope abundances in evaporites and in ancient oceans. In: Vinogradov AP (ed) *Proc Geochem Conf Commemorating the Centenary of V I Vernadskii's Birth*, vol 2, 630 p
- Thode HG, Macnamara J, Collins CB (1949) Natural variations in the isotopic content of sulphur and their significance. *Can J Res* 27B:361
- Thode HG, Monster J, Dunford HB (1958) Sulphur isotope abundances in petroleum and associated materials. *Am Assoc Petrol Geol Bull* 42:2619–2641
- Thode HG, Harrision AG, Monster J (1960) Sulphur isotope fractionation in early diagenesis of recent sediments of Northeast Venezuela. *Am Assoc Petrol Geol Bull* 44:1809–1817
- Thode HG, Monster J, Dunford HB (1961) Sulphur isotope geochemistry. *Geochim Cosmochim Acta* 25:159–174
- Thode HG, Cragg CB, Hulston JR, Rees CE (1971) Sulphur isotope exchange between sulphur dioxide and hydrogen sulphide. *Geochim Cosmochim Acta* 35:35–45
- Thompson AB (1983) Fluid absent metamorphism. *J Geol Soc London* 140:533–547
- Touret J (1971) Le faciès granulite en Norvège méridionale. Les inclusions fluids. *Lithos* 4:423–436
- Tracy RJ, Rye DM, Hewitt DA, Schiffries CM (1983) Petrologic and stable isotopic studies of fluid-rock interactions, south central Connecticut. I. The role of infiltration in producing reaction assemblages in impure marbles. *Am J Sci* 283A:589–616
- Trofimov A (1949) Isotopic constitution of sulfur in meteorites and in terrestrial objects. *Dokl Akad Nauk SSSR* 66:181 (in Russian)
- Trudinger PA, Chambers LA (1973) Reversibility of bacterial sulfate reduction and its relevance to isotope fractionation. *Geochim Cosmochim Acta* 37:1775–1778
- Truesdell AH (1974) Oxygen isotope activities and concentrations in aqueous salt solution at elevated temperatures: Consequences for isotope geochemistry. *Earth Planet Sci Lett* 23:387–396

- Truesdell AH, Hulston JR (1980) Isotopic evidence on environments of geothermal systems. In: Fritz P, Fontes J (eds) Handbook of environmental isotope geochemistry, vol 1. Elsevier, New York Amsterdam, pp 179–226
- Truesdell AH, Nathenson M, Rye RO (1977) The effects of subsurface boiling and dilution on the isotopic compositions of Yellowstone thermal waters. *J Geophys Res* 82:3694–3704
- Tsai HM, Shieh Y, Meyer HOA (1979) Mineralogy and $^{34}\text{S}/^{32}\text{S}$ ratios of sulfides associated with kimberlite xenoliths and diamonds. In: Boyd FR, Meyer HOA (eds) The mantle samples: inclusions in kimberlites and other volcanics. AGU, Washington, pp 87–103
- Tucker ME (1983) Diagenesis, geochemistry and origin of a Precambrian dolomite: The Beck spring dolomite of eastern California. *J Sediment Petrol* 53:1097–1119
- Tudge AP (1960) A method of analysis of oxygen isotopes in orthophosphate – its use in the measurement of paleotemperatures. *Geochim Cosmochim Acta* 18:81–93
- Tudge AP, Thode HG (1950) Thermodynamic properties of isotope compounds of sulphur. *Can J Res* 28:567
- Turner JV (1982) Kinetic fractionation of carbon-13 during calcium carbonate precipitation. *Geochim Cosmochim Acta* 46:1183–1192
- Ueda A, Sakai H (1983) Simultaneous determinations of the concentration and isotope ratio of sulfate- and sulfide-sulfur and carbonate-carbon in geological samples. *Geochemical J* 17:185–196
- Ueda A, Sakai S (1984) Sulfur isotope study of Quaternary volcanic rocks from the Japanese Island Arc. *Geochim Cosmochim Acta* 48:1837–1848
- Urey HC (1947) The thermodynamic properties of isotopic substances. *J Chem Soc* 1947:562
- Urey HC, Brickwedde FG, Murphy GM (1932a) An isotope of hydrogen of mass 2 and its concentration (Abstr). *Phys Rev* 39:864
- Urey HC, Brickwedde FG, Murphy GM (1932b) A hydrogen isotope of mass 2 and its concentration. *Phys Rev* 40:1
- Urey HC, Lowenstam HA, Epstein S, McKinney CR (1951) Measurement of paleotemperatures and temperatures of the Upper Cretaceous of England, Denmark and the Southeastern United States. *Bull Geol Soc Am* 62:399–416
- Uzdowski HE (1982) Reactions and equilibria in the systems $\text{CO}_2\text{--H}_2\text{O}$ and $\text{CaCO}_3\text{--CO}_2\text{--H}_2\text{O}$ ($0^\circ\text{--}50^\circ$). A review. *N Jahrb Miner Abh* 144:148–171
- Uzdowski HE, Hoefs J, Menschel G (1979) Relationship between ^{13}C and ^{18}O fractionation and changes in major element composition in a recent calcite-depositing spring – a model of chemical variations with inorganic calcite precipitation. *Earth Planet Sci Lett* 42:267–276
- Valley JW (1986) Stable isotope geochemistry of metamorphic rocks. In: Valley JW, Taylor HP, O'Neil JR (eds) Stable isotopes in high temperature geological processes. *MSA Rev Mineral* 16 (in press)
- Valley JW, O'Neil JR (1981) $^{13}\text{C}/^{12}\text{C}$ exchange between calcite and graphite: a possible thermometer in Grenville marbles. *Geochim Cosmochim Acta* 45:411–419
- Valley JW, O'Neil JR (1984) Fluid heterogeneity during granulite facies metamorphism in the Adirondacks: stable isotope evidence. *Contrib Mineral Petrol* 85:158–173
- Veizer J, Hoefs J (1976) The nature of $\text{O}^{18}/\text{O}^{16}$ and $\text{C}^{13}/\text{C}^{12}$ secular trends in sedimentary carbonate rocks. *Geochim Cosmochim Acta* 40:1387–1395
- Veizer J, Holser WT, Wilgus CK (1980) Correlation of $^{13}\text{C}/^{12}\text{C}$ and $^{34}\text{S}/^{32}\text{S}$ secular variations. *Geochim Cosmochim Acta* 44:579–587

- Vigino JA, Harmon RS, Borthwick J, Nehring NL, Motyka RJ, White LD, Johnston DA (1985) Stable-isotope evidence for a magmatic component in fumarole condensates from Augustine volcano, Cook Inlet, Alaska, USA. *Chem Geol* 49: 141–157
- Vincent E, Killingley JS, Berger WS (1981) Stable isotope composition of benthic foraminifera from the equatorial Pacific. *Nature (London)* 289:639–643
- Vinogradov AP, Grinenko VA, Ustinov VI (1962) Isotopic composition of sulfur compounds in the Black Sea. *Geochemistry* 1962:973
- Vogel DE, Garlick GD (1970) Oxygen isotope ratios in metamorphic eclogites. *Contr Mineral Petrol* 28:183–191
- Vogel JC, Urk H van (1975) Isotopic composition of groundwater in semiarid regions of South Africa. *J Hydrol* 25:23
- Wachter EA, Hayes JM (1985) Exchange of oxygen isotopes in carbon dioxide-phosphoric acid systems. *Chem Geol Isotope Geosci Sect* 52:365–374
- Wada H, Suzuki K (1983) Carbon isotopic thermometry calibrated by dolomite-calcite solvus temperatures. *Geochim Cosmochim Acta* 47:697–706
- Warren CG (1972) Sulfur isotopes as a clue to the genetic geochemistry of a roll-type uranium deposit. *Econ Geol* 67:759–767
- Way K, Fano L, Scott MR, Thew K (1950) Nuclear data. A collection of experimental values of half-lives, radiation energies, relative isotopic abundances, nuclear moments and cross-sections. *Natl Bur Stand U S Circ* 499
- Weber JN (1968) Fractionation of the stable isotopes of carbon and oxygen in calcareous marine invertebrates – the Asteroidea, Ophiuroidea and Crinoidea. *Geochim Cosmochim Acta* 32:33–70
- Weber JN, Raup DM (1966a) Fractionation of the stable isotopes of carbon and oxygen in marine calcareous organisms – the Echinoidea. I. Variation of ^{13}C and ^{18}O content within individuals. *Geochim Cosmochim Acta* 30:681–703
- Weber JN, Raup DM (1966b) Fractionation of the stable isotopes of carbon and oxygen in marine calcareous organisms – the Echinoidea. II. Environmental and genetic factors. *Geochim Cosmochim Acta* 30:705–736
- Wedeking KW, Hayes JM, Matzigkeit U (1983) Procedures of organic geochemical analysis. In: Schopf JW (ed) *Earth's earliest biosphere: Its origin and evolution*. Princeton Univ Press
- Wellmann RP, Cook FD, Krouse HR (1968) Nitrogen-15: Microbiological alteration of abundance. *Science* 161:269–270
- Welte DH, Kalkreuth W, Hoefs J (1975) Age-trend in carbon isotopic composition in Paleozoic sediments. *Naturwissenschaften* 62:482–483
- Wenner DB, Taylor HP (1973) Oxygen and hydrogen isotope studies of the serpentinization of ultramafic rocks in oceanic environments and continental ophiolite complexes. *Am J Sci* 273:207–239
- Wenner DB, Taylor HP (1974) D/H and $^{18}\text{O}/^{16}\text{O}$ ratios of serpentinization of ultramafic rocks. *Geochim Cosmochim Acta* 38:1255–1286
- Whalen M, Yoshinara T (1985) Oxygen isotope ratios of N_2O from different environments. *Nature (London)* 313:697–782
- White DE (1974) Diverse origins of hydrothermal ore fluids. *Econ Geol* 69:954–973
- Whiticar MJ, Faber E, Schoell M (1986) Biogenic methane formation in marine and freshwater environments: CO_2 reduction vs. acetate fermentation – Isotopic evidence. *Geochim Cosmochim Acta* 50:693–709
- Wickham SM, Taylor HR (1985) Stable isotope evidence for large-scale seawater infiltration in a regional metamorphic terrane; the Trois Seigneurs Massif, Pyrenees, France. *Contrib Mineral Petrol* 91:122–137

- Wickman FE (1952) Variation in the relative abundance of carbon isotopes in plants. *Geochim Cosmochim Acta* 2:243–254
- Willan RCR, Coleman ML (1983) Sulfur isotope study of the Aberfeldy barite, zinc, lead deposit and minor sulfide mineralizations in the Dalradian metamorphic terrain, Scotland. *Econ Geol* 78:1619–1656
- Williams DF, Sommer MA, Bender ML (1977) Carbon isotopic compositions of recent planktonic foraminifera of the Indian Ocean. *Earth Planet Sci Lett* 36:391–403
- Williams DF, Röttger R, Schmaljohann R, Keigwin L (1981) Oxygen and carbon isotopic fractionation and algal symbiosis in the benthic foraminifera "Heterostegina depressa". *Palaeogeogr Palaeoclim Palaeoecol* 33:231–251
- Wilson AF, Baski AK (1983) Widespread ^{18}O -depletion in some Precambrian granulites of Australia. *Precambrian Res* 23:33–56
- Wilson AF, Green DC, Davidson LR (1970) The use of oxygen isotope geothermometry on the granulites and related intrusives, Musgrave Ranges, Central Australia. *Contrib Mineral Petrol* 27:166–178
- Wong WW, Sackett WM (1978) Fractionation of stable carbon isotopes by marine phytoplankton. *Geochim Cosmochim Acta* 42:1809–1815
- Wong WW, Benedict CR, Kohel JR (1979) Enzymatic fractionation of the stable isotope of carbon dioxide by RudP-carboxylase. *Plant Physiol* 63:852–856
- Wright IP, McNaughton NJ, Fallick AE, Gardiner LR, Pillinger CT (1983) A high-sensitivity-high precision stable isotope mass spectrometer. *J Phys (E)* 16:497–504
- Wyllie PJ (1979) Mantle fluid compositions buffered in peridotite– CO_2 – H_2O by carbonates, amphibole and phlogopite. *J Geol* 86:687–713
- Yang J, Epstein S (1982) On the origin and composition of hydrogen and carbon in meteorites. *Meteoritics* 17:301
- Yang J, Epstein S (1983) Interstellar organic matter in meteorites. *Geochim Cosmochim Acta* 47:2199–2216
- Yang J, Epstein S (1984) Relic interstellar grains in Murchison meteorite. *Nature (London)* 311:544–547
- Yapp CJ (1979) Oxygen and carbon isotope measurements of land snail shell carbonate. *Geochim Cosmochim Acta* 43:629–635
- Yeh HW (1980) D/H ratios and late stage hydration of shales during burial. *Geochim Cosmochim Acta* 45:341–352
- Yeh HW, Epstein S (1978) Hydrogen isotope exchange between clay minerals and seawater. *Geochim Cosmochim Acta* 42:140–143
- Yeh HW, Epstein S (1981) Hydrogen and carbon isotopes of petroleum and related organic matter. *Geochim Cosmochim Acta* 45:753–762
- Yeh HW, Savin SM (1976) The extent of oxygen isotope exchange between clay minerals and seawater. *Geochim Cosmochim Acta* 40:743–748
- Yeh HW, Savin SM (1977) Mechanism of burial metamorphism of argillaceous sediments. 3. O-isotope evidence. *Geol Soc Am Bull* 88:1321–1330
- Yoshida N, Matsuo S (1983) Nitrogen isotope ratio of atmospheric N_2O as a key to the global cycle of N_2O . *Geochem J* 17:231–239
- Yoshida N, Hattori A, Saino T, Matsuo S, Wada E (1984) $^{15}\text{N}/^{14}\text{N}$ ratio of dissolved N_2O in the eastern tropical Pacific Ocean. *Nature (London)* 307:442–444
- Yuen G, Blair N, DesMarais DJ, Chang S (1984) Carbon isotopic composition of individual, low molecular weight hydrocarbons and monocarboxylic acids from Murchison meteorite. *Nature (London)* 308:252–254

- Yund RA, Anderson TF (1974) Oxygen isotope exchange between potassium feldspar and KCl solution. In: Geochemical transport and kinetics. Carnegie Inst Washington, Publ 634, pp 99–105
- Yurtsever Y (1975) Worldwide survey of stable isotopes in precipitation. Rep Sect Isotope Hydrol IAEA, November 1975, 40 pp
- Zierenberg RA, Shanks WC, Bischoff JL (1984) Massive sulfide deposit at 21°N, East Pacific Rise: chemical composition, stable isotopes, and phase equilibria. Bull Geol Soc Am 95:922–929
- ZoBell CE (1958) Ecology of sulfate-reducing bacterial. Prod Mongr 22:12

Subject Index

- absolute isotope abundance 22
- achondrite 68f.
- activated complex 12, 156
- activation energy 14, 46
- activity ratio 31, 47
- aerosols 149
- age curve 138
- algae 151
- amino acids 133, 152f.
- ammonia volatilization 60, 187
- amphiboles 80f.
- amphibolite-facies metamorphism 187
- anaerobic conditions 51
- anatexis 94
- animals 150, 154f.
- anoxic oceanic event 141
- anthropogenic pollution 133, 143, 149f.
- aragonite 16, 171, 172, 177, 178
- aromatic hydrocarbons 160
- asphaltenes 160
- assimilation of crustal rocks 86, 87f., 93
- atmosphere 75, 132, 141, 143ff., 176
- atomic weight 1, 32, 42
- Au-Ag vein deposits 106
- authigenic minerals 128, 168, 180

- bacteria 59, 151
- bacterial oxidation 160
 - reaction 26, 31, 51f., 145
 - sulfate reduction 51f., 115, 137, 139, 178, 182f.
- banded iron formation 190
- basalt 47, 63, 73, 77, 78, 83, 86, 91f., 95, 113, 179
- batch volatilization 185
- benthic foraminifera 172f.
- bicarbonate 133f., 141, 171
- biodegradation 134, 159, 162
- biogenic gas 164f.
 - ore deposit 115, 184
 - sulfur 111, 182f.
- biological carbon fixation 33f., 151f.
 - system 26, 35, 65, 155
- biosphere 32, 49, 141, 150ff.
- black shale 166
- boiling of fluids 101
- bond length 30
 - strength factor 41f., 54
- boron isotopes 63f.
- brine 47, 64, 129f., 136, 186

- calcite 16, 18, 35, 36, 45, 99, 142, 170f., 177, 180, 190
- calcium isotopes 64f.
- calibration curves 29f., 36, 43f., 56, 188
- Calvin cycle 34, 151
- CAM metabolism 151
- carbohydrate 34, 154, 158
- carbon dioxide 147f.
 - isotopes 31ff., 147f.
 - –, fractionation mechanisms 33f.
 - –, preparation techniques 32f.
 - –, standards 32f.
- carbonaceous chondrites 67f.
 - matter 101, 191, 196
- carbonate cement 177, 178
 - concretion 37, 179
- carbonates 32, 33f., 39f., 42f., 70, 100, 116f., 128, 135, 141, 158, 170f., 181, 187, 190, 192
- carbonatites 82
- carboxylation reaction 34f.
- carboxyl groups 155, 158
- cation exchange 18, 44
- cellulose 152, 155, 157
- channelized fluids 185, 195
- cherts 128, 142, 167, 169f., 181, 190
- chlorine isotopes 64f.
- clay minerals 88, 108, 128, 167f.

- closed system condition 47f., 52, 182f., 195
 closure temperature 30
 coal 49, 150, 163f.
 coalification 163
 concordant temperatures 17, 188f.
 connate waters 55, 107, 118, 186
 contact aureoles 191, 194
 – metamorphism 179, 191f.
 continental basalts 78, 91
 cross-over phenomena 8, 185
 crude oil 49, 150, 159f.
 crustal contamination 87
 crystal fractionation 77, 87f.

 decarbonation 101, 108, 185f., 196
 decarboxylation 158
 degassing 78, 83, 96, 143
 dehydration 107, 185f., 189
 delta value, definition 9f., 23f.
 denitrification 59f., 131, 145
 detrital minerals 168
 deuterium excess 118
 diagenesis 141, 142, 157, 167, 169, 172, 177, 179
 – of clastic rocks 180f.
 – of limestones 178f.
 diffusion 13f., 19, 33, 45, 60, 64, 179, 183, 187, 188
 – coefficients 13, 186
 – rate 31, 46
 Dole effect 145
 dolomites 176f., 196

 eclogite 83, 197
 electric field 21
 elemental sulfur 102
 equilibrium constant 7f., 9, 12, 45, 54, 56
 – effects 34, 54, 60
 euphotic zone 133
 evaporation 125, 131, 136, 155, 176
 evaporation-condensation process 10f.
 evaporite 49, 137, 138f., 142
 exchange rates 18, 30, 102f.
 – reactions 45, 51
 experimental calibration methods 43f.

 Faraday cage 21
 fermentation 164, 180
 fertilizer 58
 Fischer-Tropsch reaction 70

 fluid flow 184f.
 – inclusions 56, 82, 97f., 197
 fluid-rock interaction 19, 47f., 184f.
 fluorination 38, 57
 foraminifera 148, 171f.
 formation water 31, 55, 106f., 118, 129, 180, 186
 fossil air 146, 148, 175
 – fuel 147, 157
 fractional crystallization 86f.
 fractionation effects 6f., 31
 – factor 9f., 17, 35, 39, 54, 59, 81, 102, 106, 120, 130, 186
 freezing point 28
 fresh water carbonates 176f.
 – –, dissolved compounds 131ff.
 fulvic acids 158
 fumarole 63, 102, 104

 gabbro 90
 galaxy 76
 galena 16, 56, 112
 gas-source rock correlations 166
 geothermal system 90, 100f.
 – water 47, 90, 101f.
 geothermometers 16ff., 38, 56f., 102f., 180, 186f.
 –, experimental calibration 18f.
 glaciation 148
 glacier 122, 142
 gneiss 196
 granite 90, 93f.
 granulite 93, 196, 197
 granulite-facies metamorphism 196f.
 graphite 16, 35, 36, 190, 196
 greenhouse gas 144, 147
 greenschist metamorphism 187
 groundwater 64, 89, 124f.

 hailstone 121
 harmonic oscillator 8
 Hatch-Slack cycle 34, 151
 H³⁺-correction 28
 heterocomponents 160
 hot springs 97ff.
 humic substance 157, 158
 hydrated salt minerals 129
 hydration 31, 47, 95, 130
 hydrocarbons 70, 150, 155, 160f.
 hydrogen bonding 30
 – isotopes 26ff.
 – –, equilibrium exchange reactions 29f.

- –, fractionation mechanisms 28f.
- –, mass spectrometric measurement 28f.
- –, preparation techniques 27f.
- –, standard 28
- hydrosphere 117ff., 143, 145, 149
- hydrothermal alteration 38, 80, 91, 101, 143
- ore deposits 110f., 184
- solution 47, 56, 88, 94, 103, 107, 110, 167
- system 48, 88, 108

- ice cores 122f., 146, 175
- volume factor 172
- igneous rocks 85ff.
- inlet system 19, 20f.
- inorganic sulfate reduction 113, 115
- instrumental errors, mass spectrometer 22, 25
- interlaboratory calibration 24
- international standards 23f.
- interplanetary dust 76
- interstellar matter 69
- interstitial water 37
- ion detector 19, 21f.
- source 19, 20f.
- ionic potential 42
- iron oxides 189
- island arc volcanics 78, 91, 96
- isotope abundance 1, 19, 22, 26
- anomaly 67f., 141
- effects 4ff., 101, 156, 186
- equilibrium 17, 19, 30, 31, 102, 113, 171, 173, 188
- exchange 6ff., 17, 30, 35, 56, 85, 94, 102, 143, 149, 168, 169, 171, 190, 197
- –, mechanisms 19, 30
- –, pressure dependence 8
- fractionation 6ff., 17, 25, 26, 30, 36, 39, 43, 65, 66, 77, 94, 104, 129, 138, 145, 153, 155, 158, 177, 180
- geothermometers 16ff., 56f., 188f.
- reversal 77
- isotopes, definition 1f.
- isotopic composition, variation with chemical composition 15f., 41f.
- –, variation with crystal structure 15f., 42

- juvenile water 80, 97

- kaolinite 108, 168, 180
- kerogen 158f.
- kimberlite 82
- kinetic effects 11ff., 19, 26, 34, 35, 41, 46, 51, 60, 62, 63, 70, 74, 102, 120, 149, 164, 187, 189, 196
- energy 21
- Kuroko-type deposits 107

- lherzolite 78f.
- lignin 152, 157
- limestone 116, 129, 141, 176, 178f., 181
- lipids 34, 133, 152, 154, 157, 158, 162
- living organic matter 151f.
- lunar rocks 72f.

- maceral 163
- mafic rocks 73
- magma genesis 86f.
- mixing 88
- magmatic water 98f., 106f., 128, 186
- magnetic field 21
- mantle, isotopic composition 76ff.
- metasomatism 79, 92
- marble 190, 194
- Mars 74f.
- mass analyzer 19, 21f.
- difference 4, 26, 27, 63, 65
- factor 41f.
- spectrometry 19, 26, 66, 75
- maturation of organic matter 107, 141, 158, 165
- mean free path length 20
- metabolic effects 171
- metamorphic rocks 93, 116, 184ff.
- water 106f., 184f.
- metamorphosed ore deposit 116
- meteoric water 89f., 94, 98, 100f., 106f., 118ff., 129, 143, 167, 177, 178, 180, 186, 190, 194
- meteorite 66f.
- impact 72
- methane 29, 32, 35, 102, 104, 117, 135, 148, 163, 164f., 178
- methanogenesis 135, 164, 178
- micas 80f., 186
- microbiological action 26, 164, 179
- microorganisms 150
- mid-ocean ridge basalt 89, 91, 96, 97
- ridges 113, 140

- migration 160, 162
 mineral synthesis 18
 Mississippi-Valley type deposit 107
 molecular flow 20
 Moon 72f.

 natural gas 164f.
 nitrification 58f., 145
 nitrogen isotopes 57ff., 144f.
 nitrous oxide 144f.
 nonmass-dependent isotope effect
 15f., 68
 NSO-compounds 160f.

 ocean water 47, 53, 88, 101, 106f.,
 110, 118, 124ff., 133, 135, 138ff.,
 148, 170, 171, 172, 177, 180
 — —, dissolved components 131ff.
 — — interaction 88f.
 oceanic basalts 78, 91
 — crust 80, 88, 107, 143, 197
 Oddo-Harkins rule 13
 oil-field brines 47, 129f.
 oil-source rock correlation 160
 oils 150, 159f.
 ophiolite 88, 190
 open-system condition 48f., 52, 177,
 182f., 195
 ore deposits 49, 56, 99, 105ff.
 — fluid 56, 105f.
 — genesis 80
 organic compounds 32, 49, 70, 107,
 116, 140
 — matter 33f., 37, 38, 51, 69, 115,
 133, 135, 141, 150, 154, 157f., 165,
 175, 183, 191
 — water 107
 organisms 59, 154
 oxygen fugacity 74, 78, 111f., 116
 — isotope shift 100f.
 oxygen isotope shift 100f.
 — isotopes 37ff., 145f.
 — —, equilibrium exchange reactions
 41f.
 — —, fractionation mechanisms 41f.
 — —, preparation techniques 38f.
 — —, standards 40f.
 — minimum zone 132
 ozone 15, 143, 146f.

 paleotemperature 40, 170f.
 partial melting 77, 93
 particulate organic matter 131, 133f.

 partition function 7f.
 pegmatites 94
 peridotites 77, 83
 permeability 195
 pervasive fluid 185, 195
 petroleum 150, 158f.
 — exploration 158, 162
 — type curves 160f.
 phase transition 18
 phosphates 38, 143, 181f.
 phosphorites 143, 181
 photochemical dissociation 144, 146
 photosynthesis 26, 33f., 46, 142, 144,
 145, 150f., 175
 plankton 131, 133, 151
 planktonic foraminifera 172f.
 plants 34, 150, 151f., 163
 —, chemical components 152f.
 polysaccharides 157
 pore water 128f., 134f., 161, 169, 179
 porphyry copper deposits 108, 114
 potential energy curve 5
 preparation techniques 27f.
 proteins 34, 154, 157, 158
 pyrite 57, 112, 116, 163, 182f.

 quartz 16, 18, 42, 90, 99, 142, 168,
 169, 180, 189, 196

 radioactive decay processes 3
 radiogenic isotopes 77, 87f., 92
 Rayleigh fractionation 16f., 52f., 62,
 119f., 185
 reaction rates 11, 25, 102f.
 recrystallization 18f.
 reduced partition function 7
 regional metamorphism 195f.
 respiration 46, 145, 147, 150, 154, 171
 respiratory processes 153f.
 retrograde exchange 86, 189
 ridge basalts 78, 84
 rotational energy 7

 salinity 125f.
 salt filtration 129
 sample preparation 25f.
 sandstone 167, 180
 sea level 175
 seawater 89, 95, 101, 111, 124f., 146,
 186, 197
 secondary alteration 85, 88f.
 — ion mass spectrometer 13

- sector field analyzer 21
- sedimentary rocks 55, 93, 116, 140, 157, 167ff.
 - sulfides 182f.
- sediment/water interface 134, 182
- selenium isotopes 57f.
- self-shielding process 15, 146
- serpentinization 190
- shale 129, 169, 180, 190
- silicates 41f.
- silicon isotopes 61f.
- skarn 107, 194
- SNC meteorites 68
- snow stratigraphy 122f.
- soil-CO₂ 154, 176
- solar system 66f.
 - wind 74
- sofataras 102
- spallogenic isotope fractionations 66f.
- sphalerite 16, 56, 99, 112
- standards 22f., 28
- static mass spectrometer 66
- statistical mechanics 5, 7, 17
- stratabound deposit 114
- stratosphere 143, 146
- subduction 80, 87, 96
- sugar 133, 152
- sulfate 38, 49f., 71, 83, 97, 135f., 138f., 149, 156, 163, 182
 - reduction 51f., 57, 135, 180, 182f.
- sulfides 49f., 83, 110f., 137, 140, 156, 163, 182f.
- sulfur isotopes 49ff.
 - –, experimental determination of sulfide systems 56f.
 - –, fractionation mechanisms 51f.
 - –, preparation techniques 50f.
 - –, standard 50
- suspended organic matter 132
- symmetry rule 1
- tektites 72
- temperature calibrations 17f.
- terrestrial fractionation 67
- thermal maturation 158, 162
- thermogenic gas 165f.
- thermometers 102f.
- three-isotope exchange 19, 43
- transition state 12
- translational energy 7
- tree rings 147, 156f.
- ultrafiltration 31, 55, 129
- ultramafic rocks 73, 77
- vapor pressure 28, 46
- vein-type deposits 114
- Venus 75f.
- vibrational energy 7
 - frequency 8, 15, 18
- viscous flow 20
- vital effect 171, 175
- vitrinite reflectance 166
- volatile elements 68f., 77, 85, 94, 97, 185f.
- volatilization 194f.
- volcanic gases 82, 97ff., 143
 - glasses 80, 85, 88, 91, 95, 96
- volcanogenic sulfide deposits 107
- voltage-to-frequency converter 22
- wall rock alteration 108f.
- water washing 159, 162
- water-rock interaction 19, 47f., 88ff.
 - ratio 47f., 88, 95, 100, 130, 184f.
- weathering 91, 137, 139, 143, 167
- wood 157
- xenolith 83
- zero point energy 5, 7